A random walk approach to stochastic neutron transport

Clélia De Mulatier

université PARIS-SACLAY

UNIVERSITÉ PARIS SUD
Comprendre le monde, construire l'avenir

NNT : 2015SACLS029

THÈSE DE DOCTORAT DE L'UNIVERSITÉ PARIS-SACLAY

préparée à L'Université Paris-Sud

ÉCOLE DOCTORALE 564
Physique en Île-de-France

Spécialité Physique

par

Clélia de Mulatier

A RANDOM WALK APPROACH TO STOCHASTIC NEUTRON TRANSPORT

Thèse soutenue à Orsay le 12 octobre 2015

Composition du Jury :

M. BÉNICHOU Olivier	Directeur de recherche CNRS, Université Pierre et Marie Curie	Président
Mme BURIONI Raffaella	Professeur, Università di Parma	Rapporteur
Mme DULLA Sandra	Professeur, Politecnico di Torino	Rapporteur
M. GOBET Emmanuel	Professeur, École Polytechnique	Examinateur
M. DIOP Cheikh	Professeur, CEA Saclay et INSTN	Directeur de thèse
M. ROSSO Alberto	Directeur de recherche CNRS, Université Paris-Sud	Co-directeur de thèse
M. ZOIA Andrea	CEA Saclay	Invité

ACKNOWLEDGEMENTS – REMERCIEMENTS

Je profite des ces quelques lignes pour remercier les personnes avec qui j'ai eu la chance de travailler, ceux qui m'ont accompagnée ou encouragée, ou, tout simplement, ceux avec qui j'ai passé de bons moments au cours de ces trois dernières années.

Mes premiers remerciement vont tout droit à Andrea sans qui cette thèse n'aurait pas été ce qu'elle est maintenant. Merci de m'avoir supportée ces trois ans, encouragée, et aidée ; merci pour la confiance que tu m'as accordé sur le plan scientifique et pour ta patience. Enfin, merci d'avoir pris le temps de répondre à mes multiples questions, et de m'avoir donné tout un tas d'équations et de calculs à dériver ! je n'aurais pas appris tant de choses nouvelles sans ton aide, ce sont toutes nos discussions qui m'ont donné envie de continuer dans la recherche. Je suis aussi ravie de ne pas t'avoir découragé et d'apprendre que tu commences l'encadrement d'une nouvelle thésarde.

Je tiens aussi à remercier tout particulièrement mes deux directeurs de thèse. Cheikh, pour sa perspicacité et son expertise en terme de thèse, qui ont fortement contribué à mener à bien cette thèse interdisciplinaire, partagée entre deux laboratoires. Et enfin, Alberto, un grand merci pour m'avoir fait découvrir le domaine de la physique statistique, ainsi que celui de la recherche ! merci de m'avoir guidé depuis le stage de M1, celui de M2, et jusqu'à la thèse. J'ai beaucoup apprécié tous les projets de recherche que tu as pu me proposer. Je me souviens du premier mail que je t'ai envoyé pour le stage de M1, j'avais peur d'essuyer un refus, jamais je n'aurais imaginé arriver jusqu'ici.

Je souhaite ensuite remercier chaleureusement l'intégralité des membres de mon jury de thèse. I'm very grateful to Sandra Dulla and Raffaella Burioni for the time they have dedicated to carefully reviewing my thesis. I was also very honoured by the presence of Olivier Bénichou and Emmanuel Gobet as jury members. I would like to express my gratitude to the members of my defense committee for their participation to my PhD defense and for the interest they showed for my work.

Je tiens aussi à remercier les différents chercheurs avec qui j'ai eu la chance de collaborer, tout particulièrement Grégory, Alain, Eric et PK. Je suis très reconnaissante envers Grégory pour le temps précieux qu'il a pu m'accorder et les projets enrichissants qu'il m'a proposé.

Merci à Emmanuel Trizac et à Franck Gabriel pour m'avoir accueillie dans vos laboratoires respectifs. En particulier, je suis reconnaissante envers Emmanuel Trizac pour m'avoir permis de recevoir des lycéens au LPTMS. Je souhaite aussi remercier les membres du LPTMS et du LTSD pour leurs conseils et le temps qu'ils ont pris pour répondre à mes questions ; merci tout particulièrement à Christophe, Martin, Raoul, Denis, Guillaume, Mikhail et François-Xavier.

Je tiens aussi à remercier tout particulièrement Claudine pour son organisation, son soutien et sa bonne humeur ! Ainsi que Vincent, ton incroyable facilité à communiquer avec nos ordinateurs quand nous en sommes complètement incapables m'a sauvée à de nombreuses reprises ! merci aussi pour tous les raccourcis bash que tu as pu m'apprendre. `echo -e "\xf0\x9f\x8d\xba"` ! Merci Thérèse pour l'attention que tu m'as accordé, tes conseils et les diverses discussions entre deux arrêts de RER B tardifs.

La thèse n'a pas seulement été axée sur la recherche, mais m'a aussi permis de passer de bons moments de « détente » en cours ! Merci aux enseignants et collègues avec qui j'ai eu la chance de travailler, Daniel, Nadia, François, Hervé, Corinne et Julien. J'ai énormément apprécié enseigner pour vos cours. Un grand merci aux étudiants, avec qui j'ai passé de super moments !

La thèse, c'est aussi de très bons moments passés entre thésards/étudiants/postdoc. Je pense tout particulièrement à Andrey, Andrii, François, Giulia, Ricardo, Pierre, Vincent, Yasar, Karim, Cyril, Arthur, Olga, France, Ben, RiCyl, et les bonhommes LEGO® ! Merci beaucoup Cyril pour avoir pris le temps de relire et commenter une partie de mon manuscrit, et pour m'avoir partagé ta passion pour la physique des réacteurs. Merci à Kevin, Olga, Ricardo et Pierre pour les divers problèmes passionnants de physique ou math sur lesquels nous avons pu échanger. J'ai beaucoup aimé nos discussions, et j'espère bien avoir encore de nombreuses occasions.

Je pense aussi à tous ces amis avec qui j'ai passé de très bons moments ces dernières années; un grand merci à la coloc'du 14e, Vivien, Émilien, Cécile, Grégoire, sans qui la thèse n'aurait pas été aussi sympathique, et à mes coloc' de fin de thèse Kar' et Pierre (!) ; et aux amis de longue date, qui m'ont conseillée et soutenue, Marine, Thibaut, Sylvain, Antoine, Jules,...

Marine, merci pour nos nombreux bavardages, ton grand talent et tes conseils de psychologue !

Mes derniers remerciements vont tout droit à ma famille « adorée », mes parents qui m'ont toujours accompagnée ; et mes frères et sœurs, Geo (merci de m'avoir aidée à percer le mystère du fonctionnement des ascenseurs !), ma chroutt' adorée (j'attends ta thèse avec impatience ! ;p), Hortichou (merci à toi de continuer à nous faire tant rêver de musique) et J-T (je sais, c'est Jean-Théophane ! ahhh, heureusement que tu es là !).

Ma dernière pensée va à Eugenio. Aussi paradoxal que cela puisse être, je suis pleine de gratitude envers ces trois années de doctorat qui m'ont permis de te rencontrer, tout comme je te remercie de m'avoir tant soutenue pour les terminer. (turtle) ! Merci pour ta patience, ta gentillesse, et tous ces instants de bonheur que tu me fais vivre.

FRENCH SUMMARY – RÉSUMÉ EN FRANÇAIS

CONTRIBUTIONS DE LA THÉORIE DES MARCHES ALÉATOIRES AU TRANSPORT STOCHASTIQUE DES NEUTRONS

Au cours de mon doctorat, j'ai effectué mon activité de recherche sous la codirection d'Alberto Rosso au LPTMS (Université Paris-Sud - CNRS) et de Cheikh Diop et Andrea Zoia au LTSD (CEA Saclay DEN/DM2S/SERMA). Cette double affiliation m'a permis de travailler à l'interface de la physique statistique et de la physique des réacteurs nucléaires. Je me suis plus spécifiquement intéressée aux propriétés des marches aléatoires branchantes et de la diffusion anormale dans le contexte du transport stochastique des neutrons au sein d'un réacteur nucléaire. En outre, quelques-uns des aspects originaux de la thèse sont l'étude des fluctuations statistiques – spatiales et temporelles – de la population de neutrons et le travail en géométrie confinée ou en présence de bords (prise en compte des bords du système). Ce travail, réalisé en collaboration avec différents chercheurs du LTSD et du LPTMS, et rapporté dans ce manuscrit, a donné lieu à plusieurs publications dans des revues internationales. Vous en trouverez ici un court résumé en français.

INTRODUCTION

L'UN des principaux objectifs de la physique des réacteurs nucléaires est de caractériser la répartition de la population de neutrons au sein d'un réacteur. Due à la nature stochastique des interactions entre ces neutrons et les noyaux fissiles composant le coeur du réacteur (combustible), cette répartition fluctue spatialement et temporellement. Pour autant, pour la majeur partie des applications en physique des réacteurs, la population de neutrons considérée est très importante – on peut citer par exemple la densité de neutrons au sein d'un réacteur de type REP à pleine puissance en conditions stationnaires qui est de l'ordre de 10^8 neutrons par centimètre cube. Dans ces conditions, les grandeurs physiques caractérisant le système (tels que flux, taux de réaction, énergie déposée) sont, en première approximation, bien représentées par leurs valeurs moyennes respectives, qui obéissent à l'équation de transport linéaire de Boltzmann. Cette approche cependant présente des limites : nous nous intéressons ici à deux aspects du transport des neutrons qui ne sont peuvent pas être décrits par cette équation.

Chapitre 1 - Transport des neutrons et physique statistique

Ce chapitre introductif présente le contexte général du transport des neutrons en physique des réacteurs et explicite le lien avec la physique statistique, plus précisément la théorie des marches aléatoires. Dû à la nature stochastique et markovienne des intéractions des neutrons avec les noyaux fissiles du milieu – diffusion, capture stérile, ou encore émission d'un ou plusieurs neutrons lors de la fission d'un noyau – le transport des neutrons au sein d'un matériau fissile peut etre modélisé par des marches aléatoires exponentielles branchantes.

Sont introduits ensuite les notations utilisées dans la thése, ainsi que les observables principales en physique des réacteurs, la densité neutronique, le taux de réaction et le flux neutronique. Les équations de bases de la neutronique sont ensuite re-dérivées : l'équation de transport linéaire de Boltzmann sous forme intégro-différentielle et sous forme intégrale, et l'équation de diffusion des neutrons. Ces équations décrivent le comportement des grandeurs moyennes, que sont la densité neutronique, le flux ou le taux de réactions, c.à.d. le comportement moyen de la population de neutrons. Bien qu'adaptée à la plupart des situations en physique des réacteurs, cette approche présente cependant des limites.

Tout d'abord, elle ne permet pas caractériser les fluctuations statistiques de la population de neutrons, qui peuvent devenir importantes dans des

systèmes où la densité de neutrons est initialement faible. Dans un réacteur REP au démarrage par exemple, la population est initialement faible; des simulations numériques Monte-Carlo réalisées avec le code TRIPOLI-4 au LTSD ont mis en évidence la formation d'amas de neutrons dispersés dans de tels systèmes. Ce comportement surprenant, que nous avons baptisé « *clustering neutronique* » [Dumonteil et al. 2014], résulte de larges fluctuations spatiales et temporelles de la population de neutron, et ne peut donc pas être expliqué à partir des équations de transport usuelles.

D'autre part, l'équation de Boltzmann caractérise le transport des neutrons dans des milieux où les positions des centres de diffusion (noyaux fissiles) sont non corrélés, c.à.d. dans lesquels le transport des neutrons est de forme exponentiel. Cependant, pour quelques applications, le milieu traversé par les neutrons est fortement hétérogène, voire désordonné (à désordre figé), de sorte que l'hypothèse de centres de diffusion non corrélés n'est plus valide. Citons par exemple le cas des réacteurs à lit de boulets, ou encore le transport radiatif dans des tissus (peau). Pour ce type de milieux, il a été observé que le transport n'obéit plus à un transport simplement exponentiel, et les équations usuelles de la neutronique ne sont alors plus valables.

Le présent manuscrit s'intéresse à ces deux aspects du transport des neutrons non décrit par l'équation de transport linéaire de Boltzmann. La première partie du manuscrit traite des fluctuations statistiques de la population de neutrons, et plus particulièrement du clustering neutronique. La deuxième partie se concentre sur le transport non-exponentiel, et s'intéresse plus spécifiquement à des propriétés du transport anormal dans un système de taille fini ou en présence de bords du système.

PARTIE I - STATISTIQUES DES FLUCTUATIONS

Nous étudions, dans un premier temps, à un aspect souvent négligé des processus de diffusion avec branchements : les fluctuations statistiques – temporelles et spatiales – de la population de particules. Due au processus de naissances (fissions) et de morts (absorption) de particules, appelé *processus de Galton-Watson*, l'amplitude de ces fluctuations croît au cours du temps, jusqu'à devenir comparable au quantités moyennes caractérisant le système (telles que la densité de particules par exemple). Ainsi, même un système critique, pour lequel le taux de naissance est égale au taux de mort (comme c'est le cas pour le fonctionnement d'un réacteur), peut voir sa population disparaître au bout d'un certain temps[1]. Ce phénomène est

[1] Le temps caractéristique correspondant est bien entendu d'autant plus long que la population initiale est importante.

connu en neutronique sous le nom de *catastrophe critique* [Williams 1974]. Ces fluctuations peuvent-elles conduire à la formation d'amas de neutrons, tels que ceux observés lors des simulations TRIPOLI-4 de réacteurs au démarrage, en dépit du fait que ces particules n'interagissent pas directement entre elles ?

Chapitre 2 – Description *backward* des fluctuations

Ce premier chapitre développe les outils nécessaires à l'étude des fluctuations de la population de neutrons. En particulier, nous nous intéressons à deux observables principales (celles d'intéret en physique des réacteurs) : la longueur totale parcourue et le nombre total de collisions effectuées, par une famille de neutrons dans un volume donné du milieu fissile. Les moyennes respectives de ces deux observables sont directement reliées au flux neutronique et au taux de réaction dans le volume considéré. L'étude des moments d'ordre supérieur de ces observables permet d'accéder aux fluctuations statistiques des grandeurs physiques d'intérêts caractérisant la population de neutrons en physique des réacteurs.

Dans ce but, nous avons utilisé le formalisme backward de Feynman-Kac afin de dériver l'équation backward gouvernant la fonction génératrice des moments pour chacune de ces deux observables. Pour se faire, nous nous sommes placés dans le cas le plus général d'un système composé d'un milieu hétérogène, où la diffusion des neutrons peut être anisotrope et les vitesses (énergies) des neutrons peuvent changer à chaque collision [SNAM-MC 2013].

Enfin, nous nous intéressons à la statistique d'occupation des neutrons dans un volume donné de milieu fissile. L'observable considérée est alors le nombre total de neutrons présents dans le volume à un instant t donné[2]. Nous retrouvons alors les équations de Pàl-Bell connues en physique des réacteurs.

Chapitre 3 – Clustering neutronique

Ce chapitre commence par un état de l'art des résultats sur le phénomène de clustering, qui a déjà été observé dans différents domaines et étudié pour des systèmes de "taille infinie". Nous remarquons que la formation des *clusters* résulte d'une compétition entre le processus de naissance et de mort, qui tend à créer des amas de particules appartenant à la même

[2]Par la suite, nous nous intéresserons de nouveau à cette observable afin de caractériser la fonction de corrélation entre paires de particules du système, centrale pour comprendre le phénomène de clustering.

famille, et le processus de diffusion, qui tend à les disperser.

Pour la suite, nous nous concentrons sur les systèmes critiques, qui correspondent aux conditions de fonctionnement des réacteurs nucléaires. Dans ce contexte, nous étudions l'impact de la prise en compte des bords du système (système de volume fini) sur le phénomène de clustering. Puis nous investiguons l'impact d'un processus de contrôle de la population globale de neutrons, tel que celui réalisé par les barres de contrôle au coeur du réacteur. Pour cela nous nous sommes intéressés à la fonction de corrélation de paire du système, pour laquelle nous obtenons les équations d'évolution en utilisant une description "backward" du transport des neutrons.

Nous observons la présence de deux types de fluctuations [Zoia et al. 2014] : a) des fluctuations locales résultant d'une compétition entre le processus de reproduction/mort qui tend à créer des amas et le processus de diffusion qui tend à mixer les particules sur l'ensemble du système en un temps caractéristique τ_D ; b) des fluctuations globales qui mènent finalement l'ensemble de la population à extinction sur un temps caractéristique τ_E (clustering "trivial" et *catastrophe critique*). L'ajout d'un processus de contrôle de la population totale de neutrons (feedback) permet de bloquer ces fluctuations globales et de prévenir ainsi l'extinction du système (et le clustering trivial). On s'intéresse alors aux clusters "stabilisés" (dus aux fluctuations locales uniquement), pour lesquels nous calculons la taille caractéristique. Celle-ci dépend du ratio τ_E/τ_D, c.à.d. de la compétition entre le processus de reproduction/mort qui tend à la réduire, et celui de diffusion qui tend à l'augmenter [de Mulatier et al. 2015].

Dans ce chapitre, nous avons approximé le transport des neutrons par un transport Brownien. En perspective, il pourrait être intéressant de considérer une modélisation plus réaliste du système, notamment l'impact des hétérogénéités ou de la dépendance en énergie, ou encore des neutrons retardés sur le clustering.

PARTIE II – TRANSPORT ANORMAL

Dans cette seconde partie, nous nous intéressons au transport non-exponentiel des neutrons, initialement motivés par le problème du transport dans des milieux fortement hétérogènes et désordonnés, tels que le coeur d'un réacteur à lit de boulets.

Chapitre 4 – Opacité d'un milieu

Certaines des propriétés physiques d'un milieu immergé dans un flot de particules sont étroitement liées à la statistique des trajectories aléatoires effectuées par les particules qui le traversent. Citons par exemple l'opacité d'un milieu, qui peut être définie comme le rapport entre la longueur totale moyenne[3] parcourue par le flot de neutrons au sein du volume et le libre parcourt moyen des neutrons dans le milieu. Plus le flot intéragit avec le milieu, plus ce milieu est considéré comme opaque. La *formule d'opacité*, connue en neutronique, exprime simplement la longueur totale moyenne parcourue par les neutrons comme proportionnelle au ratio du volume V et de la surface S du milieu.

Il s'agit là d'un résultat connu sous le nom de *propriété de Cauchy*, qui est vérifiée pour toute marche aléatoire exponentielle branchante critique : la longueur moyenne $\langle L \rangle$ parcourue par une telle marche au travers d'un domaine de taille finie dépend uniquement des propriétés géométriques du domaine, $\langle L \rangle = \eta_d V/S$, où η_d est une constante dépendant de la dimension. Dans ce chapitre nous montrons que la propriété de Cauchy (et donc la formule d'opacité) reste valide dans le cas d'un transport anormal.

Propriété universelle de marches aléatoires de Pearson en géométrie confinée

En collaboration avec A. Mazzolo, nous avons caractérisé la statistique d'occupation de marches aléatoires branchantes de Pearson en géométrie confinée, pour une loi de sauts quelconque[4] (sous la condition que la loi admette un libre parcours moyen). Nous avons montré que l'ensemble de ces marches vérifient une même propriété, la longueur totale moyenne passée par ces marches dans un domaine de taille fini ne dépend que du ratio du volume sur la surface du domaine, et que cette propriété est en réalité locale [Mazzolo et al. 2014; De Mulatier et al. 2014].

Chapitre 5 – Vols de Lévy asymétriques en présence de bords absorbants (système non confiné)

Dans ce chapitre, nous considérons un marcheur évoluant à une dimension, effectuant des sauts successifs indépendants et identiquement distribués suivant une loi de probabilité asymétrique avec des queues en loi de puissance (vol de Lévy asymétrique). En particulier, nous nous intéressons à la probabilité de survie et à la statistique d'occupation d'un tel marcheur en présence de bords absorbants.

[3] Observables introduites au chapitre 2

[4] y compris en loi de puissance

En l'absence de bords, la fonction de densité de probabilité des positions du marcheur converge, après un grand nombre de sauts, vers une loi asymétrique stable (de Lévy) dont toutes les caractéristiques sont connues grâce au théorème central limite généralisé.

En présence de bords absorbants, ce théorème ne s'applique plus. La fonction de densité de probabilité des positions du marcheur est alors plus complexe à calculer. En collaboration avec G. Schehr, et par la suite P. K. Mohanty, j'ai travaillé sur la détermination des paramètres caractérisant la queue de cette densité de probabilité (c.à.d. loin des bords du système) [De Mulatier et al. 2013]. Nous caractérisons aussi la probabilité de survie du marcheur, par le biais du calcul de son exposant de persistance. Enfin quelques pistes sont explorées quant à la généralisation en dimension supérieure.

CONTENTS

INTRODUCTION

ONE of the key goals of nuclear reactor physics is to determine the distribution of the neutron population within a reactor core. This population indeed fluctuates in space and time due to the stochastic nature of the interactions between the neutrons and the nuclei of the surrounding medium. For most applications in reactor physics though, the neutron population considered is very large. For instance, in standard light-water reactors (LWR) at operating condition, the typical neutron density within the reactor core is about 10^8 neutrons per cubic centimeter. In these cases, all physical observables related to the behaviour of the population, such as the heat production due to fissions, are well characterised by average values, which are governed by the classical linear neutron transport equation, called Boltzmann equation.

However there exist some situations for which a description based on averaged observables provides a misleading characterisation of the behaviour of the neutron population. For example, during the start-up of a LWR, the neutron population is rather small. For such a low-density configuration, numerical investigations, performed with the Monte Carlo TRIPOLI-4 code at the LTSD[5], have highlighted a peculiar behaviour of the neutrons, which spontenously form clusters of highly grouped particles with empty regions in between. This phenomenon, named "neutron clustering" [Dumonteil et al. 2014], results from strong fluctuations in space and time of the population. As a consequence, average quantities become insufficient to characterise the system: neutron clustering can not be explained using the mean-field Boltzmann equation.

These strong fluctuations are in fact intrinsic to the process that govern the neutron transport in the phase space, resulting from the interplay of three fundamental mechanisms: scattering with the nuclei, emission (birth) of several neutrons from the fission of a nucleus, and capture (death) by nuclear absorption. These physical mechanisms confer a random branching structure to the neutron paths; from the point of view of statistical physics,

[5]Laboratoire de Transport Stochastique et Déterministe - CEA

the stochastic process performed by neutrons is a branching random walk, called branching Pearson random walk. Strong fluctuations are in fact typical of branching processes and their analysis will be achieved, in the thesis, by resorting to random walk theory. In particular, I have applied the Feynman-Kac path-integral formalism for branching processes, first to the treatment of fluctuations in the field of nuclear reactor physics, and, then, more precisely, to the study of the clustering phenomenon [Zoia et al. 2014; de Mulatier et al. 2015].

Moreover, another aspect of classical neutron transport theory, is that it relies on the fact that neutrons evolve without memory (Markovian transport process) in a landscape of uncorrelated scattering centres (nuclei). For instance, in an homogeneous medium, the lengths travelled by neutrons between two collisions are exponentially distributed. However, in many important applications, the traversed medium can be highly heterogeneous or disordered (such as in a Pebble-bed reactor, or during the partial meltdown of a reactor core in case of accident), and the hypothesis of uncorrelated scattering centers is deemed to fail. It has been proposed that the transport of particles in such media can be described in terms of non-exponential random walks (anomalous transport).

In the thesis I will tackle this aspect of neutron transport, in the context of another fundamental question in nuclear reactor physics: the occupation statistics of the transported particles within a domain when entering from the outer surface, i.e. the distribution of the travelled length l and the number of collisions n performed by the stochastic process inside the domain. These quantities are directly related to the opacity properties of a body with respect to an incident radiation flow of particles, which are important for a number of applications emerging in radiation shielding and microdosimetry calibration. In this context, the Markovian nature of the transport process leads to remarkably simple Cauchy-like formulas that relate the surface to the volume averages of l and n. However, a key ingredient in such derivation is the hypothesis that the flight lengths are exponentially distributed [Mazzolo et al. 2014]. By resorting to the integral form of the linear transport equations, I have then shown that such formulas strikingly carry over to the much broader class of branching processes with arbitrary jumps, and have thus a universal character. Furthermore this property is, remarkably, a local property of the system [De Mulatier et al. 2014].

During my PhD I have thus been mainly interested in branching random walks and anomalous diffusion in the context of stochastic particle transport (neutrons) in nuclear reactor physics. Using tools from statistical mechanics and transport theory, I tackled several problems of parti-

cle transport that cannot be approached by the usual strategy of applying mean field theory to branching Brownian motion. In particular, my work has been structured along two main axes.

– First, the study of fluctuation statistics: a population of particles that can reproduce or die is naturally subjected to very strong fluctuations, which will be characterised thanks to a Feynman-Kac formalism in Chapter II, and which are responsible for the neutron clustering phenomenon discussed in Chapter III.

– The last two chapters will then focus on the anomalous transport problem: first in the context of the issue of occupation statistics (Chapter IV), finally moving on to the problem of the statistics of asymmetric Lévy flights in the presence of absorbing boundaries [De Mulatier et al. 2013] (Chapter V).

One of the interesting aspects of this thesis is that problems are treated in the presence of boundaries. Indeed, even though real systems are finite (confined geometries), most of previously existing results concern infinite systems. The results presented in this thesis have led to the publication of 6 peer-reviewed articles (cited throughout this introduction), and may apply more broadly to physical and biological systems with diffusion, reproduction and death.

The general context of neutron transport that will be used in the thesis will be now introduced in Chapter I.

CHAPTER I

A Statistical Mechanics Approach to Reactor Physics

One of the central aims of nuclear reactor physics is to characterise the behaviour of a neutron population and to predict its distribution inside a reactor core. This requires accounting for the motion of neutrons and their random interactions with the nuclei of the fuel within the reactor core. We start this chapter by analysing the stochastic behaviour of neutrons in the fuel using tools from statistical physics. We then derive the main equations of the neutron transport theory, which allow to assess the distribution in space, energy and angle of neutrons inside the reactor core.

Contents

We will start this introductory chapter by recalling the general context of neutron transport in the framework of nuclear reactor physics. We will thus introduce fundamental concepts of neutron transport and statistical physics that will be useful for the understanding of the thesis. The ideas discussed in this introduction have been treated at length in several popular reactor physics books cited throughout the chapter. We start the first section (Sec. I.1) by describing the physical processes that govern the transport of neutrons in nuclear reactors, and we analyse their stochastic behaviour in the framework of statistical physics. Then, in the second section (Sec. I.2), we derive the main equations of neutron transport theory, which allow to characterise the distribution of neutrons inside a reactor core. Finally, in section I.3, we discuss some shortcomings of this transport theory that will be illustrated on two examples taken from reactor physics. These examples will show that, in some circumstances, an improved theoretical framework is needed. They will provide the key motivation for the thesis, which will thus be directed at finding new ways of describing the neutron behaviour when usual transport equations do not apply anymore.

1 NEUTRON TRANSPORT IN REACTOR PHYSICS

Similarly to a gas-fired station, a nuclear power plant generates electricity by converting thermal energy to mechanical energy, which is then converted to electricity [Reuss 2012]. In a nuclear reactor, the initial energy (heat source) comes from the fission of heavy nuclei into lighter nuclei inside the reactor core. The heat is then passed (directly or not) to a working fluid (water or gas), which runs through turbines. Figure I.1 illustrates the functioning of a Pressurized Water Reactor (PWR). However the

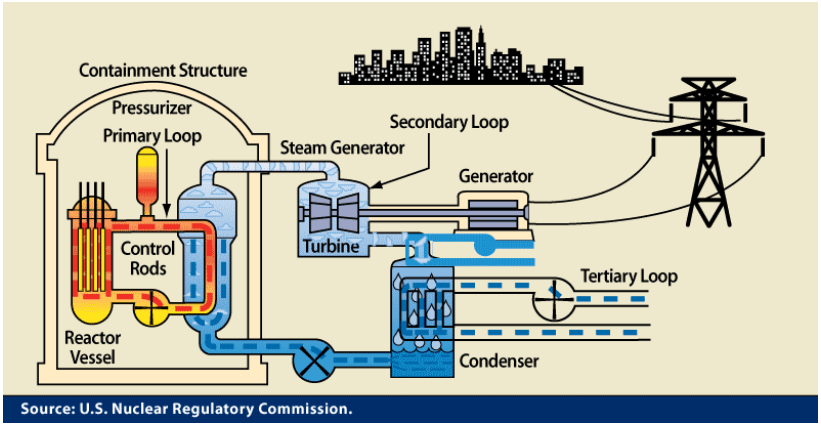

Figure I.1: Conceptual scheme of a Pressurized Water Reactor (PRW).

heavy nuclei used in a nuclear reactor, typically uranium ^{235}U or pluto-

nium ^{239}Pu, rarely undergo spontaneous fission (for instance the ^{235}U has a long half-life of 710 million years [Reuss 2012]). Fissions are in fact mainly induced by neutrons that collide with the nuclei constituting the surrounding medium (fuel). Then, conveniently, the fission of these heavy nuclei produce new neutrons that can thus also collide with other nuclei and start a *nuclear chain reaction* (see Fig. I.2). This type of medium that supports the multiplication of neutrons is called a *multiplying medium* or *fissile material*. For instance, the induced fission of the ^{235}U gives rise to two lighter nuclei, called *fission products*, and to a certain number of new neutrons n. A typical induced fission reaction is [Reuss 2012]:

$$n + {}^{235}\mathrm{U} \rightarrow {}^{92}\mathrm{Kr} + {}^{141}\mathrm{Ba} + 3\,n\,, \tag{I.1}$$

which liberates an energy of $\sim$ 200 MeV[1]. The neutrons released by this reaction are emitted with a high mean energy of approximately 2 MeV. In a PWR, the chain reaction in fact requires neutrons to be slowed down to a *thermal energy* of the order of $\sim$ meV (*slow neutrons*) in order to induce a fission (in heavy water, the thermal energy of neutrons is $\sim$ 25 meV [Bussac and Reuss 1978]); this is not true for a *fast neutron nuclear reactor*.

I.1.1 Neutron as a *Point Particle*

The aim of neutron transport theory is to describe the behaviour of the neutron population inside a nuclear reactor. For this purpose, neutrons are considered as *point particles* evolving within the reactor, where they interact only with the nuclei of the medium. This representation, which could seem too simplified, proves to be appropriate most of the time. In this section we briefly discuss its validity; then, we will assume that this representation holds in the rest of the thesis.

a. No relativistic effects

Neutron energy in a nuclear reactor typically goes up to 20 MeV (see Fig. I.5), i.e. a classical speed

$$v = \sqrt{\frac{2E}{m}} \simeq 1.38 \times 10^4 \sqrt{E\,(\mathrm{eV})}\ \ \mathrm{m/s}\,, \tag{I.2}$$

of the order of $\sim 10^7$ m/s, where $m \simeq 939.565378\ \mathrm{MeV/c^2}$ is the rest mass of the neutron. Indeed, the mean velocity of fast neutrons (released from fission) is more precisely 1.9×10^7 m/s. This order of magnitude of the speed of the fastest neutrons is small enough, compared to the light speed $c \sim 3 \times 10^8$ m/s, to consider that relativistic effects can be reasonably neglected [Schwarz and Schwarz 2004].

[1] This is a huge amount of energy (compare to the amount produce by a gas-fired power station):1 g of ^{235}U could potentially provide 2×10^4 kWh of power, enough to run a 100 W lamp for about 22 years [Schwarz and Schwarz 2004]

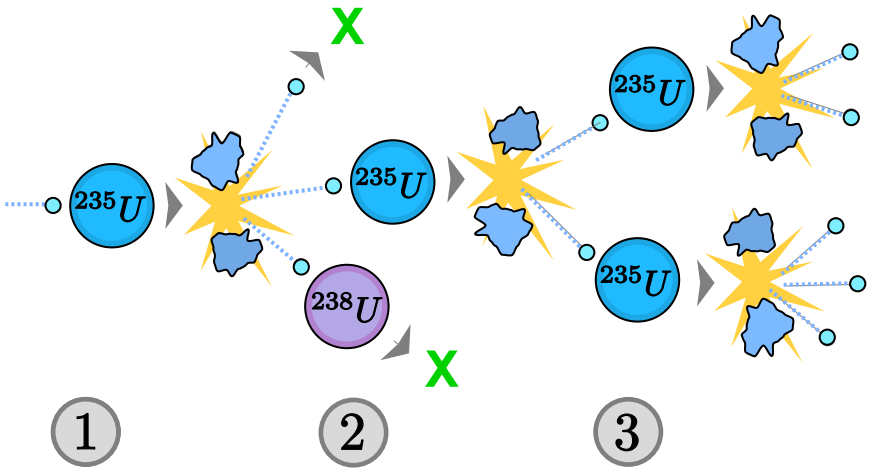

Figure I.2: Scheme of a fission chain reaction, adapted from wikipedia.

1) An first neutron, leaving from a source, is absorbed by a nucleus of Uranium-235, causing its fission into two lighter nuclei and 3 neutrons (second *generation* of neutrons) according to reaction Eq.(I.1). This fission also releases/liberates a binding energy of ~ 200 MeV.

2) Among the 3 neutrons, two are lost for the chain reaction: one is absorbed by a ^{238}U that does not undergo a fission, the other for instance leave the system (absorbed by its boundaries). The last neutron collides with an other ^{235}U, which then divides/splits into two lighter nuclei and gives rise to a third *generation* of neutrons, with 2 neutrons.

3) Each of these 2 neutrons undergoes a collision with a ^{235}U causing their fission into lighter nuclei and a fourth *generation* of neutrons.

The chain reaction is thus maintained until there is not enough heavy nuclei (aging of a reactor) or no neutron anymore (stopping of a reactor) in the system.

b. No interference: particle description

In transport theory, neutrons are considered as particles that can be fully described by their position and their velocity [Bell and Glasstone 1970]. In fact, quantum effects affecting the neutron transport, such as diffraction or interferences, can be neglected if the characteristic length of the medium (inter-nucleus distance ~1Å) is significantly larger than the neutron wave length. De Broglie's wavelength of a neutron [De Broglie 1924], λ_B, is given by the relation:

$$\lambda_B = \frac{h}{p} \simeq \frac{2.86 \times 10^{-11}}{\sqrt{E\,(eV)}}\ m\,, \tag{I.3}$$

where $h \simeq 4.1343359 \times 10^{-15}$ eV·s is the Planck constant and p denotes the momentum of the neutron considered,

$$p = \sqrt{2mE}\,, \tag{I.4}$$

for a non relativistic particle. $m \simeq 939.565378$ MeV/c^2 is the rest mass of the neutron and E its energy. In a nuclear reactor, *fast neutrons* emitted from a fission have an energy of several MeV, for which $\lambda_B \sim 10^{-14}$ m, i.e. several orders of magnitude smaller than the characteristic distance between nuclei $\sim 10^{-10}$ m.

Moreover, Heisenberg's uncertainty principle [Heisenberg 1930] states a condition on the precision that can be accessed for the position and the momentum of a particle, formulated by [Kennard 1927]:

$$\Delta x \Delta p \geqslant \frac{\hbar}{2}\,, \tag{I.5}$$

where Δx and Δp are respectively the standard deviation of the position and the momentum of the particle, and $\hbar = h/(2\pi)$ is the reduced Planck constant. Inside a reactor core (in most materials), neutrons have a mean free path (between two collisions with nuclei) of the order of a centimeter [Reuss 2012]. For this reason, we could considered for instance that an uncertainty of 10^{-4} cm on the position of a neutron can be tolerated. Thus, using Eq. (I.4) in the relation Eq. (I.5), we find that the minimum uncertainty accessible on the energy ΔE of the particle would be [Bell and Glasstone 1970]

$$\Delta E\,(eV) \sim 10^{-5}\sqrt{E\,(eV)}\,, \tag{I.6}$$

which is negligible compare to the energy E itself. The position and the energy (or speed) of a neutron in neutron transport theory can thus be considered with a good precision without violating Heisenberg's uncertainty

principle. As a consequence, it is reasonable to consider neutrons as particles (as opposed to waves) that can be characterised by their position and velocity.

Interference effects can be relevant for a tiny fraction of neutrons with very low energy (down to several meV). The wave length becomes in this case very large ($\lambda_B \sim 10^{-10}$ - 10^{-9} m) and neutrons can not be localized. Because of the negligible number of neutrons concerned, this effect is usually reasonably neglected in neutron transport theory [Bell and Glasstone 1970].

Note that in reactor physics, distances are often measured in centimeters, as a reference to the centimeter mean free path of neutrons [Reuss 2012].

c. Neutrons interact only with the nuclei of the medium

Neutron-neutron interactions are neglected [Rozon 1998]. Indeed the probability of such an interaction is negligible compared to the probability of a neutron-nucleus interaction, due to the huge difference in density: even in a thermal reactor, operating at high neutron flux, the neutron density is still less than 10^{11} neutrons per cm^3, whereas the nuclei density is of the order of 10^{22} nuclei per cm^3 [Bell and Glasstone 1970].

As a consequence of paragraph *b.* and *c.*, the spatial extension of neutrons is not relevant for the problem of their transport through matter. For these reasons, they can be considered as *point particles* (i.e. 0-dimensional particles), and the neutron population can be thought of as an *ideal gas* (defined as a gas of particles that do not interact which each other).

d. Neutron radioactive instability is neglected

Outside a nucleus, a free neutron is unstable and can decay into a proton (beta decay):

$$n \longrightarrow p^+ + e^- + \bar{\nu}_e \,,$$

where p^+, e^- and $\bar{\nu}_e$ respectively denotes the proton, the electron and the electron antineutrino. Within this decay, neutrons have a life time of about 15 min [Yue et al. 2013][2], which is very large compared to the millisecond characteristic life time of a neutron within a nuclear reactor [Bussac and Reuss 1978]. The probability that a free neutron actually undergoes a beta decay in a nuclear reactor before encountering a nucleus is thus very small and this effect is as a consequence neglected.

[2] more precisely, a life time of 887.7 ± 1.2[stat]± 1.9[syst] s was recently measured by [Yue et al. 2013]

e. Other hypotheses

Very frequently, two other hypotheses are made in neutron transport theory: that the fluctuations of the neutron population can be neglected [Bell and Glasstone 1970], and that the displacements performed by neutrons inside a nuclear reactor belong to a class of processes called *exponential displacements* (described in the next section). The discussion of these two last hypotheses will be at the heart of this thesis.

I.1.2 From Neutron Transport in Multiplying Media to Branching Exponential Flights

In this section, we recall the processes that govern neutron transport in (locally homogeneous) multiplying media. We will see that this transport can be described in terms of a specific type of random walks, called *branching exponential flights*.

a. Transport - Exponential Random Walks

Consider a single neutron[3] flowing through and interacting with a background material. Based on the previous considerations, this neutron undergoes a sequence of displacements, separated by collisions with the nuclei of the surrounding medium. We also assume that, between two collisions, no forces act upon the particle, such that its momentum is preserved along each of its displacements (free displacements): between collisions, the neutron therefore travels in a straight line and with a constant speed [Pomraning 1991]. Consider now that the neutron leaves a collision at a time t_0 from a position $\mathbf{r}_0$ with a speed v_0 in a direction $\boldsymbol{\omega}_0$: its path from $\mathbf{r}_0$ to the next collision then follows the trajectory

$$\begin{cases} \mathbf{r}' &= \mathbf{r}_0 + s' \, \boldsymbol{\omega}_0 \, , \\ t' &= t_0 + \dfrac{s'}{v_0} \, . \end{cases} \tag{I.7}$$

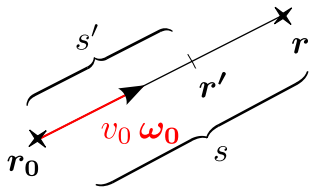

The curvilinear coordinate s' parametrises the rectilinear trajectory, varying from 0 at the initial point $\mathbf{r}_0$, to s at the next collision (s thus corresponds to the distance travelled between the two collisions). Due to the quantum nature of the neutron-nucleus interaction and to the huge number of nuclei inside the reactor core, the exact position $\mathbf{r}$ of this collision can not be assessed deterministically. In fact, as the neutron travels through the fissile

[3] Even though our work mostly focuses on neutron transport, most of the results presented throughout the thesis also apply, with minor modifications, to other "neutral particles", i.e. particles which do not interact with matter until they undergo a collision with the traversed medium, such as photons in the classical limit [Kalos and Whitlock 2008].

material it has, at anytime, a certain probability to interact with a nucleus that depends only on the local properties of the surrounding medium. It is thus reasonable to assume that a neutron evolves in the medium with *no memory* of its past history [Pomraning 1991]. This property of the neutron transport is said *Markovian*[4]. As a consequence, the probability that a neutron interacts with the surrounding medium while travelling a small distance ds' about s' is proportional to the distance travelled ds' (and independent on the length already travelled) and given by

$$\text{Probability of interaction} \qquad \Sigma(\mathbf{r}', v_0)\, ds' . \tag{I.8}$$

The proportionality constant Σ depends only on the local properties of the medium in the phase space position[5] $(\mathbf{r}', v_0)$. The dependence in the direction of travel ω_0 of the particle is omitted, as the medium is generally assumed to be isotropic. In transport theory, the quantity Σ is called [Pomraning 1991]

$$\textit{Total cross section}\ (\mathrm{cm}^{-1}) \qquad \Sigma(\mathbf{r}, v_0)\,; \tag{I.9}$$

it is the probability of interaction per unit length. Note that this cross section is a *macroscopic cross section*[6]. As a result of Eq. (I.8), the distance s travelled by a neutron between two collisions, along the trajectory Eq. (I.7), is given by the *probability density function (pdf)* $T(s)$ [Kalos and Whitlock 2008; Hughes 1996; Weiss 2005]:

Intercollision distances for a non-homogeneous Poisson process

$$T(s) = \Sigma(s)\, \exp\left[-\int_0^s \Sigma(s')\, ds'\right] \qquad \text{for } s > 0\,. \tag{I.10}$$

In this equation, the parameter s' contains the information about the local position $r'(s')$ of the particle, given by Eq. (I.7).

Here, scattering centres encountered by neutrons along their trajectory are

[4] In a Monte Carlo simulation for example this property implies that the neutron can be stopped at any moment and then restarted without taking into account what happened before it was stopped: the knowledge of the current phase-space position of the walker $(\mathbf{r}, \mathbf{v})$ is sufficient to determine its future evolution. Note that the knowledge of the current position only is not sufficient to ensure the Markovianity, as it would be instead the case for a Brownian particle [Chung 2013].

[5] We consider that the density of nuclei (scattering centres) is high enough that the multiplying medium can be described as a continuous medium, characterised by cross-section that is homogeneous at the scale of a volume element $d\mathbf{r}$ (*locally homogeneous*).

[6] Various types of collisions can happen in the medium. The macroscopic cross section for a collision type i, $\Sigma_i(\mathbf{r}, v_0)$, is given by the density of nuclei in the vicinity of $\mathbf{r}$ multiplied by the *microscopic cross section* of the nuclei $\sigma_i(v_0)$ (cm^2 or barns) for this type of collisions: $\Sigma_i(\mathbf{r}, v_0) = n(\mathbf{r})\sigma_i(v_0)$ [Reuss 2012]. The total macroscopic total cross section is then $\Sigma_t = \sum_i \Sigma_i$.

non necessarily uniformly distributed, and the process performed by neutrons while travelling (jumps separated by collisions given by $\Sigma(s)$) is called *non-homogeneous Poisson process*[7] [Ross 2013]. In Eq. (I.10), the second factor, $\exp\left[-\int_0^s \Sigma(s')\,ds'\right]$, is the marginal probability that the path gets as far as s (without collisions in the meanwhile), whereas the first factor $\Sigma(s)$ corresponds to the conditional probability, $\Sigma(s)ds$, that the collision occurs in ds about s. In analogy with optics, the exponent $\int_0^s \Sigma(s')\,ds'$ is often called *optical path length* [Bell and Glasstone 1970]. In homogeneous media, for which the cross-section Σ is constant, this exponent reduces to $s\,\Sigma$, and the jumps pdf becomes independent of the local position of the particle, taking simply the exponential form:

Intercollision distances for a homogeneous Poisson process

Exponential Distribution $$T(s) = \Sigma\,\exp\left[-\Sigma\,s\right]\ . \qquad \text{(I.11)}$$

In this case, the scattering centres encountered by the neutrons are uniformly distributed in space ($\Sigma = \text{cst}$), and the collision process followed by neutrons is called *homogeneous Poisson process*.

Proof

To demonstrate Eq. (I.10), we refer to Kalos and Whitlock's book on *Monte Carlo methods* [2008, sec. 6.3]. By definition the pdf T must be normalised on positive values, and can thus be associated to a

cumulative distribution $$\int_0^s T(s')\,ds' = 1 - U(s)\ . \qquad \text{(I.12)}$$

Its complement $U(s) = \int_s^{+\infty} T(s')\,ds'$ is the marginal probability that the next collision is at a distance s' larger than s. It can be decomposed into the sum of two probabilities:

$$U(s) = U(s+ds) + P(s \leqslant s' < s+ds), \qquad \text{for } ds > 0\ , \quad \text{(I.13)}$$

the probability that the collision occurs after $s+ds$, and the probability $P(s \leqslant s' < s+ds)$ that it occurs between s and $s+ds$. This latter probability can be rewritten using Bayes' formula[a] for conditional probabilities:

$$P(s \leqslant s' < s+ds) = U(s)\,P(s \leqslant s' < s+ds \,|\, s' \geqslant s)\,. \qquad \text{(I.14)}$$

[7] Along the trajectory, the number of nuclei distributed along the interval $(s, s+s_1)$ is a random variable that follows a Poisson law ([Poisson and Schnuse 1841]) with a mean $\int_s^{s+s_1} \Sigma(s')\,ds'$ [Ross 2013].

This latter conditional probability is the probability that a collision occurs between s and $s + ds$ for a process starting from s; for small ds it can thus be easily expanded using equation (I.8): $P(s \leqslant s' < s + ds \,|\, s' \geqslant s) = \Sigma(s)\, ds + o(ds)$. Replacing these results in equation (I.13) in the limit where ds goes to 0 leads to a first order differential equation verified by U:

$$-U'(s) = U(s)\,\Sigma(s) + o(1)\,, \tag{I.15}$$

whose solution is:

$$U(s) = \exp\left[-\int_0^s \Sigma(s')\, ds'\right]\,, \tag{I.16}$$

knowing that $U(0) = \int_0^{+\infty} T(s)\, ds = 1$ by normalisation of the pdf T. The result Eq. (I.10) then stems from the definition of the complementary cumulative: $T(s) = -U'(s)$.

[a] Bayes' formula for two propositions A and B: $P(A \mid B) = \dfrac{P(A \cap B)}{P(B)}$

Note that the jump pdf Eq. (I.10) commonly takes an other form, where the current position and speed of the particle are clearly specified [Spanier and Gelbard 1969; Lux and Koblinger 1991]:

Intercollision Length Probability Density Function

$$T(s|\mathbf{r}, \boldsymbol{\omega}_0, v_0) = \Sigma(\mathbf{r},\, v_0)\, \exp\left[-\int_0^s \Sigma(\mathbf{r} - s'\,\boldsymbol{\omega}_0,\, v_0)\, ds'\right]\,, \tag{I.17}$$

is the pdf of the jump length s performed by a particle arriving at a collision in $\mathbf{r}$ with a velocity $v_0\,\boldsymbol{\omega}_0$ (see Eq. (I.7)). This expression of the jump pdf is widely used in reactor physics. Observe that this pdf is not a density of the three space dimensions, but only of one, corresponding to the travelled length s. In the same way, we can also rewrite the marginal probability Eq. (I.16),

$$U(s|\mathbf{r}, \boldsymbol{\omega}_0, v_0) = \exp\left[-\int_0^s \Sigma(\mathbf{r} - s'\,\boldsymbol{\omega}_0,\, v_0)\, ds'\right]\,, \tag{I.18}$$

being the probability that a particle arriving in $\mathbf{r}$ has travelled a distance s with a constant velocity $v_0\,\boldsymbol{\omega}_0$ without encountering any collision.

Following this process of random jumps separated by collisions, the path performed by a neutron is thus random, called *random walk*, or, more precisely, *exponential walk* in the case of an homogeneous medium. For numerical simulation purposes, the sampling of a random variable from an

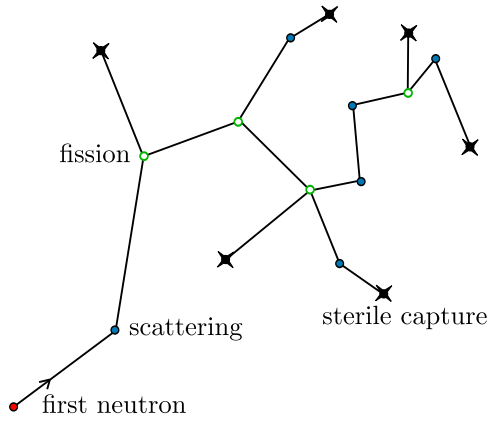

Figure I.3: Schematic representation of one initial neutron and its descendants. Neutron-nucleus interactions are commonly grouped in three main types: *scattering* (blue dots), *fission* (green circles), and *sterile capture* (black stars). These events confer a branching structure to the neutron path.

exponential distribution Eq. (I.11) is illustrated in appendix 4.

b. Collision - Branching process

Neutron-nucleus interactions are very complex, in that they are governed by quantum physics and involve the strong nuclear interaction. However, they can be conceptually grouped in three main types [Reuss 2012]: sterile capture, scattering or fission (see Fig. I.3). In the following, each of these events will be briefly recalled, and their physical meaning will be related to the corresponding statistical physics interpretation. In doing so, we will introduce the notation commonly used in reactor physics.

Capture events occur with a probability $p_c(\mathbf{r}, v)$ for particles arriving at a collision about $\mathbf{r}$ with a speed v: the incoming particle disappears, absorbed by a nucleus, and its branch of the walk ends (see Fig. I.4). In reactor physics, this event corresponds to a *sterile capture* (absorption that does not cause fission) and is associated with the macroscopic *capture cross section*:

capture cross section
$$\Sigma_c(\mathbf{r}, v) = p_c(\mathbf{r}, v)\, \Sigma(\mathbf{r}, v)\,. \tag{I.19}$$

where $\Sigma(\mathbf{r}, v)$ is the *total cross section* defined in Eq. (I.9). According to its definition above, $\Sigma_c(\mathbf{r}, v)$ is the rate at which absorption events occur. As for the total cross section, this quantity is known to depend on the position $\mathbf{r}$ and the speed v of the considered particle.

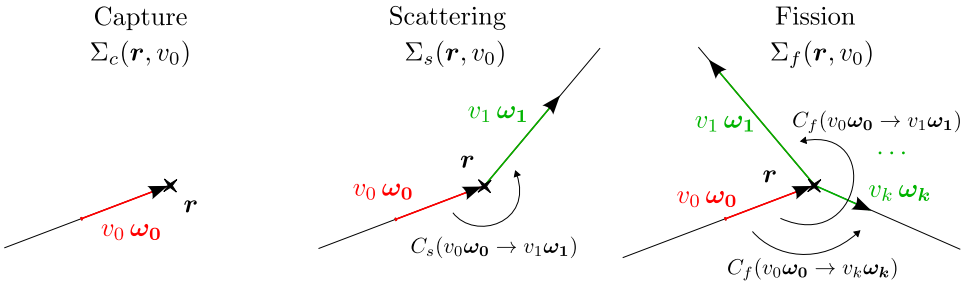

Figure I.4: Neutron-nucleus interactions can be conceptually grouped in three main types:
- *Sterile capture*: the incoming neutron is absorbed;
- *Scattering*: the speed and the direction of the neutron change, from $v_0\,\boldsymbol{\omega}_0$ to $v_1\,\boldsymbol{\omega}_1$;
- *Fission*: the incoming neutron is absorbed, k new neutrons are emitted with new speeds $v_{1..k}$ and directions $\boldsymbol{\omega}_{1..k}$.

Scattering events occur with a probability $p_s(\mathbf{r}, v)$, whereupon the velocity (direction and speed) of the walker is redistributed at random, following the probability density function $C_s(\mathbf{v} \to \mathbf{v}'|\mathbf{r})$ (see Fig. I.4), called *scattering kernel*. This scattering *kernel* is in general speed dependent and anisotropic (more precisely it depends on the angle θ between the incoming and the outgoing directions: $\boldsymbol{\omega} \cdot \boldsymbol{\omega}' = \cos(\theta)$). This type of event is related to the macroscopic

scattering cross section
$$\Sigma_s(\mathbf{r}, v) = p_s(\mathbf{r}, v)\,\Sigma(\mathbf{r}, v)\,. \tag{I.20}$$

Fission events give rise to two different types of neutrons, the *prompt neutrons*, emitted instantaneously[8] after the fission event, and the *delayed neutrons*, emitted from a few milliseconds to a few minutes later. As prompt neutrons represent more than 99% of the emitted neutrons, we will first focus on them, without taking into account delayed neutrons. We will then see in Sec. I.2.2 how the existence of delayed neutrons modifies the dynamics of the neutron population. At a collision, a *fertile capture* (fission, see Fig. I.4) occurs with a probability $p_f(\mathbf{r}, v)$: the incoming neutron is absorbed and k new neutrons are emitted with respective probabilities p_k in a new direction $\boldsymbol{\omega}'$ with a new velocity v' given by the probability density $C_f(\mathbf{v} \to \mathbf{v}'|\mathbf{r})$. Generally, new directions $\boldsymbol{\omega}'$ are isotropically distributed and the pdf $C_f(\mathbf{v} \to \mathbf{v}'|\mathbf{r})$ depends only weakly on the incoming velocity $\mathbf{v}$:

$$C_f(\mathbf{v} \to \mathbf{v}'|\mathbf{r}) = \frac{1}{4\pi} F_p(v')\,, \tag{I.21}$$

where $F_p(v')$ is the speed spectrum of prompt fission neutrons, called *average*

[8] within 10^{-13} to 10^{-14}s after the fission event

Average Prompt Fission Neutron Spectrum

The kinetic energy of an outcoming fission neutron is distributed over several decades, from fractions of meV to about 10 MeV. In 1960, Terrell [1957] proposes two approaches to model the prompt fission neutron spectrum: the Maxwellian and the Watt-Cranberg spectrum representations. Most modern assessments of prompt fission neutrons rely on a model developed by Madland and Nix [1982] in the 80s.

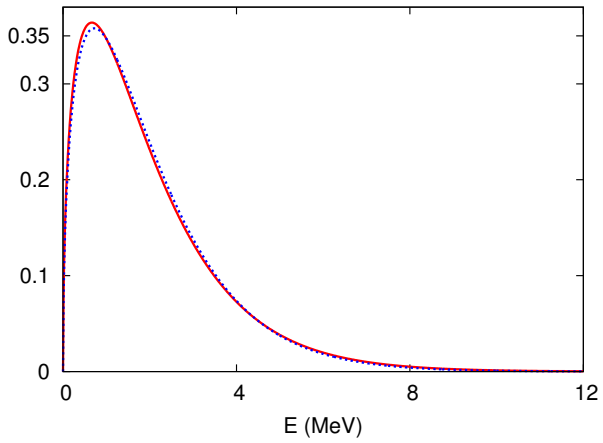

Figure I.5: Maxwell (in red) and Watt (dash curve) spectrum for Uranium. Parameters are optimally adjusted to the experimental spectrum for each fissioning system at a given excitation energy [Antoni and Bourgois 2013]. For Uranium, the mean energy of a prompt neutron is about 2 MeV.

prompt fission neutron spectrum (see Fig. I.5). The normalisation factor $4\pi = \Omega_3$ is the maximum solid angle in a 3-dimensional space:

$$\Omega_3 = \iint_{Sp_3} d^2\boldsymbol{\omega} = 4\pi\,, \tag{I.22}$$

which corresponds to the surface of the 3-dimensional unit sphere Sp_3. $d^2\boldsymbol{\omega}/(4\pi)$ is the probability for a neutron to be emitted in the solid angle element $d^2\boldsymbol{\omega}$ about the direction $\boldsymbol{\omega}$ (isotropic distribution of the outgoing directions). By definition, the probability family $\{p_k\}_{k\geqslant 0}$ verifies the normalisation

$$\sum_{k\geqslant 0} p_k \;=\; 1\,. \tag{I.23}$$

In principle the number k of emitted neutrons after a fission could vary from 0 to $+\infty$, but in practice k only varies from 0 to 7 [Reuss 2012]. The

mean number of neutrons produced per fission,

$$\nu = \sum_{k \geqslant 0} k\, p_k \,, \tag{I.24}$$

is a relevant parameter to characterise the production of neutrons. The occurrence of fission events is defined in terms of the macroscopic

fission cross section $$\Sigma_f(\mathbf{r}, v) = p_f(\mathbf{r}, v)\, \Sigma(\mathbf{r}, v) \,. \tag{I.25}$$

The three events The probability of occurrence of each of these three events is normalised, $p_c + p_s + p_f = 1$, so that the cross sections similarly add up to

$$\Sigma(\mathbf{r}, v) = \Sigma_c(\mathbf{r}, v) + \Sigma_s(\mathbf{r}, v) + \Sigma_f(\mathbf{r}, v) \,, \tag{I.26}$$

where the three types of event composing the *total cross section* appear clearly.

Therefore, submitted to these three types of collisions, each neutron of the population can, at any moment, die by *absorption* or give birth to other neutrons by *fission*. Each neutron has thus *descendants* (except for the ones that die) and an *ancestry* (except for the ones emitted from a source). In this sense, the dynamics of reproduction and death of neutrons in the population is similar to the one of families, which was first studied by Bienaymé (1845) [Heyde and Seneta 1977] and by Galton and Watson [Watson and Galton 1875] on their investigation of the extinction of family names. The process of reproduction and death is known as *Galton-Watson process* or *branching process* [Harris 1963], in reference to the branching structure that it confers to the family (like a family tree - see Fig. I.3). Depending on the value of ν, defined in Eq. (I.24), the process is then said to be [Harris 1963]:

subcritical	$\nu < 1$;	
critical	$\nu = 1$;	(I.27)
or *supercritical*	$\nu > 1$.	

Note that, in reactor physics, the dynamics of a neutron family can thus be followed in time, but also in *generation* (see Fig. I.2): neutrons leaving from a source are considered as the first generation of neutrons; then at each event (scattering or fission) a neutron leaving a collision belongs to the generation after that of the one entering the collision.

Monte Carlo Numerical Simulations for Neutron Transport

The different processes we have seen in this section are at the basis of Monte Carlo simulations developed for the transport of neutrons in a multiplying medium [Spanier and Gelbard 2008]. Indeed this type of simulation involves following the trajectory of each particle within the medium from its source to the end of its history (by absorption or exit of the medium) [CEA monographie 2013]. Along this trajectory, one or several physical observables (random variables) are recorded, such as the total length travelled inside a certain region of the medium, or the total number of collisions performed in this region. Simulations of the full history of the system are performed a large number of times, in order to obtain the mean of each observable over the various realisations of the system. These averaged values are called *estimators*, and will be seen more in detail in Chapter 2. Monte Carlo methods are not limited to neutron transport, and have many applications involving stochastic processes in physics, life sciences and finance [Gobet 2013; Krauth 2006].

c. Generalised process and unified notation for branching random walk

The mechanisms governing neutron behaviour in *multiplying media* confer a random branching structure to the neutron paths, with random displacements, death and reproduction events. Neutrons inside the reactor core thus perform random walks with a branching structure, known as *branching random walk* in statistical physics[9]. Besides, since the length of the displacements are exponentially distributed (if the medium is homogeneous), such random walks are called *branching exponential walks*.

However, the complexity of the reactor physics formalism and notation, with different type of collisions (various cross sections $\Sigma_{c/s/f}$ and probability density functions $C_{c/s/f}$), may hinder the statistical analysis of some of the key physical mechanisms of the neutron transport. For the sake of simplicity, we consider the general branching random walk process with only one type of collision (see Fig. I.6), upon which the incoming particle disappears, and k new particles are emitted with a probability $p_k(\mathbf{r}, v)$. The velocities $\mathbf{v}'$ of the new particles are then redistributed, following a single probability density function $C(\mathbf{v} \to \mathbf{v}'|\mathbf{r})$. Each descendant will then behave as the mother particle, undergoing a new sequence of displacements and collisions, giving thus rise to a branched structure. It is finally possible, for

[9] In particular, when $p_k = \delta_{k,1}$ (i.e. without branching), the walk described in the current section, with random jumps separated by random reorientation of the walker, is known as *Pearson random walk* [Hughes 1996; Weiss 2005].

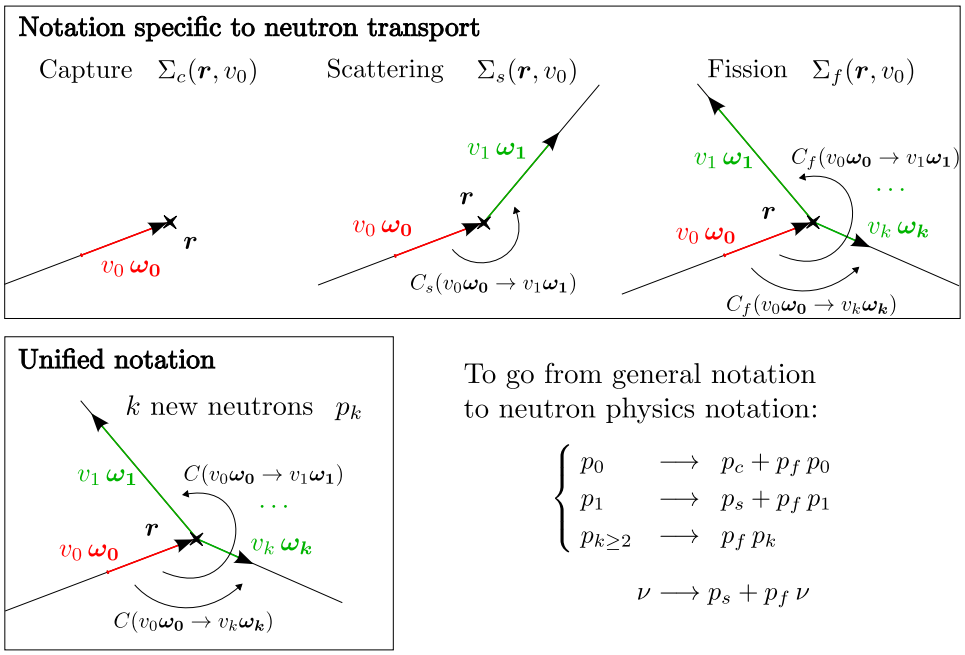

Figure I.6: Conceptual representation of the three groups of collisions in nuclear reactor physics with its specific notation, and of the generalised branching process with a unified notation.

practical applications, to replace the general notation by the one specific to reactor physics, using the transformation (see Fig. I.6):

From unified notation to reactor physics notation

$$\nu\,\Sigma(\mathbf{r}, v)\,C(\mathbf{v} \to \mathbf{v}'\,|\,\mathbf{r})$$

$$\downarrow \tag{I.28}$$

$$\Sigma_s(\mathbf{r}, v)\,C_s(\mathbf{v} \to \mathbf{v}'\,|\,\mathbf{r}) + \nu\,\Sigma_f(\mathbf{r}, v)\,C_f(\mathbf{v} \to \mathbf{v}'\,|\,\mathbf{r})$$

Results specific to nuclear reactor physics will then be identified by a yellow bar on the left margin of the text, as it is on Eq. (I.28).

I.1.3 Characterisation of the neutron population: phase space densities

Neutron transport in nuclear reactors is intrinsically stochastic, due to the random nature of the different physical phenomena (random collisions and changes of velocity) that govern the neutron behaviour. As a consequence neutron transport problem must be handled within the framework of a sta-

tistical description. In order to fully characterise the neutron dynamics in the phase space, each neutron requires six variables at any time t or current generation i of the particle:

- the three spatial coordinates $\mathbf{r}$;
- the three velocity coordinates $\mathbf{v}$, which contain information about the speed v (or any related variable such as the kinetic energy E) and the direction $\boldsymbol{\omega}$ of the particle.

Although the neutron population is very diluted compared to the population of nuclei, it is still very large $\sim 10^8$ neutrons/cm^3 in a power reactor [Duderstadt and Hamilton 1976]. As consequence, the statistical analysis of all the individual positions can be, most the time, replaced by a mean analysis using the concept of *expected densities*[10] in the phase space [Duderstadt and Hamilton 1976]. For this purpose, we replace the microscopic description of each neutron by a description at a mesoscopic scale, assuming that the neutron density is *locally homogeneous*: homogeneous over any volume element $d\tau = d\mathbf{r}\, d\mathbf{v}$ of the phase space.

We are thus interested in densities in the phase space: spatial and angular densities with respect to the six variables, $\mathbf{r}, \mathbf{v}$. The dependence on time or generation will be denoted with a small index, or a seventh variable, t or i, which will stand for distinguishing out of equilibrium cases from stationary cases.

Speed and Kinetic Energy

In transport theory it is convenient to use the kinetic energy E and the direction $\boldsymbol{\omega}$ of the particle, rather than the three momentum or velocity variables $\mathbf{v} = v\,\boldsymbol{\omega}$, for easier reference and comparison with experimental data [Pomraning 1991]. In the following, however, we will keep the notation with the velocity for the sake of simplicity. Note that these two notations are perfectly equivalent, as E and v are related by the classical mechanics relation $E = m\,v^2/2$. Thus, any density function p can be written in term of the variable v or E, using the identity:

$$p(v)dv = p(E)dE\,, \tag{I.29}$$

where the relation between dv and dE is then given by

$$dE = m\,v\,dv \qquad \text{or} \qquad dv = dE/\sqrt{2\,m\,E}\,. \tag{I.30}$$

[10] This idea and its limits will be discuss at the end of this chapter, section I.3.1.

a. Particle Density ($\sim 10^8$ *n.cm*$^{-3}$ *in a power reactor) [Duderstadt and Hamilton 1976]*

For instance, let us first start with a central quantity, the

Particle angular density (n.cm^{-3}.sr^{-1}.MeV^{-1}) $\qquad n(\mathbf{r}, \mathbf{v}, t)$. (I.31)

As a density in the phase space, $n(\mathbf{r}, v, \boldsymbol{\omega}, t)\, d^3\mathbf{r}\, dv\, d^2\boldsymbol{\omega}$ corresponds, at a certain time t, to the mean number of particles

- located in a small volume $d^3\mathbf{r}$ about $\mathbf{r}$,
- whose speed is between v and $v + dv$,
- and which travel in a direction given by the solid angle $d^2\boldsymbol{\omega}$ about $\boldsymbol{\omega}$ [Bell and Glasstone 1970].

The integration of this particle angular density over all possible directions, leads to the *particle density* (n.cm^{-3}.MeV^{-1}):

$$\textit{particle density} \qquad n(\mathbf{r}, v, t) = \iint_{\Omega_3} d^2\boldsymbol{\omega}\; n(\mathbf{r}, \boldsymbol{\omega}, v, t) \; . \tag{I.32}$$

This quantity gives the distribution in space and energy (speed) of neutrons in the system at any time. The ensemble of the possible directions is given by the solid angle $\Omega_3 = 4\pi$ defined in Eq. (I.22). The *neutron density* captures most of the information needed to describe the statistical behaviour of the neutron population inside nuclear reactors. In fact, this quantity lies at the heart of two other physical observables that are more commonly used in reactor physics: the *neutron flux* and the *reaction rate* [Bell and Glasstone 1970].

b. Collision Rate Density, or Reaction Rate Density

The neutron density allows us to compute the rate at which neutron-matter interactions occur at any position in the reactor [Reuss 2012; Bell and Glasstone 1970]. Between two collisions, a neutron keeps a constant velocity $v\,\boldsymbol{\omega}$. During a time interval dt, it thus travels a straight path of length $v\,dt$, and therefore has the probability $\Sigma(\mathbf{r}, v)\, v\, dt$ to interact with the surrounding medium about $\mathbf{r}$. Multiplying this probability by $n(\mathbf{r}, \mathbf{v}, t)\, d^3\mathbf{r}\, d^3\mathbf{v}$ (the mean number of neutrons in the vicinity of $\mathbf{r}$ with a velocity $\mathbf{v}$) leads to the mean number of collisions that occur during dt in the volume element $d^3\mathbf{r}\, d^3\mathbf{v}$ of the phase space, and thus to define the

$$\textit{Collision rate angular density} \qquad \psi(\mathbf{r}, \boldsymbol{\omega}, v, t) \doteq n(\mathbf{r}, \boldsymbol{\omega}, v, t)\, \Sigma(\mathbf{r}, v)\, v \; , \tag{I.33}$$

(collisions cm^{-3}.MeV^{-1}.sr^{-1}.s^{-1}). In other terms, $\psi(\mathbf{r}, v, \boldsymbol{\omega}, t)\, d^3\mathbf{r}\, d^3\mathbf{v}$ is the rate at which collisions happened in the vicinity of the phase space position

$(\mathbf{r}, \mathbf{v})$ at time t. Integrating the angular density ψ over all possible directions for $\boldsymbol{\omega}$, gives the *collision rate density* (collisions $\mathrm{cm}^{-3}.\mathrm{MeV}^{-1}.\mathrm{s}^{-1}$):

Collision rate density
$$\Psi(\mathbf{r}, v, t) \doteq \iint_{\Omega_3} d^2\boldsymbol{\omega}\, \psi(\mathbf{r}, \boldsymbol{\omega}, v, t) = n(\mathbf{r}, v, t)\, \Sigma(\mathbf{r}, v, t)\, v \,. \tag{I.34}$$

In practice it can be useful to distinguish the different types of *reaction* (collision) by decomposing Σ into the different partial macroscopic cross-sections Σ_r (the index r standing for c, s or f), so that we get a *reaction rate density* for each type of reaction: absorption, scattering and fission.

c. Neutron Flux *($\sim 10^{13}$ $n.cm^{-2}.s^{-1}$ in a PWR)*

The product $n\,v$ appearing in Eq. (I.33) and (I.34) occurs very often in reactor theory, such that it is given a special name, the "*neutron flux*". Then, as for the neutron density, it is possible to define a density in the phase space, the neutron *angular flux* ($\mathrm{n.cm}^{-2}.\mathrm{MeV}^{-1}.\mathrm{sr}^{-1}.\mathrm{s}^{-1}$):

Angular flux
$$\varphi(\mathbf{r}, \boldsymbol{\omega}, v, t) \doteq v\, n(\mathbf{r}, \boldsymbol{\omega}, v, t) \,, \tag{I.35}$$

and a density in the simple space, called the *scalar flux* ($\mathrm{n.cm}^{-2}.\mathrm{MeV}^{-1}.\mathrm{s}^{-1}$) [Bell and Glasstone 1970]:

Scalar flux
$$\phi(\mathbf{r}, v, t) \doteq v\, n(\mathbf{r}, v, t) = \iint_{\Omega_3} d^2\boldsymbol{\omega}\, \varphi(\mathbf{r}, \boldsymbol{\omega}, v, t) \,. \tag{I.36}$$

The expression "*Neutron Flux*" is very specific to the field of reactor physics. Indeed this quantity does not match the usual definition of a particle flux in physics, but correspond to the magnitude of the particle current density $n\,\mathbf{v}$.

d. Current Density

The neutron *angular current density*, also called *vector flux* (as it is the vector version of the *neutron flux*), is the particle current density:

Angular current density
$$\mathbf{j}(\mathbf{r}, \boldsymbol{\omega}, v) \doteq \mathbf{v}\, n(\mathbf{r}, \boldsymbol{\omega}, v, t) = \varphi(\mathbf{r}, \boldsymbol{\omega}, v, t)\, \boldsymbol{\omega} \,. \tag{I.37}$$

In the case of a monokinetic theory, $\mathbf{j}(\mathbf{r}, v, \boldsymbol{\omega}, t) = \mathbf{j}(\mathbf{r}, \boldsymbol{\omega}, t)\, \delta(v)$, it is very common to introduce the current density $\mathbf{J}(\mathbf{r}, t)$ (a space density only)

Current density
$$\mathbf{J}(\mathbf{r}, t) \doteq \iint_{\Omega_3} d^2\boldsymbol{\omega}\, \mathbf{j}(\mathbf{r}, \boldsymbol{\omega}, t) \,, \tag{I.38}$$

whose direction gives the mean direction of the neutrons within the volume element $d^3\mathbf{r}$ about $\mathbf{r}$ (unit: $\mathrm{n.cm}^{-2}.\mathrm{s}^{-1}$).

To proceed further, we will now derive the evolution equation for the phase space neutron density $n(\mathbf{r}, \mathbf{v}, t)$, which takes the name of *linear transport equation*, or *linear Boltzmann equation*. The different problems that will be tackled in the thesis will then emerge from a discussion of the limits of this equation.

2 BOLTZMANN EQUATION FOR NEUTRON TRANSPORT

The behaviour of a nuclear reactor is governed by the distribution in the phase space of the neutron population, $n(\mathbf{r}, \mathbf{v}, t)$. In theory this distribution can be predicted by solving the associated transport equation, which describes the equilibrium or out of equilibrium behaviour of the neutron population inside the nuclear reactor. In this part, we recall the two possible forms of this transport equation. The first form is an integro-differential equation, which expresses the balance between neutrons loss and gain in a volume element of a multiplying medium [Reuss 2012]. Then, integrating this equation (using the method of characteristics [Bell and Glasstone 1970]) leads to a purely integral form of the transport equation. Finally, the respective properties of these two forms will be briefly discussed.

I.2.1 Integro-differential Transport Equation

From the definition of the particle density in section I.1.3, the number of neutrons within an elementary six dimensional box $d^3\mathbf{r}\, d^2\boldsymbol{\omega}\, dv$ about the phase space position $(\mathbf{r}, \boldsymbol{\omega}, v)$ at time t is:

$$\text{number of particles at } t \qquad n(\mathbf{r}, \boldsymbol{\omega}, v, t)\, d^3\mathbf{r}\, d^2\boldsymbol{\omega}\, dv\,. \tag{I.39}$$

The first form of the transport equation is then obtained by enforcing neutron balance in this elementary volume, $d\tau = d^3\mathbf{r}\, d^2\boldsymbol{\omega}\, dv$, during a time interval dt [Reuss 2012]. The variation of the total number of neutrons within $d\tau$ between times t and $t + dt$ is due to particles that leave (*loss*) or enter (*gain*) the box during this time interval:

$$\begin{aligned} n(\mathbf{r}, \boldsymbol{\omega}, v, t + dt)\, d^3\mathbf{r}\, d^2\boldsymbol{\omega}\, dv = {} & n(\mathbf{r}, \boldsymbol{\omega}, v, t)\, d^3\mathbf{r}\, d^2\boldsymbol{\omega}\, dv \\ & - \text{loss during } dt \\ & + \text{gain during } dt \end{aligned} \tag{I.40}$$

During dt, particles can leave or enter the phase space volume $d\tau$ by changing their position (by transport) or their velocity (by collision).

a. Loss by collision

A neutron of the phase space volume $d\tau$ can undergo a collision during the time interval dt and thus leave $d\tau$ by changing velocity. Moving with a

speed v, this neutron covers a distance $v\,dt$ during dt, so that its probability of colliding with a nucleus of the surrounding medium along its path is $\Sigma(\mathbf{r}, v)\, v\, dt$[11]. The mean number of neutrons thus lost during dt is

$$\text{total loss by collision} \qquad \Sigma(\mathbf{r}, v)\, v\, dt\, n(\mathbf{r}, \mathbf{v}, t) d\tau\,. \tag{I.41}$$

b. Gain by collision and from an external source

After encountering a collision (scattering or fission) in the vicinity of $\mathbf{r}$, a neutron may enter the phase space volume $d\tau$ by changing its (initial) velocity to $\mathbf{v}$. Let us denote by $\chi(\mathbf{r}, \mathbf{v}, t)\, dt$ the density of particles thus produced in $d\tau$ during dt. To this first source of particles for the volume $d\tau$, we must add, if there is one, an external source of particles of rate density $Q(\mathbf{r}, \mathbf{v}, t)$. The resulting density of neutrons produced in $d\tau$ during dt is therefore:

$$q(\mathbf{r}, \mathbf{v}, t)dt = \chi(\mathbf{r}, \mathbf{v}, t)dt + Q(\mathbf{r}, \mathbf{v}, t)dt\,. \tag{I.42}$$

From Eq. (I.41), we know that the mean number of neutrons of velocity $\mathbf{v}' = v'\,\boldsymbol{\omega}'$ undergoing a collision in the volume $d^3\mathbf{r}$ during dt is

$$\Sigma(\mathbf{r}, v')\, v'\, n(\mathbf{r}, \mathbf{v}', t) d\tau'\, dt\,. \tag{I.43}$$

Each of these collisions then gives rise to a random number k of neutrons of velocity $\mathbf{v}$ with the probability: $p_k(\mathbf{r}, v')\, C(\mathbf{v}' \to \mathbf{v})$. Integrating over the possible incoming velocity $\mathbf{v}'$, and summing over the number of descendants k produced per fission, we finally obtain the total number of neutrons gained by collisions during dt:

$$\begin{aligned}\chi(\mathbf{r}, \mathbf{v}, t)\, dt\, d^3\mathbf{r} &= \sum_k \iiint k\, p_k\, \Sigma(\mathbf{r}, v')\, v'\, C(\mathbf{v}' \to \mathbf{v}\,|\,\mathbf{r})\, n(\mathbf{r}, \mathbf{v}', t)\, d\tau\, dt \\ &= \iint_{\Omega_3} d^2\boldsymbol{\omega}' \int_0^{+\infty} dv' \nu\, \Sigma(\mathbf{r}, v')\, v'\, C(\mathbf{v}' \to \mathbf{v}\,|\,\mathbf{r})\, n(\mathbf{r}, \mathbf{v}', t)\, d^3\mathbf{r}\, dt\end{aligned} \tag{I.44}$$

In reactor physics, it is customary to introduce the *collision operator* $\mathcal{C}[\cdot]$ [Reuss 2012], which relates the density of neutrons leaving a collision about $\mathbf{r}$ with a velocity $\mathbf{v}$ to the density of neutrons entering the collision with a velocity $\mathbf{v}'$. In terms of the quantities already introduced, the *collision operator* can thus express the *outgoing collision rate density* $\chi(\mathbf{r}, \mathbf{v}, t)$ as a function of

[11] Total cross sections are assumed to be continuous functions of the position in the vicinity of $\mathbf{r}$.

the incoming *collision rate density* $\psi(\mathbf{r},\mathbf{v}',t) = v'\,\Sigma(\mathbf{r},v')\,n(\mathbf{r},\mathbf{v}',t)$ (defined in Eq. (I.33)):

Collision Operator

$$\chi(\mathbf{r},\mathbf{v},t) = \mathcal{C}\left[\,\psi(\mathbf{r},\mathbf{v}',t)\,\right]\,. \tag{I.45}$$

The expression of the operator can be obtained from Eq. (I.44):

$$\mathcal{C}\left[\,\psi\,\right] = \iiint d^3\mathbf{v}'v\,C(\mathbf{v}'\to\mathbf{v}\,|\,\mathbf{r})\,\psi(\mathbf{r},\mathbf{v}',t)\,. \tag{I.46}$$

Eq. (I.44) then takes a simpler form:

$$\chi(\mathbf{r},\mathbf{v},t) = \mathcal{C}\left[\,\Sigma(\mathbf{r},v')\,v'\,n(\mathbf{r},\mathbf{v}',t)\,\right]\,. \tag{I.47}$$

In practice there is a distinction between the physical processes of scattering and fission [Reuss 2012] (see Sec. I.1.2), such that, using Eq.(I.28),

$$\mathcal{C}[\Sigma\,\varphi] = \mathcal{C}_s[\Sigma_s\,\varphi] + \mathcal{C}_f[\Sigma_f\,\varphi]\,, \tag{I.48}$$

where the *scattering* and the *fission operator* are respectively:

$$\mathcal{C}_s[\cdot] = \iiint d^3\mathbf{v}'\,C_s(\mathbf{v}'\to\mathbf{v}\,|\,\mathbf{r})\,\left[\,\cdot\,\right]\,. \tag{I.49}$$

and

$$\mathcal{C}_f[\cdot] = \iiint d^3\mathbf{v}'\,\nu(\mathbf{r},v')\,C_f(\mathbf{v}'\to\mathbf{v}\,|\,\mathbf{r})\,\left[\,\cdot\,\right] \tag{I.50}$$

$$= \frac{1}{4\pi}F_p(v)\int dv'\nu(\mathbf{r},v')\,\left[\,\cdot\,\right]\,, \tag{I.51}$$

using Eq. (I.21) for $C_f(\mathbf{v}'\to\mathbf{v}\,|\,\mathbf{r})$.

c. Flux of particles entering and leaving the volume element $d^3\mathbf{r}$

During dt, the net number of neutrons leaving the volume V through its boundary $\mathcal{S}$ is[12]:

$$\iint_{\mathcal{S}}\left(\mathbf{j}\cdot d^2\mathbf{S}\right)\,dt = \iiint_V \nabla\cdot\mathbf{j}\,d^3\mathbf{r}\,dt\,. \tag{I.52}$$

where $d^2\mathbf{S}$ is the outward surface elementary vector of the surface $\mathcal{S}$ and $\mathbf{j} = n\mathbf{v}$ the angular current defined in Eq. (I.37). The right hand side of (I.52) comes from the use of the divergence theorem.

[12]Note that $\iint_{\mathcal{S}}\mathbf{j}\cdot d^2\mathbf{S}$ is an actual flux of particles (by opposition to the *neutron flux* defined in Eq. (I.35)).

d. Total balance

Finally, the balance on the phase space volume element,

$$n(\mathbf{r},\mathbf{v},t+dt) = n(\mathbf{r},\mathbf{v},t) + \left[q(\mathbf{r},\mathbf{v},t) - v\,\Sigma(\mathbf{r},v)\,n(\mathbf{r},\mathbf{v},t) - \nabla\cdot[n(\mathbf{r},\mathbf{v},t)\,\mathbf{v}]\right] dt\,, \quad \text{(I.53)}$$

leads to the equation for the angular density:

$$\frac{\partial}{\partial t}\,n(\mathbf{r},\boldsymbol{\omega},v,t) + \mathbf{v}\cdot\nabla n + \Sigma(\mathbf{r},v)\,n\,v = q(\mathbf{r},\boldsymbol{\omega},v,t)\,, \quad \text{(I.54)}$$

where we have used $\nabla\cdot[n(\mathbf{r},\mathbf{v},t)\,\mathbf{v}] = \mathbf{v}\cdot\nabla n(\mathbf{r},\mathbf{v},t)$, as the nabla only contains derivatives with respect to the three space variables $\mathbf{r}$. The total source of neutrons q is given by Eq. (I.42) and (I.44), from which we can see that Eq.(I.54) is a linear equation.

Boltzmann Integro-differential Transport Equation

$$\frac{1}{v}\frac{\partial}{\partial t}\,\varphi(\mathbf{r},\boldsymbol{\omega},v,t) + \boldsymbol{\omega}\cdot\nabla\varphi + \Sigma(\mathbf{r},v)\,\varphi = q(\mathbf{r},\boldsymbol{\omega},v,t)\,, \quad \text{(I.55)}$$

where q is the total rate at which neutrons appear about $\mathbf{r}$ at time t, with a velocity $v\boldsymbol{\omega}$, as a result of both collisions (scattering and fission) and an independent source Q:

$$q(\mathbf{r},\boldsymbol{\omega},v,t) = \chi(\mathbf{r},\boldsymbol{\omega},v,t) + Q(\mathbf{r},\boldsymbol{\omega},v,t)\,. \quad \text{(I.56)}$$

The phase space density χ is called the *outgoing collision rate density*. It is the rate density of particle leaving a collision about $\mathbf{r}$ at time t with a velocity $v\,\boldsymbol{\omega}$:

$$\chi(\mathbf{r},\boldsymbol{\omega},v,t) = \int_{\Omega_3} d\boldsymbol{\omega}' \int_0^{+\infty} dv'\,\nu\,\Sigma(\mathbf{r},v')\,C(\mathbf{v}'\to\mathbf{v}|\mathbf{r})\,\varphi(\mathbf{r},\boldsymbol{\omega}',v',t)\,. \quad \text{(I.57)}$$

In the framework of neutron transport, Eq. (I.55) is still valid as it is: only the expression of the *outgoing collision rate density* (I.57) is modified. Using Eq.(I.48) to change to the notation of reactor physics (see Sec. I.1.2) yields:

$$\begin{aligned}\chi(\mathbf{r},\boldsymbol{\omega},v,t) &= \int_{\Omega_3} d\boldsymbol{\omega}' \int_0^{+\infty} dv'\,\Sigma_s(\mathbf{r},v')\,C_s(\mathbf{v}'\to\mathbf{v}|\mathbf{r})\,\varphi(\mathbf{r},\boldsymbol{\omega}',v',t) \\ &\quad + F_p(v)\int_0^{+\infty} dv'\,\nu\,\Sigma_f(\mathbf{r},v')\int_{\Omega_3}\frac{d\boldsymbol{\omega}'}{4\pi}\varphi(\mathbf{r},\boldsymbol{\omega}',v',t)\,, \quad \text{(I.58)} \\ &= \mathcal{C}_s[\Sigma_s\,\varphi] + \mathcal{C}_f[\Sigma_f\,\varphi]\,, \quad \text{(I.59)}\end{aligned}$$

in terms of collision operators.

Boltzmann equation

This equation can also be obtain from the *Boltzmann equation* developed by Ludwig Boltzmann in 1872 to study the kinetic theory of gases[a], and, has thus inherited its name in the field of reactor physics. Indeed, the neutron population can be seen as an *ideal gas* of particles (see Sec. I.1.1) that evolves on an immobile gas of nuclei that it interacts with [CEA collectif et al. 2013], with a chemical reaction-like terms to take into account absorption and "multiplication" of neutrons by fission [Cercignani 1988]. The resulting transport equation (I.54) is then linear as a consequence of the neglect of the neutron-neutron interactions. In the kinetic theory of gases, collisions among the particles are important, which leads to the presence of nonlinear collision terms in the Boltzmann equation [Bell and Glasstone 1970].

[a] half a century before the discovery of the neutron [Chadwick 1932]

In transport theory, it is common to introduce the linear operator referring to the transport of the particle (displacement, absorption and scattering) called [Bell and Glasstone 1970; Spanier and Gelbard 1969]

$$\textit{transport operator} \qquad \mathcal{L}\,\cdot = \boldsymbol{\omega}\cdot\nabla\,\cdot + \Sigma(\mathbf{r},v)\,\cdot - \mathcal{C}_s[\,\Sigma_s\,\cdot\,], \tag{I.60}$$

such that the integro-differential transport equation becomes:

$$\left[\frac{1}{v}\frac{\partial}{\partial t} + \mathcal{L}\right]\varphi(\mathbf{r},\mathbf{v},t) = Q(\mathbf{r},\mathbf{v},t) + \mathcal{C}_f[\,\Sigma_f\,\varphi\,], \tag{I.61}$$

with on the left-hand-side, the transport, and on the right-hand side, the sources (external source and source from fission).

Deterministic numerical simulation in reactor physics

In the field of reactor physics, deterministic numerical simulations consist in solving numerically the neutron transport equation (the Boltzmann equation or one of its variants) on a mesh in phase space [CEA collectif et al. 2013]. The mesh in energy is, most of the time, realised by considering coupled groups of neutrons with the same energy (*multi-group* description). The variety of situations that need to be studied in reactor physics give rise to various numerical strategies (different modelisations and discretisations) for simulating a system [Duderstadt and Martin 1979; Dulla et al. 2008, 2011].

I.2.2 Delayed Neutrons

The Boltzmann equation (I.55) gives the evolution of the flux in space and time (for non stationary problems). In reactor physics, time-dependent problems arise in the start-up and the shutdown of a reactor. They are also of fundamental practical importance in investigating the stability and controllability of a reactor, both under normal operating conditions and as a result of an accident [Bell and Glasstone 1970]. However, delayed neutrons, briefly introduced in Sec. b., play a key role in the out-of-equilibrium behaviour of the neutron population inside a reactor, so that time-dependent problems require taking into account the presence of delayed neutrons in Eq. (I.55) to obtain physically meaningful results. In this section we briefly recall what are the *delayed neutrons* and why they change the dynamics of the neutron population. Finally we derive the time-dependent transport equation that accounts for delayed neutrons.

a. Delayed Fission Neutrons

Controlled by the nuclear force, the emission of a prompt neutron is almost instantaneous (within 10^{-13}s to 10^{-14}s after the fission event), whereas a delayed neutron decay, associated with the beta decay of one of the fission products (controlled by the weak interaction), can occur anytime from a few milliseconds to a few minutes later [Reuss 2003]: the beta decay of a fission product (called *precursors*) can produce, with a certain delay, an excited-state radioisotope (*delayed-neutron emitter*) that immediately undergoes a neutron emission. For instance:

$$^{87}\mathrm{Br} \longrightarrow ^{87}\mathrm{Kr}^{*} \longrightarrow ^{86}\mathrm{Kr} + ^{1}\mathrm{n}\,, \tag{I.62}$$

where the Bromine ^{87}Br has a beta half-life of 54.5 s [Reuss 2012]. This delay is of several order of magnitude larger than the microsecond characteristic lifetime of a neutron in a reactor core. For this reason, even though delayed neutrons represent less than 1% of the emitted neutrons, they play a key role in the dynamics of the neutron population (their decay constant will often determine the time behaviour of the neutron population). They are in fact of major importance in nuclear reactor kinetic control and safety analysis [Reuss 2003].

b. Transport Equation

Several fission products are precursors of the delayed-neutron emitters, with various decay rate and energy of emission. However, for practical reasons, it is possible to divide them into six or eight groups, indexed by ℓ, of similar characteristic half-life [Bell and Glasstone 1970]. A precursor of group ℓ thus decays exponentially with a rate[13] λ_ℓ, and then gives

[13] mean decay rate, averaged over the different precursors of the group

rise to one (delayed) neutron. Therefore, provided that the precursors decay where they were formed by fission[14], delayed neutrons spontaneously emitted about $\mathbf{r}$ at time t by the decay of precursors ℓ, constitute a new source term of emission rate $\lambda_\ell\, c_\ell(\mathbf{r},t)$ in the transport equation (I.55):

$$\begin{aligned}\chi(\mathbf{r},\boldsymbol{\omega},v,t) = &\int_{\Omega_3} d\boldsymbol{\omega}' \int_0^{+\infty} dv'\, \Sigma_s(\mathbf{r},v')\, C_s(\mathbf{v}'\to\mathbf{v}|\mathbf{r})\, \varphi(\mathbf{r},\boldsymbol{\omega}',v',t)\\ &+ F_p(v)\int_0^{+\infty} dv'\,(1-\beta)\,\nu\,\Sigma_f(\mathbf{r},v')\int_{\Omega_3}\frac{d\boldsymbol{\omega}'}{4\pi}\varphi(\mathbf{r},\boldsymbol{\omega}',v',t)\\ &+ \sum_\ell F_\ell(v)\,\lambda_\ell\, c_\ell(\mathbf{r},t)\,, \end{aligned} \tag{I.63}$$

where c_ℓ is the atom density of precursors ℓ, and the distribution $F_\ell(v)$ is the average spectrum of delayed neutrons produced by precursors of type ℓ [Bell and Glasstone 1970]. Modifications to Eq. (I.58) due to delayed neutrons were underlined in red in the latter equation. Here $\nu(\mathbf{r},v')$ is the mean number of neutrons emitted at a fission about $\mathbf{r}$ due to a neutron of speed v', including both prompt and delayed neutrons, and $\beta_\ell(\mathbf{r},v)$ is the fraction of this number that comes from precursors of type ℓ, so that

$$\beta(\mathbf{r},v) = \sum_\ell \beta_\ell(\mathbf{r},v) \tag{I.64}$$

is the total fraction of delayed neutrons. Moreover, the transport equation (I.55) should now be coupled to a kinetic equation for the atom density $c_\ell(\mathbf{r},t)$ of precursor ℓ:

$$\frac{\partial c_\ell}{\partial t}(\mathbf{r},t) = -\lambda_\ell\, c_\ell + \underbrace{\int_0^{+\infty} dv'\,\beta_\ell\,\nu\,\Sigma_f(\mathbf{r},v')\int_{\Omega_3}\frac{d\boldsymbol{\omega}'}{4\pi}\varphi(\mathbf{r},\boldsymbol{\omega}',v',t)}_{\text{rate of precursor produced by fission}}\,, \tag{I.65}$$

The first term on the right-hand-side (rhs) corresponds to the exponential spontaneous decay of precursors, whereas the second is a source term of precursors resulting from fission: $\beta_\ell(\mathbf{r},v')\,\nu(\mathbf{r},v')$ is the mean number of precursors produced by fissions about $\mathbf{r}$ caused by incoming neutron of speed v'.

[14] It is the case most of the time. However, in a reactor with circulating fuel (fluid), precursors may move after being emitted from a fission [Bell and Glasstone 1970]. We can cite for instance the molten-salt reactors [Dulla et al. 2006]. This case is ignored here.

I.2.3 Boundary and Initial Conditions

The transport equation (I.55) is a first order differential equation in space and time, admitting an infinite number of possible solutions. In order to determine which of these solutions correspond to the physical problem, appropriate boundary and initial conditions on the neutron phase space density are required to complete the transport equation.

a. Boundary conditions

Consider a spatial region of a physical system where we would like to solve the neutron transport equation (I.55). This region can have an arbitrary shape, but we will make the assumption that it is surrounded by a *non-reentrant surface*: a neutron leaving the system by its surface can not reenter it [Pomraning 1991; Bell and Glasstone 1970]. Under this hypothesis, neutrons entering the region of interest from its surface are considered as coming from an external source. Then, in order to solve the transport equation, this incoming flux of neutrons through the surface needs to be specified (boundary condition) at any point $\mathbf{r}_S$ of the surface S and for any inward direction $\boldsymbol{\omega}$:

$$\varphi(\mathbf{r}_S, \boldsymbol{\omega}, v, t) = \Lambda_S(\mathbf{r}_S, \boldsymbol{\omega}, v, t)\,, \qquad \text{for } \mathbf{n}\cdot\boldsymbol{\omega} < 0\,, \tag{I.66}$$

where Λ_S is a specified function, and $\mathbf{n}$ the unit outward normal vector at the point $\mathbf{r}_S$. In the particular case of *absorbing boundary condition*, no neutron enter from outside and neutrons that leave the body never come back:

$$\varphi(\mathbf{r}_S, \boldsymbol{\omega}, v, t) = 0\,, \qquad \mathbf{n}\cdot\boldsymbol{\omega} < 0\,. \tag{I.67}$$

This case is also called *vacuum* or *free surface* boundary condition. It is an interesting case, because any boundary condition, with the hypothesis of a non reentrant surface, can be directly replaced by a free surface, coupled with a (surface) source term Q_S, of the form:

$$Q_S(\mathbf{r}, \boldsymbol{\omega}, v, t) = \Lambda_S(\mathbf{r}, \boldsymbol{\omega}, v, t)\,\mathbb{1}_S(\mathbf{r})\,\mathcal{H}(t)\,, \tag{I.68}$$

which contributes to Q in equation (I.56). The function $\mathbb{1}_S$ is the *marker function* of the surface S: it is equal to 1 for positions $\mathbf{r}$ located on the surface and 0 elsewhere; and $\mathcal{H}$ is the Heaviside function, which ensures that time is positive (considering that the process was started at $t = 0$).

Non-reentrant surface hypothesis

Let us focus on the non-reentrant hypothesis in greater detail.

- If the boundaries are closed (such as absorbing or reflecting boundaries), the system of interest does not exchange particles with the external world, and of course no hypothesis is needed. This hypothesis is in fact relevant only when exchanges of particles between the region of interest and the outside are possible.
- Moreover, the hypothesis becomes useless when the region of interest is at thermodynamic equilibrium with the external world. Indeed, in that case the surrounding system plays the role of a "particle thermal bath", and a reentering neutron can not be distinguished from a new neutron actually coming from outside.

Therefore this hypothesis is necessary only in the case where the system of interest exchanges particles with an external world with which it is not in equilibrium.

b. Initial condition

The initial condition specifies the shape of the neutron phase space density at time $t = 0$:

$$\varphi(\mathbf{r}, \boldsymbol{\omega}, v, t = 0) = \Lambda_0(\mathbf{r}, \boldsymbol{\omega}, v) \, , \tag{I.69}$$

where Λ_0 is a specified function. Of course one can also start the system at any positive time t_0, and in that case, the temporal part in the surface source term Eq. (I.68) would be replaced by $\mathcal{H}(t - t_0)$. As for the boundary conditions, the initial condition can be also placed in a volume source term that will impact the transport equation only at initial time $t = 0$:

$$Q_0(\mathbf{r}, \boldsymbol{\omega}, v, t) = \Lambda_0(\mathbf{r}, \boldsymbol{\omega}, v) \, \delta(t) \, \mathbb{1}_V(\mathbf{r}) \, . \tag{I.70}$$

The function $\mathbb{1}_V$ is the *marker function* of the region of interest V, equal to 1 for positions $\mathbf{r}$ located within the region V and to 0 elsewhere. The distribution δ is the *Dirac delta function*, defined [Weisstein 2010], for a function f, as[15]

$$\int dt \, \delta(t) \, f(t) = f(0) \, . \tag{I.71}$$

[15] this convenient notation is generally used in physics. However it is an abused notation: not a standard (Riemann or Lebesgue) integral.

c. Boundary and initial conditions in the source term

Boundary and Initial Conditions - Source Term

To summarise, the initial and boundary conditions can be both placed in the source term Q of equation (I.56), which takes the form:

$$\begin{aligned} Q(\mathbf{r},\boldsymbol{\omega},v,t) &= Q_0 + Q_S + Q_V \\ &= \Lambda_0(\mathbf{r},v,\boldsymbol{\omega})\,\delta(t)\,\mathbb{1}_V(\mathbf{r}) + \Lambda_S(\mathbf{r},\boldsymbol{\omega},v,t)\,\mathbb{1}_S(\mathbf{r})\,\mathcal{H}(t) + Q_V\ , \end{aligned} \tag{I.72}$$

where Q_V is a specified volume source:

$$Q_V(\mathbf{r},\boldsymbol{\omega},v,t) = \Lambda_V(\mathbf{r},\boldsymbol{\omega},v,t)\,\mathbb{1}_V(\mathbf{r})\,\mathcal{H}(t)\ . \tag{I.73}$$

I.2.4 Integral Transport Equation

Thus far, we have focused on the integro-differential form of the transport equation (I.55). Since this equation is a linear first-order partial differential equation, it can be integrated thanks to a general technique known as method of characteristics [Courant and Hilbert], which yields the integral form of the transport equation. In this section, we will first derive the integral transport equation following the arguments of Bell and Glasstone in their book *Nuclear Transport Theory* [1970, Sec. 1.2 p.21]. We will then discuss the physical implications of this equation. Finally, we will analyse the impact of initial and boundary conditions, in the spirit of Pomraning in *Linear Kinetic theory and particle transport in stochastic mixtures* [1991, Sec. 1.4 p.21 Eq. (1.112)]. Results of this section are useful for the understanding of Chapter 3.

a. Integrating the Integro-differential Equation

Let us recall the integro-differential form of the transport equation (I.55):

$$\frac{1}{v}\frac{\partial}{\partial t}\varphi(\mathbf{r},\boldsymbol{\omega},v,t) + \boldsymbol{\omega}\cdot\nabla\varphi + \Sigma(\mathbf{r},v)\,\varphi = q(\mathbf{r},\boldsymbol{\omega},v,t)\ . \tag{I.74}$$

The aim of the method of characteristics is to find the curves, called the characteristic curves or characteristics, along which a partial differential equation (PDE) becomes an ordinary differential equation that can be formally integrated [Courant and Hilbert]. In the previous equation, the partial derivatives are taken with respect to the time coordinate, ∂_t, and the three space coordinates, ∇. Therefore one can find the characteristics by introducing a new variable s and choosing the following form for the total

derivative of φ with respect to it:

$$-\frac{d\varphi}{ds}(\mathbf{r},\boldsymbol{\omega},v,t) = \frac{1}{v}\frac{\partial}{\partial t}\varphi(\mathbf{r},\boldsymbol{\omega},v,t) + \boldsymbol{\omega}\cdot\nabla\varphi(\mathbf{r},\boldsymbol{\omega},v,t)\,. \tag{I.75}$$

Moreover, as we know that

$$\frac{d\varphi}{ds}(\mathbf{r},\boldsymbol{\omega},v,t) = \frac{dt}{ds}\frac{\partial\varphi}{\partial t} + \frac{d\mathbf{r}}{ds}\cdot\nabla\varphi\,, \tag{I.76}$$

and upon identifying terms in these two expressions, we find that:

$$\begin{cases} \dfrac{d\mathbf{r}}{ds} &= -\boldsymbol{\omega}\,, \\ \dfrac{dt}{ds} &= -\dfrac{1}{v}\,. \end{cases} \quad\Longrightarrow\quad \begin{cases} \mathbf{r} &= \mathbf{r}_0 - s\,\boldsymbol{\omega}\,, \\ t &= t_0 - \dfrac{s}{v}\,, \end{cases} \tag{I.77}$$

where $\mathbf{r}_0$ and t_0 are arbitrary constants. The curves $\mathbf{r}(s)$ and $t(s)$ are the characteristics of the differential equation (I.74), and for a fixed direction $\boldsymbol{\omega}$ and speed v, the curve passing through the point $\mathbf{r}_0$ at time t_0 is precisely the straight path followed by a particle arriving in r_0 at t_0 with velocity $v\,\boldsymbol{\omega}$ since its last collision (see fig. I.7 Left). As a consequence, along the

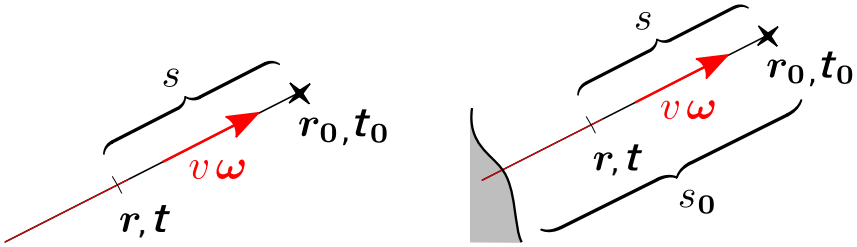

(a) Characteristic curve **(b)** in the presence of boundaries

Figure I.7: Characteristic curve

characteristics, the partial differential equation (I.74) for neutron transport becomes the ordinary equation[16]:

$$\frac{d\varphi}{ds}(s) - \Sigma(s)\,\varphi(s) = -q(s)\,, \tag{I.78}$$

where

$$\begin{cases} \varphi(s) &= \varphi\left(\mathbf{r}_0 - s\,\boldsymbol{\omega},\boldsymbol{\omega},v,t_0 - \dfrac{s}{v}\right)\,, \\ \Sigma(s) &= \Sigma(\mathbf{r}_0 - s\,\boldsymbol{\omega},v) \end{cases} \tag{I.79}$$

To integrate this equation and take care of the presence of boundaries, we assume that there exists a positive value s_0 of s (s_0 can be $+\infty$) such that

$$\varphi(s_0) = 0\,. \tag{I.80}$$

[16] One can also check that $\frac{d\varphi}{ds}(\mathbf{r}_0 - s\,\boldsymbol{\omega},\boldsymbol{\omega},v,t_0 - \frac{s}{v}) = -\frac{1}{v}\frac{\partial}{\partial t}\varphi(\mathbf{r},\boldsymbol{\omega},v,t) - \boldsymbol{\omega}\cdot\nabla\varphi$

At this point s_0, the characteristic curve crosses a boundary of the system (see Fig. I.7 Right): it can be a spatial boundary or the initial time. Equation (I.80) then makes the assumption that outside this boundary the flux is null, corresponding to the free surface case (see Sec. I.2.3), and absence of particles in the system at initial time. Other types of boundary conditions, as well as the initial condition, can thereafter be included via the source term, using Eq. (I.72). We now integrate equation (I.78) along the characteristics from $s = 0$ to s_0:

$$-\varphi(0)\, e^{-\int^0 \Sigma(s')ds'} = -\int_0^{s_0} q(s)\, e^{-\int^s \Sigma(s')ds'} ds\,,$$

and obtain the solution of the ordinary equation (I.78)

$$\varphi(0) = \int_0^{s_0} q(s)\, e^{-\int_0^s \Sigma(s')ds'} ds\,. \tag{I.81}$$

This solution can be transformed into the solution of the original PDE, using Eq. (I.79), and finally leads to the so-called *integral transport equation for the neutron flux* [Bell and Glasstone 1970; Pomraning 1991]:

Integral Transport Equation For the Neutron Flux

$$\varphi(\mathbf{r},\boldsymbol{\omega},v,t) = \int_0^{s_0} \exp\left[-\int_0^s \Sigma(\mathbf{r}-s'\boldsymbol{\omega},v)\, ds'\right] q\Big(\mathbf{r}-s\boldsymbol{\omega},\boldsymbol{\omega},v,t-\frac{s}{v}\Big)\, ds\,, \tag{I.82}$$

where $q(\mathbf{r}-s\boldsymbol{\omega},\boldsymbol{\omega},v,t-\frac{s}{v})$, defined in equation (I.56), corresponds to the density rate of neutrons leaving a collision or emitted by an external source at $\mathbf{r}-s\boldsymbol{\omega}$, with velocity $v\,\boldsymbol{\omega}$.

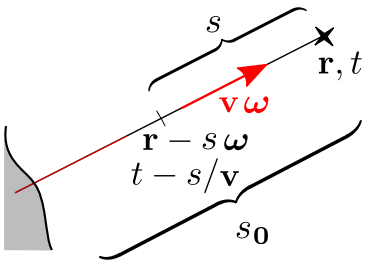

Figure I.8

b. Physical Interpretation

For the neutron flux Equation (I.82) can be rewritten in terms of the *outgoing collision rate density* χ and the external source Q [Duderstadt and Martin

1979; Case and Zweifel 1967]:

$$\varphi(\mathbf{r},\boldsymbol{\omega},v,t) = \int_0^{s_0} \underbrace{U(s|\mathbf{r},\boldsymbol{\omega},v)}_{\substack{\text{probability to have}\\ \text{no collision between}\\ \mathbf{r}-s\boldsymbol{\omega} \text{ and } \mathbf{r}}} \underbrace{\left[(\chi+Q)\left(\mathbf{r}-s\boldsymbol{\omega},\boldsymbol{\omega},v,t-\frac{s}{v}\right)\right] ds}_{\substack{\text{flux of particles emitted}\\ \text{about } \mathbf{r}-s\boldsymbol{\omega}\\ \text{in the direction } \boldsymbol{\omega}}}, \tag{I.83}$$

where $U(s|\mathbf{r},\boldsymbol{\omega},v) = \exp\left[-\int_0^s \Sigma(\mathbf{r}-s'\boldsymbol{\omega},v)\,ds'\right]$ is the complementary cumulative distribution of the jump length pdf[17], which represents the marginal probability that no collision occurs between $\mathbf{r}-s\,\boldsymbol{\omega}$ and $\mathbf{r}$. The physical meaning of the transport equation (I.83) is apparent in the form of the equation: the flux of particles about $\mathbf{r}$ in a direction $\boldsymbol{\omega}$ at time t results from the transport of the (density of) particles that are leaving a collision or are emitted from a source about $\mathbf{r}-s\,\boldsymbol{\omega}$ in the direction $\boldsymbol{\omega}$ at time $t-s/v$ and that did not undergo any collision in between (see Fig.I.8).

For the collision density Multiplying both sides of equation (I.82) by the total cross-section $\Sigma(\mathbf{r},v)$, we obtain a similar transport equation for the *incident collision rate density* $\psi(\mathbf{r},\boldsymbol{\omega},v,t)$ [Duderstadt and Martin 1979; Case and Zweifel 1967]:

$$\psi(\mathbf{r},\boldsymbol{\omega},v,t) = \int_0^{s_0} \underbrace{ds\,T(s|\mathbf{r},\boldsymbol{\omega},v)}_{\substack{\text{probability to encounter}\\ \text{a collision about } \mathbf{r}\\ \text{(after travelling a distance } s\text{)}}} \underbrace{\left[(\chi+Q)\left(\mathbf{r}-s\boldsymbol{\omega},\boldsymbol{\omega},v,t-\frac{s}{v}\right)\right]}_{\substack{\text{rate density of particles}\\ \text{emitted about } \mathbf{r}-s\boldsymbol{\omega}\\ \text{in the direction } \boldsymbol{\omega}}}, \tag{I.84}$$

where $T(s|\mathbf{r},\boldsymbol{\omega},v) = \Sigma(\mathbf{r},v)\exp\left[-\int_0^s \Sigma(\mathbf{r}-s'\boldsymbol{\omega},v)\,ds'\right]$ is the exponential inter-collision pdf, introduced in section I.1.2. Here as well the integral equation can be given a physical interpretation: the collision rate density for particles entering a collision about $\mathbf{r}$ with the direction $\boldsymbol{\omega}$ at time t results from the density rate of particles, emitted about $\mathbf{r}-s\,\boldsymbol{\omega}$ in the direction $\boldsymbol{\omega}$ at the earlier time $t-s/v$, undergoing a collision about $\mathbf{r}$ at a time s/v later (see Fig.I.8).

In reactor physics, it is very common to introduce the *displacement operator* $\mathcal{T}$ [Reuss 2012], which "transports" particles leaving a collision, or

[17] **Reminder** U is the complementary cumulative distribution of the exponential jumps pdf: $U(s) = \int_s^{+\infty} T(s')ds'$ (see Sec. I.1.2)

emitted by a source, to their next collision:

$$\mathcal{T}[\chi] = \int_0^{s_0} ds\, T(s|\mathbf{r},\boldsymbol{\omega},v)\, \chi\left(\mathbf{r}-s\boldsymbol{\omega},\boldsymbol{\omega},v,t-\frac{s}{v}\right) . \tag{I.85}$$

The integral transport equation for the collision rate density $\psi(\mathbf{r},\boldsymbol{\omega},v,t)$ then takes the concise form:

$$\psi = \mathcal{T}\mathcal{C}[\psi] + \psi_1 , \tag{I.86}$$

by recalling that the outgoing collision rate density χ is related to the incident density by $\chi = \mathcal{C}[\psi]$ (see Eq. (I.46)). The quantity

$$\psi_1 = \mathcal{T}[Q] , \tag{I.87}$$

called the *first-collision rate density* or *uncollided density* [Reuss 2012; Bell and Glasstone 1970; Case and Zweifel 1967], represents the contribution to ψ due to particles coming straight from the source. It is also common to define the *uncollided flux*,

$$\varphi_1(\mathbf{r},\boldsymbol{\omega},t) = \int_0^{s_0} U(s|\mathbf{r},\boldsymbol{\omega},v)\, \left[Q\left(\mathbf{r}-s\boldsymbol{\omega},\boldsymbol{\omega},v,t-\frac{s}{v}\right)\right] ds , \tag{I.88}$$

which represents the contribution to the angular flux due to particles that have not undergone collisions since they were emitted from the source.

Note that from these physical considerations, we can see that the two integral transport equations Eq. (I.83) and (I.84) could have been established directly from a neutron balance in the phase space.

Method of Characteristics for Numerical Simulations

Like the Boltzmann equation (I.55), the integral form of the transport equation can also lead to the derivation of some numerical methods [Barbarino et al. 2013]. In particular, the method of characteristics is especially well adapted to the numerical deterministic resolution of transport equations [CEA monographie 2013]: the transport equation is integrated along a *characteristics*. This method allows resolving the transport equation with a good compromise between precision and speed, on system of complex geometries with irregular shape (thanks to the possibility to use a non structured grid), with general boundary condition and less approximations on the anisotropy of the scattering. For these reason, this method is more and more employed for industrial codes.

c. Initial and boundary conditions and general integral transport equation

Let us recall the integral transport equation (I.82) for the neutron flux:

$$\varphi(\mathbf{r},\boldsymbol{\omega},v,t)=\int_0^{s_0}\exp\left[-\int_0^{s}\Sigma(\mathbf{r}-s'\boldsymbol{\omega},v)\,ds'\right]q\left(\mathbf{r}-s\boldsymbol{\omega},\boldsymbol{\omega},v,t-\frac{s}{v}\right)ds\,, \tag{I.89}$$

where q is the total rate, defined in Eq. (I.56), at which neutrons appear as a result of both collisions and an independent source Q. In Sec. I.2.4.a., Eq. (I.89) was established for a free surface case, with no particle at initial time. As seen in Sec. I.2.3, initial and boundary conditions can be then added as external source terms of the transport equation (I.89) – see Eq. (I.72): the initial condition is equivalent to a volume source Q_0 at the initial time, and the boundary conditions to a surface source of particles Q_S. In this section, we derive explicitly the contribution to $\varphi(\mathbf{r},\boldsymbol{\omega},v,t)$ in Eq. (I.89) due to these two sources.

Initial conditions – Let us call φ_1^0 the contribution to φ due to the transport of initial source $Q_0(\mathbf{r},\boldsymbol{\omega},v,t)=\Lambda_0(\mathbf{r},\boldsymbol{\omega},v)\,\delta(t)\,\mathbb{1}_V(\mathbf{r})$ (Eq. (I.70)):

$$\varphi_1^0(\mathbf{r},\boldsymbol{\omega},v,t)=\int_0^{s_0}U(s)\,\Lambda_0(\mathbf{r}-s\boldsymbol{\omega},\boldsymbol{\omega},v)\,\delta\left(t-\frac{s}{v}\right)\,\mathbb{1}_V(\mathbf{r}-s\boldsymbol{\omega})ds\,, \tag{I.90}$$

$$=\begin{cases}U(v\,t)\,\Lambda_0(\mathbf{r}-v\,t\,\boldsymbol{\omega},\boldsymbol{\omega},v) & \text{if } (\mathbf{r}-v\,t\,\boldsymbol{\omega})\in V\\ 0 & \text{elsewhere.}\end{cases} \tag{I.91}$$

We define $\mathbf{r}_S$ the intersection of the characteristic curve $\mathbf{r}-v\,t\,\boldsymbol{\omega}$ and the surface S (see Fig. I.9). The condition $\mathbf{r}-v\,t\,\boldsymbol{\omega}\in V$ is then equivalent to $v\,t\leqslant\|\mathbf{r}_S-\mathbf{r}\|=(\mathbf{r}-\mathbf{r}_S)\cdot\boldsymbol{\omega}$, so that the contribution due to the initial source is finally:

Contribution due to the initial source (initial condition)

$$\varphi_1^0(\mathbf{r},\boldsymbol{\omega},v,t)=U(v\,t)\,\Lambda_0(\mathbf{r}-v\,t\,\boldsymbol{\omega},\boldsymbol{\omega},v)\,\mathcal{H}\big((\mathbf{r}-\mathbf{r}_S)\cdot\boldsymbol{\omega}-v\,t\big)\,, \tag{I.92}$$

$$\psi_1^0(\mathbf{r},\boldsymbol{\omega},v,t)=T(v\,t)\,\Lambda_0(\mathbf{r}-v\,t\,\boldsymbol{\omega},\boldsymbol{\omega},v)\,\mathcal{H}\big((\mathbf{r}-\mathbf{r}_S)\cdot\boldsymbol{\omega}-v\,t\big)\,. \tag{I.93}$$

Boundary conditions – Let us now call φ_1^S the contribution to φ due to the surface source equivalent to the boundary conditions, given in Eq. (I.68):

$$\varphi_1^S(\mathbf{r},\boldsymbol{\omega},v,t)=\int_0^{s_0}U(s)\,\Lambda_S\left(\mathbf{r}-s\boldsymbol{\omega},\boldsymbol{\omega},v,t-\frac{s}{v}\right)\,\mathbb{1}_S(\mathbf{r}-s\boldsymbol{\omega})\,\mathcal{H}\left(t-\frac{s}{v}\right)ds\,. \tag{I.94}$$

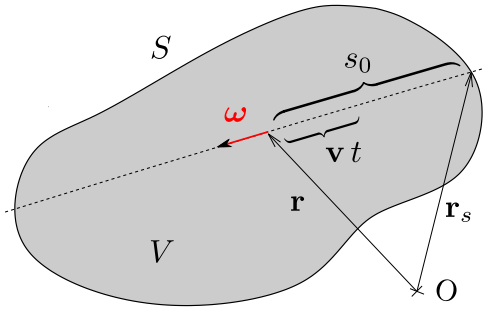

Figure I.9: The position $\mathbf{r}_S$ is at the intersection of the characteristic curve, straight line defined by the point $\mathbf{r}$ and the direction $\boldsymbol{\omega}$ (dash line), and the surrounding surface S of the system.

By definition of the intersection point $\mathbf{r}_S$, the vectors $\mathbf{r}-\mathbf{r}_S$ and $\boldsymbol{\omega}$ are aligned (see Fig. I.9), and $\mathbb{1}_S(\mathbf{r}-s\boldsymbol{\omega})$ can be written as a one dimension delta distribution in the direction of $\boldsymbol{\omega}$:

$$\mathbb{1}_S(\mathbf{r}-s\boldsymbol{\omega}) = \delta((\mathbf{r}-\mathbf{r}_S)\cdot\boldsymbol{\omega}-s) = \delta(\|\mathbf{r}-\mathbf{r}_S\|-s)\,. \tag{I.95}$$

As a consequence, performing the integration over s in Eq. (I.94) leads to the final contribution due to the surface source.

Contribution due to the surface source (boundary condition)

$$\varphi_1^S(\mathbf{r},\mathbf{v},t) = U\big((\mathbf{r}-\mathbf{r}_S)\cdot\boldsymbol{\omega}\big)\,\Lambda_S\Big(\mathbf{r}_S,\mathbf{v},t-\frac{(\mathbf{r}-\mathbf{r}_S)\cdot\boldsymbol{\omega}}{v}\Big)\,\mathcal{H}\Big(t-\frac{(\mathbf{r}-\mathbf{r}_S)\cdot\boldsymbol{\omega}}{v}\Big) \tag{I.96}$$

It represents the contribution to the neutron flux about r due to the rate of particles emitted from the surface S at a positive time $t-\|\mathbf{r}-\mathbf{r}_S\|/v$ and transported until $\mathbf{r}$.

$$\psi_1^S(\mathbf{r},\mathbf{v},t) = T((\mathbf{r}-\mathbf{r}_S)\cdot\boldsymbol{\omega})\,\Lambda_S\Big(\mathbf{r}_S,\mathbf{v},t-\frac{(\mathbf{r}-\mathbf{r}_S)\cdot\boldsymbol{\omega}}{v}\Big)\,\mathcal{H}\Big(t-\frac{(\mathbf{r}-\mathbf{r}_S)\cdot\boldsymbol{\omega}}{v}\Big) \tag{I.97}$$

Replacing these two contributions in the integral transport equation (I.89), we recover the general integral transport equation obtained in [Pomraning 1991, Sec. 1.4 p.18] where boundary and initial conditions Eq. (I.66) and (I.69) were directly used to integrate the integro-differential transport equation.

Note that in the case of a volume source, the integration over s can not be directly calculated, and the general integral can not be simplified:

$$\varphi_1^V(\mathbf{r},\boldsymbol{\omega},v,t) = \int_0^{s_0} U(s|\mathbf{r},\boldsymbol{\omega})\,Q_V\big(\mathbf{r}-s\boldsymbol{\omega},\boldsymbol{\omega},v,t-\frac{s}{v}\big)\,ds\,. \tag{I.98}$$

I.2.5 Diffusion Equation

An important aspect of transport theory involves the development of approximate descriptions that can be solved analytically. One very common approximate description consists in removing the velocity dependence of the transport equation, replacing it by a set of approximate equations in the real space $\mathbf{r}$. To start with, it is customary to consider neutrons with constant speed v[18]. These neutrons obey to the *one speed transport equation*, (one speed version of the neutron transport equation (I.61)):

$$\frac{1}{v}\frac{\partial}{\partial t}\varphi(\mathbf{r},\boldsymbol{\omega},t)+\boldsymbol{\omega}\cdot\nabla\varphi+\Sigma(\mathbf{r})\,\varphi = \Sigma_s(\mathbf{r})\int d\boldsymbol{\omega}' C_s(\boldsymbol{\omega}'\to\boldsymbol{\omega})\varphi(\mathbf{r},\boldsymbol{\omega}',t)+q'(\mathbf{r},\boldsymbol{\omega},t)\,, \tag{I.99}$$

where $q'(\mathbf{r},\boldsymbol{\omega},t)=Q_f(\mathbf{r},\boldsymbol{\omega},t)+Q(\mathbf{r},\boldsymbol{\omega},t)$ contains the sources from fission $Q_f=\mathcal{C}_f[\,\Sigma_f\,\varphi\,]$, plus an external source Q.

a. Conservation equation

Integrating the one speed transport equation (I.99) over the angular dependence and using the definitions Eq. (I.36) and (I.38), we obtain the conservation equation:

Conservation equation

$$\frac{1}{v}\frac{\partial}{\partial t}\phi(\mathbf{r},t)+\nabla\cdot\mathbf{J}+\Sigma_a(\mathbf{r})\,\phi=q'(\mathbf{r},t)\,, \tag{I.100}$$

where

$$\mathbf{J}(\mathbf{r},t)=\int d\boldsymbol{\omega}\mathbf{j}(\mathbf{r},\boldsymbol{\omega},t)\qquad \phi(\mathbf{r},t)=\int d\boldsymbol{\omega}\varphi(\mathbf{r},\boldsymbol{\omega},t)\qquad q'(\mathbf{r},t)=\int d\boldsymbol{\omega}q'(\mathbf{r},\boldsymbol{\omega},t)$$

and $\Sigma_a=\Sigma_c+\Sigma_f$ is the absorption cross-section that corresponds to the occurrence of neutron absorption by nuclei for sterile capture or fission events. Note that the number of neutrons is conserved during a scattering event, such that the flux of neutron leaving a scattering (in any direction) about $\mathbf{r}$ is equal to the flux of neutrons entering it:

$$\int d\boldsymbol{\omega}\int d\boldsymbol{\omega}'\Sigma_s(\mathbf{r})\,C_s(\boldsymbol{\omega}'\to\boldsymbol{\omega})\varphi(\mathbf{r},\boldsymbol{\omega}',t)=\int d\boldsymbol{\omega}\Sigma_s(\mathbf{r})\,\varphi(\mathbf{r},\boldsymbol{\omega},t)\,. \tag{I.101}$$

Equation (I.100) is the conservation equation of the system. It can also be obtained directly from a neutron balance (see Sec. I.2.1) in the real space.

[18] This is coherent with the multi-group description used for deterministic numerical simulations, which considers coupled groups of neutrons with the same energy.

b. P_1 *equations and diffusion approximation*

Multiplying Eq. (I.99) by $\boldsymbol{\omega}$ and integrating again over $\boldsymbol{\omega}$, we obtain

$$\frac{1}{v}\frac{\partial}{\partial t}\mathbf{J}(\mathbf{r},t)+\int d^2\boldsymbol{\omega}\,\boldsymbol{\omega}\,[\boldsymbol{\omega}\cdot\nabla\varphi]+\Sigma_t(\mathbf{r})\,\mathbf{J}=\mu_0\,\Sigma_s\mathbf{J}(\mathbf{r},t)+Q_1(\mathbf{r},t)\,, \quad \text{(I.102)}$$

where $Q_1(\mathbf{r},t)=\int d^2\boldsymbol{\omega}\boldsymbol{\omega}\,Q(\mathbf{r},\boldsymbol{\omega},t)$ and μ_0 is the mean value of the cosine of the scattering angle [Duderstadt and Martin 1979]:

$$\mu_0=\langle\boldsymbol{\omega}\cdot\boldsymbol{\omega}'\rangle=\int d^2\boldsymbol{\omega}\,(\boldsymbol{\omega}\cdot\boldsymbol{\omega}')\,C_s(\boldsymbol{\omega}\cdot\boldsymbol{\omega}'\,|\,\mathbf{r})\,. \quad \text{(I.103)}$$

Indeed, considering that the medium is isotropic[19], the scattering kernel $C_s(\boldsymbol{\omega}\to\boldsymbol{\omega}'\,|\,\mathbf{r})$ does not depend on the direction of the incoming particle $\boldsymbol{\omega}$, but only on the angle between the two directions $\boldsymbol{\omega}$ and $\boldsymbol{\omega}'$:

$$C_s(\boldsymbol{\omega}\to\boldsymbol{\omega}'\,|\,\mathbf{r})=C_s(\boldsymbol{\omega}\cdot\boldsymbol{\omega}'\,|\,\mathbf{r})\,.$$

The mean value of the cosine of this scattering angle can then be defined as in Eq. (I.103)[20]. Note that, if the scattering is isotropic, $C_s(\boldsymbol{\omega}\to\boldsymbol{\omega}'\,|\,\mathbf{r})=1/(4\pi)$ and $\mu_0=0$, and the scattering term vanishes in Eq. (I.102). Furthermore, to establish Eq. (I.102), we have also used the fact that the fission source $Q_f(\mathbf{r},\boldsymbol{\omega},t)$ is isotropic (see Eq. (I.21)), such that, $Q_f(\mathbf{r},\boldsymbol{\omega},t)=\nu\Sigma_f\phi(\mathbf{r},t)/(4\pi)$, and $\int d^2\boldsymbol{\omega}\,\boldsymbol{\omega}Q_f(\mathbf{r},\boldsymbol{\omega},t)=0$.

To go further, we assume that the angular flux is only weakly dependent on the angle, and expand it at first order [Duderstadt and Martin 1979]:

$$\varphi(\mathbf{r},\boldsymbol{\omega},t)=\frac{1}{4\pi}\left[\int d^2\boldsymbol{\omega}\,\varphi\right]+\frac{3}{4\pi}\left[\int d^2\boldsymbol{\omega}\,\mathbf{j}\right]\cdot\boldsymbol{\omega}\,, \quad \text{(I.104)}$$

$$=\frac{1}{4\pi}\phi(\mathbf{r},t)+\frac{3}{4\pi}\mathbf{J}(\mathbf{r},t)\cdot\boldsymbol{\omega}\,. \quad \text{(I.105)}$$

This approximation is known as the P_1 *approximation*, as it corresponds to the expansion in the first order of the angular flux in Legendre Polynomials in $\mu=\boldsymbol{\omega}\cdot\boldsymbol{\omega}'$ [Duderstadt and Martin 1979; Pomraning 1991; Bell and Glasstone 1970]. Using this approximation in Eq. (I.102), we obtain the system of equations [Duderstadt and Martin 1979]:

$$\frac{1}{v}\frac{\partial}{\partial t}\phi(\mathbf{r},t)+\nabla\cdot\mathbf{J}+\Sigma_a(\mathbf{r})\,\phi=Q(\mathbf{r},t)\,, \quad \text{(I.106)}$$

$$\frac{1}{v}\frac{\partial}{\partial t}\mathbf{J}(\mathbf{r},t)+\frac{1}{3}\nabla\phi+(\Sigma_t-\mu_0\Sigma_s)(\mathbf{r})\,\mathbf{J}=Q_1(\mathbf{r},t)\,, \quad \text{(I.107)}$$

[19] which is the case all along the thesis

[20] μ_0 can be rewritten, in the spherical coordinate system (r,θ,φ), setting $\boldsymbol{\omega}'$ along e_z: $\mu_0=\langle\boldsymbol{\omega}\cdot\boldsymbol{\omega}'\rangle=\int_0^{2\pi}d\varphi\int_0^{\pi}d\theta\sin(\theta)\,\cos(\theta)\,C_s(\cos(\theta)\,|\,\mathbf{r})$

known as the P_1 *equations*.

The first order equation (I.107) can be further simplified by introducing two other reasonable approximations [Duderstadt and Martin 1979]:

- we consider that the external source $Q(\mathbf{r}, \omega, t)$ is isotropic: the source term Q_1 then vanishes in Eq.(I.107);
- we assume that the variations in time of the current density $\mathbf{J}(\mathbf{r}, t)$ are slow compared to the collision process, so that we can neglect the time derivative $v^{-1}\partial\mathbf{J}/\partial t$ in comparison with $\Sigma_t\mathbf{J}$:

$$\frac{1}{|\mathbf{J}|}\frac{\partial|\mathbf{J}|}{\partial t} \ll v\Sigma_t\,; \tag{I.108}$$

  the rate of variation of the current density in time must be small compared to the collision frequency $v\Sigma_t$, which is typically $v\Sigma_t \gtrsim 10^5\ s^{-1}$.

Under these approximations, Eq. (I.107) becomes

$$\mathbf{J}(\mathbf{r}, t) = -\frac{1}{3(\Sigma_t - \mu_0\,\Sigma_s(\mathbf{r}))}\,\nabla\phi(\mathbf{r}, t)\,; \tag{I.109}$$

the current density is proportional to the spatial gradient of the flux. Note that, recalling the relation between the flux and the density, $\phi(\mathbf{r}, t) = v\,n(\mathbf{r}, t)$, the same type of relation arise for the neutron density:

$$\mathbf{J}(\mathbf{r}, t) = -D(\mathbf{r})\,\nabla n(\mathbf{r}, t)\,, \tag{I.110}$$

where we introduced the *diffusion coefficient*

$$D(\mathbf{r}) = \frac{v}{3(\Sigma_t - \mu_0\,\Sigma_s(\mathbf{r}))}\,. \tag{I.111}$$

Taken together, the assumptions done in this section are known as the *diffusion approximation*, and Eq. (I.110) is known as *Fick's first law* of diffusion [Diu et al. 2007]. Finally, substituting this relation into Eq. (I.106) yields

One-speed diffusion equation

$$\frac{1}{v}\frac{\partial}{\partial t}\,\phi(\mathbf{r}, t) - \frac{1}{v}\,\nabla\cdot D(\mathbf{r})\nabla\phi + \Sigma_a(\mathbf{r})\,\phi = q'(\mathbf{r}, t)\,, \tag{I.112}$$

know as the *one-speed diffusion equation*. This equation is one of the simplest description of a transport process [Duderstadt and Martin 1979].

In case of an homogeneous medium, the cross-sections $\Sigma_{t/a}$ and the diffusion coefficient D do not depend on $\mathbf{r}$; the one-speed diffusion equation (I.112) simplifies to

$$\frac{1}{v}\frac{\partial}{\partial t}\phi(\mathbf{r},t) - \frac{1}{v}D\Delta\phi + \Sigma_a\,\phi = q'(\mathbf{r},t)\,. \tag{I.113}$$

Moreover, if the scattering is isotropic, $C_s(\boldsymbol{\omega}\cdot\boldsymbol{\omega}') = 1/(4\pi)$, then $\mu_0 = 0$ and the diffusion coefficient, Eq.(I.111), reads

$$D = \frac{v}{3\Sigma_t}\,. \tag{I.114}$$

Along the thesis, we will resort to the *diffusion approximation* described above at several occasions. Generally, we will further consider that the medium is homogeneous and the scattering isotropic, for which we can use the equations:

Diffusion equations

For the flux,
$$\frac{1}{v}\frac{\partial}{\partial t}\phi(\mathbf{r},t) - \frac{1}{v}D\Delta\phi + \Sigma_a\,\phi = q'(\mathbf{r},t)\,; \tag{I.115}$$

For the density,
$$\frac{\partial}{\partial t}n(\mathbf{r},t) - D\Delta n + v\,\Sigma_a\,n = q'(\mathbf{r},t)\,, \tag{I.116}$$

where the constant $\Sigma_a = \Sigma_c + \Sigma_f$ and the

diffusion coefficient is
$$D = \frac{v}{3\Sigma_t}\,. \tag{I.117}$$

The source term $q' = Q_f + Q$ contains an external isotropic source Q

and the fission source
$$Q_f(\mathbf{r},\boldsymbol{\omega},t) = \frac{1}{4\pi}\nu\Sigma_f\phi(\mathbf{r},t)\,. \tag{I.118}$$

3 Limits of the Transport Equation

In this last section we will discuss two phenomena, observed in the field of reactor physics, that highlight several limits of the transport theory presented in this chapter. First, the observation of *neutron clustering* in some Monte Carlo simulations of nuclear reactors [Dumonteil et al. 2014] will lead us to question the approximation made by neglecting the fluctuation of the neutron population in a multiplying medium. Then, the observation of non-exponential transport of neutrons (or photons) in strongly heterogeneous media, such as pebble-bed reactors [Larsen and Vasques 2011], motivates the need for a new transport theory in this type of medium. The key motivations for the thesis will follow from here.

I.3.1 Fluctuations Problem

A *neutron clustering* effect, has been recently observed in Monte Carlo (criticality) simulations of nuclear reactors. This effect was brought to light in the article [Dumonteil et al. 2014], illustrated on a "small" example: a Monte Carlo criticality simulation of a PWR pin-cell performed with the Tripoli-4® code developed at the CEA Saclay [Brun et al. 2011, 2013]. In this work, the pin-cell system is composed of a single UO_2 fuel rod, enclosed in a Zircaloy cladding (see Fig. I.10). A water moderator surrounds the cladding, which is modelled, in the Monte Carlo simulations, by reflecting boundary conditions for the pin-cell. Simulations start with a uniform source of neutrons along the axis of the pin-cell, which corresponds to the equilibrium state of a system with reflecting boundaries. The neutron flux is then recorded over a regular spatial grid composed of 40 bins along the axial direction, indexed by i (see Fig. I.10). Three sets of simulations were run for different values of the pin-cell length L: $L = 10$ cm, $L = 100$ cm and $L = 400$ cm, with the same number of simulated particles $N = 10^4$. Resulting time evolutions of the flux after convergence of the simulations are displayed on Fig. I.11.

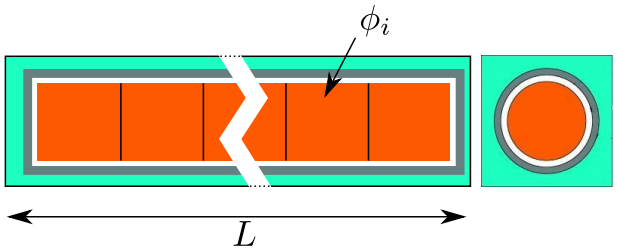

Figure I.10: Representation of a pin-cell.

We first observe that, for a small system ($L = 10$ cm, Fig. I.11 Left), the flux stays more or less uniform in the pin-cell over time, and fluctuations around the "average flux" are small. The second simulation ($L = 100$ cm, Fig. I.11 Left) exhibits much stronger fluctuations in space and time of the neutron flux. This behaviour is further enhanced when taking $L = 400$ cm (Fig. I.11 Right): fluctuations of the population are so strong that neutrons tend to gather into *clusters* separated by empty space, while the total neutron population is preserved (as the system is critical, $\nu = 1$). Clusters then seem to wander around indefinitely. This effect is amplified by decreasing the initial density of neutrons in the system.

This distribution of the flux is far from the one expected in such a system, i.e. a uniform flux in a pin-cell with reflecting boundaries. Even more surprisingly, the Monte Carlo simulation has actually converged (in that the parameter used for measuring convergence of these simulations has

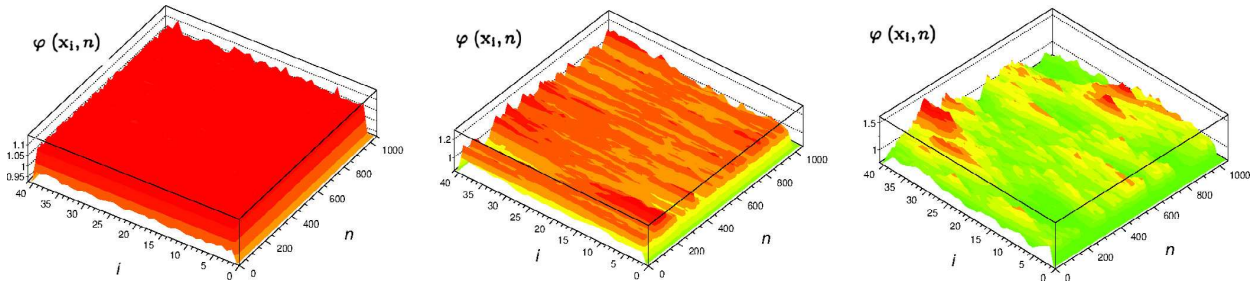

Figure I.11: Figure reproduced from [Dumonteil et al. 2014]. Monte Carlo criticality simulations for a PWR pin-cell with varying axial length L, at fixed number of particles per cycle, $N = 10^4$. The neutron flux $\phi(x_i, n)$ over an axially-distributed spatial mesh is displayed as a function of the mesh index i and the cycle number n. Left: $L = 10$ cm. Center: $L = 100$ cm. Right: $L = 400$ cm.

reached a stationary value). One of the first conclusions of this observations would be to consider that the criteria of convergence of the simulation could be misleading in large systems with a relatively small number of simulated particles. However, one is led to wonder whether this problem could be even more fundamental [Dumonteil et al. 2014].

In fact, branching random walks have been studied since a long time in connection with mathematical modelling of biological populations, such as bacteria, plankton or amoebae [Athreya and Ney 2012b; Young et al. 2001; Houchmandzadeh 2008]. In these systems, several experiments have shown the tendency of *neutral clustering*: even in absence of particle-particle interactions, a population of individuals that are initially uniformly distributed tends to form clusters [Houchmandzadeh 2002, 2009]. Moreover, several other situations have already been reported in the context of nuclear physics in which the neutron population undergoes large fluctuations, such that the population state in the system is quite unpredictable [Prinja 2012] (in that the mean is not representative of the instantaneous distribution of the population).

The first part of the thesis will focus on the fluctuations of the neutron population around its mean value. More generally the part will deal with the fluctuations of a population of individuals that can diffuse, reproduce or die. It will be divided into two chapters: the first one will establish equations for the various moments of quantities that characterise the neutron population (such as the instantaneous density, the number of collisions, the), whereas the second one will aim to explain and characterise the clustering phenomenon.

I.3.2 Non Exponential Transport

In this chapter we have seen that neutron transport in multiplying media can be modeled by Pearson random walks coupled to a birth-death mechanism (see Sec. I.1.2). More generally, linear transport[21] is modeled in terms of Pearson random walks: particles, such as photons or neutrons, move at constant speed along straight paths of random length, interrupted by collisions with the medium, whereupon directions are randomly redistributed [Duderstadt and Martin 1979; Case and Zweifel 1967]. By nature, the process followed by the transported particles is Markovian, and therefore the distances travelled by the particles between two collisions depend only on the properties of the medium. Assuming that this medium is homogeneous and that scattering centres are uncorrelated, these inter-collision distances are exponentially distributed (see Sec. I.1.2). In this case, the (mean[22]) behaviour of the transported particles is well described by the Boltzmann equation (with or without the branching term) derived in Sec. I.1.2, and, in the diffusion limit, the transport of the particles is characterised by a mean square displacement which grows linearly with time

$$\langle (\Delta r(t))^2 \rangle \sim D\, t\,, \tag{I.119}$$

where D is the diffusion parameter (see Sec. I.2.5).

However, in many applications of linear transport theory, the hypothesis of homogeneous and uncorrelated scattering centres is deemed to fail. We can cite for instance light propagation through turbid media [Davis and Marshak 2004; Davis 2006; Kostinski and Shaw 2001] or engineered optical materials [Barthelemy et al. 2008; Svensson et al. 2013, 2014], neutron diffusion in pebble-bed reactors [Larsen and Vasques 2011], and radiation trapping in hot atomic vapours [Mercadier et al. 2009]. In these systems, the presence of spatially extended non-scattering regions induces longer inter-collision distances (compared to typical jumps in the medium), which increase the diffusivity of the particles; the resulting jump distribution is no longer exponential. On the other hand, *quenched* heterogeneities, i.e. heterogeneities that do not change in time, such as those linked to quenched disorder, lead to correlations between jumps that tend to counteract the increase of diffusivity [Svensson et al. 2014]. These two effects can be observed in Fig. I.12, illustrating the example of photon transport in a *Lévy glass* [Barthelemy et al. 2008].

[21] where particles are fairly diluted, i.e., interact with the surrounding medium but not with each other

[22] In this section, we do not consider the issue of fluctuations raised in the previous section.

In reactor physics, the issue of particle transport in quenched disordered media is, for example, central for neutron transport in pebble bed reactors [Larsen and Vasques 2011; Vasques and Larsen 2014a,b], whose core is filled with about 10^5 randomly placed spherical fuel elements, called pebbles[23] [Grimod 2010]. These pebbles have all the same radius of 3 cm, which is comparable to the neutron mean free path. Correspondingly it has been observed that neutron transport in these systems is strongly affected by the empty spaces[24] between pebbles: jump distributions appear broader than exponential, and mean free paths are increased [Behrens 1949; Lieberoth and Stojadinović 1980].

For these systems, the Boltzmann equation derived in Sec. I.1.2 does not hold [Larsen and Vasques 2011], and, in the diffusion limit, the diffusion relation (I.119) breaks down [Svensson et al. 2014], being replaced by [Barthelemy et al. 2008]

$$\langle (\Delta r(t))^2 \rangle \sim D\, t^{\gamma}\,, \tag{I.120}$$

where $\gamma \neq 1$, which deviates from the linear dependence on time found for the diffusive case. We say then that the transport is *anomalous* [Metzler and Klafter 2000], and it is characterised by the parameter γ: the process is called *super-diffusive* if $\gamma > 1$, and *sub-diffusive* if $0 < \gamma < 1$. More precisely, anomalous transport through strong heterogeneous media is characterised by a *super-diffusive* behaviour ($\gamma > 1$).

In the context of heterogeneous media, important insights have been provided by the development of generalised transport equation (generalised Boltzmann equation) and homogeneisation theory [Larsen and Vasques 2011; Frank and Goudon 2010; Davis and Marshak 2004; Scholl et al. 2006]. In the case of quenched disorder, most works were carried out within the framework of anomalous diffusion [Fogedby 1994; Barthelemy et al. 2010; Buonsante et al. 2011; Groth et al. 2012; Bernabó et al. 2014]. The reference model for this class of phenomena is the so-called *Lévy walk* [Zaburdaev et al. 2015]: particles evolve with a constant finite speed, performing random steps distributed according to a power-law distribution, i.e. with an algebraic tail of the form:

$$T(\ell) \underset{\ell\infty}{\sim} \frac{1}{\ell^{\alpha+1}}, \qquad \text{with } 0 < \alpha < 2\,. \tag{I.121}$$

The parameter α characterising the jump distribution is called *stability index*: for $0 < \alpha < 2$ the distribution has no variance, and for $0 < \alpha \leqslant 1$

[23] Each pebble is made of graphite (the moderator) containing microscopic fuel particles.

[24] These empty spaces are random in placement and geometry and of size comparable to the neutron mean free path within the fuel.

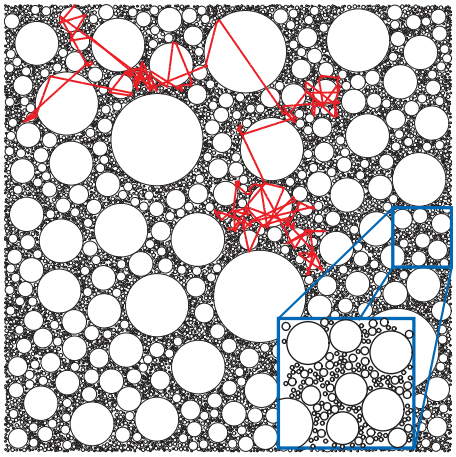

Figure I.12: Figure reproduced from [Barthelemy et al. 2008]. Monte Carlo simulation of a photon walk through a two-dimensional version of a *Lévy glass*. Lévy glasses are obtained by modifying the local density of scattering particles within an initially homogeneous medium, by inserting glass microspheres that do not scatter with a power-law diameter (The inset shows the scale invariance of the glass). The photon transport within this system is dominated by long jumps performed by photon through the glass spheres. Experimental evidence from [Barthelemy et al. 2008] shows that the transmission of light through a Lévy glass corroborates the hypothesis of photons performing Lévy walks inside a Lévy glass [Davis and Marshak 1997].

it has no mean. However, the description of neutron and photon propagation in such systems remains particularly challenging, and a comprehensive theoretical framework is still missing, especially in the presence of boundaries [Larsen and Vasques 2011; Svensson et al. 2013, 2014; Bernabó et al. 2014].

In the second part of the thesis, we will thus explore different aspects of anomalous transport. First, we will focus on the issue of occupation statistics of non-exponential random walks, including Lévy walks, in a finite domain (Chapter IV). Finally, in Chapter V, we will move on to the problem of the statistics of asymmetric Lévy flights in the presence of absorbing boundaries.

First part

Fluctuation Statistics

CHAPTER II

BACKWARD DESCRIPTION OF THE FLUCTUATIONS

In this chapter, we are interested in the fluctuation statistics of the neutron population (in a reactor core). For that purpose, we develop backward equations for each moment of quantities of interest in reactor physics, in the general case of systems composed of an inhomogeneous medium, where the speed of neutrons can change at each collision and their scattering can be anisotropic.

Contents

1 THE FLUCTUATION PROBLEM

II.1.1 Useful combinatorial quantities

Before dealing with the core of the fluctuation problem, let us first have a closer look at the discrete probability law $\{p_k\}_{k\geqslant 0}$ defined in Sec. I.1.2. As seen in the previous chapter, the mean behaviour of a branching process does not depend explicitly on the different values taken by the probabilities p_k, but only on the corresponding first factorial moment[1]

$$\nu = \langle\, k \,\rangle = \sum_{k\geqslant 0} k\, p_k = p_1 + 2\, p_2 + 3\, p_3 + \dots . \tag{II.1}$$

This quantity physically represents the mean number of particles created at a collision. In the same way, we will see in this chapter that the first order of the fluctuations of a branching process will depend only on the two first factorial moments $\nu \doteq \nu_1$ and $\nu_2 = \langle\, k(k-1) \,\rangle$. Given the importance that these factorial moments take in branching processes, in this paragraph we will focus on understanding the physical meaning of the higher moments:

***Falling factorial moment* of the number of descendants at a collision**

$$\nu_i = \langle\, k(k-1)(\dots)(k-i+1) \,\rangle = \sum_{k\geqslant 0} k(k-1)(\dots)(k-i+1)\, p_k\,. \tag{II.2}$$

Let us consider first the second factorial moment ν_2. Using factorial and combinatorial notations, ν_2 can be rewritten as:

$$\begin{aligned} \nu_2 &= \sum_{k\geqslant 0} k(k-1)\, p_k = \sum_{k\geqslant 0} \frac{k!}{(k-2)!}\, p_k \\ \nu_2 &= 2 \sum_{k\geqslant 0} \binom{k}{2} p_k\,, \qquad \text{where } \binom{k}{2} = \frac{k!}{2!\,(k-2)!}\,. \end{aligned} \tag{II.3}$$

This binomial coefficient represents the number of particle pairs that can be formed from a set of k particles. Therefore,

$$\frac{\nu_2}{2} = \sum_{k\geqslant 0} \binom{k}{2} p_k = \left\langle \binom{k}{2} \right\rangle, \tag{II.4}$$

corresponds to the mean number of particle pairs that are created at a collision, and thus ν_2 **represents the mean number of *ordered* particle pairs**

[1] see for instance the Boltzmann equation (I.55) and (I.57), where the first factorial moment were denoted ν without any index.

that are emitted per collision [Bell 1965] (here "ordered" means that particles have been given a label). For the same reasons, the third factorial moment

$$\nu_3 = 3! \sum_{k \geqslant 0} \binom{k}{3} p_k \,, \qquad \text{where } \binom{k}{3} = \frac{k!}{3!\,(k-3)!} \tag{II.5}$$

represents the mean number of ordered particle triplets that are emitted at a collision, as 3! is the number of permutations that can be done between 3 labelled particles. More generally, for all $i \geqslant 1$, the factorial moment ν_i corresponds to the mean number of ordered sets of i particles that are emitted at a collision.

Example for a binary branching process **-** $\forall k \geqslant 3$**,** $p_k = 0$

$$\begin{cases} \nu_1 = p_1 + 2\,p_2 \\ \nu_2 = 2\,p_2 \\ \nu_i = 0, \qquad \forall i > 2 \end{cases} \tag{II.6}$$

At a collision, 1 pair is emitted with a probability p_2, and so, 2 ordered pairs are emitted with a probability p_2. As a consequence, the mean number of ordered pairs emitted at a collision is $2\,p_2$, which is exactly the value of ν_2.

II.1.2 The Birth and Death Process

The *Galton-Watson process* introduced in Chapter 1 has been already pointed out as being responsible for very strong fluctuations of the size of a population of individuals that can reproduce or die [Harris 1963; Athreya and Ney 2012a; Pázsit and Pál 2007]. In this section we work on a zero dimensional system, where we neglect the spatial displacements of the particles and consider the population as a whole. This simpler system is a good starting point to understand the origin of strong fluctuations in branching processes. We will then highlight a phenomenon called *critical catastrophe* by Williams [1974].

Consider a system in which we initially deposit N_0 particles that are then allowed to randomly reproduce or die with a rate λ, following the *Galton-Watson process* described in the first chapter (Sec. I.1.2): events occur with a rate λ; at each event, a random particle is absorbed and k new neutrons are emitted with a probability p_k. We neglect the spatial displacements of the particles and consider the population as a whole[2] (zero dimensional model). The total number $N(t)$ of particles in the system at time t is

[2] Either particles are not allowed to diffuse in the system, either we consider the whole system as a single point system (cf *point reactor*)

a random variable. We thus denote by $P(N,t)$ the probability of observing exactly N individuals in the system at time t. In order to characterise the fluctuations of the population size $N(t)$, we must compare the

mean size of the population $$\langle N(t) \rangle = \sum_{N \geqslant 0} N(t)\, P(N,t)\,, \tag{II.7}$$

to the fluctuations of the population around this mean, i.e. to the

variance $$\sigma^2(t) = \langle N^2(t) \rangle - \langle N(t) \rangle^2\,, \tag{II.8}$$

where $\langle N^2(t) \rangle = \sum_{N \geqslant 0} N^2\, P(N,t)$. For the zero dimensional model, we can show, thanks to the detailed balance, that the probability $P(N,t)$, obeys the master equation (A.13) (see Ann. 2) [Harris 1963]:

$$\frac{dP}{dt}(N,t) = -\lambda\, N\, P(N,t) + \sum_{i=0}^{N} \lambda_i\, (N+1-i)\, P(N+1-i,t)\,, \tag{II.9}$$

where $\lambda_i = \lambda p_i$ is the rate at which an event that gives rise to i new neutrons occurs in the system. We can then derive the equation for each moment of $N(t)$ using the definition $\langle N^k \rangle = \sum_{N \geqslant 0} N^k\, P(N,t)$. In particular, we get the equation verified respectively by the mean and the variance: Eq. (A.15) and (A.17) in the annex 2. Solving these equations yields the evolution in time of the mean number of particles in the system:

$$\langle N(t) \rangle = N_0\, e^{\lambda\,(\nu_1 - 1)\,t}\,, \tag{II.10}$$

and of the variance

$$\sigma^2(t) = \left[\frac{\nu_2}{(\nu_1 - 1)} - 1 \right] \left[\frac{\langle N(t) \rangle^2}{N_0} - \langle N(t) \rangle \right]\,, \tag{II.11}$$

with the initial conditions $\langle N \rangle(0) = N_0$ and $\sigma^2(0) = 0$. To characterise the behaviour of the total number of particles in the system, we can compare these two quantities in different ways:

- the *variance-to-mean ratio* (VMR) [Cox and Lewis 1966], also called *dispersion index* or *Fano factor* [Fano 1947],

  $$\mathrm{VMR}(t) = \frac{\sigma^2}{\langle N \rangle}(t)\,, \tag{II.12}$$

  gives an estimation of the dispersion of the random variable N, by comparison with a Poisson variable with the same mean[3] (for which

[3] The use of this comparison is easier to understand in the context of a spatially extended problem: starting from a uniform distribution of walkers in the system and dividing the space into small identical squares (quadrats), the random number N_i of particles in each quadrat will initially follow a Poisson law [Poisson and Schnuse 1841] (for which VMR = 1). It will then stay Poissonian in the case of Brownian walker/purely diffusing walker, i.e. the VMR will stay at 1. A VMR becoming significantly higher than 1 will denote a clustered distribution of particles in space [Houchmandzadeh 2009].

VMR $= 1$). In particular, the variable is said "over dispersed" if VMR > 1, and "under dispersed" if VMR < 1;

- the ratio between the standard deviation $\sigma(t)$ and the mean $\langle N(t)\rangle$, called *relative standard deviation* (RSD) or *coefficient of variation* [Everitt and Skrondal 2002]. Here we will use its square:

$$\mathrm{RSD}^2(t) = \frac{\sigma^2}{\langle N\rangle^2}(t) = \frac{\langle N(t)^2\rangle - \langle N(t)\rangle^2}{\langle N(t)\rangle^2}\,. \tag{II.13}$$

  If this ratio is larger then 1, the fluctuations of N around its mean are larger than the mean itself. In other words, the population size fluctuates between twice its mean and 0. Obviously, the death of the whole population is then very likely to happen. This is due to a fundamental asymmetry of the system: birth events can not happen anymore if the population size becomes 0, whereas a population that has doubled its size can still die later on.

Let us now see how these quantities behave in the different regimes defined in Eq. (I.27): subcritical, supercritical and critical.

Subcritical $\nu_1 < 1$ In this case,

$$\mathrm{RSD}^2(t) = \frac{1}{N_0}\left(1 + \frac{\nu_2}{(1-\nu_1)}\right)\left(e^{\lambda(1-\nu_1)\,t} - 1\right)\,, \tag{II.14}$$

grows exponentially with a characteristic time $\tau_{sub} = [\lambda(1-\nu_1)]^{-1}$. This observation is coherent with the evolution of the mean number of particles in the system that decreases with the same characteristic time, $\langle N\rangle(t) = N_0 \exp(-\lambda(1-\nu_1)\,t)$. The RSD^2 becomes thus larger than 1 for a time $\propto \ln(N_0/\nu_2)[\lambda(1-\nu_1)]^{-1}$, after which strong fluctuations of the system kill the whole population. The VMR, starting from 0, only increases in time with the characteristic time τ_{sub},

$$\mathrm{VMR}(t) = \left(1 + \frac{\nu_2}{1-\nu_1}\right)\left(1 - e^{-\lambda(1-\nu_1)\,t}\right)\,, \tag{II.15}$$

to saturate to a constant larger then 1[4].

[4]Note that in a spatially extended case, with an initial uniform distribution of particles, dividing the space into small identical squares, the random number N_i of particles in each quadrat is initially Poisson distributed, such that its $\mathrm{VMR}(0) = 1 \Leftrightarrow \sigma_0 = \sqrt{N_0}$. Then, starting the branching process, $\mathrm{VMR}(t)$ increases monotonically, so that the random variable N_i is always over-dispersed for any positive time $t > 0$.

Supercritical $\nu_1 > 1$ In this case, the variance to mean square ratio initially increases in time, to eventually saturate at large time to a constant

$$\mathrm{RSD}^2(t) = \frac{\nu_2 - (\nu_1 - 1)}{N_0(\nu_1 - 1)} \left(1 - e^{-\lambda(\nu_1 - 1)\, t}\right) \underset{t \to +\infty}{\longrightarrow} \frac{1}{N_0} \left[\frac{\nu_2}{(\nu_1 - 1)} - 1\right] . \tag{II.16}$$

Therefore fluctuations of the population size $N(t)$ can stay smaller than its mean or become larger than it[5], depending on this ratio. These fluctuations thus

- increase with the relative fluctuations of the number of particles emitted by collision, i.e., with the ratio of the mean number of pairs to the mean number of new particles created at a collision: $\nu_2/(\nu_1 - 1)$. The fluctuations thus increase with the process of pair production at a collision (parametrised by ν_2), but also when the system get closer to criticality ($\nu_1 \to 1$).

- decrease when the initial size N_0 of the population is increased.

The reproduction process tends to increase the fluctuations, whereas a larger initial population naturally decreases them. However, as the size of the whole population, given in Eq. (II.10), grows exponentially with time (which can compensate increasing fluctuations), this it not sufficient to fully characterise the dispersion of the population size. In fact, the variance-to-mean ratio also grows exponentially in time[6],

$$\mathrm{VMR}(t) = \left(\frac{\nu_2}{\nu_1 - 1} - 1\right) \left(e^{\lambda(\nu_1 - 1)\, t} - 1\right) , \tag{II.17}$$

so that the random variable N becomes significantly over-dispersed for large time.

Critical $\nu_1 = 1$**,** the mean number of particles in the system is constant, equal to

$$\langle N \rangle(t) = N_0 , \qquad \text{for all } t. \tag{II.18}$$

However, the VMR $\sim \lambda \nu_2\, t$ grows linearly: the number of particles in the system becomes highly dispersed with time. Furthermore, the relative standard deviation squared also grows linearly in time,

$$\mathrm{RSD}^2(t) = \frac{\sigma^2}{\langle N \rangle^2}(t) \sim \frac{\lambda \nu_2}{N_0} t . \tag{II.19}$$

[5]These fluctuations can explain why, in the case $\nu_1 > 1$, the probability that such a system "survives", i.e. $N(t) > 0$, at large time t can be strictly smaller than 1, even though $\langle N(t) \rangle$ grows [Harris 1963; Zoia et al. 2012a]. This probability is called *survival probability*. This argument will be seen more in details in Sec. II.3.3.b

[6]Note that $\frac{\nu_2}{\nu_1 - 1} > 2$

such that the RSD can become larger than 1. We thus expect an extinction of the whole population in a characteristic *extinction time*

Characteristic extinction time

$$\tau_E = \frac{N_0}{\lambda \nu_2}, \tag{II.20}$$

after which the variance σ becomes larger than the mean $\langle N \rangle$ (RSD > 1). This phenomenon was named "*critical catastrophe*" by Williams [1974]. Note that this time is longer for a larger initial population N_0, and is shorter for a faster reproduction process ($\lambda\nu_2$ is the rate at which pairs of particles are created in the system).

The existence of this finite extinction time may seem to contradict Eq. (II.18), which states that the mean number of particles is a constant. However, the average $\langle \cdot \rangle$ is taken over all realisations of the system (*ensemble average*): while most realisations will be empty at a time $t \geqslant \tau_E$, few others will have exploded, compensating for the empty ones, and thus resulting in a constant population size on average. This is the reason why representing the size of the population by its ensemble average seems to be particularly misleading here. In fact, a system where the ensemble average is representative of a single realisation is said *self-averaging*. In our system, the contradiction highlighted above indicates a failure of *self-averaging* [Young et al. 2001]: as a direct consequence, the knowledge of the mean becomes useless to characterise a single realisation of the system. We can thus question the appropriateness of the transport equations introduced in the first chapter in characterising the fluctuations of the system.

II.1.3 Limits of the usual transport equations to describe fluctuations

Let us keep on working with the zero-dimensional problem, and compare two quantities:

▷ the probability $P_1(t)$ to find one particle in the cell at time t, starting with a single particle in the cell at initial time, $P_1(0) = 1$;

▷ the mean number of particles in the cell at time t: $\langle N(t) \rangle$.

We then focus on two different systems: a first one (case *a.*), where particles can only be absorbed (without birth), and a second one (case *b.*), where particles can reproduce or die, like in the previous system.

a. Without particle birth

Following the lines of Annex 2, the master equation for a system where particles can only die, with a rate λ_0, is

$$\frac{dP_N}{dt}(t) = -\lambda_0 N\, P_N(t) + \lambda_0 (N+1) P_{N+1}(t)\,. \tag{II.21}$$

On one hand, starting the system with a single particle, we have that $P_N(t) = 0$ for all $N > 1$, and obtain for $P_1(t)$:

$$\frac{dP_1}{dt}(t) = -\lambda_0 P_1(t)\,. \tag{II.22}$$

The variation of the probability $P_1(t)$ is due to the death of the initial single particle of the system, which happens with a rate λ_0. On the other hand, the equation for the mean number of particles can be extracted directly from the master equation (II.21), using the definition $\langle N(t) \rangle = \sum_{N \geqslant 0} N\, P_N(t)$:

$$\frac{d\langle N \rangle}{dt}(t) = -\lambda_0 \langle N \rangle(t)\,. \tag{II.23}$$

In this simple system, we observe that the mean number of particles $\langle N \rangle$ and the probability P_1 (of finding one particle in the system, starting with a single particle) obey the same time evolution equation.

Adding diffusion in the problem – we consider an homogeneous system where particles can die and diffuse (with constant speed and isotropic scattering), as described at the end of Sec. (I.2.5) – we know already that the density of particles in the system is given by the diffusion equation (I.116) without the fission source term:

$$\frac{\partial}{\partial t} n(\mathbf{r}, t) - D\Delta n(\mathbf{r}, t) + \lambda_c n(\mathbf{r}, t) = 0\,, \tag{II.24}$$

where λ_c is the rate at which particles are captured ($\lambda_c = v\,\Sigma_c$ for particles with finite speed v). Consider now the probability density $p(\mathbf{r}, t)$ of finding a particle in the vicinity of $\mathbf{r}$ at time t in the system. This probability density is known to obey the Fokker-Planck equation for Brownian motion with no drift and with absorption [Kadanoff 2000], which is exactly the same equation than Eq. (II.24). The density $n(\mathbf{r}, t)$ and the probability density $p(\mathbf{r}, t)$ thus follow exactly the same equation. The same correspondence exists in the case of particles performing exponential flight (described in the first chapter): in absence of branching, the evolution equation for the probability density $p(\mathbf{r}, \mathbf{v}, t)$ to find a particle in the vicinity of the phase-space position $(\mathbf{r}, \mathbf{v})$ can be obtained using exactly the same detailed balance realised in Sec. I.2.1 to obtain the equation for the density in the phase space

$n(\mathbf{r}, \mathbf{v}, t)$. As a consequence, the two equations (for p and for n) are identical, both given by the transport Eq. (I.54) without the fission term.

In these three examples (zero dimensional problem, diffusion and exponential walks), the density n and the probability density p (mean $\langle N \rangle$ and probability P_1 for the first example) follow the same equation. In fact, this is always the case for a process with particles that can diffuse and die, without branching. Moreover, the initial density of particles can be related to the initial probability density of particles in the system: $\langle N(0) \rangle = N_0 P_1(0)$ for the zero-dimension case, $n(\mathbf{r}, 0) = N_0 p(\mathbf{r}, 0)$ for the Brownian motion, and $n(\mathbf{r}, \mathbf{v}, 0) = N_0 p(\mathbf{r}, \mathbf{v}, 0)$ for the exponential flight. Solving, in each case, for the time course of n and p with the above respective initial conditions, we obtain for all t,

$$\begin{cases} \langle N \rangle(t) = N_0 P_1(t)\,, & \text{for the zero-dimensional case;} \\ n(\mathbf{r}, t) = N_0 p(\mathbf{r}, t)\,, & \text{for Brownian motion;} \\ n(\mathbf{r}, \mathbf{v}, t) = N_0 p(\mathbf{r}, \mathbf{v}, t)\,, & \text{for exponential flights,} \end{cases} \tag{II.25}$$

i.e. that mean and probability are simply proportional. For this reason, in the three cases mentioned above, the mean quantities ($\langle N \rangle$, $n(\mathbf{r}, t)$ and $n(\mathbf{r}, \mathbf{v}, t)$) can be given a probabilistic interpretation, and the particle behaviour in the system is, as a consequence, well represented by them.

b. With birth of particles

Let us now consider the simplest branching process, called *binary branching process*, where particles can die, with a rate $\lambda_0 = \lambda p_0$, or replicate, with a rate $\lambda_2 = \lambda p_2$ (the initial particle is absorbed, giving birth to two new particles, resulting in a net increase of one particle in the system). For this binary branching process, for all $i > 2$, $\lambda_i = \lambda p_i = 0$, and the master equation (II.9) gives for $P_1(t)$,

$$\frac{dP_1}{dt}(t) = -(\lambda_0 + \lambda_2)P_1(t) + 2\lambda_0 P_2(t)\,, \tag{II.26}$$

whereas the equation for the mean number of particles in the system Eq. (A.15) becomes

$$\frac{d\langle N \rangle}{dt}(t) = (\lambda_2 - \lambda_0)\langle N \rangle(t)\,. \tag{II.27}$$

The time evolution equation for the probability P_1 is thus very different from the equation for the mean number of particles $\langle N \rangle$. Furthermore the equation for P_1 is in fact coupled to the equation for $P_2(t)$:

$$\frac{dP_2}{dt}(t) = -2(\lambda_0 + \lambda_2)P_2(t) + 3\lambda_0 P_3(t) + \lambda_2 P_1(t)\,, \tag{II.28}$$

which is coupled to the equation for $P_3(t)$, etc. The equation for P_1 is thus associated to a hierarchy of coupled equations, all given by Eq. (II.9).

c. Conclusion

In a system where particles can only move or die, the particle density is a relevant tool to understand the behaviour of the whole population, in that it is directly proportional to the probability density of particles. However, adding branching to the system significantly alters its behaviour, breaking the link between density and probability density that exists in the absence of branching. In particular, the *critical catastrophe* highlighted by Williams and the "non *self-averaging* property" of the system are some of the consequences of this peculiarity of branching systems.

The "non *self-averaging*" property of the system is enhanced when the number of particles gets smaller. For most applications in reactor physics, the neutron population in a nuclear reactor is sufficiently large (10^8 n/cm^3 in a PWR at operating condition [Duderstadt and Hamilton 1976]) for the neutron density to give a good characterisation of the neutron population and of its dynamics within the reactor core. Thanks to the large number of neutrons, fluctuations around the mean remain relatively small. In theses cases, it is meaningful to use the classical transport equations (such as the Boltzmann equation (I.55)) to predict the behaviour of the neutron population in the reactor core, even though they are equations for the density of particles, and not for the probability density.

However, as we have just seen, the branching process that is inherent to the fission chain is at the origin of strong fluctuations, which increase when the system is closer to criticality (see Eq. (II.16)). In fact it is known that there exist some situations for which the knowledge of the mean or the variance provides an incomplete description of the state of the neutron population [Prinja 2012], as illustrated by the example of the clustering phenomenon in Sec. I.3.1. For these cases, we need a better description of the system, which, for instance, can be provided by the probability density function of finding a particle at a given position in the system.

In the following we will attempt to give a deterministic description of the fluctuations in the system. For this purpose, a forward or a backward approach can be adopted. Whereas a forward description of a branching process would provide an infinite family of coupled equations (see for instance Eq. (II.21) in the previous section), a backward description would give a single equation containing a non linear term [Prinja 2012]. In this chapter, will focus on establishing the backward equations for every moments of interesting quantities in the field of reactor physics, using a for-

malism known as *Feynman-Kac formalism* [Kac 1949; Zoia et al. 2012b].

2 Feynman-Kac Backward Equations

A central question for reactor physics, and for random walks in general, is to determine the occupation statistics of the stochastic paths in a given region V of the space [Condamin et al. 2007; Grebenkov 2007; Berezhkovskii et al. 1998; Agmon 2011; Bénichou et al. 2005]. In this context, the two natural observables of the system are the total length[7] l_V travelled by neutrons in V and the number n_V of collisions occurred in V during a certain time [Spanier and Gelbard 1969; Lux and Koblinger 1991; Blanco and Fournier 2006; Mazzolo 2004; Zoia et al. 2011]. In reactor physics, for instance, the knowledge of the mean length $\langle\, l_V \,\rangle$ allows assessing the neutron flux due to the chain reaction, and thus the deposited power, whereas the mean number of collision $\langle\, n_V \,\rangle$ allows assessing the reaction rate, and thus to the number of radiation-induced structural defects [Pázsit and Pál 2007; Bell and Glasstone 1970]. In this section, we will see how to establish backward evolution equations for every moment of l_V; other quantities of interest will then be studied in the next section. For this purpose, we will closely follow the derivation of [Zoia et al. 2012b] valid for systems with homogeneous medium, with constant particle speed and isotropic scattering, and extend their result by relaxing these constraints.

II.2.1 "Backward" quantities

a. Definitions

Consider one neutron starting from $(\mathbf{r}_0, \mathbf{v}_0)$ at time $t = 0$. The total length that this neutron and all its descendants travel up to a time t in a subvolume V of the system is the length $l_V(t \,|\, \mathbf{r}_0, \mathbf{v}_0)$ introduced above. This quantity is a stochastic variable that depends on the realisation of the walk of each neutron. By definition it can be computed, for one realisation of the branching random walk, as the sum of the length travelled in V by each paths of the branching trajectory:

$$l_V(t \,|\, \mathbf{r}_0, \mathbf{v}_0) = \sum_{\text{every path}} \int_0^t \mathbb{1}_V\big[\mathbf{r}(t')\big]\, v(t')\, dt' \,, \tag{II.29}$$

where t is the observation time and $\mathbb{1}_V[\mathbf{r}]$ is the *marker function* of the region V

$$\mathbb{1}_V[\mathbf{r}] = \begin{cases} 1 & \text{for } \mathbf{r} \in V \,, \\ 0 & \text{elsewhere} \,. \end{cases} \tag{II.30}$$

[7] Here we are essentially focusing on walks with finite velocities. In the case of walks with infinite velocity (Brownian motion, Lévy flight), the residence time is a better observable than the total length l_V.

The length $l_V(t\,|\,\mathbf{r}_0,\mathbf{v}_0)$, resulting from a single neutron emitted in $(\mathbf{r}_0,\mathbf{v}_0)$ at $t=0$, contributes to the total length $l_V(t\,|\,S_0)$ resulting from an initial source S_0 of neutrons in the system:

$$l_V(t|S_0) = \int_{S_0} d^3\mathbf{r}_0\, d^3\mathbf{v}_0\, l_V(t|\mathbf{r}_0,\mathbf{v}_0)\, S_0(\mathbf{r}_0,\mathbf{v}_0)\,, \tag{II.31}$$

where $S_0(\mathbf{r}_0,\mathbf{v}_0)$ denotes the distribution of the initial source of neutrons. Clearly, $l_V(t\,|\,S_0)$ is also a random variable. Its mean over the different realisations of the system, denoted $\langle\, l_V\,\rangle\,(t|S_0)$, is commonly used in the field of Monte Carlo simulations of nuclear reactors, where it is called *track-length estimator* [Lux and Koblinger 1991]. By definition, $\langle\, l_V\,\rangle\,(t|S_0)$ is related to neutron angular flux $\varphi_{S_0}(\mathbf{r},\mathbf{v},t)$ resulting from an initial source S_0 of neutrons, through[8] the integrals [Zoia et al. 2012b]:

$$\langle\, l_V\,\rangle(t|S_0) = \int_0^t dt \int_V d^3\mathbf{r} \int_{4\pi} d^2\boldsymbol{\omega} \int_0^{+\infty} dv\, \varphi_{S_0}(\mathbf{r},\boldsymbol{\omega},v,t)\,. \tag{II.32}$$

The symbol $\langle\cdot\rangle$ denotes the *ensemble average*, which is an average over all the possible realisations of the system. For instance, $\langle\, l_V(t|\mathbf{r}_0,\mathbf{v}_0)\,\rangle$ is the average of $l_V(t|\mathbf{r}_0,\mathbf{v}_0)$ over all the possible paths that the initial neutron and its descendants can take.

b. Forward vs Backward quantities

In Eq. (II.32), taking a point source $S_0 \equiv (\mathbf{r}_0,\mathbf{v}_0)$, the quantity $\langle\, l_V\,\rangle(t\,|\,\mathbf{r}_0,\mathbf{v}_0)$ is expressed as the integral of a *forward quantity*: the flux $\varphi_{S_0}(\mathbf{r},\mathbf{v},t)$ resulting from a point source in $(\mathbf{r}_0,\mathbf{v}_0)$. $\langle\, l_V\,\rangle$ can thus be given a "*forward*" interpretation: it is the mean total length travelled in V up to time t, with, for initial condition, a point source in $(\mathbf{r}_0,\mathbf{v}_0)$ at time $t=0$. However, a "*backward*" interpretation can be more natural for $\langle\, l_V\,\rangle$, as it can be seen as the mean total length travelled in V as *a function of* the initial position and direction of the first neutron:

$$\langle\, l_V\,\rangle(t|\mathbf{r}_0,\mathbf{v}_0) \doteq \underbrace{\langle\, l_V\,\rangle(\mathbf{r}_0,\mathbf{v}_0,t)}_{\text{backward notation}}\,, \tag{II.33}$$

This is in fact true for the stochastic variable $l_V(\mathbf{r}_0,\mathbf{v}_0,t)$ and for each of its moments $\langle\, l_V^m\,\rangle(\mathbf{r}_0,\mathbf{v}_0,t)$, that we will denote:

Moment of order m $$L_m(\mathbf{r}_0,\mathbf{v}_0,t) \doteq \langle\, l_V^m(\mathbf{r}_0,\mathbf{v}_0,t)\,\rangle\,, \tag{II.34}$$

Each moment[9] $\langle\, l_V^m\,\rangle(\mathbf{r}_0,\mathbf{v}_0,t)$ will thus satisfy a *backward equation*, with, for final condition, the region V ("detector") where the length l_V is estimated (see Fig. II.1b).

[8] $\varphi_{S_0}(\mathbf{r},\mathbf{v},t)\,d^3\mathbf{r}\,d^3\mathbf{v}\,dt$ is the total length travelled by neutrons of the system in the volume element $d^3\mathbf{r}\,d^3\mathbf{v}$ during the time interval dt, and $\mathbf{v} = v\,\boldsymbol{\omega}$.

[9] The probability density function of the total length l_V also satisfy a backward equation.

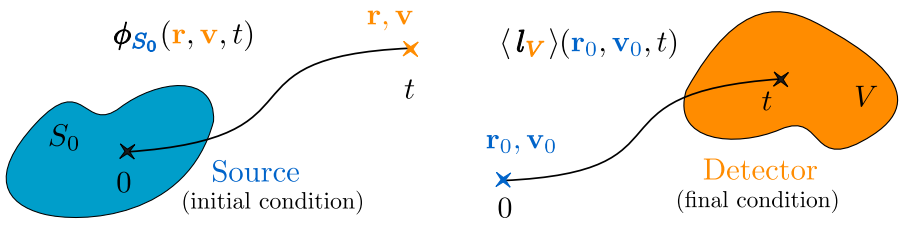

(a) Forward **(b)** Backward

Figure II.1: Forward vs backward quantities

Forward vs Backward quantities

$\langle \, l_V \, \rangle(\mathbf{r}_0, \mathbf{v}_0, t)$ can be seen as a backward quantity, in contrast with the forward quantity $\varphi_{S_0}(\mathbf{r}, \mathbf{v}, t)$.

Forward quantity $\quad \varphi_{S_0}(\mathbf{r}, \mathbf{v}, t)$

Solution of a forward differential equation,
$\longrightarrow$ integrated on a source S_0 (initial conditions);
$\longrightarrow$ which gives the quantity φ_{S_0} at time t as a function of the arrival positions $(\mathbf{r}, \mathbf{v})$ in the phase-space.

Backward quantity $\quad \langle \, l_V \, \rangle(\mathbf{r}_0, \mathbf{v}_0, t)$

Solution of a backward differential equation,
$\longrightarrow$ integrated on a detector V (final conditions);
$\longrightarrow$ which gives the quantity $\langle \, l_V \, \rangle$ at time t as a function of the starting positions $(\mathbf{r}_0, \mathbf{v}_0)$ in the phase-space.

In the context of nuclear reactor physics, the *track-length estimator* $\langle \, l_V \, \rangle$ is computed with a Monte Carlo simulation (for instance with the Tripoli-4® code developed at the CEA Saclay [Brun et al. 2011, 2013]). On the other hand, thanks to Eq. (II.32), $\langle \, l_V \, \rangle$ is directly related to the neutron flux φ_{S_0}, which can also be assessed by solving numerically the Boltzmann equation (I.55), with a deterministic simulation. However, as pointed out in the last section, due to the branching process, the Boltzmann equation does not contain any further information about the higher moments of l_V (as it is intrinsically an equation for averaged observables). Thus, whereas higher moments of l_V can be obtained by Monte Carlo simulation, we have not introduced yet any corresponding equations for them, which could be indeed useful for characterising the behaviour of the fluctuations in the system through deterministic numerical simulation.

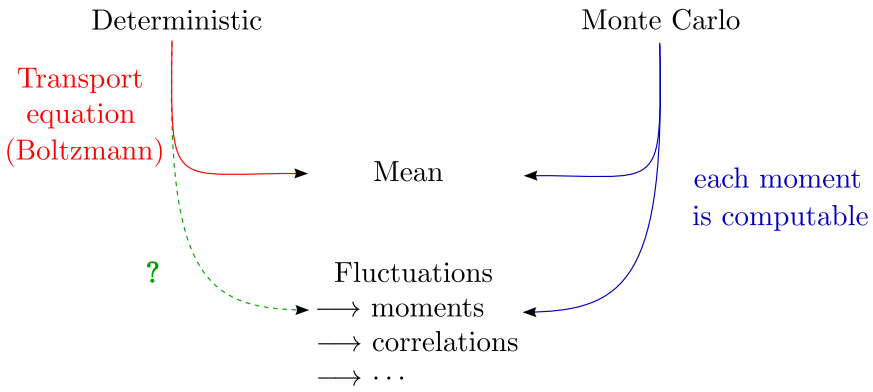

To go beyond the average description, we need another formalism that will allow us to compute all the moments of l_V. This can be achieved with the Feynman-Kac formalism [Zoia et al. 2012b], which allows us to derive a backward equation for each moment of l_V, called *backward Feynman-Kac equation*.

Numerical Simulation in Reactor Physics

Deterministic simulations solve the transport equation for the whole neutron population [CEA collectif et al. 2013].

⟶ *advantages*: fast; can simulate the behaviour of the whole population of neutrons in a reactor core.

⟶ *disadvantages*: approximation due to the discretisation and to the modelisation chosen for the simulation.

Monte Carlo Simulations simulate the physics of the system at a microscopic scale by following the history of each neutron in the system [CEA collectif et al. 2013].

⟶ *advantages*: - no need for discretisation, they simulate directly the physics of the system. Thus, neutrons can be followed continuously in energy, and the simulations can take into account 3-dimensional systems with any type of geometry, such as, in particular, stochastic media. Representative of the physics of the system, they are considered as reference codes.

⟶ *disadvantages*: - Time consuming, indeed the statistical convergence of Monte Carlo simulations is very slow compared to the convergence of deterministic simulations.
- Memory intensive, as the history of each individual neutron is followed. To give an idea, a PWR at operating condition generates 10^{19} neutrons per second [CEA collectif et al. 2013], which can not be simulated with the power of current computers.
- Not ready yet for simulations of neutron transport out of equilibrium, nor for the computation of the *adjoint flux* [CEA collectif et al. 2013].

> These two types of simulations should be seen as complementary rather than competing. Indeed, for instance, deterministic simulations can provide tools to accelerate Monte Carlo simulations (for example with a method of *importance sampling* [Krauth 2006]). Inversely, Monte Carlo simulations are already used as reference codes to *validate* deterministic simulations [CEA collectif et al. 2013]. They can also be used to adapt real nuclear data for the purpose of discretisation in deterministic simulations [CEA collectif et al. 2013].

II.2.2 Feynman-Kac formalism

The total length $l_V(\mathbf{r}_0, \mathbf{v}_0, t)$ travelled in V up to a time t is a stochastic variable. Ideally, one would like to derive an equation for the probability density function of $l_V(t, \mathbf{r}_0, \mathbf{v}_0)$. However, this equation is particularly hard to obtain directly. A solution is to establish an equation for the moment generating function [Grimmett and Stirzaker 2001]

moment generating function
$$Q_t(s|\mathbf{r}_0, \mathbf{v}_0) = \left\langle e^{-s\, l_V(\mathbf{r}_0, \mathbf{v}_0, t)} \right\rangle , \tag{II.35}$$

from which each moment can be directly obtained by derivation[10]:

$$L_m(\mathbf{r}_0, \mathbf{v}_0, t) = (-1)^m \left. \frac{\partial^m Q_t(s \,|\, \mathbf{r}_0, \mathbf{v}_0)}{\partial\, s^m} \right|_{s=0} . \tag{II.36}$$

In this section, we will derive the backward equation for $Q_t(s \,|\, \mathbf{r}_0, \mathbf{v}_0)$ by closely following the lines of [Zoia et al. 2012b]. The approach that they take was originally proposed by Kac for Brownian motion [Kac 1949] and is based on the Feynman path integral formalism [Zoia et al. 2012b], such that it is commonly called *Feynman-Kac formalism*. This method applies more generally to continuous-time Markov processes [Kac 1951; Majumdar 2005] and has been recently extended to non-Markovian walks [Turgeman et al. 2009]. The derivation of [Zoia et al. 2012b] was done for systems that are homogeneous, with isotropic scattering and where particles evolve with a constant speed only. However, in realistic situations, the physical parameters characterising the neutron transport process, such as the cross-sections and the moments ν_k, depend on the position and the energy of the neutrons, and the scattering angular distribution is often strongly anisotropic [Bell and Glasstone 1970]. Here we will relax the constraint on the isotropy of the scattering kernel, introduce speed and space dependent cross-sections, and consider particles with non-constant speed.

[10] In the following, we will keep the notation $L \doteq L_1$ for the first moment (mean of l_V).

a. The system

In this section we will first use the general notation of branching exponential walks introduced in Sec. I.1.2.c. to derive the backward equation for the moment generating function. As moment equations can be useful for the purpose of numerical simulations in reactor physics, we will work on systems as realistic as possible, considering (see Fig. II.2)

▷ that particle speeds are non constant and can change at each collision;

▷ an inhomogeneous background material: $\Sigma(\mathbf{r}, v)$, $p_k(\mathbf{r}, v)$, $\nu(\mathbf{r}, v)$;

▷ anisotropic scattering: $C(\mathbf{v} \to \mathbf{v}')$.

Finally, we will adapt more specifically the final equations to the field of reactor physics, using the change of notation Eq. (I.28).

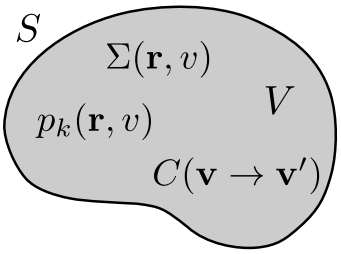

Figure II.2: The system of interest can be inhomogeneous, with anisotropic scattering, and neutron speed is not necessarily constant.

b. How to establish a backward equation?

In general, we are used to work with forward equations, that we establish by building the forward quantity at time $t + dt$ from the one at time t following the evolution of the process between t and $t + dt$ (see Fig. II.3a). Backward equations are not as commonly used. In the previous section, the differences between forward and backward quantities were stressed. Let us see now how to build a backward equation; this is illustrated in Figure II.3b.

$Q_t(s|\mathbf{r}'_0, \mathbf{v}'_0)$ denotes the moment generating function observed at time $t_0 + t$ for one neutron emitted from $(\mathbf{r}'_0, \mathbf{v}'_0)$ at an arbitrary time t_0. Setting $t_0 = dt$, this quantity can be related to the moment generating function $Q_{t+dt}(s|\mathbf{r}_0, \mathbf{v}_0)$ observed at time $t + dt$ for one neutron emitted from $(\mathbf{r}_0, \mathbf{v}_0)$ at time 0. For this purpose, we need to understand how one neutron can be emitted in $\mathbf{r}'_0, \mathbf{v}'_0$ at time dt as a result of one neutron emitted in $\mathbf{r}_0, \mathbf{v}_0$ at time $t = 0$ (see Fig. II.3b). Note that all of this is possible thanks to the Markovian property of the process we are interested in: the branching

random walk performed by neutrons, described in Sec. I.1.2. Thanks to this property, $Q_t(s|\mathbf{r}'_0, \mathbf{v}'_0)$ is independent on the history of the particle before the "start" at the position $(\mathbf{r}'_0, \mathbf{v}'_0)$ [Pázsit and Pál 2007].

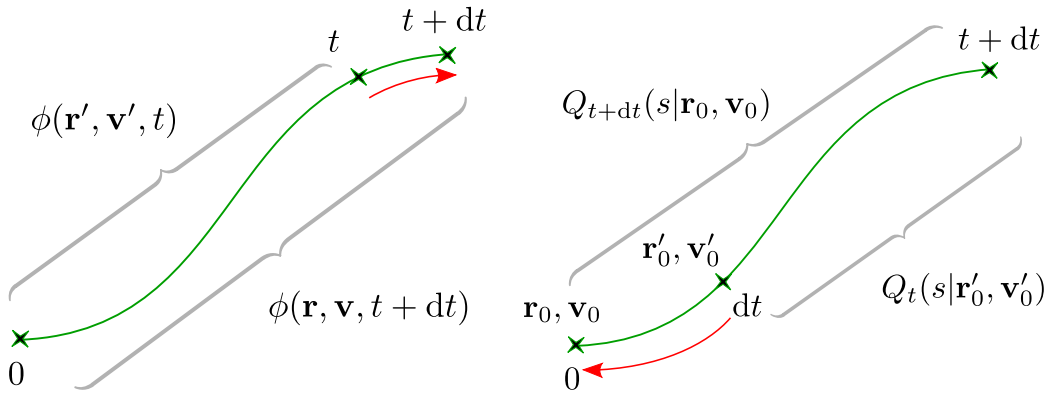

(a) Forward **(b)** Backward

Figure II.3: Conceptual scheme of the differences in construction of forward (a) and backward (b) equations.

c. Backward equation for the moment generating function

In order to relate $Q_t(s|\mathbf{r}'_0, \mathbf{v}'_0)$ to $Q_{t+\mathrm{d}t}(s|\mathbf{r}_0, \mathbf{v}_0)$ for a small $\mathrm{d}t$, we need to understand exactly what happened between $t = 0$ and $\mathrm{d}t$. Let us detail the different possible histories for a single neutron emitted in $\mathbf{r}_0, \mathbf{v}_0$ to arrive in $\mathbf{r}'_0, \mathbf{v}'_0$ at a time $\mathrm{d}t$ later:

(a) with probability $1 - \Sigma(\mathbf{r}_0, v_0)\, v_0\, \mathrm{d}t$, **the neutron does not interact with the medium** and goes straight with a constant speed v_0, from $\mathbf{r}_0$ to $\mathbf{r}_0 + \mathrm{d}\mathbf{r}_0 = \mathbf{r}_0 + \mathbf{v}_0\, \mathrm{d}t$ (see Fig. II.4a);

(b) with probability $\Sigma(\mathbf{r}_0, v_0)\, v_0\, \mathrm{d}t$, **the neutron undergoes a collision in $\mathbf{r}_0$** giving then rise to k neutrons with probability p_k (see Fig. II.4b).

Case (a) - the particle does not interact with the medium (see Fig. II.4a) The total length travelled in V from the start to $t + \mathrm{d}t$ can be decomposed in two terms,
$\longrightarrow$ the length travelled until $\mathrm{d}t$ by the first neutron (in yellow on the figure), performing a straight line with a constant speed v_0, i.e. a length $\mathbb{1}_V(\mathbf{r}_0)\, v_0\, \mathrm{d}t$;
$\longrightarrow$ the length travelled from $\mathrm{d}t$ to $t + \mathrm{d}t$ by the first neutron and its descendants, starting from $(\mathbf{r}'_0, \mathbf{v}'_0) = (\mathbf{r}_0 + \mathrm{d}\mathbf{r}_0, \mathbf{v}_0)$ at time $\mathrm{d}t$ (in green on the figure), i.e. the length $l_V(\mathbf{r}_0 + \mathrm{d}\mathbf{r}_0, \mathbf{v}_0, t)$;

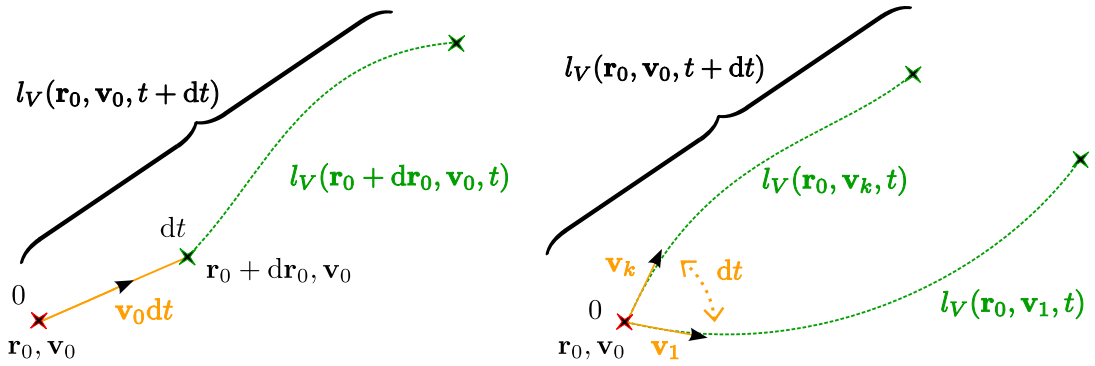

(a) Straight line **(b)** Branching

Figure II.4: Different possible histories for a neutron during dt.

Thus the total length reads:

$$l_V(\mathbf{r}_0, \mathbf{v}_0, t+dt) = \underbrace{\mathbb{1}_V(\mathbf{r}_0)\, v_0\, dt}_{\text{travelled in } V \text{ by the 1rst neutron}} + l_V(\mathbf{r}_0+d\mathbf{r}_0, \mathbf{v}_0, t)\,. \quad \text{(II.37)}$$

Using the definition Eq. (II.35), the contribution to $Q_{t+dt}(s|\mathbf{r}_0, \mathbf{v}_0)$ due to case (a) is therefore

$$\begin{aligned} Q^a_{t+dt}(s|\mathbf{r}_0, \mathbf{v}_0) &= \big(1 - v_0\, \Sigma(\mathbf{r}_0, \mathbf{v}_0)\, dt\big)\, e^{-s\, v_0\, \mathbb{1}_V(\mathbf{r}_0)\, dt} \left\langle\, e^{-s\, l_V(\mathbf{r}_0+d\mathbf{r}_0, \mathbf{v}_0, t)} \,\right\rangle \\ &= \big(1 - v_0\, \Sigma(\mathbf{r}_0, \mathbf{v}_0)\, dt\big)\, e^{-s\, v_0\, \mathbb{1}_V(\mathbf{r}_0)\, dt}\; Q_t(s|\mathbf{r}_0+d\mathbf{r}_0, \mathbf{v}_0) \end{aligned} \quad \text{(II.38)}$$

Case (b) - the particle interacts with the medium In this case, the initial particle is absorbed in $\mathbf{r}_0$, the length thus travelled in V between 0 and dt is zero. Then, with a probability $p_k(\mathbf{r}_0, v_0)$, k particles are emitted with velocities $\{\mathbf{v}_i\}_{0\leqslant i\leqslant k}$, such that l_V is equal to the sum of the total length travelled by each of these new particles and their descendants (see Fig. II.4b). Therefore,

with probability p_0, $\quad l_V(\mathbf{r}_0, \mathbf{v}_0, t+dt) = 0$
with probability p_1, $\quad l_V(\mathbf{r}_0, \mathbf{v}_0, t+dt) = l_V(\mathbf{r}_0, \mathbf{v}_1, t)$
with probability p_2, $\quad l_V(\mathbf{r}_0, \mathbf{v}_0, t+dt) = l_V(\mathbf{r}_0, \mathbf{v}_1, t) + l_V(\mathbf{r}_0, \mathbf{v}_2, t)$
with probability p_k, $\quad l_V(\mathbf{r}_0, \mathbf{v}_0, t+dt) = l_V(\mathbf{r}_0, \mathbf{v}_1, t) + \cdots + l_V(\mathbf{r}_0, \mathbf{v}_k, t)$

where the velocities $\{\mathbf{v}_i\}_{0\leqslant i\leqslant k}$ are given by the pdf $C(\mathbf{v}_0 \to \mathbf{v}_i)$.

Thus, for example, the contribution to $Q_{t+dt}(s|\mathbf{r}_0, \mathbf{v}_0)$ due to the creation of 1 new particle in $\mathbf{r}_0$ during dt is

$$Q^{b,k=1}_{t+dt}(s|\mathbf{r}_0, \mathbf{v}_0) = \big(v_0\, \Sigma(\mathbf{r}_0, \mathbf{v}_0)\, dt\big)\; p_1\; \langle\, Q_t(s|\mathbf{r}_0, \mathbf{v}_1)\,\rangle_{\mathbf{v}_1}\,, \quad \text{(II.39)}$$

using the definition $Q_t(s|\mathbf{r}_0,\mathbf{v}_1) = \left\langle\, e^{-s\, l_V(\mathbf{r}_0,\mathbf{v}_1,t)} \,\right\rangle$. The expectation $\langle\cdot\rangle_{\mathbf{v}_1}$ denotes an average over all possible velocities $\mathbf{v}_1$ of the particle leaving the collision. Similarly, the contribution due to the creation of k new particles in $\mathbf{r}_0$ involves a term of the form:

$$\begin{aligned}\left\langle\, e^{-s\, l_V(\mathbf{r}_0,\mathbf{v}_1,t)} \cdots e^{-s\, l_V(\mathbf{r}_0,\mathbf{v}_k,t)} \,\right\rangle &= \left\langle\, e^{-s\, l_V(\mathbf{r}_0,\mathbf{v}_1,t)} \,\right\rangle \left\langle\, \cdots \,\right\rangle \left\langle\, e^{-s\, l_V(\mathbf{r}_0,\mathbf{v}_k,t)} \,\right\rangle \\ &= Q_t(s|\mathbf{r}_0,\mathbf{v}_1) \cdots Q_t(s|\mathbf{r}_0,\mathbf{v}_k) \qquad \text{(II.40)}\end{aligned}$$

where the expectation of the product becomes the product of the expectations, as it is assumed that descendant particles are independent. Furthermore the velocities of the descendants are independent, all given by the same pdf $C(\mathbf{v}_0 \to \mathbf{v}_1)$, such that we can successively write:

$$\begin{aligned}Q^{b,k}_{t+dt}(s|\mathbf{r}_0,\mathbf{v}_0) &= \big(v_0\,\Sigma(\mathbf{r}_0,v_0)\,dt\big)\; p_k \,\langle\, Q_t(s|\mathbf{r}_0,\mathbf{v}_1) \cdots Q_t(s|\mathbf{r}_0,\mathbf{v}_1) \,\rangle_{\mathbf{v}_1\cdots\mathbf{v}_k}, \\ &= \big(v_0\,\Sigma(\mathbf{r}_0,v_0)\,dt\big)\; p_k \,\langle\, Q_t(s|\mathbf{r}_0,\mathbf{v}_1) \,\rangle_{\mathbf{v}_1} \cdots \langle\, Q_t(s|\mathbf{r}_0,\mathbf{v}_1) \,\rangle_{\mathbf{v}_k}, \\ &= \big(v_0\,\Sigma(\mathbf{r}_0,v_0)\,dt\big)\; p_k \,\big(\langle\, Q_t(s|\mathbf{r}_0,\mathbf{v}_1) \,\rangle_{\mathbf{v}_1}\big)^k. \qquad \text{(II.41)}\end{aligned}$$

The expectation $\langle\, Q_t \,\rangle_{\mathbf{v}_1}$ over the random velocity $\mathbf{v}_1$ of the leaving particle is given by the integral over $\mathbf{v}_1$ weighted by the adjoint probability density $C^*(\mathbf{v}_1 \to \mathbf{v}_0\,|\,\mathbf{r}_0)$, conjugate of the collision probability density $C(\mathbf{v}_0 \to \mathbf{v}_1\,|\,\mathbf{r}_0)$ [Dynkin 1965]:

$$\begin{aligned}\langle\, Q_t \,\rangle_{\mathbf{v}_1}(s|\mathbf{r}_0,\mathbf{v}_0) &= \iiint d^3\mathbf{v}_1 C^*(\mathbf{v}_1 \to \mathbf{v}_0|\mathbf{r}_0)\, Q_t(s|\mathbf{r}_0,\mathbf{v}_1)\,, \qquad \text{(II.42)} \\ &= \mathcal{C}^*\big[Q_t\big](s|\mathbf{r}_0,\mathbf{v}_0)\,. \qquad \text{(II.43)}\end{aligned}$$

where we defined the *adjoint collision operator* $\mathcal{C}^*[\cdot]$ associated to C^*[11]. Therefore, the contribution due to the creation of k new particles in $\mathbf{r}_0$ is:

$$Q^{b,k}_{t+dt}(s|\mathbf{r}_0,\mathbf{v}_0) = \big(v_0\,\Sigma(\mathbf{r}_0,v_0)\,dt\big)\; p_k \left(\mathcal{C}^*\big[Q_t\big]\right)^k(s|\mathbf{r}_0,\mathbf{v}_0)\,. \qquad \text{(II.44)}$$

Differential equation The final expression for $Q_{t+dt}(s|\mathbf{r}_0,\mathbf{v}_0)$ resulting from all these contributions is

$$\begin{aligned}Q_{t+dt}(s|\mathbf{r}_0,\mathbf{v}_0) = &\underbrace{\big(1 - v_0\,\Sigma(\mathbf{r}_0,v_0)\,dt\big)\, e^{-s\,v_0\,\mathbb{1}_V(\mathbf{r}_0)\,dt}\; Q_t(s|\mathbf{r}_0 + d\mathbf{r}_0,\mathbf{v}_0)}_{\text{transport } \mathbf{r}_0 \to \mathbf{r}_0 + d\mathbf{r}_0} \\ &+ \underbrace{\big(v_0\,\Sigma(\mathbf{r}_0,v_0)\,dt\big)\; G\Big(\mathcal{C}^*\big[Q_t(s|\mathbf{r}_0,\mathbf{v}_0')\big]\Big)}_{\text{collision in } \mathbf{r}_0}, \qquad \text{(II.45)}\end{aligned}$$

[11] Note that the backward collision operator defined here, is not a proper backward version of the forward collision operator defined in Eq. (I.46), as the parameter ν_1 appearing in Eq. (I.46) is not taken into account here.

where G is the generating function of the descendant number k:

$$G[z] = \sum_{k \geqslant 0} p_k \, z^k \, . \tag{II.46}$$

An expansion in the leading order in dt of the transport term, with $d\mathbf{r}_0 = \mathbf{v}_0 dt$,

$$\begin{cases} e^{-s\, v_0 \, \mathbb{1}_V(\mathbf{r}_0)\, dt} = 1 - s\, v_0\, \mathbb{1}_V(\mathbf{r}_0)\, dt + O(dt^2) \\ Q_t(s|\mathbf{r}_0 + d\mathbf{r}_0, \mathbf{v}_0) = Q_t(s|\mathbf{r}_0, \mathbf{v}_0) + v_0\, \boldsymbol{\omega}_0 \cdot \nabla_{\mathbf{r}_0} Q_t(s|\mathbf{r}_0, \mathbf{v}_0)\, dt + O(dt^2)\,, \end{cases}$$

finally leads to the backward differential equation for the moment generating function $Q_t(s|\mathbf{r}_0, \mathbf{v}_0)$, known as [Zoia et al. 2012b]

Backward Feynman-Kac equation for $Q_t(s|\mathbf{r}_0, \mathbf{v}_0)$

$$\frac{1}{v_0}\frac{\partial Q_t}{\partial t} = \underbrace{\boldsymbol{\omega}_0 \cdot \nabla_{\mathbf{r}_0} Q_t}_{\text{Transport}} \underbrace{-s\, \mathbb{1}_V(\mathbf{r}_0)\, Q_t}_{\text{Counts}} \underbrace{-\Sigma(\mathbf{r}_0, v_0)\, Q_t}_{\text{Capture}} + \underbrace{\Sigma(\mathbf{r}_0, v_0)\, G\big(\mathcal{C}^*[Q_t]\big)}_{\text{Descendant contribution}} . \tag{II.47}$$

This equation should be considered together with the initial condition $Q_0(s|\mathbf{r}_0, \mathbf{v}_0) = 1$ and appropriate boundary conditions. Here we recognise the form of several terms already introduced in the first chapter:

▷ the first term $\boldsymbol{\omega}_0 \cdot \nabla_{\mathbf{r}_0} Q_t$ is a transport term, whose form is specific to exponential random walks (it is the differential form of the exponential transport kernel, see Chap 1);

▷ the term $-\Sigma(\mathbf{r}_0, v_0)\, Q_t$ corresponds to the absorption of the incoming particle at each collision.

Regarding the two other terms, we can say that:

▷ The term $-s\, \mathbb{1}_V(\mathbf{r}_0)\, Q_t$ is a counting term, appearing here because l_V is a quantity that is summed along the trajectory.

▷ The last term finally is the contribution of the descendants, including a branching term: it corresponds to the increase of Q_t due the creation of particles at a collision. In particular, note that given the form of $G[z]$ in Eq. (II.46), this branching term is non linear. Observe also that the *adjoint collision operator* $\mathcal{C}^*$ contains an integral (see Eq. (II.42)), such that Eq. (II.47) is in fact a non linear integro-differential equation.

d. Backward equation for each moment of the total length travelled in a region V

The moment generating function of a random variable is an alternative specification of its probability density function[12], and thus it also contains

[12] From a inverse Laplace Transform of the latter equation, it is possible to obtain the equation for the pdf of l_V [Appel 2013]. However, the resulting equation will be also a non

all the information about the random variable. However, the equation (II.47) verified by $Q_t(s|\mathbf{r}_0, \mathbf{v}_0)$ is a non linear integro-differential equation, which is, in general, difficult to solve. Nevertheless, in practice, we can reduce the problem to the study of the first moments of l_V, and, from the definition of the moment generating function Eq. (II.35), we can directly derive the equation for the moment of order m by taking the m-th derivative of Eq. (II.47). Using the Faà di Bruno formula[13] [Faà di Bruno 1855; Craik 2005] for computing multiple derivatives of the composition of functions $G\big(\mathcal{C}^*\big[Q_t\big]\big)$ (see Eq. (A.7) in Annexe 1), the equation for $L_m(\mathbf{r}_0, \mathbf{v}_0, t)$ reads

Equation for $L_m(\mathbf{r}_0, \mathbf{v}_0, t)$

$$\frac{1}{v_0}\frac{\partial L_m}{\partial t} = \underbrace{\boldsymbol{\omega}_0 \cdot \nabla_{\mathbf{r}_0} L_m}_{\text{Transport}} + \underbrace{m\, \mathbb{1}_V(\mathbf{r}_0)\, L_{m-1}}_{\text{Counting term}} \underbrace{- \Sigma(\mathbf{r}_0, v_0)\, L_m}_{\text{Loss at collisions}}$$
$$+ \underbrace{\Sigma(\mathbf{r}_0, v_0)\left[\nu_1\, \mathcal{C}^*\big[L_m\big] + \sum_{j=2}^{m} \nu_j \mathcal{B}_{m,j}\Big(\mathcal{C}^*\big[L_i\big]\Big)\right]}_{\text{Contribution of the descendants at each collision}}, \qquad \text{(II.48)}$$

with the initial condition $L_m(\mathbf{r}_0, \mathbf{v}_0, 0) = 0$ for all m. The functions $\mathcal{B}_{m,j}[x_1, \cdots, x_{m-j+1}]$, whose notation was simplified in $\mathcal{B}_{m,j}[x_i]$, are the Bell polynomials (see Annexe 1). They commonly appear when dealing with the combinatorics of branched structures [Pitman 2006]. The constants ν_j are the falling factorial moments (of order j) for the number of descendants per collision, given by the j-th derivative of the generating function G:

$$\nu_j \doteq \langle\, k(k-1)(...)(k-j+1)\,\rangle$$
$$= \sum_{k\geqslant 0} k(k-1)(...)(k-j+1)\, p_k \qquad \text{(II.49)}$$
$$\nu_j = G^{(j)}[1]\,. \qquad \text{(II.50)}$$

Observe that, as announced in Sec. (II.1.1), the first moment L_1 depends only on ν_1, the second moment L_2 only on ν_1 and ν_2, and so on.

Interestingly, it turns out that equation (II.48) has exactly the same form as the one derived by Zoia et al. [2012b] for branching random walks evolving in a simpler system (an homogeneous medium, with isotropic scattering and constant speed along the paths), except that

▷ Σ and ν_j depend on the position $\mathbf{r}_0$ (inhomogeneous medium);

▷ the speed v_0 is now a variable of the problem instead of a constant

linear integro-differential equation.

[13] also known in french as Arbogast's formula [Arbogast 1800]

parameter, such that Σ and ν_j also depend on v_0 (particle speed changes at any collision);

▷ the collision kernel $C(\mathbf{v}_0 \to \mathbf{v}')$ is not necessarily isotropic.

In this section we have thus showed that the equation of [Zoia et al. 2012b] carries over to our more general case with the different interpretation and minor changes mentioned above. For applications in reactor physics, this generalisation is of course very useful, and in the next section we illustrate this result on a simple example in reactor physics (see Sec. II.3.1).

II.2.3 Comments on the form of the equation

a. Reactor physics notation

To transpose Eq. (II.48) from the general branching random walk notation to the one used in reactor physics (see Sec. I.1.2), we have to replace:

$$\begin{gathered} \nu_1 \, \Sigma(\mathbf{r}_0, v_0) \, C^*(\mathbf{v}_0 \to \mathbf{v}_1 \,|\, \mathbf{r}_0) \\ \downarrow \text{ by} \end{gathered} \tag{II.51}$$

$$\Sigma_s(\mathbf{r}_0, v_0) \, C_s^*(\mathbf{v}_0 \to \mathbf{v}_1 \,|\, \mathbf{r}_0) + \nu_1 \, \Sigma_f(\mathbf{r}_0, v_0) \, C_f^*(\mathbf{v}_0 \to \mathbf{v}_1 \,|\, \mathbf{r}_0) \,,$$

and, for the branching terms:

$$\begin{cases} \nu_{i \geqslant 2} \, \Sigma(\mathbf{r}_0, v_0) & \xrightarrow{\text{by}} \quad \nu_{i \geqslant 2} \, \Sigma_f(\mathbf{r}_0, v_0) \\ C^*(\mathbf{v}_0 \to \mathbf{v}_1 \,|\, \mathbf{r}_0) & \xrightarrow{\text{by}} \quad C_f^*(\mathbf{v}_0 \to \mathbf{v}_1 \,|\, \mathbf{r}_0) \end{cases} \tag{II.52}$$

where Σ_s and Σ_f are respectively the scattering and the fission cross-section and C_s^* and C_f^* are the adjoint of the probability densities respectively associated with the scattering and the fission kernel defined in Sec. I.1.2. Note that this transformation extends the one of Eq. (I.28) to the study of the fluctuations, by taking into account higher order properties of the process ($\nu_{i \geqslant 2}$). The backward equation (II.48) finally becomes

$$\begin{aligned} \frac{1}{v_0} \frac{\partial L_m}{\partial t} &= \mathcal{L}^* L_m + m \mathbb{1}_V(\mathbf{r}_0) \, L_{m-1} + \Sigma_f \sum_{j=1}^{m} \nu_j \mathcal{B}_{m,j}\big(\mathcal{C}_f^*\big[L_i\big]\big) \\ \mathcal{L}^* \cdot &= \boldsymbol{\omega} \cdot \nabla_{\mathbf{r}_0} \cdot - \Sigma(\mathbf{r}_0, v_0) \cdot + \Sigma_s(\mathbf{r}_0, v_0) \, \mathcal{C}_s^*\big[\,\cdot\,\big] \,, \end{aligned} \tag{II.53}$$

where we introduced the *backward transport operator* $\mathcal{L}^*$ [Zoia et al. 2012a; Pázsit and Pál 2007]. Observing that the operator

$$\Sigma_s(\mathbf{r}_0, v_0) \, \mathcal{C}_s^*\big[\,\cdot\,\big] = \iiint \mathrm{d}^3\mathbf{v}_1 \, \Sigma_s(\mathbf{r}_0, v_0) \, C_s^*(\mathbf{v}_1 \to \mathbf{v}_0 | \mathbf{r}_0) \, [\cdot] \,, \tag{II.54}$$

is actually the adjoint of the forward operator

$$\mathcal{C}_s\left[\Sigma_s\,\cdot\,\right] = \iiint d^3\mathbf{v}_0\;\Sigma_s(\mathbf{r}_0,v_0)\,C_s(\mathbf{v}_0\to\mathbf{v}_1|\mathbf{r}_0)\,[\cdot]\,, \tag{II.55}$$

appearing in the definition Eq. (I.60) of the transport operator $\mathcal{L}$, we can check that the backward transport operator $\mathcal{L}^*$ is the *adjoint operator* of $\mathcal{L}$ [Bell and Glasstone 1970].

b. Equation for the mean, link with the forward equation

Eq. (II.53) becomes for the average total length $L(\mathbf{r}_0,\mathbf{v}_0,t)$ travelled in V ($m=1$):

$$\left[\frac{1}{v_0}\frac{\partial}{\partial t} - \mathcal{L}^*\right] L(\mathbf{r}_0,\mathbf{v}_0,t) = \Sigma_f\,\nu_1\,\mathcal{C}_f^*\left[\,L\,\right] + \mathbb{1}_V(\mathbf{r}_0) \tag{II.56}$$

where $\mathcal{L}^*$ is the *backward transport operator* introduced above. Here, we can observe that the backward equation for the first moment is the adjoint of the forward transport equation (I.61) (Boltzmann equation), with a supplementary source term $\mathbb{1}_V(\mathbf{r}_0)$ (in this chapter we have not considered any external source). Indeed, the backward operator

$$\nu_1(\mathbf{r}_0,v_0)\,\Sigma_f(\mathbf{r}_0,v_0)\,\mathcal{C}_f^*\left[\,\cdot\,\right] = \iiint d^3\mathbf{v}_1\;\nu_1\,\Sigma_f(\mathbf{r}_0,v_0)\,C_f^*(\mathbf{v}_1\to\mathbf{v}_0|\mathbf{r}_0)\,[\cdot]\,, \tag{II.57}$$

is the adjoint of the operator

$$\mathcal{C}_f\left[\Sigma_f\,\cdot\,\right] = \iiint d^3\mathbf{v}_0\;\nu_1\,\Sigma_f(\mathbf{r}_0,v_0)\,C_f(\mathbf{v}_0\to\mathbf{v}_1|\mathbf{r}_0)\,[\cdot]\,, \tag{II.58}$$

where $\mathcal{C}_f\left[\,\cdot\,\right]$ is given by Eq. (I.50). As seen earlier, the supplementary source term $\mathbb{1}_V(\mathbf{r}_0)$ is here because we are computing a quantity that is accumulated along the time[14].

c. Second and other moments - non linear term responsible for large fluctuations

For higher moments, Eq. (II.53) can be rewritten

$$\left[\frac{1}{v_0}\frac{\partial}{\partial t} - \mathcal{L}^*\right] L_m = \Sigma_f\,\nu_1\,\mathcal{C}_f^*\left[L_m\right] + m\,\mathbb{1}_V(\mathbf{r}_0)\,L_{m-1} + \Sigma_f\sum_{j=2}^{m}\nu_j\,\mathcal{B}_{m,j}\left(\mathcal{C}_f^*\left[L_i\right]\right) \tag{II.59}$$

[14]For instance, we will see in the next section, that this term disappears in the equation for the mean number of particles in a region V at a time t, $N_V(t)$ (which is a quantity related to the density of particle and that is not integrated along the trajectory).

Due to the presence of the Bell polynomials, we could expect this equation to inherit the non linearity from the equation of the moment generating function Eq. (II.47). However, for each moment, the non-linear terms depend only on the moments of lower order. For example, the equation for the variance L_2 exhibits a term in $\{L_1\}^2$,

$$\frac{1}{v_0}\frac{\partial L_2}{\partial t} = \mathcal{L}^* L_2 + \nu_1 \Sigma_f \mathcal{C}_f^*\left[L_2\right] + \underbrace{2\,\mathbb{1}_V(\mathbf{r}_0)\,L_1 + \Sigma_f \nu_2 \left(\mathcal{C}_f^*\left[L_1\right]\right)^2}_{\text{additional source terms}}, \quad \text{(II.60)}$$

that corresponds to an extra source term for the equation. The resulting equation is therefore linear, and this is true for all the moments of order $m \geqslant 2$. Furthermore, the importance of moments of lower order in this supplementary source term is amplified by the presence of the powers in the Bell polynomials. This suggests that fluctuations in branching systems are enhanced by positive feedback. This could provide a first justification of the strong fluctuations and the clustering behaviour observed in chapter 1; a finer analysis will be given in chapter 3.

3 QUANTITIES OF INTEREST IN REACTOR PHYSICS

Thanks to the Feynman-Kac approach, in the last section, we were able to derive backward equations for the various moments of the travelled length l_V, allowing us to fully characterise the statistics of l_V for branching random walks. Several other physical observables of the branching process can be assessed with the same formalism. In the following, we will discuss some of them that are interesting in the field of reactor physics.

II.3.1 Numerical simulation for the travelled length statistics

In order to illustrate the generalisation appearing in Eq. (II.48) to systems with inhomogeneous media and where the speed of neutrons can change at each collision, we revisit here a relevant example of a one-dimensional transport inspired by reactor physics. Consider a one-dimensional bounded system of size $[0, B]$ where neutrons can move only in two directions: $\boldsymbol{\omega} = \pm e_x$ (see Fig. II.5). Neutrons evolve in the system, performing branching exponential walks: at a collision, the incoming neutron is captured with the probability p_0, scattered with the probability p_1 and gives rise to a fission with probability $p_{k\geqslant 2}$. This simple one-dimensional model is known in the field of reactor physics as the *rod model*. Despite the simplifications, the model captures the key features of neutron transport and has been already widely adopted [Harris 1963; Wing 1962].

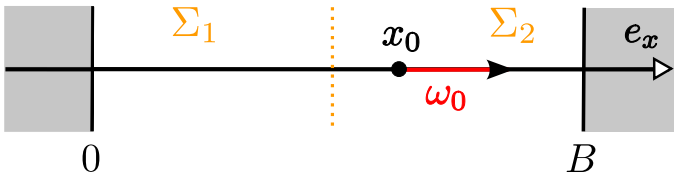

Figure II.5: Simple one-dimensional model of a reactor.

For the simulations, we start the system with one single particle in x_0 located inside the detector (within the domain $[0, B]$, see Fig. II.5), so that $\mathbb{1}_V(\mathbf{r}_0) = 1$. We also assume the boundaries in 0 and B to be absorbing. In this model, $\boldsymbol{\omega}_0$ can take only two values, $\boldsymbol{\omega}_0 = \pm e_x$, such that we can define, for each order m, the two quantities $L_m^+(x_0, t) = L_m(x_0, +e_x, t)$ and $L_m^-(x_0, t) = L_m(x_0, -e_x, t)$ that do not depend on the variable $\boldsymbol{\omega}_0$. For the purpose of deterministic numerical simulations, we can then rewrite Eq. (II.48) as a system of two coupled differential equations:

$$\begin{cases} \dfrac{1}{v_0}\dfrac{\partial L_m^+}{\partial t} = \dfrac{\partial L_m^+}{\partial x_0}(x_0,t) + m\,L_{m-1}^+ - \Sigma\,L_m^+ + \Sigma\,\nu_1\,\mathcal{C}^*\left[L_m\right]^+ \\ \qquad\qquad + \Sigma\sum_{j=2}^{m}\nu_j\mathcal{B}_{m,j}\left(\mathcal{C}^*\left[L_i\right]^+\right), \\ \dfrac{1}{v_0}\dfrac{\partial L_m^-}{\partial t} = \dfrac{\partial L_m^-}{\partial x_0}(x_0,t) + m\,L_{m-1}^- - \Sigma\,L_m^- + \Sigma\,\nu_1\,\mathcal{C}^*\left[L_m\right]^- \\ \qquad\qquad + \Sigma\sum_{j=2}^{m}\nu_j\mathcal{B}_{m,j}\left(\mathcal{C}^*\left[L_i\right]^-\right). \end{cases}$$

Introducing the vector:

$$\vec{L_m} = \begin{pmatrix} L_m^+ \\ L_m^- \end{pmatrix}, \tag{II.61}$$

the scattering collision operator can be then written as a 2×2 matrix:

$$C = \begin{pmatrix} c(+\to+) & c(-\to+) \\ c(+\to-) & c(-\to-) \end{pmatrix}, \tag{II.62}$$

where $c(+ \to -)$, for instance, is the probability that a particle, arriving at the collision with a direction $\boldsymbol{\omega} = +e_x$, leaves along the direction $\boldsymbol{\omega} = -e_x$; and similarly for the other entries of the matrix. We can finally compute the terms containing the adjoint collision operator $\mathcal{C}^*\left[L_m\right]^\pm$ in Eq. (II.61), using:

$$\begin{pmatrix} \mathcal{C}^*[L_m]^+ \\ \mathcal{C}^*[L_m]^- \end{pmatrix} = \begin{pmatrix} c(+\to+)\,L_m^+ + c(+\to-)\,L_m^- \\ c(-\to+)\,L_m^+ + c(-\to-)\,L_m^- \end{pmatrix} \tag{II.63}$$

$$= C^*\,\vec{L_m}, \tag{II.64}$$

where C^* is the adjoint matrix of C. Concerning the Monte Carlo simulations, the details of the algorithm used here are provided in Appendix 5.

Fig. II.6 displays a plot of the first moment $L(t)$ of the total length travelled by a single particle starting from x_0 in a direction ω_0 and all its descendants within $[0, B]$, as a function of the time t. This length grows in time, saturating at a maximum value when, on average, there are no particles in the system anymore. Simulations were performed for a critical system ($\nu_1 = 1$), in the case of a piecewise inhomogeneous medium composed of two homogeneous sub-domains of respective cross-section Σ_1 and Σ_2, as illustrated on Fig. II.5. We consider dimensionless variables: we set the particle speed $v = 1$ and take $B = 2$; the frontier between the two sub-domains is in the centre of the box, in $x = 1$; and the initial particle is started from $x_0 = 1.75$ with a direction $\omega_0 = +e_x$. For Fig. II.6 two types of simulations were performed:

- first, a deterministic numerical solution of Eq. (II.48) for $m = 1$ (red circles, and blue crosses), using a spatial mesh of 2.10^3 points, and a time resolution of $dt = 1.10^{-3}$;

- then, a Monte-Carlo simulation of the system (red and blue curves), realised with a time step of $dt = 2.10^{-4}$. Averages are taken over 10^5 realisations of the system, so that the statistical uncertainties are of the order of 10^{-3} (as the variance of the total length is ~ 0.5 – see Fig. II.7).

The plots show a good agreement between the results of the Monte Carlo simulations and the numerical solutions of Eq. (II.48) with $m = 1$, for the inhomogeneous cases, $(\Sigma_1, \Sigma_2) = (1, 0.5)$ and $(0.5, 1)$. The black curves correspond to the deterministic simulations for the uniform cases, $\Sigma_1 = \Sigma_2 = 1$ and $\Sigma_1 = \Sigma_2 = 0.5$.

Fig. II.7 compares two critical systems ($\nu_1 = 1$): one is purely diffusive ($p_1 = 1$ and $\forall i \neq 1, p_i = 0$) corresponding to the dark and the blue curves; the other has branching with $p_0 = p_2 = 0.5$ and $\forall i \neq \{0, 2\}, p_i = 0$. The data are obtained by deterministic simulations (numerical solutions of Eq. (II.48) for $m = 1$ and for $m = 2$). As expected, the first moment L is identical in these two cases (black curve and red crosses). Indeed, the behaviour of L depends only on the value of ν_1. Note that the second moment L_2 increases much faster in the branching case.

II.3.2 Collision Statistics

An other fondamental quantity in Monte Carlo simulation of nuclear reactor is the total number of collisions n_V undergone by neutrons in a region V of the system. Its stochastic definition, for a single neutron starting from

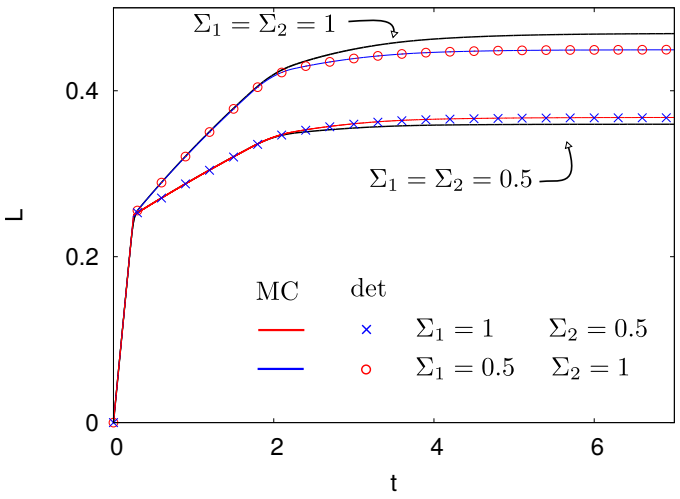

Figure II.6: Mean length L travelled, in the inhomogeneous one-dimensional box $[0, 2]$ displayed in Fig. II.5, by a single particle starting from $x_0 = 1.75$ in a direction $\omega_0 = +e_x$ and all its descendants; obtained by Monte Carlo simulations (blue and red curves) and by deterministic simulations (circles and crosses). The two black curves correspond to a uniform system of constant cross-section $\Sigma_1 = \Sigma_2$.

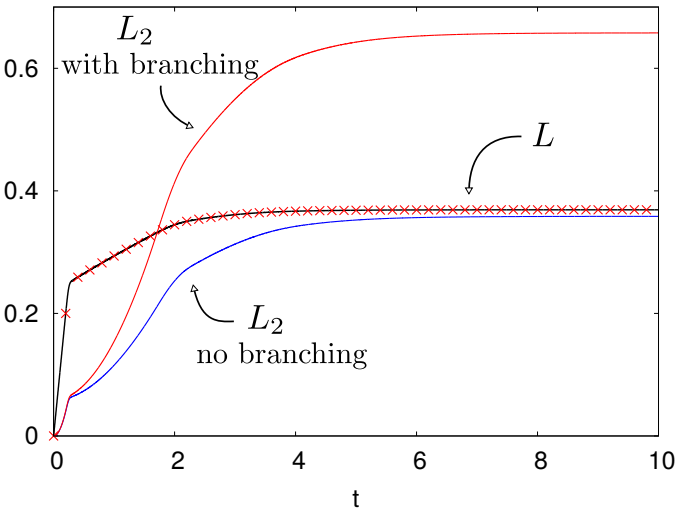

Figure II.7: First and second moment of the length travelled, in the inhomogeneous one-dimensional box $[0, 2]$ displayed in Fig. II.5, by a single particle starting from $x_0 = 1.75$ in a direction $\omega_0 = +e_x$ and all its descendants. Simulations are performed with branching (red curve and crosses), or without branching (blue and dark curves).

$(\mathbf{r}_0, \mathbf{v}_0)$ at time $t = 0$ is

$$n_V(\mathbf{r}_0, \mathbf{v}_0, t) = \int_0^t dt' \sum_{\text{every path}} \mathbb{1}_V(\mathbf{r}(t')) \,, \tag{II.65}$$

where t is the observation time and $\mathbb{1}_V[\mathbf{r}]$ is the *marker function* of the region V. In the context of Monte Carlo simulations for neutron transport, the mean of this stochastic variable is referred to as the *collision estimator* [Lux and Koblinger 1991]. This estimator is associated with the total reaction rate density (or collision rate density), defined in Eq. (I.33):

$$\langle\, n_V \,\rangle(S_0, t) = \int_0^t dt' \int_V d^3\mathbf{r} \int d^3\mathbf{v}\; \psi(\mathbf{r}, \mathbf{v}, t') \,, \tag{II.66}$$

where $\psi(\mathbf{r}, \mathbf{v}, t) = \Sigma(\mathbf{r}, \mathbf{v})\, n(\mathbf{r}, \mathbf{v}, t)$. The equation for the various moments of n_V are derived in [Zoia et al. 2012b] for the case of an homogeneous medium, with isotropic scattering and neutrons with constant speed. Relaxing these constraints in their equations remains as a possible line of further research.

II.3.3 Occupation Statistics: Escape, Survival and Extinction Probability

In this section, we will see that other interesting observables can be assessed thanks to the same formalism (backward Feynman-Kac formalism), with minor changes [Zoia et al. 2012b]. We are first interested in the instantaneous number of particles in a domain V at time t, denoted $N_V(S_0, t)$ for a source S_0 of initial neutrons. Indeed, we will see in the next chapter that this quantity is at the heart of the clustering problem. Unlike the two quantities l_V and n_V, this new N_V is not integrated over time [Pázsit and Pál 2007].

As for the travelled length l_V (see Eq. (II.35)), we define the moment generating function[15] of the discrete random variable N_V [Grimmett and Stirzaker 2001]

$$W_t(\mathbf{r}_0, \mathbf{v}_0, s) = \langle\, s^{N_V(\mathbf{r}_0, \mathbf{v}_0, t)} \,\rangle \,, \tag{II.67}$$

from which every moment of N_V can be directly derived:

$$\langle\, N_V^m \,\rangle(\mathbf{r}_0, \mathbf{v}_0, t) = \frac{\partial^m W_t(\mathbf{r}_0, \mathbf{v}_0|s)}{\partial\, s^m}\bigg|_{s=0} \,. \tag{II.68}$$

To obtain the backward equation for the moment generating function W_t we can follow exactly the lines of the derivation proposed in Sec. II.2.2 for

[15] Note that N_V is a discrete random variable, whereas l_V was a continuous one, and as a consequence the moment generating functions are defined in a slightly different way.

the stochastic variable l_V [Pázsit and Pál 2007]. We decompose the process into two parts, from time 0 to dt and from dt to $t+dt$. Thanks to the Markovian property of the process performed by neutrons (branching exponential walks - see Sec. I.1.2), these two parts are independent. Just as in Sec. II.2.2, two types of events can happen during dt:

(a) with a probability $(1-\Sigma v_0 dt)$ the initial particle travelled in straight line from $\mathbf{r}_0$ to $\mathbf{r}_0+\mathbf{v}_0 dt$. In this case, regarding the final state of the system (number of particles in V at time $t+dt$), there is no distinction between starting the process from $\mathbf{r}_0$ at time $t=0$ or starting it from $\mathbf{r}_0+d\mathbf{r}_0$ at time dt later. As a consequence, the contribution of this case *(a)* to the total number of particles is

$$N_V^a(\mathbf{r}_0,\mathbf{v}_0,t+dt) = N_V(\mathbf{r}_0+d\mathbf{r}_0,\mathbf{v}_0,t)\,, \tag{II.69}$$

and the moment generating function reads

$$\begin{aligned} W^a_{t+dt}(s|\mathbf{r}_0,\mathbf{v}_0) &= \big(1-v_0\,\Sigma(\mathbf{r}_0,v_0)\,dt\big)\,\left\langle\, s^{\,N_V(\mathbf{r}_0+d\mathbf{r}_0,\mathbf{v}_0,t)}\,\right\rangle \\ &= \big(1-v_0\,\Sigma(\mathbf{r}_0,v_0)\,dt\big)\,W_t(s|\mathbf{r}_0+d\mathbf{r}_0,\mathbf{v}_0) \end{aligned} \tag{II.70}$$

(b) with probability $\Sigma v_0 dt$ the first particle encounters a collision during dt, giving birth to k descendants. The number of particles in V at time $t+dt$ then results from the history of each of the k families directly descending from this initial particle. As a consequence, the contribution of this case *(b)* to the total number of particles is

$$N_V^b(\mathbf{r}_0,\mathbf{v}_0,t+dt) = N_V(\mathbf{r}_0,\mathbf{v}_1,t)+\cdots+N_V(\mathbf{r}_0,\mathbf{v}_k,t)\,, \tag{II.71}$$

where the velocities $\{\mathbf{v}_i\}_{1\leqslant i\leqslant k}$ are given by the pdf $C(\mathbf{v}_0\to\mathbf{v}_i)$. Exactly as for the moment generating function of l_V (see Eq. (II.44)) we obtain:

$$W^b_{t+dt}(s|\mathbf{r}_0,\mathbf{v}_0) = \big(v_0\,\Sigma(\mathbf{r}_0,v_0)\,dt\big)\;G\Big(\mathcal{C}^*\big[W_t(s|\mathbf{r}_0,\mathbf{v}_0')\big]\Big)\,, \tag{II.72}$$

where G is the generating function of the descendant number k defined in Eq. (II.46).

Combining these two terms, $W_{t+dt}(s|\mathbf{r}_0,\mathbf{v}_0) = W^a_{t+dt}+W^b_{t+dt}$, and expanding Eq. (II.70) in the first order in dt, finally yields the differential equation for $W_t(s|\mathbf{r}_0,\mathbf{v}_0)$:

Pál-Bell equation for $W_t(s\,|\,\mathbf{r}_0,\mathbf{v}_0)$

$$\frac{1}{v_0}\frac{\partial W_t}{\partial t} = \underbrace{\boldsymbol{\omega}_0\cdot\nabla_{\mathbf{r}_0}W_t}_{\text{Transport}} \quad \underbrace{-\Sigma(\mathbf{r}_0,v_0)\,W_t}_{\text{Capture at each collision}} \quad + \underbrace{\Sigma(\mathbf{r}_0,v_0)\,G\Big(\mathcal{C}^*\big[W_t\big]\Big)}_{\text{descendant contribution}}\,. \tag{II.73}$$

This equation is known in reactor physics as the *Pál-Bell equation* and is widely used for analysing the statistics of particle counting at a given detector [Bell 1965; Pal 1958; Pázsit and Pál 2007]. We recognise the different terms also appearing in Eq. (II.47): a transport term (corresponding to the markovian exponential transport), an absorption term corresponding to the absorption of the incoming particle at each collision and finally a non linear branching term. Note that the counting term found in Eq. (II.47) does not appear here. Indeed, N_V is an instantaneous quantity, whereas l_V is a quantity that is accumulated along the trajectory. The Pál-Bell equation can also be written in the framework of the diffusion approximation introduced in the first chapter (see Sec. I.2.5):

Pál-Bell equation for $W_t(s\,|\,\mathbf{r}_0)$ in the diffusion approximation

$$\frac{\partial W_t}{\partial t}(s\,|\,\mathbf{r}_0) = \underbrace{D\,\nabla^2_{\mathbf{r}_0} W_t}_{\text{Diffusion}} \underbrace{-\,\lambda\, W_t}_{\text{Capture}} + \underbrace{\lambda\, G\big[W_t\big]}_{\text{descendant contribution}}\,, \qquad \text{(II.74)}$$

where

$$W_t(s|\mathbf{r}_0) = \int_{\Omega_3} W_t(s|\mathbf{r}_0,\boldsymbol{\omega}_0)\,d^3\boldsymbol{\omega}_0\,, \qquad \text{(II.75)}$$

and for which we have considered that, $\longrightarrow$ the system is homogeneous, $\Sigma = \text{cst}$;
$\longrightarrow$ particles evolve with a constant speed, $v_0 = \text{cst}$, and we thus define the rate (in time) at which particles encounter an event: $\lambda = v_0\Sigma = \text{cst}$;
$\longrightarrow$ the scattering is isotropic: $C(\mathbf{v}\to\mathbf{v}_0) = 1/\Omega_3$.
The derivation of this equation can be found in [Pázsit and Pál 2007; Bell 1965].

a. Occupation statistics

We can now directly get the equation for each moment of the instantaneous number of particles N_V in any sub-domain V of the system by taking the successive derivatives of Eq. (II.73). The m-th derivative thus yields for the moment of order m, $\langle\, N_V^m \,\rangle = N_m$, the equation:

Equation for $N_m(\mathbf{r}_0,\mathbf{v}_0,t)$

$$\frac{1}{v_0}\frac{\partial N_m}{\partial t} = \underbrace{\boldsymbol{\omega}_0\cdot\nabla_{\mathbf{r}_0} N_m}_{\text{Transport}} \underbrace{-\,\Sigma(\mathbf{r}_0,v_0)\,L_m}_{\text{Loss at collisions/Capture}} + \underbrace{\Sigma(\mathbf{r}_0,v_0)\left[\nu_1\,\mathcal{C}^*\big[N_m\big] + \sum_{j=2}^{m}\nu_j\mathcal{B}_{m,j}\Big(\mathcal{C}^*\big[N_i\big]\Big)\right]}_{\text{Contribution of the descendants at each collision}}. \qquad \text{(II.76)}$$

Using, as in the previous section, the Faà di Bruno formula [Faà di Bruno 1855; Craik 2005] for computing the m-th derivative of the composition of functions $G\Big(\mathcal{C}^*\big[W_t\big]\Big)$ (see Eq. (A.8) in Annexe 1).

b. Survival probability and extinction probability

Let us consider now a system of volume V surrounded by an absorbing boundary. Any particle that leaves the system from its boundaries is absorbed and thus can not reenter it. In this system, a particle and its family can survive or die, depending on the interplay between the branching process and the leakages through the boundaries. We can thus define the probability that the family descending a single particle emitted from $(\mathbf{r}_0, \mathbf{v}_0)$ at time 0 will survive in the system until a time t [Redner 2001], namely the

survival probability $$q_S(t\,|\,\mathbf{r}_0, \mathbf{v}_0)\,. \tag{II.77}$$

In other terms, considering that we start the system with a single particle in $(\mathbf{r}_0, \mathbf{v}_0)$ at time $t = 0$, $S(t\,|\,\mathbf{r}_0, \mathbf{v}_0)$ is the probability that there is still a particle in the system at time $t > 0$. In the same way, we can define the

extinction probability $$E(t) = 1 - q_S(t)\,, \tag{II.78}$$

which is the probability that the system is extinct at a time t, i.e. that there are no particles left in the system at time t: $N_V(t) = 0$. Note that if a system is extinct at time t, then the system will stay extinct for any time $t' > t$. Furthermore we can notice that [Pázsit and Pál 2007]:

$$\begin{cases} \text{if } N_V(t) = 0 \text{ (extinct system), then } s^{N_V}\big|_{s=0} = 1\,, \\ \text{whereas if } N_V(t) > 0, \text{ then } W_t(s)|_{s=0} = s^{N_V}\big|_{s=0} = 0\,; \end{cases} \tag{II.79}$$

such that the probability that a system is extinct at time t is given by:

$$E(t) = \langle\, s^{N_V}\big|_{s=0} \,\rangle = W_t(s)|_{s=0}\,. \tag{II.80}$$

As a consequence, the extinction probability $E(t, \mathbf{r}_0, \mathbf{v}_0)$ obeys to the same equation than $W_t(s|\mathbf{r}_0, \mathbf{v}_0)$, Eq. (II.73), and the survival probability $q_S(t, \mathbf{r}_0, \mathbf{v}_0)$ satisfies the equation:

$$\frac{1}{v_0}\frac{\partial q_S}{\partial t}(t, \mathbf{r}_0, \mathbf{v}_0) = \underbrace{\boldsymbol{\omega}_0 \cdot \nabla_{\mathbf{r}_0} q_S}_{\text{Transport}} \quad \underbrace{-\Sigma(\mathbf{r}_0, v_0)\, q_S}_{\text{Capture at each collision}} + \underbrace{\Sigma(\mathbf{r}_0, v_0)\, F\Big(\mathcal{C}^*\big[q_S\big]\Big)}_{\text{descendant contribution}}\,. \tag{II.81}$$

where $F[z] = \sum_{k\geqslant 1} \alpha_k\, z^k$, with $\alpha_k = (-1)^k\, \nu_k/k!$ [Bell 1965; Zoia et al. 2012b].

In the case of $\nu_1 \leqslant 1$, we have seen that the process of birth and death will lead to the death of the whole population in the long time regime[16], independently of the volume V of the medium [Harris 1963]. For $\nu_1 > 1$, it exists a critical volume V_c of the system below which the particle losses due to absorptions and leakages through the boundaries are larger than the gain due to population growth [Pázsit and Pál 2007], and for large time t the system goes to extinction: $q_S(\mathbf{r}_0, \mathbf{v}_0, t) \underset{t\to\infty}{\longrightarrow} 0$. However, when $\nu_1 > 1$ and $V > V_c$ a branching system has a finite probability to survive indefinitely, and the survival probability admits a non-trivial limit when t goes to infinity: $q_S(\mathbf{r}_0, \mathbf{v}_0, t) \underset{t\to\infty}{\longrightarrow} q_S^\infty(\mathbf{r}_0, \mathbf{v}_0) > 0$. Finding this asymptotic survival probability constitutes a long standing issue [Brunet and Derrida 2009; Derrida and Simon 2007].

II.3.4 Conclusion and perspectives

In this chapter we have seen that a population of N_0 individuals that can reproduce or die intrinsically undergoes very strong fluctuations of its community size in time. These fluctuations become even stronger when the system gets closer to criticality ($\nu_1 = 1$), which is the regime in which nuclear reactor are normally operating [Dumonteil et al. 2014]. In particular, in a critical system, these strong fluctuations result in an unexpected behaviour: whereas the mean number of individuals in the system stays constant in time $\langle N \rangle(t) = N_0$, the entire population is destined for death in a characteristic time $\tau_E = N_0/(\lambda\nu_2)$. This phenomenon, for which the standard deviation of the system size becomes larger than its mean, was named *critical catastrophe* by Williams [1974]. The mean number of particles $\langle N \rangle(t)$ is in fact an average over all realisations of the system (ensemble average), and the contradiction highlighted here only indicates that the system is not *self-averaging* [Young et al. 2001].

For most applications in reactor physics, the neutron population considered is sufficiently large (10^8 n/cm^3 in a PWR at operating condition [Duderstadt and Hamilton 1976]) for the neutron density to give a good characterisation of the behaviour of the neutron population. In these cases, it is meaningful to use the classical transport equations (such as the Boltzmann equation (I.55)). However there exist some situations for which a description based on averaged observables provides a misleading characterisation of the behaviour of the neutron population [Prinja 2012], such as for the clustering phenomenon [Dumonteil et al. 2014] introduced in the first chapter. Thanks to the Feynman-Kac formalism, we have established the backward equations for each moment of the main quantities of interest in reactor physics, generalising the results of [Zoia et al. 2012b]. Moments

[16] decreasing population for $\nu_1 < 1$ and critical catastrophe for $\nu_1 = 1$ (see Sec. II.1.2)

of order higher than one allow us to study the fluctuations of the neutron population:

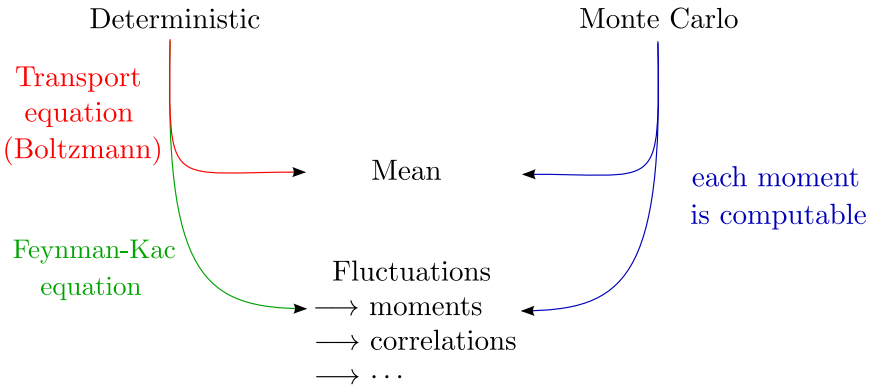

While commenting these moment equations, we saw that the form of the branching term (corresponding to the reproduction process) could explain the presence of strong fluctuations in a system with branching (see Sec. II.2.3). This observation could provides a first explanation for the clustering phenomenon presented in chapter 1. Moreover, using the Feynman-Kac formalism, it is now possible to derive a backward equation for the pair correlation function between particles of the system. In the next chapter, a large part will be dedicated to this quantity, at the heart of the understanding of the neutron clustering behaviour.

CHAPTER III

NEUTRON CLUSTERING

In this chapter, we bring an exhaustive review on the clustering phenomenon introduced in chapter 1, which has been studied across different fields. In particular we focus on systems evolving at criticality, which corresponds to the operating condition of a nuclear reactor. In this context, we investigate the impact of the finite size of the system (confined geometry and finite number of neutrons) and of a population control on the clustering phenomenon.

Contents

THE neutron population in a prototype model of nuclear reactor can be described in terms of a collection of particles undergoing three key random mechanisms: diffusion, reproduction due to fissions, and death due to absorption events. When the reactor is operated at the critical point (i.e., fissions are exactly compensated by absorptions), the whole neutron population might in principle go to extinction because of the wild fluctuations induced by births and deaths (see Chapter II). This *critical catastrophe*, is nonetheless never observed in practice: feedback mechanisms acting on the total population, such as human intervention, have a stabilising effect. However, these fluctuations can also give rise to local extinctions of the population, at the origin of the clustering phenomenon observed in [Dumonteil et al. 2014] (see Sec. I.3.1), and a non-uniform neutron density in the reactor fuel elements might lead to local peaks in the deposited energy (hot spots) and represent thus a most unwanted event with respect to the safe operation of nuclear power plants [Dumonteil et al. 2014]. In practice, several parameters can affect this phenomenon. In this chapter, we revisit the clustering phenomenon (the critical catastrophe at a local scale), by investigating the effects of the finite extension of the system (presence of boundaries and finite number of individuals) and of a population control on the spatial behaviour of the fluctuations. The work presented here results from a collaboration with Eric Dumonteil, Alain Mazzolo, Alberto Rosso and Andrea Zoia, and has been published in [Dumonteil et al. 2014; Zoia et al. 2014; de Mulatier et al. 2015].

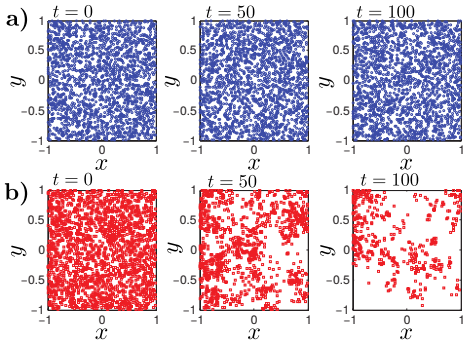

Figure III.1: Monte Carlo simulation of the evolution of a collection of particles in a two-dimensional box. Particles are initially prepared with a uniform spatial distribution. **Case a).** Particles follow regular Brownian motions: as time increases, positions are shuffled by diffusion, but the spatial distribution of the particles stays uniform. **Case b).** Particles perform branching Brownian motions with equal birth and death rates: as time increases, the population undergoes large fluctuations, and the particle density displays a wild patchiness.

Branching processes and clustering issue

Many physical and biological systems can be represented in terms of a collection of individuals governed by the competition of the two basic random mechanisms of birth and death. Examples are widespread and encompass neutron multiplication [Pázsit and Pál 2007; Williams 1974], nuclear collision cascades [Harris 1963; Athreya and Ney 2012a; Bharucha-Reid 1968], epidemics and ecology [Bailey 1968; Jagers et al. 1975; Murray 1989; Zhang et al. 1990; Meyer et al. 1996; Tilman and Kareiva 1997], bacterial growth [Golding et al. 1998; Houchmandzadeh 2008], and genetics [Sawyer and Fleischman 1979; Lawson and Jensen 2007]. Neglecting particle–particle correlations and non-linear effects, the evolution of such systems can be effectively explained by the Galton–Watson model [Harris 1963]. In most of these examples, individuals also interact with the surrounding environment and are typically subject to random displacements [Williams 1974; Zhang et al. 1990; Meyer et al. 1996; Tilman and Kareiva 1997]. The interplay between the fluctuations stemming from birth-death events and those stemming from diffusion will thus subtly affect the spatial distribution of the particles in such systems [Le Gall 2012; Brunet and Derrida 2009; Ramola et al. 2014, 2015]. In particular, at and close to the critical point a collection of such individuals (spatially uniform at the initial time) may eventually display a wild patchiness (see Fig. III.1) [Zhang et al. 1990; Meyer et al. 1996; Young et al. 2001; Houchmandzadeh 2008]. Spatial clustering phenomena have been first identified in connection with mathematical models of ecological communities [Dawson 1977; Cox and Griffeath 1985], and since then have been thoroughly investigated for both infinite and finite collections of individuals in unbounded domains [Zhang et al. 1990; Meyer et al. 1996; Young et al. 2001; Houchmandzadeh 2008, 2009]. In this chapter, we will revisit the critical catastrophe of neutron chains in a prototype model of a nuclear reactor, with special emphasis on the spatial distribution of neutrons in confined geometries.

1 ABOUT THE PROCESS

III.1.1 A prototype model of a nuclear reactor

A nuclear reactor is a device conceived to extract energy from the fission chains induced by neutrons [Bell and Glasstone 1970]. To fix the ideas, here we will focus on the widely used light-water reactors. The nuclear fuel is made of uranium, arranged in a regular lattice and plunged in light water. A fission chain begins with a neutron emitted at high energy from a fission event (see Fig. III.2). The neutron enters the surrounding water, slows down towards thermal equilibrium, and then starts diffusing. If the neutron eventually re-enters the fuel, it may i) be absorbed on the ^{238}U isotope of uranium, in which case the chain is terminated; or ii) give rise to a new fission event by colliding with the ^{235}U fissile isotope, whereupon a random number of high-energy neutrons are emitted. The water surrounding the fuel lattice acts as a reflector and prevents the neutrons from escaping from the core. A number of control rods are inserted into the core, with the aim of absorbing the excess neutrons and keep the population constant (this ensures a constant power output). When the neutron population grows, the control rods are inserted more deeply into the core, slowing down the chain reaction. On the contrary, when the population decreases, the control rods are raised, accelerating the chain reaction.

The energy- and spatial-dependent behaviour of a nuclear reactor can be fully assessed only by resorting to large-scale numerical simulations including a realistic description of the heterogeneous geometry [Dumonteil et al. 2014; Brun et al. 2013; CEA collectif et al. 2013]. However, for the purposes of this work we will use the simplified prototype model of a nuclear reactor introduced in Chapter I, which retains all the key ingredients of a real system. We assume that the reactor can be represented as a collection of N neutrons evolving in an homogeneous multiplying medium of finite volume V, surrounded by reflecting or absorbing boundaries: neutrons undergo scattering, reproduction and absorption in a confined system. The medium is thus characterised by a constant cross-section Σ, and the stochastic paths of neutrons are known to follow position- and velocity-dependent exponential flights (see Sec. 2). For our model, we approximate these paths by regular Brownian motions with a constant diffusion coefficient D. This corresponds to developing our study in the framework of the one-speed *diffusion approximation* introduced in Sec. I.2.5, considering furthermore that scattering events are isotropic. In particular:

- particles are moving with a constant velocity v, which defines a constant collision rate $\lambda = \Sigma * v = cst$;
- directions of new particles, created at each collision, are isotropically

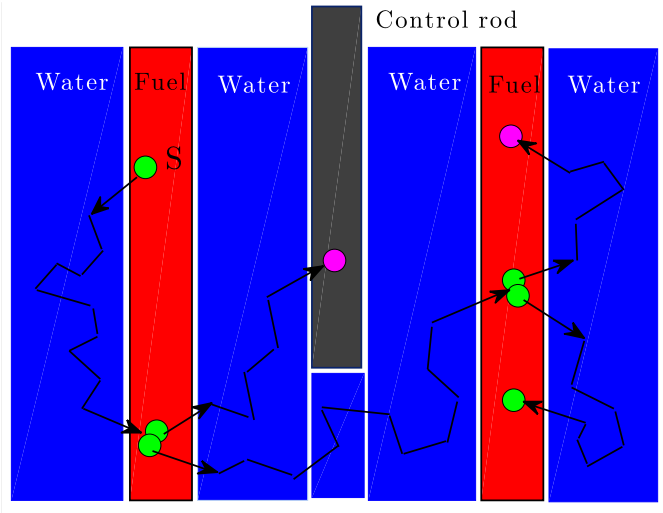

Figure III.2: Simplified scheme of neutron propagation within a nuclear reactor. A fission chain begins with a source neutron S born from a fission event in the fuel. The neutron diffuses in the water and may eventually come back to a fuel element, where it can either be absorbed (magenta dots) and the trajectory terminates; or give rise to a new fission, upon which additional neutrons are set free (green dots). The system is operated at the critical point, where the average number of neutrons produced by fission is exactly compensated by the losses by absorptions. To adjust the total population and enforce the critical regime, a control rod can be inserted to absorb the excess neutrons.

distributed: $C(\mathbf{v} \to \mathbf{v}') = \text{cst} = 1/\Omega_d$;

- the diffusion coefficient is then given by $D = \dfrac{v}{3\Sigma}$ (see Eq. (I.117)).

A diffusing walker then undergoes collisions at rate λ: the incoming neutron "disappears" (captured by a nucleus) and is replaced, with probability p_k, by k of descendants. With probability p_0, the incoming neutron has no descendants (*sterile capture*), which corresponds to a "death event". For $k \geqslant 2$, the incoming neutron "gives birth" to new neutrons. In order for the reactor to be exactly critical, the mean number of descendants per collision, $\nu_1 = \sum_k k p_k$, must be equal to $\nu_1 = 1$ (see Eq. (I.27)).

III.1.2 Elementary clustering with zero-dimensional systems

In Chapter II, we saw that the birth/death process is by itself responsible for very strong fluctuations of the whole population. This observation puts

this process at the heart of the clustering problem. In this section we tackle the clustering problem, starting from the zero dimensional system introduced in Sec. II.1.2.

Let us consider a collection of many copies of a zero-dimensional cell placed side by side. Each cell starts with the same number N_0 of non-diffusing particles, and then evolves independently. Despite the spatial extension of this new system, the problem is still the zero dimensional one studied in Sec. II.1.2; we now observe simultaneously different realisations of the same single-cell system. For a critical system, the mean number of particles in each cell is N_0 at any time (see Eq. (II.18)):

$$\langle N \rangle(i,t) = N_0 \text{ at any time and for every cell } i, \tag{III.1}$$

from which we may expect a uniform and constant distribution of particles among the cells. However, as a consequence of the fluctuations discussed in Sec. II.1.2, most of the cells will be empty in a characteristic time $\tau_E = N_0/(\lambda\nu_2)$, whereas few others will become highly populated, resulting in a clustered system: the conflict between Eq. (III.1) and one realisation of the system illustrates the failure of *self-averaging* [Young et al. 2001]. The clustering appearing here is a local effect of the *critical catastrophe*: before decimating the whole population, strong fluctuations are responsible for local community death, creating holes in the population and thus giving rise to a "trivial clustering" of particles. This phenomenon is then enhanced by the asymmetry between birth and death events: particles can die anywhere, whereas new particles can be created only where there are already other particles (parents), such that, if a cell is empty, it will stay empty.

Therefore, in the spatially extended system, the temporal fluctuations caused by birth/death process in each cell lead to spatial fluctuations of the population across cells. These spatial and temporal fluctuations give rise to a trivial clustering of the population appearing in the characteristic time τ_E. Up to now, particles were not allowed to diffuse over the system. As diffusion has a mixing property, we may expect it to prevent the formation of clusters (by repopulating the empty spaces).

2 FREE POPULATION

Let us consider now the interplay between spatial displacements and birth-and-death events. For the sake of simplicity, the whole chapter we will be placed in the context of the diffusion approximation introduced in Sec. I.2.5. For applications to nuclear reactors, we start the system from a state which corresponds to the equilibrium state of the corresponding critical system with the same boundary conditions. We then let the particles evolve freely:

they can diffuse, reproduce or die in the system. Three different cases will be tackled here, with different initial and boundary conditions:

- the case of an infinite system (that has no boundary) with an infinite number of particle; the system starts with a uniform distribution of particles;
- the case of a finite medium with reflecting boundaries, with a finite number of initial particles starting with a uniform distribution over the system;
- the case of a finite medium with absorbing boundaries, with a finite number of initial particles starting with a "cosine distribution" over the system;

III.2.1 General considerations - Pair Correlation Function

Particles evolve now in a continuous space. In order to characterise the physical properties of the system, we introduce a (local) *instantaneous density*, which is defined for each realisation of the system as

instantaneous density
$$\rho(\mathbf{x}, t) = \lim_{d\mathbf{x}\to 0} \frac{N(\mathbf{x}, t)}{d\mathbf{x}}\,, \tag{III.2}$$

where $N(\mathbf{x}, t)$ is the number of particles in a volume element $d\mathbf{x}$ about $\mathbf{x}$ in the realisation considered. The density $n(\mathbf{x}, t)$ of particles in the vicinity of $\mathbf{x}$ at time t is then defined by the ensemble average of $\rho(\mathbf{x}, t)$,

density
$$n(\mathbf{x}, t) = \langle \rho(\mathbf{x}, t) \rangle\,. \tag{III.3}$$

Here, we start the system from a state which corresponds to the equilibrium state of the corresponding critical system with the same boundary conditions, i.e. $n(\mathbf{x}, t = 0) \doteq n_0(\mathbf{x})$ is solution of the diffusion equation (I.116) in the stationary case at criticality,

$$\Delta n_0(\mathbf{x}) = 0\,, \tag{III.4}$$

and with the appropriate boundary conditions (absorbing or reflecting). If the system is critical, $n(\mathbf{x}, t)$ will then remain unchanged in time. However, as seen previously, this mean density is not necessarily representative of one realisation of the system (which is the property of a self-averaging system). In section II.1.2, to characterise the fluctuations in time of the population and emphasise the non self-averaging character of the system, we introduced the variance of the population size. As the system is now spatially extended, we need a new tool to characterise also the fluctuations in space of the population. This is the role of the *covariance*

$$Cov(\mathbf{x}, \mathbf{y}, t) = \langle \rho(\mathbf{x}, t)\rho(\mathbf{y}, t) \rangle - \langle \rho(\mathbf{x}, t) \rangle \langle \rho(\mathbf{y}, t) \rangle\,. \tag{III.5}$$

Note that $Cov(\mathbf{x}, \mathbf{x}, t) = \sigma^2(\mathbf{x}, t)$, is the variance of the density ρ.

Pair correlation function The correlation function can be defined in many different ways, and among the various definitions, we should choose the one that is the most appropriate for our problem. A common mathematical definition is the correlation coefficient introduced by Pearson, known as *Pearson's correlation coefficient*,

$$g(\mathbf{x},\mathbf{y},t) = \mathrm{Cov}(\mathbf{x},\mathbf{y},t)/(s(\mathbf{x},t)\,s(\mathbf{y},t))\,, \tag{III.6}$$

$s(\mathbf{x},t) = \sqrt{\langle\rho(\mathbf{x},t)^2\rangle - \langle\rho(\mathbf{x},t)\rangle^2}$ is the standard deviation of the instantaneous density $\rho(\mathbf{x},t)$. This coefficient is equal to 1 when $x = y$. However the idea would be to choose a function that also allow us to verify the criteria Eq. (II.13), that push us to rather adopt the slightly different definition:

$$g(\mathbf{x},\mathbf{y},t) = \frac{\mathrm{Cov}(\mathbf{x},\mathbf{y},t)}{\langle\rho(\mathbf{x},t)\rangle\,\langle\rho(\mathbf{y},t)\rangle} = \frac{\langle\rho(\mathbf{x},t)\rho(\mathbf{y},t)\rangle - n(\mathbf{x},t)\,n(\mathbf{y},t)}{n(\mathbf{x},t)\,n(\mathbf{y},t)}\,, \tag{III.7}$$

so that $g(\mathbf{x},\mathbf{x},t) = \mathrm{RSD}_\rho^2$ corresponds to the square of the *relative standard deviation* of $\rho(\mathbf{x},t)$. Indeed the RSD, defined in Eq. (II.13), has appear in Sec. II.1.2 to be the interesting quantity to characterise global fluctuations of the population. On the other hand, note that the definition $\langle\rho(\mathbf{x},t)\rho(\mathbf{y},t)\rangle$ includes the particle *self-contributions* when $\mathbf{x} = \mathbf{y}$, i.e., the contributions due to correlation between each particle with itself. These self-contributions will make $g(\mathbf{x},\mathbf{y},t)$ diverging when in the limit $\mathbf{x} = \mathbf{y}$, as particles are infinitely correlated with themselves. Subtracting the self-contributions, we obtain the pair correlation:

$$h(\mathbf{x},\mathbf{y},t) = \langle\rho(\mathbf{x},t)\rho(\mathbf{y},t)\rangle - \underbrace{\delta(\mathbf{x}-\mathbf{y})\,n(\mathbf{x},t)}_{\text{self-contributions}}\,. \tag{III.8}$$

Formally, $h(\mathbf{x},\mathbf{y},t)$ is the density of pairs of distinct particles formed by one particles about $\mathbf{x}$ and one about $\mathbf{y}$ at time t. We finally define the *centered and normalised pair correlation function* as [Houchmandzadeh 2009]:

$$g(\mathbf{x},\mathbf{y},t) = \frac{h(\mathbf{x},\mathbf{y},t) - h_{\mathrm{ind}}(\mathbf{x},\mathbf{y},t)}{n(\mathbf{x},t)\,n(\mathbf{y},t)}\,, \tag{III.9}$$

where $h_{\mathrm{ind}}(\mathbf{x},\mathbf{y},t)$ corresponds to the pair correlation function $h(\mathbf{x},\mathbf{y},t)$ assuming that particles in the system at time t are all independent. In the limit of a large number of particles in the system, $h_{\mathrm{ind}}(\mathbf{x},\mathbf{y},t) \to n(\mathbf{x},t)\,n(\mathbf{y},t)$.

III.2.2 System of Infinite Size

The case of a system of infinite size has been discussed by Houchmandzadeh [2008, 2002, 2009] for a binary birth/death process (particles can have up to 2 descendants at a collision). Consider a collection of Brownian particles

starting with a uniform distribution in space ($n(\mathbf{x},0) = n_0$[1]); they can move randomly with a diffusion constant D, duplicate with a rate $\lambda_2 = \lambda p_2$ and die with a rate $\lambda_0 = \lambda p_0$. Note that the total number of particles in this system is infinite, such that the extinction time $\tau_E = N_0/(\lambda\nu_2)$ is infinite: this system will never be extinct.

Writing the master equation for the probability $P(N_{\mathbf{x}}, t)$ that a volume element of size $d\mathbf{x}$ about $\mathbf{x}$ contains $N_{\mathbf{x}}$ individuals at time t, and taking the continuous limit when $d\mathbf{x}$ goes to zero, we can extract the equation for any moment of $\rho(\mathbf{x}, t)$ [Houchmandzadeh 2009]. In particular, thanks to the invariance of the problem under spatial translations, the mean density $n(\mathbf{x}, t) = \langle\rho(\mathbf{x}, t)\rangle$ does not depend on the position $\mathbf{x}$ and thus verifies the equation [Houchmandzadeh 2009]:

$$\frac{dn}{dt}(t) = (\lambda_2 - \lambda_0)\, n(t)\,. \tag{III.10}$$

Therefore, starting the system with a uniform distribution of particles n_0,

$$n(t) = n_0\, e^{(\lambda_2 - \lambda_0)\, t}\,. \tag{III.11}$$

For the same reason, the centered and normalised pair correlation function, denoted $g_\infty(\mathbf{x}, \mathbf{y}, t)$ here, depends only on the distance $r = \|\mathbf{x} - \mathbf{y}\|$ between the two positions $\mathbf{x}$ and $\mathbf{y}$, which allows to extract its equation from the master equation [Houchmandzadeh 2009]:

$$\frac{\partial g_\infty}{\partial t}(r, t) = 2D\Delta g_\infty(r, t) + \frac{2\lambda_2}{n_0}\delta(r)\,, \tag{III.12}$$

where $\delta(r)$ is the Dirac delta function. Solving this equation for a system of infinite size (boundary conditions), yields:

$$g_\infty(r, t) = 2\lambda_2 \int_0^t dt'\, \frac{G_\infty^{2D}(r, t - t')}{n(t')}\,, \tag{III.13}$$

where $G_\infty^{2D}(r, t - t')$ is the Green function solution of the homogeneous heat equation with a diffusion coefficient $2\,D$[2] for a system with no boundaries (infinite system) in dimension d:

$$G_\infty^{2D}(r, t) = \frac{1}{(8\pi D t)^{d/2}}\, e^{-\frac{r^2}{8Dt}}\,. \tag{III.14}$$

[1] The uniform density $n(\mathbf{x}, 0) = n_0$ corresponds to the solution of Eq. (III.4) in the case of a system with an infinite size. Note that the total number N_0 of particles in the system is thus infinite.

[2] the homogeneous diffusion equation $\frac{\partial g_\infty}{\partial t}(r, t) = 2D\Delta g_\infty(r, t)$.

Rearranging the terms in the integral (translation in time), the pair correlation function finally reads:

$$g_\infty(r,t) = \frac{2\lambda_2}{n_0}\int_0^t dt' \, \frac{1}{(8\pi D t')^{d/2}} \, e^{-\frac{r^2}{8Dt'} - (\lambda_2 - \lambda_0)(t-t')} . \qquad \text{(III.15)}$$

The coefficient $2\lambda_2$, appearing in the numerator, corresponds to the rate at which pairs of particles are created in the system[3]. Thus increasing the reproduction process, i.e. increasing $2\lambda_2$, increases the correlation between particles. Whereas increasing the diffusion coefficient D or the initial density of particles n_0 (both appearing in the denominator of g) will tend to decrease correlations between particles. This observations confirm the tendency expected in Sec. III.1.2. Moreover, the limit (in the sense of distributions) of the sequence of zero-centered normal distributions, $\frac{1}{a\sqrt{\pi}} e^{-r^2/a^2}$ when $a \to 0$, is the Dirac delta function $\delta(r)$. Thus, in the limit when the diffusion coefficient D goes to zero, we can expect the pair correlation function to converges to the Dirac distribution: as particles do not move, clusters are "point located", just like in the model of Sec. III.1.2 (after τ_E few zero-dimensional cells are over-populated, surrounded by empty cells). Thus, in case of clustering, diffusion seems to increase the spatial extension of the clusters (increasing the correlation length).

Let us consider the critical case $\lambda_2 = \lambda_0$ (equivalent to $\nu_1 = 1$ for a *binary branching process*). In dimension $d = 1$, the pair-correlation function Eq. (III.15) reads

$$g_\infty(r,t) = \frac{2\lambda_2}{n_0}\int_0^t dt' \, \frac{1}{\sqrt{8\pi D t'}} \, e^{-\frac{r^2}{8Dt'}} . \qquad \text{(III.16)}$$

Figure III.3 Left shows a good correspondence between this theoretical solution and a Monte-Carlo simulation of the pair correlation function. The figure also shows the plots of $g_\infty(r,t)$ for different times: the pair correlation function displays a peak when r goes to zero, which characterises a system in which particles tend to cluster [Zhang et al. 1990; Meyer et al. 1996; Young et al. 2001; Houchmandzadeh 2008, 2009]. Indeed, this peak reflects the increased probability of finding particles lying at short distances. The amplitude of the peak increases with time, but also its width. Rewriting $g_\infty(x,t)$ with the change of variables, $u = r/\sqrt{8Dt'}$ in the integral, we

[3] λ is the rate at which collisions happened in the system, and, for a *binary branching process*, $\nu_2 = 2p_2$ is the number of pairs created per collision (see Sec. II.1.1), so that $\lambda\nu_2 = 2\lambda_2$ represents the rate at which pairs of particles are created in the system.

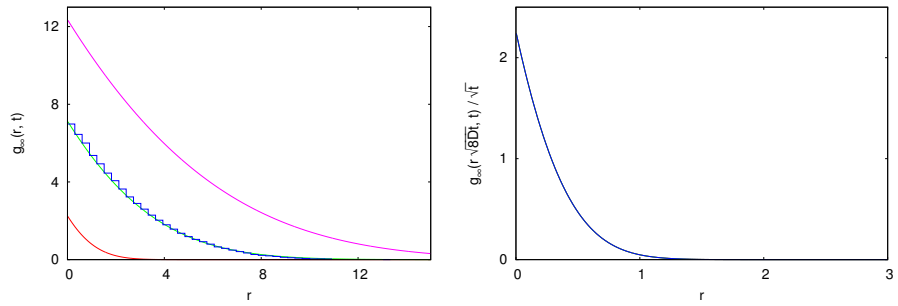

Figure III.3: **Left.** Pair correlation function $g_\infty(r,t)$ for a one-dimensional system of infinite size, with $D = 1$, $\lambda_2 = 1$ and $n_0 = 0.5$, at time $t = 1.$ (red), $t = 10$ (green) and $t = 30$ (purple). Comparison with the pair correlation function obtained by Monte Carlo simulation (blue) for time $t = 10$. **Right.** Self-similarity – exact overlapping of the curves $g_\infty(r\sqrt{8Dt})/\sqrt{t}$ for different time, $t = 1$, 10 and 30.

obtain

$$g_\infty(r,t) = \frac{2\lambda_2}{n_0 4D\sqrt{\pi}}\, r \int_{\frac{r}{\sqrt{8Dt}}}^{+\infty} \frac{e^{-u^2}}{u^2}\, du\,. \tag{III.17}$$

Then, integrating by parts leads to

$$g_\infty(r,t) = \frac{2\lambda_2}{n_0\sqrt{2D}}\,\sqrt{t}\,F\left(\frac{r}{\sqrt{8Dt}}\right), \tag{III.18}$$

$$\text{where } F(X) = \left[\frac{e^{-X^2}}{\sqrt{\pi}} - X\,\mathrm{erfc}(X)\right]. \tag{III.19}$$

The function $\mathrm{erfc}(X)$ is the *complementary error function* defined for $X \in \mathbb{R}$ as

$$\mathrm{erfc}(X) = \frac{2}{\sqrt{\pi}} \int_X^\infty e^{-u^2}\, du\,. \tag{III.20}$$

Note that $F(0) = 1/\sqrt{\pi}$ is finite, so that

$$g_\infty(0,t) \;=\; \frac{2\lambda_2}{n_0\sqrt{2D}}\,\sqrt{t} \;=\; \frac{\sqrt{\tau_D}}{\tau_P}\,\frac{\sqrt{t}}{\sqrt{\pi}}\,. \tag{III.21}$$

The amplitude of $g_\infty(0,t)$ is governed by the ratio $\sqrt{\tau_D}/\tau_P$, and thus results from a competition between a diffusion process, of a characteristic time $\tau_D = (2Dn_0^2)^{-1}$, and a process of production of particle pairs, of characteristic time $\tau_P = (2\lambda_2)^{-1}$. Increasing diffusion (smaller τ_D) will reduce

the correlation between particles, whereas increasing the reproduction process (smaller τ_P) will tend to increase the correlations. Observe that both the amplitude and the width of the peak grow with $\sqrt{t}$ (more precisely the width increases with $\sqrt{8Dt}$, see Eq. (III.18)). In fact, Eq. (III.18) exhibits a *self-similarity* property of the system (see Fig. III.3 Right.), which is a consequence of the infinite spatial extension of the system, and of the infinite source of particles.

In dimension $d \geqslant 2$, the pair-correlation function Eq. (III.15) can be rewritten using the change of variable $u = r^2/(8Dt')$ in the integral:

$$g_\infty(r,t) = \frac{2\lambda_2}{n_0(8\pi D)^{d/2}} \frac{1}{t^{\frac{d}{2}-1}} \left(\frac{8Dt}{r^2}\right)^{\frac{d}{2}-1} \int_{\frac{r^2}{8Dt}}^{+\infty} u^{\frac{d}{2}-2} e^{-u}\, du\,. \quad \text{(III.22)}$$

The coefficient in front of this equation has the dimension of a time to the power $(d/2-1)$: we recognise the pair production time $\tau_P = (\lambda\nu_2)^{-1}$ and the diffusion characteristic time $\tau_D = (2Dn_0^2)^{-1}$, such that

$$\frac{2\lambda_2}{n_0(2D)^{d/2}} = \frac{{\tau_D}^{d/2}}{\tau_P}\,, \quad \text{(III.23)}$$

as a signature of the competition between mixing from diffusion and clustering from birth and death events. Here also the system exhibits a self-similarity property:

$$g_\infty(r,t) = \frac{{\tau_D}^{d/2}}{\tau_P} \frac{1}{t^{\frac{d}{2}-1}} F_d\left(\frac{r^2}{8Dt}\right)\,, \quad \text{(III.24)}$$

$$\text{where} \qquad F_d(X) = \frac{1}{(4\pi)^{d/2}} \frac{1}{X^{\frac{d}{2}-1}} \Gamma\left(\frac{d}{2}-1, X\right)\,. \quad \text{(III.25)}$$

The function $\Gamma(a,X)$ is the *upper incomplete gamma function* defined for $X \in \mathbb{R}^+$ and $a > 0$ as

$$\Gamma(a,X) = \int_X^\infty u^{a-1} e^{-u}\, du\,. \quad \text{(III.26)}$$

However a series expansion[4] of $F_d(X)$ about $X = 0$ ($r = 0$),

$$\begin{cases} F_d(X) = \dfrac{1}{4\pi}\left[-\gamma - \log(X) + \mathcal{O}(X)\right]\,, & \text{for } d = 2 \\ F_d(X) = \dfrac{1}{(4\pi)^{d/2}}\left[\dfrac{1}{X^{\frac{d}{2}-1}}\Gamma\left(\dfrac{d}{2}-1\right) - \dfrac{2}{d-2} + \mathcal{O}(X)\right]\,, & \text{for } d > 2\,, \end{cases}$$

[4] where $\Gamma(a) = \Gamma(a,0)$ and $\gamma = -\int_0^\infty e^{-u}\log(u)\, du$ is the Euler-Mascheroni constant

shows that the pair correlation function, in dimension higher than 1, is always diverging when r goes to 0 at any time $t > 0$.

To summarise, the pair correlation function between particles separated by a distance r displays a pic when r goes to zero, which characterises the tendency of particle clustering. The phenomenon then results from a competition between diffusion that tend to mix the system (decreases short range correlation and increase the correlation length) and the creation of particle pairs that correlate particles of the same family (increases short range correlations). However, the size of the system and the source of particles being infinite here, none of these two processes can actually "win", which results in a self-similar pair correlation function. In higher dimension, we notice that the mixing effect of diffusion is weaker.

III.2.3 System of finite size - Feynman-Kac backward formalism and general solution

In a nuclear reactor, the medium where neutrons evolve has of course a finite size, and the number of initial particles is also finite (although large). This is more generally the case for any physical systems. For instance, a nuclear fuel rod in a PWR can be modeled by a thin cylinder ($\sim$ 3 mm of radius and $\sim$ 4 m high - see Fig. I.10), with absorbing boundaries at its top and bottom, and surrounding by water in which neutrons are driven back to the fuel (reflecting boundaries). It then seems natural to wonder how the finite size of the medium affects the clustering phenomenon. (In the following we will consider finite size system, with reflecting boundaries or absorbing boundaries).

So far, we have used a forward description of the problem, establishing the equations for $n(\mathbf{x}, t)$ and $g(\mathbf{x}, \mathbf{y}, t)$ from a master equation of the system [Houchmandzadeh 2009]. Because of the branching nature of the process, this approach requires to use combinatorial tools (see the derivation of the master equation in Ann. 2), and becomes particularly cumbersome in presence of boundaries, where the translational symmetry of the system is broken. For these systems, it is more convenient to resort to the backward formalism introduced in Chapter II. Fig. III.4 illustrates this idea: whereas one particle taken at time 0 can have zero, one, or several descendants at any positive time $t' > 0$ (see Fig. III.4 Left), a particle, randomly chosen at time t, has a single ancestor at any earlier time t' ($0 < t' < t$), as illustrated on Fig. III.4 Right. Therefore, instead of following several branches, which requires combinatorial analysis in the forward method, we simply follow a single (generalised) trajectory defined by the trajectories of each ancestor (red path on Fig. III.4 Right) in the backward method.

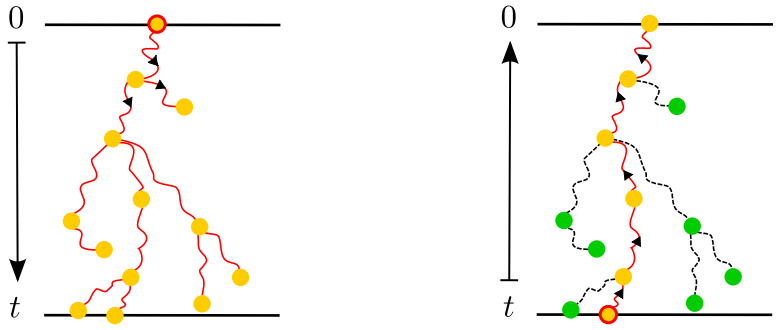

Figure III.4: Schematic representation of the evolution of a particle family descending from a single particle at time 0. Branching and death events are represented by yellow or green dots. This figure illustrates why, with a forward method (on the left hand side), we need to perform a combinatorial analysis at each branching point of the family, whereas, with a backward method (on the right hand side), the analysis consists in tracing back a particle trajectory up to the ancestor at time $t = 0$.

In the following, we will establish the general equation for the density $n(\mathbf{x}, t)$ and the pair correlation function $g(\mathbf{x}, \mathbf{y}, t)$ for a system surrounded by boundaries. We will then derive explicit solutions for reflecting or absorbing boundaries.

a. Backward equation and general solution for the mean density

Backward equations Consider a system of finite volume V starting with a single particle in $\mathbf{r}_0 \in V$ at time $t = 0$. We denote by $N_X(t|\mathbf{r}_0)$ the instantaneous number of particles that are located within a sub-domain X at time t (for a system initially starting with one single particle in $\mathbf{r}_0$). This random variable was already introduced in Chapter II. It is associated with the moment generating function

$$W_t(s\,|\,\mathbf{r}_0) = \langle\, s^{N_X(t\,|\,\mathbf{r}_0)} \,\rangle\,, \tag{III.27}$$

whose equation of evolution of can be formulated using the Feynman-Kac backward formalism (see Sec. II.3.3) in the context of the diffusion approximation [Pázsit and Pál 2007; Bell 1965]:

$$\frac{\partial W_t}{\partial t}(s\,|\,\mathbf{r}_0) = \underbrace{D\,\nabla^2_{\mathbf{r}_0} W_t}_{\text{Diffusion}} \underbrace{-\,\lambda\, W_t}_{\text{Capture}} + \underbrace{\lambda\, G\big[W_t\big]}_{\text{descendant contribution}}\,, \tag{III.28}$$

where $G[z] = \sum_k p_k z^k$ is the moment generating function of the number of particles emitted at a collision. This equation if known as the Pál-Bell equation (see Eq. II.74).

Every moment of $N_X(t|\mathbf{r}_0)$ can be obtained by derivation of the moment generating function $W_t(s\,|\,\mathbf{r}_0)$. In particular the mean number of particles in X is given by:

$$\langle\, N_X(t\,|\,\mathbf{r}_0)\,\rangle = \partial_s W_t(s|\mathbf{r}_0)\Big|_{s=0}. \tag{III.29}$$

Using this definition and recalling that $G'[1] = \nu_1$, we obtain, from Eq. (III.28) the evolution equation for $\langle\, N_X(t\,|\,\mathbf{r}_0)\,\rangle$, associated with the initial condition:

$$\begin{cases} \partial_t \langle\, N_X(t\,|\,\mathbf{r}_0)\,\rangle = D\Delta_{\mathbf{r}_0}\langle\, N_X\,\rangle + \lambda(\nu_1 - 1)\langle\, N_X\,\rangle\,, \\ \langle\, N_X(0\,|\,\mathbf{r}_0)\,\rangle = \mathbb{1}_X(\mathbf{r}_0)\,, \end{cases} \tag{III.30}$$

where $\mathbb{1}_X(\mathbf{r})$ is the *marker function* of the domain X, equal to 1 if $\mathbf{r} \in X$ and 0 otherwise. Let us set now the sub-domain X to the volume element $d\mathbf{x}$ located in $\mathbf{x}$. The number of particles within the volume element $d^3\mathbf{x}$ about $\mathbf{x}$ at time t then corresponds to $N(\mathbf{x}, t\,|\,\mathbf{r}_0) = N_X(t\,|\,\mathbf{r}_0)$, and the instantaneous density (III.2) is given by

$$\rho(\mathbf{x}, t\,|\,\mathbf{r}_0) = \lim_{d\mathbf{x}\to 0} \frac{N(\mathbf{x}, t\,|\,\mathbf{r}_0)}{d\mathbf{x}} = \lim_{d\mathbf{x}\to 0} \frac{N_X(t\,|\,\mathbf{r}_0)}{d\mathbf{x}}\,. \tag{III.31}$$

Dividing Eq. (III.30) by $d\mathbf{x}$ and taking its limit when $d\mathbf{x}$ goes to 0, we finally obtain the backward evolution equation of the density of particles at time t in the vicinity of $\mathbf{x}$, $n(\mathbf{x}, t\,|\,\mathbf{r}_0) = \langle \rho(\mathbf{x}, t\,|\,\mathbf{r}_0)\rangle$:

Backward equation for the particle concentration $n\,(\mathbf{x}, t\,|\,\mathbf{r}_0)$

$$\begin{cases} \partial_t\, n\,(\mathbf{x}, t\,|\,\mathbf{r}_0) = D\,\nabla^2_{\mathbf{x}_0} n\,(\mathbf{x}, t\,|\,\mathbf{r}_0) + \lambda(\nu_1 - 1)\, n\,(\mathbf{x}, t\,|\,\mathbf{r}_0)\,, \\ n\,(\mathbf{x}, 0\,|\,\mathbf{r}_0) = \delta(\mathbf{x} - \mathbf{r}_0)\,, \\ + \text{ Boundary Conditions} \end{cases} \tag{III.32}$$

More generally, the system is started with a finite number N_0 of particles distributed over the volume V with a pdf $p(\mathbf{r}_0)$. These N_0 initial particles are emitted independently, and each of them gives rise to a family which evolves independently of the others. The density resulting from this N_0 independent particle sources then reads

$$\boxed{n\,(\mathbf{x}, t) = N_0 \int_V p(\mathbf{r}_0)\, n\,(\mathbf{x}, t\,|\,\mathbf{r}_0) d\mathbf{r}_0\,.} \tag{III.33}$$

Note that we can also arrive at this result starting from the moment generating function. At time $t = 0$, each particle is independently emitted from a position $\mathbf{r}_0$ of the system with a probability density $p(\mathbf{r}_0)$. It thus results a source S whose distribution in space is given by:

$$n_0(\mathbf{r}_0) = N_0\, p(\mathbf{r}_0)\,. \tag{III.34}$$

Let us denote by $N_X(t\,|\,S)$ the number of particles in the domain X at time t resulting from the source S of particles in the system at $t = 0$. This random variable can be associated with a moment generating function $W_t(u\,|\,S)$, such that:

$$\langle\, N_X(t\,|\,S)\,\rangle = \partial_u\, W_t(s\,|\,S)\Big|_{s=0}\,. \tag{III.35}$$

By definition, since the initial positions of the N_0 particles are independent,

$$\begin{aligned} W_t(s\,|\,S) &= \int_V p(\mathbf{r}_1)\,\cdots\,p(\mathbf{r}_{N_0})\,W_t(s\,|\,\mathbf{r}_1)\cdots W_t(s\,|\,\mathbf{r}_{N_0})\,d\mathbf{r}_1\cdots d\mathbf{r}_{N_0}\,,\\ &= \Big[\int_V p(\mathbf{r}_0)\; W_t(s\,|\,\mathbf{r}_0)\,d\mathbf{r}_0\Big]^{N_0}\,. \end{aligned} \tag{III.36}$$

which, using the property Eq. (III.35) and the definition Eq. (III.34), leads to

$$\langle\, N_X(t\,|\,S)\,\rangle = \int_V n_0(\mathbf{r}_0)\,\langle\, N_X(t\,|\,\mathbf{r}_0)\,\rangle\,d\mathbf{r}_0\,, \tag{III.37}$$

and finally to the result of equation (III.41).

General Solution The general solution of Eq. (III.32) reads

$$n\,(\mathbf{x}, t\,|\,\mathbf{r}_0) = e^{\lambda(\nu_1-1)t}\int_V d\mathbf{r}'_0\,\delta(\mathbf{x}-\mathbf{r}'_0)\,G_D(\mathbf{r}_0, t\,;\,\mathbf{r}'_0, t'=0)\,, \tag{III.38}$$

hence, by definition of the Dirac delta function,

$$n\,(\mathbf{x}, t\,|\,\mathbf{r}_0) = e^{\lambda(\nu_1-1)t}\,G_D(\mathbf{x}, t;\,\mathbf{r}_0)\,, \tag{III.39}$$

where $G_D(\mathbf{x}, t;\,\mathbf{r}_0)$ is the Green function solution of the diffusion equation

$$\boxed{\begin{cases} \left(\partial_t - D\,\nabla^2_{\mathbf{r}_0}\right)\,G_D(\mathbf{r}, t;\,\mathbf{r}_0, t_0) = \delta(\mathbf{r}-\mathbf{r}_0)\,\delta(t-t_0)\,,\\ + \text{ Boundary Conditions.} \end{cases}} \tag{III.40}$$

The general from of density for an extended source of particles is then

Particle concentration

$$n\,(\mathbf{x}, t) = e^{\lambda(\nu_1-1)t}\int_V n_0(\mathbf{r}_0)\,G_D(\mathbf{x}, t;\,\mathbf{r}_0)\,d\mathbf{r}_0\,. \tag{III.41}$$

To go further now, we need to add boundary conditions, and the expression of the initial source of particles $n_0(\mathbf{r}_0)$.

b. Backward equation and general expression for the pair correlation function

Backward equation Consider a system of finite volume V starting with a single particle in $\mathbf{r}_0 \in V$ at time $t = 0$. To characterise correlations between particles, we focus on the mean number of particle pairs formed by one particle in a sub-domain $X \subset V$ and one in a sub-domain $Y \subset V$ at time t:

$$\langle\, N_X(t\,|\,\mathbf{r}_0)\, N_Y(t\,|\,\mathbf{r}_0)\,\rangle\,. \tag{III.42}$$

Observe that this definition includes the self-contributions of particles when $X = Y$, i.e., the contributions due to the N_X pairs formed by each particle with itself. We then define the correlation function

$$\begin{aligned} \mathcal{G}(\mathbf{x},\mathbf{y},t\,|\,\mathbf{r}_0) &= \langle\, \rho(\mathbf{x},t\,|\,\mathbf{r}_0)\,\rho(\mathbf{y},t\,|\,\mathbf{r}_0)\,\rangle\,, &\text{(III.43)}\\ &= \lim_{d\mathbf{x}\to 0}\lim_{d\mathbf{y}\to 0}\left\langle \frac{N_X(t\,|\,\mathbf{r}_0)}{d\mathbf{x}}\,\frac{N_Y(t\,|\,\mathbf{r}_0)}{d\mathbf{y}}\right\rangle, &\text{(III.44)}\end{aligned}$$

by taking the subdomain X as the volume element $d\mathbf{x}$ about $\mathbf{x}$, and the subdomain Y as the volume element $d\mathbf{y}$ about $\mathbf{y}$. The various *moments* of the random variable $N_X(t|\mathbf{r}_0)\,N_Y(t|\mathbf{r}_0)$ can be obtained by derivation of the moment generating function:

$$W_t^{X,Y}(u,w\,|\,\mathbf{r}_0) = \left\langle\, u^{\,N_X(t\,|\,\mathbf{r}_0)}\, w^{\,N_Y(t\,|\,\mathbf{r}_0)}\,\right\rangle. \tag{III.45}$$

For simplicity, we will discard the superscript X, Y in the following[5]. In particular,

$$\langle\, N_X(t\,|\,\mathbf{r}_0)\, N_Y(t\,|\,\mathbf{r}_0)\,\rangle = \partial_u\partial_w\, W_t(u,w|\mathbf{r}_0)\Big|_{\substack{w=0\\u=0}}. \tag{III.46}$$

Using the Feynman-Kac method to formulate the evolution equation of $W_t(u,w\,|\,\mathbf{r}_0)$, it can be shown that $W_t(u,w\,|\,\mathbf{r}_0)$ satisfies the same backward equation as the moment generating function $W_t(u\,|\,\mathbf{r}_0)$ [Pázsit and Pál 2007; Bell 1965], namely,

$$\partial_t\, W_t(u,w\,|\,\mathbf{r}_0) = D\nabla^2_{\mathbf{r}_0} W_t - \lambda W_t + \lambda G[W_t]\,. \tag{III.47}$$

Then by taking the mixed derivative of Eq. (III.46), we get

$$\partial_t\,\langle\, N_X\, N_Y(t\,|\,\mathbf{r}_0)\,\rangle = D\nabla^2_{\mathbf{r}_0}\langle\, N_X\, N_Y\,\rangle + \lambda(\nu_1 - 1)\langle\, N_X\, N_Y\,\rangle + \lambda\nu_2\langle\, N_X\,\rangle\,\langle\, N_Y\,\rangle\,,$$

recalling that $G'[1] = \nu_1$ and $G^{(2)}[1] = \nu_2$. With the definitions Eq. (III.44) and Eq. (III.31) we finally obtain the

[5] The distinction with the moment generating function $W_t(s)$ in Eq. (III.27) is already explicit thanks to the variables u, v instead of s.

Backward equation for the correlation function $\mathcal{G}$

$$\begin{cases} \partial_t\, \mathcal{G}(\mathbf{x},\mathbf{y},t\,|\,\mathbf{r}_0) = D\,\nabla^2_{\mathbf{r}_0}\mathcal{G} + \lambda(\nu_1-1)\,\mathcal{G} + \lambda\nu_2\, n(\mathbf{x},t\,|\,\mathbf{r}_0)\, n(\mathbf{y},t\,|\,\mathbf{r}_0) \\ \mathcal{G}(\mathbf{x},\mathbf{y},0\,|\,\mathbf{r}_0) = \delta(\mathbf{x}-\mathbf{r}_0)\,\delta(\mathbf{y}-\mathbf{r}_0) \\ + \text{Boundary Conditions.} \end{cases} \tag{III.48}$$

To express the correlation function $\mathcal{G}_{\mathcal{S}}(\mathbf{x},\mathbf{y},t)$ resulting from a source $\mathcal{S}$ of N_0 independent particles at $t=0$, let us restart from the definition

$$\mathcal{G}_{\mathcal{S}}(\mathbf{x},\mathbf{y},t) = \langle\, \rho(\mathbf{x},t)\,\rho(\mathbf{y},t)\,\rangle\,, \tag{III.49}$$

$$= \lim_{dx\to 0}\lim_{dy\to 0}\left\langle \frac{N_X(t\,|\,\mathcal{S})}{dx}\,\frac{N_Y(t\,|\,\mathcal{S})}{dy}\right\rangle, \tag{III.50}$$

generalising Eq. (III.44) to any source $\mathcal{S}$ of particles. This correlation function can be associated with the generating function $W_t(u,w\,|\,\mathcal{S})$, such that

$$\langle\, N_X(t|\mathcal{S})\, N_Y(t|\mathcal{S})\,\rangle = \partial_u\partial_v W_t(u,w\,|\,\mathcal{S})\Big|_{\substack{u=0\\w=0}}. \tag{III.51}$$

The N_0 particles emitted from the source are independent and their initial positions are identically distributed according to the pdf $p(\mathbf{r}_0)$. Thus, by definition,

$$W_t(u,w\,|\,\mathcal{S}) = \int_V p(\mathbf{r}_1)\cdots p(\mathbf{r}_{N_0})\, W_t(u,w\,|\,\mathbf{r}_1)\cdots W_t(u,w\,|\,\mathbf{r}_{N_0})\,d\mathbf{r}_1\cdots d\mathbf{r}_{N_0}\,,$$

$$= \Big[\int_V p(\mathbf{r}_0)\, W_t(u,w\,|\,\mathbf{r}_0)\,d\mathbf{r}_0\Big]^{N_0}. \tag{III.52}$$

Applying the definition (III.51) and using Eq. (III.35) then leads to

$$\langle\, N_X N_Y(t\,|\,\mathcal{S})\,\rangle = N_0(N_0-1)\int_V p(\mathbf{r}_0)\,\langle\, N_X(t|\mathbf{r}_0)\,\rangle\,d\mathbf{r}_0 \int_V p(\mathbf{r}_0)\,\langle\, N_Y(t|\mathbf{r}_0)\,\rangle\,d\mathbf{r}_0$$
$$+ N_0\int_V p(\mathbf{r}_0)\,\langle\, N_X\, N_Y(t|\mathbf{r}_0)\,\rangle\,d\mathbf{r}_0\,,$$

and we finally obtain the correlation function

$$\boxed{\mathcal{G}_{\mathcal{S}}(\mathbf{x},\mathbf{y},t) = N_0(N_0-1)\, n(\mathbf{x},t|\mathcal{S}_1)\, n(\mathbf{y},t|\mathcal{S}_1) + N_0\int_V d\mathbf{r}_0\, p(\mathbf{r}_0)\,\mathcal{G}(\mathbf{x},\mathbf{y},t|\mathbf{r}_0)} \tag{III.53}$$

The density $n(\mathbf{x},t|\mathcal{S}_1)$ is the density of particles about $\mathbf{x}$ at time t resulting from a source of a single particle distributed over V according to $p(\mathbf{r}_0)$:

$$n(\mathbf{x},t|\mathcal{S}_1) = \int_V p(\mathbf{r}_0)\, n(\mathbf{x},t|\mathbf{r}_0)\,d\mathbf{r}_0\,. \tag{III.54}$$

As the N_0 particles of the source are independent, $n(\mathbf{x},t|\mathcal{S}) = N_0\, n(\mathbf{x},t|\mathcal{S}_1)$, and we recover Eq. (III.41). In Eq. (III.53), observe that

$$N_0(N_0-1)\, n(\mathbf{x},t|\mathcal{S}_1)\, n(\mathbf{y},t|\mathcal{S}_1) \doteq h_{\text{ind}}(\mathbf{x},\mathbf{y},t)\,, \tag{III.55}$$

corresponds to the pair correlation function in the system at time t in absence of correlation (as if particles in the system at time t were all independent).

Pair correlation function – Just like $\langle\, N_X(t\,|\,\mathbf{r}_0)\, N_Y(t\,|\,\mathbf{r}_0)\,\rangle$, the correlation function $\mathcal{G}_{\mathcal{S}}(\mathbf{x},\mathbf{y},t)$, defined in Eq. (III.50), includes self-contributions of particles when $X = Y$. Subtracting these contributions to $\mathcal{G}(\mathbf{x},\mathbf{y},t\,|\,\mathcal{S})$, we obtain the pair correlation defined in Sec. III.2.1 [Houchmandzadeh 2009],

$$\boxed{h(\mathbf{x},\mathbf{y},t) = \mathcal{G}(\mathbf{x},\mathbf{y},t\,|\,\mathcal{S}) - \underbrace{\delta(\mathbf{x}-\mathbf{y})\, n(\mathbf{x},t\,|\,\mathcal{S})}_{\text{self-contributions}}\,.} \tag{III.56}$$

Indeed, when $X = Y$ the mean number of particle pairs in $X = Y$ is

$$\big\langle\, N_X(t\,|\,\mathcal{S})\,\big(\,N_X(t\,|\,\mathcal{S})-1\big)\,\big\rangle = \langle\, N_X(t\,|\,\mathcal{S})^2\,\rangle - \langle\, N_X(t\,|\,\mathcal{S})\,\rangle\,, \tag{III.57}$$

whereas, it is $\langle\, N_X(t\,|\,\mathcal{S})\, N_Y(t\,|\,\mathcal{S})\,\rangle$ when $X \neq Y$. $h(\mathbf{x},\mathbf{y},t)$ is the density of pairs of distinct particles formed by one particles about $\mathbf{x}$ and one about $\mathbf{y}$, that results at time t from a source $\mathcal{S}$ of particles at time $t = 0$.

General Solution The general solution of Eq. (III.48) reads

$$\begin{aligned}\mathcal{G}\,(\mathbf{x},\mathbf{y},t\,|\,\mathbf{r}_0) &= e^{\lambda(\nu_1-1)t}\int_V d\mathbf{r}_0'\,\delta(\mathbf{x}-\mathbf{r}_0')\,\delta(\mathbf{y}-\mathbf{r}_0')\,G_D(\mathbf{r}_0,t\,;\,\mathbf{r}_0',0)\\ &+\int_0^t dt'\int_V d\mathbf{r}_0'\,\lambda\nu_2\, n(\mathbf{x},t'|\mathbf{r}_0')\, n(\mathbf{y},t'|\mathbf{r}_0')\, e^{\lambda(\nu_1-1)(t-t')}\, G_D(\mathbf{r}_0,\mathbf{r}_0',t-t')\,.\end{aligned}$$

Using Eq. (III.38), the first term of this solution, is equal to $\delta(\mathbf{x}-\mathbf{y})\, n(\mathbf{x},t|\mathbf{r}_0)$. Replacing then Eq. (III.39), $e^{\lambda(\nu_1-1)(t-t')}\, G_D(\mathbf{r}_0,\mathbf{r}_0',t-t') = n(\mathbf{r}_0',t-t'|\mathbf{r}_0)$, in the second term, we can rewrite the correlation function $\mathcal{G}$:

$$\begin{aligned}\mathcal{G}\,(\mathbf{x},\mathbf{y},t\,|\,\mathbf{r}_0) &= \delta(\mathbf{x}-\mathbf{y})\, n(\mathbf{x},t|\mathbf{r}_0)\\ &\quad+\lambda\nu_2\int_0^t dt'\int_V d\mathbf{r}_0'\, n(\mathbf{x},t'|\mathbf{r}_0')\, n(\mathbf{y},t'|\mathbf{r}_0')\, n(\mathbf{r}_0',t-t'|\mathbf{r}_0)\,.\end{aligned} \tag{III.58}$$

Therefore, for an extended source $\mathcal{S}$ of particles, the correlation function $\mathcal{G}_{\mathcal{S}}(\mathbf{x},\mathbf{y},t)$ given by Eq. (III.53) becomes

$$\begin{aligned}\mathcal{G}_{\mathcal{S}}(\mathbf{x},\mathbf{y},t) = \underbrace{h_{\text{ind}}(\mathbf{x},\mathbf{y},t)}_{\text{independent pairs}} &+ \underbrace{N_0\,\delta(\mathbf{x}-\mathbf{y})\, n(\mathbf{x},t\,|\,\mathcal{S}_1)}_{\text{self-contributions}}\\ &+ \underbrace{N_0\,\lambda\nu_2\int_0^t dt'\int_V d\mathbf{r}_0'\, n(\mathbf{x},t'|\mathbf{r}_0')\, n(\mathbf{y},t'|\mathbf{r}_0')\, n(\mathbf{r}_0',t-t'\,|\,\mathcal{S}_1)}_{\text{correlated pairs from the same family}}\,,\end{aligned} \tag{III.59}$$

where $h_{\text{ind}}(\mathbf{x}, \mathbf{y}, t)$ is given by Eq. (III.55). Here we can identify different contributions to the correlation function $\mathcal{G}_{\mathcal{S}}$:

- the first term corresponds to the pair correlation function of the system at time t computed as if particles were all independent;
- then, we recognise the term of *self-contributions*, $N_0\,\delta(\mathbf{x}-\mathbf{y})\,n(\mathbf{x}, t|\mathcal{S}_1) = \delta(\mathbf{x}-\mathbf{y})\,n(\mathbf{x}, t|\mathcal{S})$ (see Eq. (III.56));
- the last term corresponds to the correlations between particles of the same family, i.e. particles that share a common ancestor. It thus represents the non-trivial contribution to the correlations due to the branching mechanism, and therefore is the key quantity for understanding the clustering phenomenon.

Using Eq. (III.56), we can reformulate Eq. (III.59) and focus on this last term:

$$h(\mathbf{x}, \mathbf{y}, t) - h_{\text{ind}}(\mathbf{x}, \mathbf{y}, t) = \tag{III.60}$$
$$+ N_0\lambda\nu_2 \int_0^t dt'\, e^{2\lambda(\nu_1-1)\,t'} \int_V d\mathbf{r}_0'\, G_D(\mathbf{x}, t'|\mathbf{r}_0')\, G_D(\mathbf{y}, t'|\mathbf{r}_0')\, n(\mathbf{r}_0', t-t'|\mathcal{S}_1)$$

where we used $n(\mathbf{x}, t\,|\,\mathbf{r}_0) = \exp(\lambda(\nu_1-1)\,t)\,G_D(\mathbf{x}, t; \mathbf{r}_0)$ from Eq. (III.39). Finally, the centered and normalised pair correlation function defined in Eq. (IV.90) becomes, with $n(\mathbf{y}, t|\mathcal{S}) = N_0\,n(\mathbf{y}, t|\mathcal{S}_1)$,

$$\boxed{g(\mathbf{x}, \mathbf{y}, t) = \frac{\lambda\nu_2}{N_0} \frac{\displaystyle\int_0^t dt'\, e^{2\lambda(\nu_1-1)\,t'} \int_V d\mathbf{r}_0'\, G_D(\mathbf{x}, t'; \mathbf{r}_0')\, G_D(\mathbf{y}, t'; \mathbf{r}_0')\, n(\mathbf{r}_0', t-t'|\mathcal{S}_1)}{n(\mathbf{x}, t|\mathcal{S}_1)\, n(\mathbf{y}, t|\mathcal{S}_1)}} \tag{III.61}$$

Particular cases – In the case of a uniform initial distribution of particles, $p(\mathbf{r}_0) = \text{cst} = 1/V$, the expression (III.41) for the density $n(\mathbf{x}, t|\mathcal{S}_1)$ can be simplified:

$$n(\mathbf{x}, t|\mathcal{S}_1) = \frac{1}{V}\, e^{\lambda(\nu_1-1)\,t} \int_V G_D(\mathbf{x}, t; \mathbf{r}_0)\, d\mathbf{r}_0 = \frac{1}{V}\, e^{\lambda(\nu_1-1)\,t}\,, \tag{III.62}$$

thanks to the normalisation property of the propagator $G_D(\mathbf{x}, t; \mathbf{r}_0)$. In this case, the density then reads

$$n(x, t) = n_0\, e^{\lambda(\nu_1-1)\,t}\,, \tag{III.63}$$

where $n_0 = N_0/V$ is the initial density of particles, and Eq. (III.61) simplifies

$$g(x, y, t) = \frac{\lambda\nu_2}{n_0} \int_0^t e^{\lambda(\nu_1-1)\,(t'-t)}\, G_{2D}(\mathbf{x}, \mathbf{y}, t')\, dt'\,, \tag{III.64}$$

where we used the property of convolution of two identical Green functions[6]. In the limit case of N_0 and V taken to infinity with keeping the ratio $n_0 = N_0/V$ constant, the Green function $G_D(\mathbf{x}, t'; \mathbf{y}) = G_D^\infty(\mathbf{x} - \mathbf{y}, t')$ is given by Eq. (III.14) and we recover the centered and normalised pair correlation function $g_\infty(x, y, t)$ of the system of infinite size (see previous section), with, in addition, a generalisation to any number of descendants per collision[7].

III.2.4 System of finite size - reflecting and absorbing boundaries

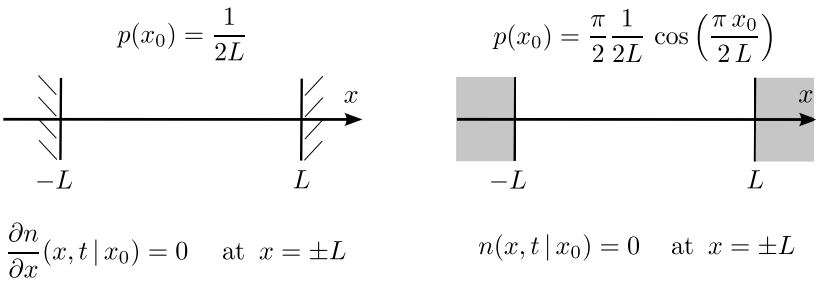

Figure III.5: One dimensional systems considered with respective initial and boundary conditions: reflecting boundary condition on the Left and absorbing on the Right.

a. Reflecting boundaries

Consider a one-dimensional system of size $V = 2L$ with reflecting boundaries (Neumann boundary conditions) in $x = -L$ and $x = L$:

$$\frac{\partial n}{\partial x}(x, t \,|\, x_0) = 0 \qquad \text{at} \qquad x = \pm L\,. \tag{III.65}$$

For instance, this system could model a one-dimensional fuel rod surrounded by water in a nuclear reactor (see Sec. III.1.1). We then start the system with N_0 branching Brownian particles prepared at equilibrium (see Eq. (III.4)), which corresponds, for reflecting boundaries, to a uniform distribution of the N_0 particles: $n_0 = N_0/2L$ (see Fig. III.5 Left). The mean density of particles in the system is then given by Eq. (III.63):

Neutron density, for reflecting boundary conditions

$$n(x, t) = n_0\, e^{\lambda(\nu_1 - 1)\, t}\,. \tag{III.66}$$

The system is thus exactly critical for $\nu_1 = 1$. For this system, the Green

[6] $\int_V d\mathbf{r}_0'\, G_D(\mathbf{x}, t'; \mathbf{r}_0')\, G_D(\mathbf{y}, t'; \mathbf{r}_0') = G_{2D}(\mathbf{x}, t'; \mathbf{y})$

[7] In the previous section, $g_\infty(x, y, t)$ was only derived for the binary branching case.

function solution of the nonhomogeneous heat equation (III.40) reads [Polyanin 2001; Polyanin; Grebenkov and Nguyen 2013]

$$G_D(x,y,t) = \frac{1}{2L} + \frac{1}{L}\sum_{n=1}^{\infty} a_n(x,y)\,\exp\left(-\frac{D\,n^2\,\pi^2\,t}{4\,L^2}\right)\,, \tag{III.67}$$

$$\text{where} \qquad a_n(x,y) = \cos\left(\frac{n\,\pi\,x}{2\,L} + \frac{n\,\pi}{2}\right)\,\cos\left(\frac{n\,\pi\,y}{2\,L} + \frac{n\,\pi}{2}\right)\,, \tag{III.68}$$

and the pair correlation function Eq. (III.64) then reads

$$g(x,y,t) = \frac{\lambda\nu_2}{N_0}\int_0^t e^{\lambda(\nu_1-1)\,(t'-t)}\left[1 + 2\sum_{n=1}^{\infty} a_n(x,y)\,e^{-\frac{2D\,n^2\,\pi^2\,t'}{4\,L^2}}\right]dt'\,. \tag{III.69}$$

Let us focus in particular on the critical case, which is of utmost importance for nuclear reactors. In this case, after integrating over t, we get

$$g(x,y,t) = \frac{\lambda\nu_2}{N_0}\left[t + \frac{4\,L^2}{D\,\pi^2}\sum_{n=1}^{\infty} a_n(x,y)\,\frac{1-e^{-\frac{2D\,n^2\,\pi^2\,t}{4\,L^2}}}{n^2}\right]. \tag{III.70}$$

Figure III.6 shows a very good agreement between this theoretical solution and the pair correlation obtained by Monte-Carlo simulation for different positions in the box $[-L, L]$. We observe here that the behaviour of the correlations between particles is governed by to different characteristic times. First we recognise the extinction characteristic time $\tau_E = \frac{N_0}{\lambda\nu_2}$, introduced in Eq. (II.20). Then, as the quantity in the exponential is dimensionless, it appears an other characteristic time related to diffusion:

Diffusion characteristic time

$$\tau_D = \frac{(2\,L)^2}{D\,\pi^2}\,. \tag{III.71}$$

Note that the same time characterise the decay of the survival probability of a purely diffusive particle in a system of size 2L with absorbing boundaries [Redner 2001]:

$$S(t) \propto e^{-t/\tau_D}\,. \tag{III.72}$$

In this case, the time τ_D characterises the decay of particles in the system. More generally, $1/\tau_D$ can thus be seen as the rate at which particles reach the system boundaries. With these two characteristic times, the pair correlation function finally reads

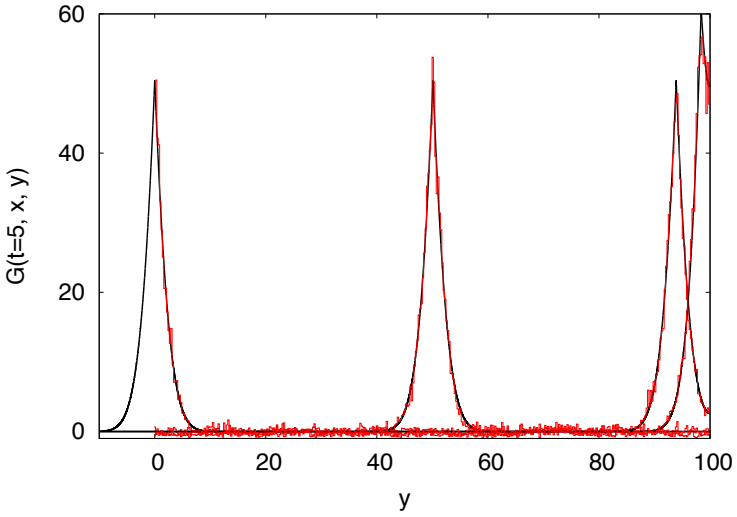

Figure III.6: Theoretical (black) and numerical (red) pair correlation function $g(x, y, t)$ at time $t = 5$ generations and positions $x = 0$, 50.1, 93.9 and 98.4, for a system of size $L = 100$ with reflecting boundaries starting with $N_0 = 10$ particles. Theoretical curves are given by Eq. (III.73). Monte Carlo simulation were realised for a critical binary branching case ($\lambda_2 = \lambda_0$ and $\lambda_{i\geqslant 3} = 0$), and the pair correlation function was computed on 10^5 realisations of the system. This figure shows a very good agreement between the theoretical pair correlation function and the one obtained by Monte Carlo simulations.

Pair correlation function, for reflecting boundary conditions

$$g(x, y, t) = \frac{t}{\tau_E} + \frac{\tau_D}{\tau_E} \sum_{n=1}^{\infty} a_n(x, y) \frac{1 - e^{-\frac{2n^2 t}{\tau_D}}}{n^2}. \qquad \text{(III.73)}$$

For $t > \tau_E$, $g(x, x, t)$ becomes larger than 1, such that the fluctuations of the neutron density in the system becomes larger than the density itself, and the whole population goes to extinction (*critical catastrophe*). If $\tau_D > \tau_E$, global effects of the boundaries of the system on the clustering will not be visible before the extinction of the population.

In a nuclear reactor however, the neutron population is very large, and generally $\tau_E \gg \tau_D$. Here, we performed Monte Carlo simulations of a crit-

ical one-dimensional fuel rod with reflecting boundaries; parameters are given in Fig. III.7. For these simulations, the diffusion time $\tau_D \simeq 40.5$ and the extinction time $\tau_E \simeq 100$, such that $\tau_D < \tau_E$. Fig. III.7 then shows the evolution in time of $g(x = 0, y, t)$ obtained by Monte Carlo simulations (and compared with the exact solution (III.73)). See Appendix 5 for details concerning the Monte Carlo simulations. We observe that the pair correlation function $g(x = 0, y, t)$ displays different regimes (see also Fig. III.7):

- Immediately after the initial time, $g(x = 0, y, t)$ displays a peak at short distances, $x = y$, which mirrors the effects of local fluctuations responsible for spatial clustering. The amplitude of the peak is proportional to the ratio τ_D/τ_E (see Eq. (III.73)), which reflects the competition between reproduction and diffusion: increasing reproduction (smaller τ_E) enhances the correlations, whereas increasing diffusion (smaller τ_D) reduces the correlations. The width of the peak, which is related to the correlation length of the system, grows with time and is enhanced by diffusion (see the exponential term in Eq. (III.73)).

- When $t \geqslant \tau_D$, the particles have explored the entire volume, and the tent-like shape of $g(xi, y, t)$ freezes into its asymptotic behaviour: the exponential vanishes in Eq. (III.73).

- The total number of neutrons in the reactor also undergoes global fluctuations due to the absence of population control and to N being finite. These global fluctuations progressively lift upwards the shape of $g(x, y, t)$ by a spatially flat term that diverges linearly in time as t/τ_E in Eq. (III.73). Finally, for $t > \tau_E$, $g(x, x, t) \geqslant 1$. This physically means that, no matter how dense the system is at time $t = 0$, global spatial fluctuations affect the whole volume with uniform (and increasing) intensity, and the neutrons are eventually doomed to extinction within a time τ_E in the absence of population control.

b. Absorbing boundaries

Absorbing boundary conditions for the one-dimensional fuel rod can be also dealt with by resorting to the same approach. Consider a one dimensional system of size $V = 2L$ with absorbing boundaries (Dirichlet boundary conditions) in $x = -L$ and $x = L$:

$$n(x, t \,|\, x_0) = 0 \qquad \text{at} \qquad x = \pm L\,, \tag{III.74}$$

illustrated on Fig. III.5 Right. We then start the system from an equilibrium configuration of the N_0 initial particles (i.e. the solution of Eq. (III.4) with

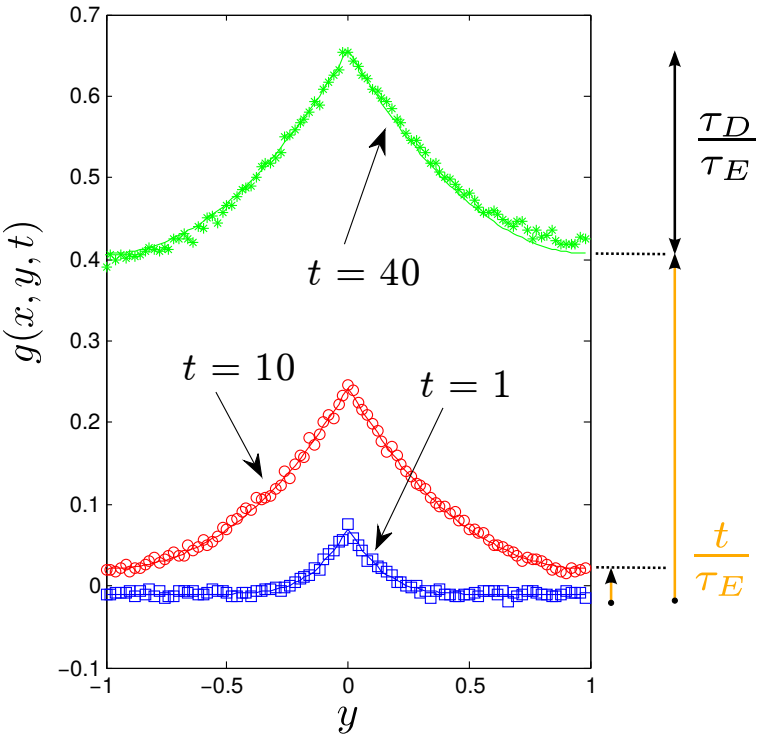

Figure III.7: The normalized and centered pair correlation function $g(x = 0, y, t)$ for a collection of $N_0 = 100$ branching Brownian motions at criticality ($\nu_1 = 1$) with diffusion coefficient $D = 0.01$ and birth-death rate $\lambda = 1$ with $\nu_2 = 1$ in a one-dimensional box of half-size $L = 1$. We took $x = 0$ and plotted $g(x, y, t)$ with respect to y at successive times $t = 1$ (blue squares), $t = 10$ (red circles) and $t = 40$ (green stars). Symbols correspond to Monte Carlo simulations with 10^5 ensembles, solid lines to exact solutions Eq. (III.73). Statistical uncertainties are of the order of 10^{-2}. For the case of a free system, $g(x, y, t)$ initially develops a peak at $x = y = 0$, which is the signature of particles undergoing spatial clustering. At later times, $g(x, y, t)$ takes an asymptotic spatial shape, and is translated upwards by a spatially uniform term growing linearly in time.

absorbing boundary conditions), corresponding to a cosine distribution of particles $n_0(x_0) = N_0 p(x_0)$:

$$p(x_0) = \frac{\pi}{2}\frac{1}{2L}\cos\left(\frac{\pi x_0}{2L}\right), \tag{III.75}$$

the probability density $p(x_0)$ begin normalised. For this system, the Green function solution of the nonhomogeneous heat equation (III.40) reads [Polyanin 2001; Polyanin; Grebenkov and Nguyen 2013]:

$$G_D(x,y,t) = \frac{1}{L}\sum_{n=1}^{\infty} b_n(x,y)\,\exp\left(-\frac{D\,n^2\,\pi^2\,t}{4\,L^2}\right), \tag{III.76}$$

$$\text{where} \qquad b_n(x,y) = \sin\left(\frac{n\,\pi\,x}{2L}+\frac{n\,\pi}{2}\right)\sin\left(\frac{n\,\pi\,y}{2L}+\frac{n\,\pi}{2}\right). \tag{III.77}$$

The mean density of particles is given by Eq. (III.41), with $n(x_0) = N_0 p(x_0)$,

$$n(\mathbf{x},t) = n_0\,e^{\lambda(\nu_1-1)t}\int_{-L}^{+L}\cos\left(\frac{\pi x_0}{2L}\right)\,G_D(t,x_0,x)\,dx_0 \tag{III.78}$$

where we set $n_0 = \pi N_0/(4L)$ as the initial concentration of particles in the center of the box. Note that,

$$\int_{-L}^{+L}\cos\left(\frac{\pi x_0}{2L}\right)\sin\left(\frac{n\,\pi\,x_0}{2L}+\frac{n\,\pi}{2}\right)dx_0 = \begin{cases} L & \text{for } n=1 \\ 0 & \text{for } n\neq 1 \end{cases}, \tag{III.79}$$

so that, after integration the mean density of particles in the system reads

$$n(x,t) = n_0\,\cos\left(\frac{\pi x}{2L}\right)\exp\left[\left(\lambda(\nu_1-1)-\frac{\pi^2 D}{4L^2}\right)t\right]. \tag{III.80}$$

The system is critical if this solution is time independent, i.e. if

$$\lambda(\nu_1-1) = \frac{\pi^2 D}{4L^2} \qquad \Longleftrightarrow \qquad \lambda(\nu_1-1) = \frac{1}{\tau_D}. \tag{III.81}$$

Here, we recognise the diffusion characteristic time $\tau_D = \frac{(2L)^2}{D\,\pi^2}$, introduced in Eq. (III.71). Note that, for a binary branching case ($\lambda(\nu_1-1) = \lambda_2 - \lambda_0$), for instance, we can rewrite this condition of criticality:

$$\lambda_2 = \lambda_0 + \frac{1}{\tau_D}. \tag{III.82}$$

The rate of particle birth (on the lhs) is equal to the rate of particle death (on the rhs). Particle absorption can happen within the volume with a rate λ_0 and on the boundaries with a rate $1/\tau_D$. Here we recover the physical

meaning of $1/\tau_D$ that was expected in the previous section (rate at which particles reach the boundaries).

In the critical case, for a system with absorbing boundaries, the pair correlation function Eq. (III.61) becomes,

$$g(x,y,t) = \frac{1}{\tau_E}\,\frac{4}{\pi L}\,\frac{\displaystyle\int_0^t dt' \sum_{n=1}^{\infty}\sum_{m=1}^{\infty} f_{n,m}(x,y)\, e^{-(n^2+m^2-2)\frac{t'}{\tau_D}}}{\cos\left(\frac{\pi x}{2L}\right)\cos\left(\frac{\pi y}{2L}\right)}\,, \quad \text{(III.83)}$$

where we have recognised the characteristic extinction times τ_E introduced in Eq. (II.20), and where the function $f_{n,m}(x,y)$ is defined for any x and y in the interval $]-L, L[$ by

$$f_{n,m}(x,y) = \int_{-L}^{L} \cos\left(\frac{\pi x_0}{2L}\right) b_n(x_0,x)\, b_m(x_0,y)\, dx_0\,. \quad \text{(III.84)}$$

Using the expression of $b_n(x,y)$ in Eq. (III.77), we obtain

$$f_{n,m}(x,y) = \begin{cases} 0 & \text{if } n \text{ and } m \text{ have different parity,} \\ \dfrac{8L}{\pi}\,\dfrac{\sin\left(\frac{n\,\pi x}{2L}+\frac{n\,\pi}{2}\right)\sin\left(\frac{m\,\pi y}{2L}+\frac{m\,\pi}{2}\right)}{\left[1-(n-m)^2\right]\left[(n+m)^2-1\right]} & \text{otherwise.} \end{cases} \quad \text{(III.85)}$$

In Eq. (III.83) the term in the exponential vanishes for $n = m = 1$, consequently the first term in the sum, for $n = m = 1$, is independent of time. Besides,

$$f_{1,1}(x,y) = \frac{8L}{3\pi}\,\cos\left(\frac{\pi x}{2L}\right)\cos\left(\frac{\pi y}{2L}\right). \quad \text{(III.86)}$$

After integrating over the time, this first term gives rise to a term of "trivial clustering"

$$g_{1,1}(x,y,t) = \frac{32}{3\pi^2}\,\frac{t}{\tau_E}\,. \quad \text{(III.87)}$$

growing linearly with time (as for the case of reflecting boundaries) and characterising the death of the whole population in an extinction time τ_E (*critical catastrophe*). The function $f_{m,n}$ behaves as $nm/(m^2+n^2)$ if m and n are equal, and as $nm/(m^4+n^4)$ otherwise, so that the double sum over m and n in Eq. (III.83) converges. However, its value is not easy to compute, and as we are interested in the behaviour of $g(x,y,t)$ in time, it could be more interesting to invert the time integral with the sums[8]:

[8] This is possible if the sum of the integral of the absolute value of the function of interest still converges, which is the case here.

Pair correlation function – for absorbing boundaries

$$g(x,y,t) = \frac{32}{3\pi^2}\frac{t}{\tau_E} + \frac{32}{\pi^2}\frac{\tau_D}{\tau_E}\sum_{\substack{n,m\geqslant 1\\ \text{same parity}\\ \setminus\{n=m=1\}}} c_{n,m}(x,y)\left[1-e^{-(n^2+m^2-2)\frac{t}{\tau_D}}\right] \tag{III.88}$$

where

$$c_{n,m}(x,y) = \frac{n\,m\,\sin\left(\frac{n\,\pi x}{2L}+\frac{n\,\pi}{2}\right)\,\sin\left(\frac{m\,\pi y}{2L}+\frac{m\,\pi}{2}\right)}{\left[2(m^2+n^2)-(n-m)^2-1\right](n^2+m^2-2)\,\cos\left(\frac{\pi x}{2L}\right)\,\cos\left(\frac{\pi y}{2L}\right)},$$

In the sum, the factor (n^2+m^2-2) is always larger than 6, so that for $t > \tau_D$, the exponential rapidly vanishes:

$$\sum_{\substack{n,m\geqslant 1\\ \text{same parity}\\ \setminus\{n=m=1\}}} c_{n,m}(x,y)\left[1-e^{-(n^2+m^2-2)\frac{t}{\tau_D}}\right] \underset{t\gg\tau_D}{\longrightarrow} \sum_{\substack{n,m\geqslant 1\\ \text{same parity}\\ \setminus\{n=m=1\}}} c_{n,m}(x,y)\,. \tag{III.89}$$

This sum is convergent for all x and y in the interval $]-L, L[$ (see fig. III.8). The sum in Eq. (III.90) then converges to an asymptotic value for large t, so that the shape of $g(x,y,t)$ becomes frozen:

$$\text{for } t > \tau_D,\quad g(x,y,t) = \underbrace{\frac{32}{3\pi^2}\frac{t}{\tau_E}}_{\text{Critical catastrophe for } t>\tau_E} + \underbrace{\frac{32}{\pi^2}\frac{\tau_D}{\tau_E}\sum_{\substack{n,m\geqslant 1\\ \text{same parity}\\ \setminus\{n=m=1\}}} c_{n,m}(x,y)}_{\text{shape of the peak frozen}}\,. \tag{III.90}$$

Finally, as for the previous case, for time $t > \tau_E$ the whole population will go to extinction do to global fluctuation of the system (critical catastrophe).

c. Conclusion and perspectives

In the two cases we have observe the same three different regimes of $g(x,y,t)$ in the system (for $0 < \tau_D < \tau_E$):

- Immediately after the initial time, g displays a peak at short distances $x = y$: the particles tend to cluster. The amplitude of the peak (correlations) is enhanced by the reproduction process whereas it is reduced

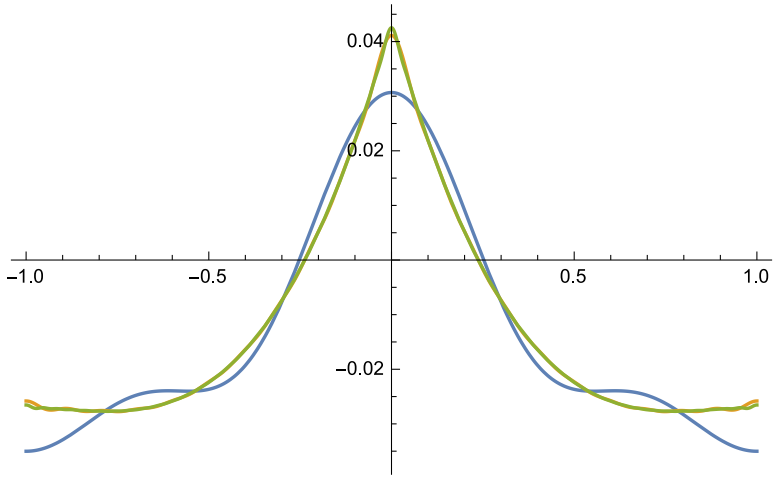

Figure III.8: Convergence of the sum in Eq. (III.89): plot of the function resulting from the sum for $L = 1$ and different values of $n_{max} = m_{max} = 7$ (blue), 40 (orange) and 100 (green).

by diffusion. Its width (~ correlation length) increase in time, due to diffusion. Note that the same observations were done for the system of infinite size (see Sec. III.2.2);

- Then, for $t > \tau_D$, the shape of the peak is frozen, such that we may expect the cluster to exhibit a characteristic size.

- and, for $t > \tau_E$, the system finally goes to extinction, due to global fluctuations (critical catastrophe).

The first regime was already observed in the case of an unbounded system (infinity size, see Sec. III.2.2), and the critical catastrophe finally happened due to the finite number of initial particle (see Sec. III.1.2). The effects of the boundaries appears in the second regime: after τ_D particles have explored the entire volume (the finite size of the system is "seen" by the particles). In this regime, we may expect cluster to exhibit a characteristic size (the shape of the peak of g is frozen), which would result from the competition between correlation by birth/death mechanism and mixing over V by diffusion. However, this regime could be visible only for $t \ll \tau_E$, and at the end, global spatial fluctuations will affect the whole population that will undergo "a trivial clustering" due to the critical catastrophe, and eventually go to extinction in a time τ_E.

3 CONTROLLED POPULATION IN A SYSTEM OF FINITE SIZE

So far, the population of neutrons was allowed to fluctuate freely in our model, which leads to strong global fluctuations of the population. However, in a nuclear reactor, different physical phenomena actually contribute to the control of the neutron population, such as the Doppler effect that tend to counteract local fluctuations of the population. An external operator also acts on the whole population to control the power delivered by the reactor, preventing it from large increase or death by inserting or removing control rods that absorb neutron excess. These actions control the whole population, introducing a feedback effect on the population fluctuations and forcing it to stay constant on average. In this section, we will focus on the effects of a global population control by imposing that the total number of neutrons in the system is preserved. We will then investigate the consequences of such constraint on spatial fluctuations.

III.3.1 The model

We consider again the simplified prototype model of a nuclear reactor described in Sec. III.1.1, introducing now a population control. We start the system with an equilibrium configuration of N_0 independent neutrons (see Sec. III.2) and let them free to evolve with a diffusion constant D; collisions then occur with a rate λ. The simplest way to enforce a constant number N_0 of neutrons in the population is to correlate reproduction and absorption events [Zhang et al. 1990; Meyer et al. 1996]: at each fission, the incoming neutron disappears and is replaced by a random number $m \geqslant 1$ of descendants, with a probability p_m; simultaneously, $m-1$ other neutrons are removed from the population (absorptions). This procedure ensures the conservation of the total number of neutrons (see the example in Fig. III.9). This mechanism has been first introduced in theoretical ecology (with binary branching $p_m = \delta_{m,2}$) [Zhang et al. 1990; Meyer et al. 1996], where similar large-scale constraints such as limited food resources have been shown to quench the wild fluctuations in the number of individuals that are expected for an unconstrained community. Similar effects have been also considered in the context of cellular growth under the effects of chemotaxis [Gelimson and Golestanian 2015].

The procedure – Start with N_0 particles, and let them diffuse. For all $k \geqslant 2$: with a rate $\lambda_k = \lambda p_k$, choose 1 particle and duplicate it $k-1$ times. Kill $k-1$ other randomly chosen particles[9].

Based on the model above, the total number of particle remains constant, being equal to N_0 at any time, as illustrated on Fig. III.9. Moreover,

[9] Note that, necessarily, for all $k \geqslant N_0$, we must have $p_k = 0$.

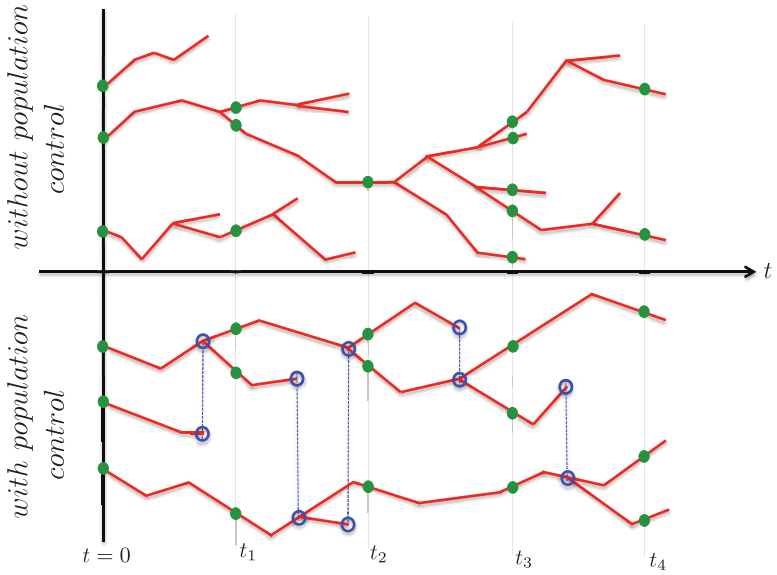

Figure III.9: Evolution of a collection of branching random walks with binary fission and $\nu_1 = 1$. At time $t = 0$, the population is composed of $N = 3$ particles; the system is then observed at successive times $t_1 < t_2 < t_3 < t_4$. **Top.** *without population control* – Birth or death events can occur at any moment, the total number of neutrons in the system undergoes important fluctuations in time. **Bottom.** *with population control* – at each fission event a new neutron appears in the system; an other neutron is simultaneous removed from the system: the total number N of neutrons in the population is preserved at any time ($N = 3$ here, for instance).

as $k-1$ deaths occur with a rate λ_k, the rate of particle death $\lambda_0 = \lambda\, p_0$ thus becomes:

$$\lambda_0 = \sum_{k \geqslant 2} (k-1)\, \lambda_k \,, \tag{III.91}$$

such that we recover $\nu_1 = 1$:

$$\nu_1 = \sum_k k\, p_k = 1 - p_0 + \sum_{k \geqslant 2} (k-1)\, p_k \,, \tag{III.92}$$

using $p_1 = 1 - p_0 - \sum_{k \geqslant 2} p_k$. For this controlled system, the Feynman-Kac method that we have used in the previous section would be cumbersome to derive. However, it is still possible to derive the pair correlation function of the system by using a simpler method introduced by [Meyer et al. 1996],

which is based on the knowledge of the common ancestor of two randomly chosen particles at any time.

III.3.2 Genealogy - the last common ancestor

The model described above can be extended to a more general process, where particles are killed with a probability p_{death} that can be, in general, smaller than 1 [Meyer et al. 1996]. This extended control also prevents the population from becoming extinct, and for $p_{death} = 1$ we recover the critical process described above. For $p_{death} < 1$, $p_0 = p_{death} \sum_{k \leqslant 2} (k-1)\, p_k$, and the process is super-critical ($\nu_1 > 1$ according to Eq. (III.92)). Concerning reactor physics, this generalised model could be interesting for a next step, as reactors are operated by perturbations close to the exact critical point.

One very interesting feature of this controlled model is the possibility to calculate, at any time $t > 0$, the probability that two randomly chosen particles among the $N(t)$ of the system have shared their last common ancestor at a time $t_a = t - \tau$ ($\tau \geqslant 0$). In this section we will be compute this probability for the generalised control model. Following the lines of [Meyer et al. 1996], we will then be able to compute the pair correlation function of the system.

a. Starting with N_0 particles

Let us denote by $A_t(t_a)\, dt_a$ the probability that a pair of particles arbitrarily chosen at a time t was generated from its last common ancestor in the time interval $[t_a - dt_a, t_a]$ (see Fig. III.10 Left). The system is started at time $t = 0$ with N_0 particles, and then follows the generalised process described above. At a positive time t, an arbitrarily chosen pair of particles may have no common ancestor (see Fig. III.10 Right), so that the marginal probability that they actually share a common ancestor is necessarily smaller than one: $\int_0^t A_t(t_a)\, dt_a < 1$, and as the time t goes to infinity, this probability necessarily converges to 1, which gives the normalisation for A_t:

$$\lim_{t \to +\infty} \int_0^t A_t(t_a)\, dt_a = 1\,. \tag{III.93}$$

Let us denote by $U_A(t)$ the complementary probability:

$$U_A(t) = 1 - \int_0^t A_t(t_a)\, dt_a \;< 1\,, \tag{III.94}$$

corresponding to the marginal probability that two particles chosen at time t do not share any common ancestor.

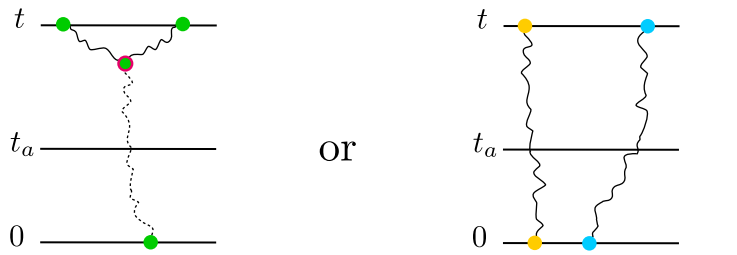

Figure III.10: **Left:** We are interested in the probability that two particles arbitrarily chosen at a time t share their last common ancestor in the time interval $[t_a - dt_a, t_a]$.
Right: At time $t > 0$, two arbitrarily chosen particles may have no common ancestor, descending respectively from two different particles at time $t = 0$.

To derive $A_t(t_a)$ we must consider the process of pair reproduction. At a time t, the exact number of ordered pairs in the system is

$$N(t)\,(N(t)-1)\,, \tag{III.95}$$

where $N(t)$ represents the total number of particles in the system at time t. Furthermore, during the time interval $[t, t+dt]$, the number of new pairs of particles that are created in the system is (see Eq. (II.3) and Sec. II.1.1)

$$\underbrace{N(t)\,\lambda\,dt}_{\text{number of collisions during } dt} \times \underbrace{\nu_2}_{\text{mean number of pairs emitted at a collision}}\,. \tag{III.96}$$

The ratio of these two quantities gives the fraction of new pairs created in the time interval $[t, t+dt]$ over the total number of pairs [Meyer et al. 1996]:

$$\lambda_p(t)\,dt = \frac{\lambda\,\nu_2}{N(t)-1}\,dt\,, \tag{III.97}$$

which allows us to define the rate $\lambda_p(t)$ of renewal of particle pairs. Let us now consider the conditional probability that two arbitrarily chosen particles at time t were generated from a common ancestor at t' in the time interval $[t_a, t_a + dt_a]$, given that $t' \leqslant t_a + dt_a$, namely $P_t\,(t' \in [t_a, t_a + dt_a] \mid t' \leqslant t_a + dt_a)$. This probability is exactly the fraction of new pairs created during the time interval, obtained in Eq. (III.97),

$$P_t\left[\,t' \in [t_a - dt_a, t_a] \mid t' \leqslant t_a\,\right] = \lambda_p(t_a)\,dt_a\,. \tag{III.98}$$

Moreover, by definition[10], this conditional probability reads

$$P_t\left[\, t' \in [t_a - dt_a, t_a] \mid t' \leqslant t_a \,\right] = \frac{P_t\left[\, t' \in [t_a - dt_a, t_a] \text{ and } t' \leqslant t_a \,\right]}{P_t\left[\, t' \leqslant t_a \,\right]} ,$$

where, from the definition of A_t, $P_t\left[\, t' \in [t_a - dt_a, t_a] \text{ and } t' \leqslant t_a \,\right] = A_t(t_a)\, dt_a$ and $P_t\left[\, t' \leqslant t_a \,\right] = \int_0^{t_a} A_t(t')\, dt'$. A_t therefore verifies the homogeneous Volterra integral equation of the second kind:

$$A_t(t_a) = \lambda_p(t_a) \int_0^{t_a} A_t(t')\, dt' . \tag{III.99}$$

As the kernel of this equation $\lambda_p(t_a)\, A_t(t')$ is separable, this equation can be solved directly. Then, using the normalisation Eq. (III.93) finally yields

Probability density $A_t(t_a)$

$$\text{for } 0 < t_a < t, \qquad A_t(t_a) = \lambda_p(t_a)\, \exp\left[-\int_{t_a}^{t} \lambda_p(s)\, ds \right] . \tag{III.100}$$

It follows the probability that two arbitrarily chosen particles at time t do not share any common ancestor:

Probability $U_A(t)$

$$U_A(t) = \exp\left[-\int_0^{t} \lambda_p(s)\, ds \right] . \tag{III.101}$$

Other quantities – Note that the probability density A_t allows defining other important physical quantities. For instance, we can define the probability $V_t(t_m)$ that two particles randomly chosen at time t come from the same initial particle and that their last common ancestor is located in time before t_m (see Fig. III.12 Left):

$$V_t(t_m) = \int_0^{t_m} A_t(t_a)\, dt_a < 1 ; \tag{III.102}$$

or its complementary probability $U_t(t_m)$ that two particles chosen at time t does not share any "last common ancestor" before t_m (either their last common ancestor is at $t' \geqslant t_m$, either they do not share any common ancestor

[10] The conditional probability of an event A assuming that B has occurred is given by $P(A \mid B) = \frac{P(A \cap B)}{P(B)}$

– see Fig. III.11)

$$\begin{aligned} U_t(t_m) &= 1 - \int_0^{t_m} A_t(t_a)\,dt_a \quad = 1 - V_t(t_m) < 1\,, \\ &= \underbrace{1 - \exp\left[-\int_{t_m}^{t} \lambda_p(s)\,ds\right]}_{\text{pba that last common ancestor between } t_m \text{ and } t} + \underbrace{\exp\left[-\int_0^t \lambda_p(s)\,ds\right]}_{\text{no common ancestor}}; \end{aligned} \tag{III.103}$$

For the critical case, due to particle number conservation, $N(t) = N_0$ for all t, the rate λ_p at which pairs are renewed in the system remains exactly constant over time. We denote by λ_c this constant:

$$\text{for all } t, \qquad \lambda_p(t) \doteq \lambda_c = \frac{\lambda \nu_2}{N_0 - 1}\,. \tag{III.104}$$

Then, from Eq. (III.100) and (III.101), the function $A_t(t_a)$ and the probability $U_A(t)$ read:

$A_t(t_a)$ and $U_A(t)$ at criticality

$$\begin{cases} A_t^c(t_a) &= \lambda_c\, e^{-\lambda_c (t - t_a)}\,, \\ U_A^c(t) &= e^{-\lambda_c t}\,. \end{cases} \tag{III.105}$$

For a super-critical case ($\nu_1 > 1$), we assume that, thanks to the population control, fluctuations are significantly reduced, so that $N(t)$ is well represented by its mean [Meyer et al. 1996], which is given in Eq. (II.10). The reproduction rate of particle pairs then decreases exponentially with time:

$$\lambda_p(t) = \frac{\lambda \nu_2}{N_0\, e^{\lambda(\nu_1 - 1)\, t} - 1} \simeq \lambda_c\, e^{-\lambda(\nu_1 - 1)\, t}\,. \tag{III.106}$$

Eq. (III.100) for the function $A_t(t_a)$ and Eq. (III.101) for the probability $U_A(t)$ then become, for large N_0:

$$\begin{cases} A_t^s(t_a) &\simeq \lambda_p(t_a)\, \exp\left[-\dfrac{\lambda_p(t_a) - \lambda_p(t)}{\lambda\,(\nu_1 - 1)}\right]\,, \\ U_A^s(t) &\simeq \exp\left[-\dfrac{\lambda_c - \lambda_p(t)}{\lambda\,(\nu_1 - 1)}\right]\,, \end{cases} \tag{III.107}$$

where we used that $\lambda_p(0) = \lambda_c$.

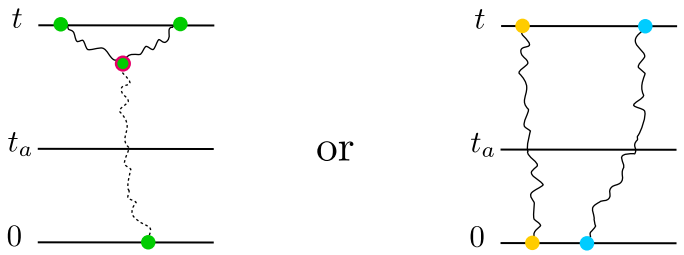

The last common ancestor is located after t_a

The two particles belong to two differents families

Figure III.11: $U_t(t_a)$ represents the probability that the last common ancestor of two particles randomly chosen at time t is not located before the time t_a: either the particles actually share a common ancestor, but after t_a (see green family on the left), either the particles come from two distinct families (see yellow and blue families on the right), and thus do not share any common ancestor.

A Markovian process of pair renewal – A simpler way to obtain $A_t(t_a)$ is to observe that the pair reproduction process is a non-homogenous Poisson process of rate $\lambda_p(t)$ (Poissonian if λ_p is constant, i.e. if the system is critical). Then, following the lines of section I.1.2 (see in particular Eq. (I.10)), we can write directly the marginal probability that two particles randomly chosen at time t do not share any common ancestor[11]:

$$U_A(t) = \exp\left[-\int_0^t \lambda_p(s)\,ds\right] . \tag{III.108}$$

Indeed, this probability can be seen as the probability that a pair of particles generated at time $t = 0$ is still "alive" at time t (i.e. that the renewal process that kills one of the two initial branches has not happened yet). We can then obtain directly $U_A(t_a)$ or $V_A(t_a)$ using the heuristic probabilistic argument illustrated on Eq. (III.103) and Fig. III.11. To determine $V_t(t_a)$ we decompose each path from $t = 0$ to t into two parts, one from $t = 0$ to t_a, and the other one from t_a to t (see Fig. III.12). As the pair reproduction process is Markovian, these two parts are completely independent, and

$$V_t(t_a) = \frac{U_A(t)}{U_A(t_a)}\,[1 - U_A(t_a)] . \tag{III.109}$$

By definition (see Eq. (III.102)), the probability density $A_t(t_a)$ can then be obtained by derivation of $V_t(t_a)$: $A_t(t_a) = V_t'(t_a)$. Using from Eq. (III.108)

[11] $U_A(t+dt) = U_A(t) - P_t\,[\,t_a \in [t, t+dt]\,]$
where $P_t\,[\,t_a \in [t, t+dt]\,] = U_A(t+dt)\,P_t\,[\,t_a \in [t, t+dt]\,|\,t_a \leqslant t+dt\,]$

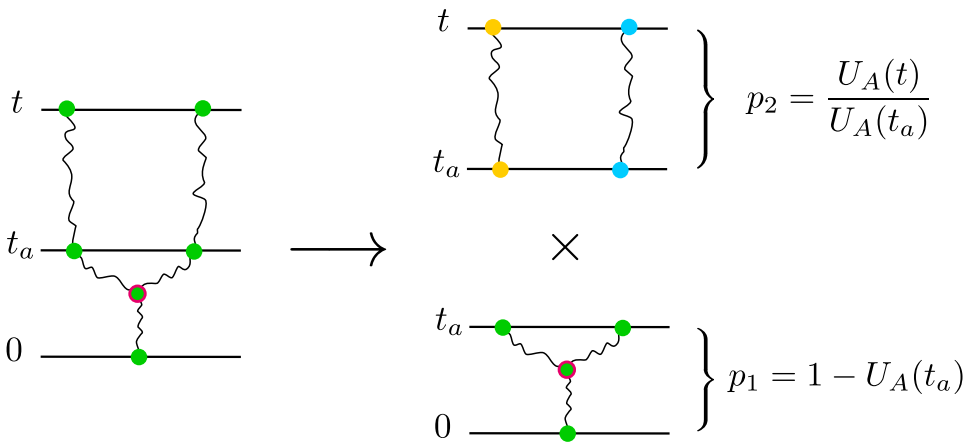

Figure III.12: **Left:** $V_t(t_a)$ represents the probability that the last common ancestor of two particles randomly chosen at time t is actually located before the time t_a, which corresponds to the situation illustrated here. Note that necessarily the two particles can not share any other common ancestor between t_a and t.
Left to right: As the process of pair renewal is Markovian, trajectories from time 0 to time t can be decomposed into two independent parts, from 0 to t_a and from t_a to t. For this reason, the probability $V_t(t_a)$ that two particles chosen at time t shared a last common ancestor before t_a, results from the product of the probability p_2 that the particles at time t come from two different families (yellow and blue) at time t_a, i.e. with no common ancestor from t_a to t, and the probability p1 that two particles taken at time t_a actually share a common ancestor.

that $U_A{}'(t) = \lambda_p(t)\, U_A(t)$ finally yields

$$A_t(t_a) = \lambda_p(t_a) \frac{U_A(t)}{U_A(t_a)} \,. \tag{III.110}$$

Thanks to the same arguments, the probability$A_t(t_a)dt_a$ could have been also directly obtained. Indeed it is the probability that two particles chosen at t have no common ancestor between t_a and t, namely $U_A(t)/U_A(t_a)$, and that their common ancestor were "generated" in the time interval $[t_a - dt_a, t_a]$, namely $\lambda_p(t_a)dt_a$. Finally, replacing the expression of $U_A(t)$ from Eq. (III.108) in this latter equation leads to the final result Eq. (III.100).

b. N_0 *particles starting from the same position*

Other types of initial conditions may also be worked out within the same approach. For instance, one might want to consider the case where all particles start from a point-source located at $\mathbf{r}_0$, which has been considered in [Meyer et al. 1996]. Assigning the initial positions of the particles does not change the results previously obtained for $A_t(t_a)$. However, for this particular example, if two randomly chosen particles at time t have no common ancestor, we know, for sure, that their respective first ancestors have at least started from the same position $\mathbf{r}_0$ at time $t = 0$. We thus define, for every particle, a unique common ancestor that is in $\mathbf{r}_0$ at $t = 0$. We then introduce the pdf of the last generalised common ancestor of two particles at time t[12] [Meyer et al. 1996]:

$$\mathcal{A}_t(t_a) = \underbrace{A_t(t_a)}_{\text{normal ancestors}} + \underbrace{U_A(t)\,\delta(t_a)}_{\text{unique ancestor at } t=0} \,, \tag{III.111}$$

which takes into account the unique ancestor at $t = 0$. At any time t, every chosen pair of particles thus always shares a generalised common ancestor, and, by definition

$$\int_0^t \mathcal{A}_t(t_a)\, dt_a = 1 \,. \tag{III.112}$$

In particular, for the critical case, using Eq. (III.105), the pdf of the last generalised common ancestor reads

$$\mathcal{A}_t^c(t_a) = \lambda_c\, e^{-\lambda_c\,(t - t_a)} + e^{-\lambda_c\, t}\, \delta(t_a) \,. \tag{III.113}$$

[12] This new pdf allows characterising the spatial relation between particles, more than the family relationship (genealogy) itself.

III.3.3 Pair correlation function - Controlled clustering

a. General Case

We start with a finite collection of N_0 particles distributed with the probability density $p_0(\mathbf{r})$ over a d-dimensional system of volume V (finite or not) and let them evolve according to the controlled process described in Sec. III.3.1. For any particle chosen in the system at time t, it is possible to trace the ancestry of its family until its unique *first* ancestor at time 0 (one of the N_0 starting particles). This defines a generalised trajectory for the particle from the initial time up to the observation time t (see Fig. III.13). Since births do not affect the diffusing process, the statistical properties of this trajectory are the same as for a single diffusing particle [Meyer et al. 1996]. Thanks to this observation, we can write the probability density to find a particle about $\mathbf{r}$ at time t as:

$$p(\mathbf{r},t) = \int_V G_D(\mathbf{r},t;\,\mathbf{r}_0,t_0)\,p(\mathbf{r}_0,t_0)\,d\mathbf{r}_0\,, \tag{III.114}$$

where $p(\mathbf{r}_0,t_0)$ is the probability density that the first particle starts from $\mathbf{r}_0$ at time 0. $G_D(\mathbf{r},t;\,\mathbf{r}_0,t_0) \doteq G_D(\mathbf{r},\mathbf{r}_0,t,t_0)$ is the propagator of a purely diffusing particle in the considered system, i.e. $G_D(\mathbf{r},t;\,\mathbf{r}_0,t_0)\,d\mathbf{r}$ gives the probability to find a regular Brownian particle about $\mathbf{r}$ at time t, knowing that the particle was at $\mathbf{r}_0$ at time t_0. This propagator satisfies the diffusion equation Eq. (III.40)[13]. Starting the system with a particle probability density $p(\mathbf{r}_0,t_0=0) \doteq p_0(\mathbf{r}_0)$, the density of particles at time t then reads[14]

$$n(\mathbf{r},t) = \langle N(t)\rangle\,p(\mathbf{r},t)\,, \tag{III.115}$$

$$= \langle N(t)\rangle \int_V G_D(\mathbf{r},t;\,\mathbf{r}_0,t_0)\,p_0(\mathbf{r}_0)\,d\mathbf{r}_0\,, \tag{III.116}$$

where $\langle N(t)\rangle$ is the mean number of particles in the system at time t, given by Eq. (II.10), $\langle N(t)\rangle = N_0\exp[\lambda(\nu_1-1)]$. Equation (III.116) is thus identical to the density obtained without population control, Eq. (III.41):

Particle density

$$n\,(\mathbf{r},t) = N_0\,e^{\lambda(\nu_1-1)t}\int_V p_0(\mathbf{r}_0)\,G_D\,(\mathbf{r},t;\,\mathbf{r}_0)\,d\mathbf{r}_0\,. \tag{III.117}$$

At criticality, $N(t) = N_0$ for all t and the neutron density also becomes indistinguishable from that of N_0 regular Brownian particles. The fact that the particle density $n(\mathbf{r},t)$ does not provide any information about spatial

[13] $G_D\,(\mathbf{r},t;\,\mathbf{r}_0,t_0)$ is given by Eq. (III.14) for an infinite system, Eq. (III.67) for a system with reflecting boundaries and Eq. (III.76) with absorbing boundaries.

[14] $n(\mathbf{r},t)$ results from $\langle N(t)\rangle$ regular Brownian walkers, see Eq.(II.25).

correlations in the system is apparent here in the way $n(\mathbf{r}, t)$ was built by considering purely diffusive (generalised) trajectories.

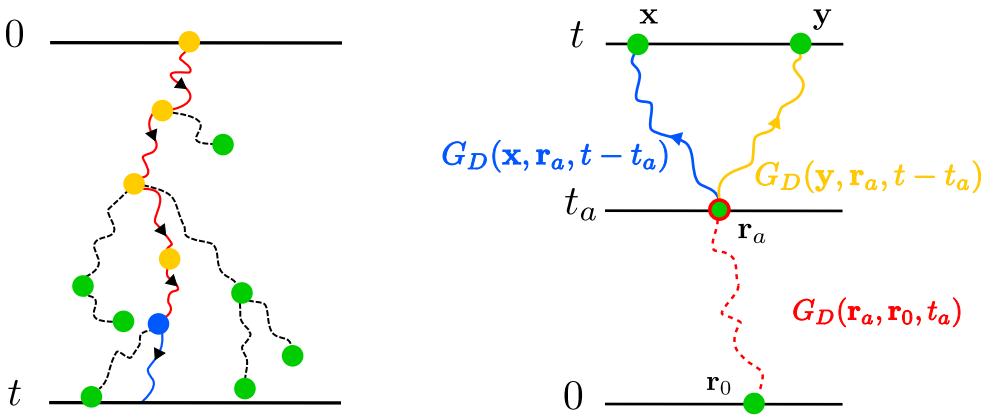

Figure III.13: **Left:** Schematic representation: real trajectory of a particle (blue) since its birth (blue point) until time t, compared with its generalised trajectory (red) that trace its ancestry since time 0. This generalised trajectory has the same statistical properties than trajectories travelled by a purely diffusing particle from $\mathbf{r}_0$ at time $t = 0$ to $\mathbf{r}$ at time t.
Right: Schematic representation: two distinct particles at time t sharing their last common ancestor at time t_a. At any time smaller than t_a, the generalised trajectories of the two particles are identical corresponding to the same Brownian trajectory, whereas, for time larger than t_a, their respective generalised trajectories correspond to two Brownian motions that have both started at time t_a from a common position $\mathbf{r}_a$.

Let us now consider the pair correlation function h_c defined in section III.2.1. The index c, for "control", will be used in this section to distinguish each quantity from its counterpart in the free case (see Sec. III.2). To derive $h_c(\mathbf{x}, \mathbf{y}, t)$, we first consider the probability density $P_2(\mathbf{x}, \mathbf{y}, t)$ to find, at time t, a pair of *distinct* particles, with one about $\mathbf{x}$ and the other about $\mathbf{y}$. Note that this definition does not include self-contributions. The pair correlation function h_c is then given by the pair probability density function $P_2(\mathbf{x}, \mathbf{y}, t)$ multiplied by the mean number of ordered particle pairs in the system at time t:

$$h_c(\mathbf{x}, \mathbf{y}, t) = \langle N(t) \rangle \left(\langle N(t) \rangle - 1 \right) P_2(\mathbf{x}, \mathbf{y}, t) \,. \tag{III.118}$$

As seen in section III.3.2, the control process allows tracking the ancestry

of any pair of particles back to their last common ancestor. Thanks to this property, we can use the genealogy of each particle pair to compute the correlation function of the system [Meyer et al. 1996]. Let us choose two distinct particles at time t, and first assume that their last common ancestor is located at time $t_a < t$ (see Fig. III.13 Right). At any time smaller than t_a, the generalised trajectories of the two particles are identical, whereas for time larger than t_a their respective trajectories correspond to two Brownian motions that have both started from a common position $\mathbf{r}_a$ at time t_a. The part of shared trajectory is responsible for correlations between the two particles, and therefore gives rise to a correlated part in the pair correlation function of the system. Thanks to this description, we can write the correlated part of the probability density $P_2(\mathbf{x}, \mathbf{y}, t)$:

$$P_2^{\text{corr}}(\mathbf{x}, \mathbf{y}, t) = \int_0^t dt_a A_t(t_a) \int_V G_D(\mathbf{x}, \mathbf{r}_a, t, t_a)\, G_D(\mathbf{y}, \mathbf{r}_a, t, t_a)\, p(\mathbf{r}_a, t_a)\, d\mathbf{r}_a \,, \tag{III.119}$$

where
- $A_t(t_a)\, dt_a$ is the probability to find the last common ancestor in the time interval $(t_a, t_a + dt_a)$;
- $p(\mathbf{r}_a, t_a)\, d\mathbf{r}_a$ is the probability that this ancestor is about $\mathbf{r}_a$, where $\mathbf{r}_a$ is the position at time t_a of a Brownian walker that has started from $\mathbf{r}_0$ at time 0 (see Eq. (III.114)):

$$p(\mathbf{r}_a, t_a) = \int_V G_D(\mathbf{r}_a, t_a; \mathbf{r}_0, 0)\, p_0(\mathbf{r}_0)\, d\mathbf{r}_0 \,; \tag{III.120}$$

- $G_D(\mathbf{x}, \mathbf{r}_a, t, t_a)\, G_D(\mathbf{y}, \mathbf{r}_a, t, t_a)\, d\mathbf{x}d\mathbf{y}$ is the probability to find a pair of regular Brownian particles at time t, one about $\mathbf{x}$ and the other one about $\mathbf{y}$, knowing that the pair was about $\mathbf{r}_a$ at time t_a.

On the other hand, the two particles may have no common ancestor, which happens with probability $U_A(t)$: they come from two independent families starting from independent positions $\mathbf{x}_0$ and $\mathbf{y}_0$ at time 0, and thus contribute to the uncorrelated part of the probability density $P_2(\mathbf{x}, \mathbf{y}, t)$:

$$\begin{aligned} P_2^{\text{unc}}(\mathbf{x}, \mathbf{y}, t) &= U_A(t) \iint_V G(\mathbf{x}, \mathbf{x}_0, t, 0)\, G(\mathbf{y}, \mathbf{y}_0, t, 0)\, p_0(\mathbf{x}_0)\, p_0(\mathbf{y}_0)\, d\mathbf{x}_0\, d\mathbf{y}_0 \,, \\ &= U_A(t)\, p(\mathbf{x}, t)\, p(\mathbf{y}, t) \,. \end{aligned} \tag{III.121}$$

The resulting probability density is the sum of these two contributions,

$$P_2(\mathbf{x}, \mathbf{y}, t) = P_2^{\text{corr}}(\mathbf{x}, \mathbf{y}, t) + P_2^{\text{unc}}(\mathbf{x}, \mathbf{y}, t) \,, \tag{III.122}$$

and, the pair correlation function h_c in Eq. (III.118) then reads

$$\begin{aligned} h_c(\mathbf{x}, \mathbf{y}, t) &= \overline{N}_t(\overline{N}_t - 1)\, U_A(t)\, p(\mathbf{x}, t)\, p(\mathbf{y}, t) \\ &+ \lambda \nu_2 \overline{N}_t \int_0^t dt_a \frac{\overline{N}_t - 1}{\overline{N}_{t_a} - 1} \frac{U_A(t)}{U_A(t_a)} \int_V G_D(\mathbf{x}, \mathbf{r}_a, t, t_a)\, G_D(\mathbf{y}, \mathbf{r}_a, t, t_a)\, p(\mathbf{r}_a, t_a)\, d\mathbf{r}_a \,, \end{aligned} \tag{III.123}$$

where $A_t(t_a)$ was replaced by its expression in Eq. (III.110). For the sake of clarity, we adopted the lighter notation $\overline{N}_t$ instead of $\langle N(t)\rangle$.

Forward interpretation of the correlated part of P_2

$U_A(t)$ is the probability that a pair of particles chosen at time t has no common ancestor. It can also be seen as the probability that a pair of particles generated at time 0 is still "alive" at time t (i.e., the process of pair renewal that kills one of the two initial branches has not occurred, yet). The correlated part of P_2 can thus also be interpreted in a slightly different way. Let us rewrite Eq. (III.119):

$$P_2^{\rm corr}(\mathbf{x},\mathbf{y},t) = \int_0^t dt_a \lambda_p(t_a) \frac{U_A(t)}{U_A(t_a)} \int_V G(\mathbf{x},\mathbf{r}_a,t,t_a)\, G(\mathbf{y},\mathbf{r}_a,t,t_a)\, p(\mathbf{r}_a,t_a)\, d\mathbf{r}_a \ ,$$

$1 \times \lambda_p(t_a)dt_a$ gives the probability to generate one pair of particles during $[t_a, t_a + dt_a]$, and $U_A(t)/U_A(t_a)$ is the probability that this pair stays "alive" from t_a to t.

Finally, to obtain the *centered and normalised pair correlation function* $g_c(\mathbf{x},\mathbf{y},t)$, we must subtract from h_c its uncorrelated part: the pair correlation function $h_c^{\rm ind}(\mathbf{x},\mathbf{y},t)$ of $\overline{N}_t$ independent diffusing particles (see Eq. (IV.90)):

$$h_c^{\rm ind}(\mathbf{x},\mathbf{y},t) = \overline{N}_t(\overline{N}_t - 1)\, p(\mathbf{x},t)\, p(\mathbf{y},t)\,. \tag{III.124}$$

This corresponds to considering that all the particles present in the system at time t have performed fully independent trajectories. Note that for $\overline{N}$ large enough $h_c^{\rm ind}(\mathbf{x},\mathbf{y},t) \underset{\overline{N}_t \gg 1}{\simeq} n(\mathbf{x},t)\, n(\mathbf{y},t)$. The centered and normalise pair correlation function Eq. (IV.90) finally reads:

$$\begin{aligned} g_c(\mathbf{x},\mathbf{y},t) \ &= \ \frac{\overline{N}_t - 1}{\overline{N}_t}\,[U_A(t) - 1] \qquad\qquad\qquad\qquad\qquad\qquad\qquad\qquad\qquad\qquad \text{(III.125)} \\ &+ \frac{\lambda\nu_2}{\overline{N}_t} \frac{\displaystyle\int_0^t dt_a\, \frac{\overline{N}_t - 1}{\overline{N}_{t_a} - 1} \frac{U_A(t)}{U_A(t_a)} \int_V G_D(\mathbf{x},\mathbf{r}_a,t,t_a)\, G_D(\mathbf{y},\mathbf{r}_a,t,t_a)\, p(\mathbf{r}_a,t_a)\, d\mathbf{r}_a}{p(\mathbf{x},t)\, p(\mathbf{y},t)} \end{aligned}$$

At criticality – for any time t, $N(t) = N_0$ and $\lambda_p(t) \doteq \lambda_c = \lambda\nu_2/(N_0 - 1)$; the particle density is $n(\mathbf{x},t) = N_0\, p(\mathbf{x},t)$, and the pair correlation function reads

$$\begin{aligned} h_c(\mathbf{x},\mathbf{y},t) &= N_0(N_0 - 1)\, e^{-\lambda_c t}\, p(\mathbf{x},t)\, p(\mathbf{y},t) \qquad\qquad\qquad\qquad\qquad\qquad \text{(III.126)} \\ &+ \lambda\nu_2 N_0 \int_0^t dt_a\, e^{-\lambda_c(t - t_a)} \int_V G_D(\mathbf{x},\mathbf{r}_a,t,t_a)\, G_D(\mathbf{y},\mathbf{r}_a,t,t_a)\, p(\mathbf{r}_a,t_a)\, d\mathbf{r}_a \end{aligned}$$

where $U_A(t)$ is given by Eq. (III.105). Finally, Eq. (III.125) becomes

Normalised and centered pair correlation function

$$g_c(\mathbf{x},\mathbf{y},t) = \frac{N_0-1}{N_0}\left[e^{-\lambda_c t}-1\right] + \frac{\lambda\nu_2}{N_0}\frac{\displaystyle\int_0^t dt_a\, e^{-\lambda_c(t-t_a)}\int_V G_D(\mathbf{x},\mathbf{r}_a,t,t_a)\,G_D(\mathbf{y},\mathbf{r}_a,t,t_a)\,p(\mathbf{r}_a,t_a)\,d\mathbf{r}_a}{p(\mathbf{x},t)\,p(\mathbf{y},t)} \quad \text{(III.127)}$$

In front of the first integral, we recognise the extinction time $\tau_E = N_0/(\lambda\nu_2)$ introduced in Sec. II.1.2 and also appearing in the pair correlation function $g(\mathbf{x},\mathbf{y},t)$ for the free case – see Eq. (IV.90). However, thanks to the control, the population can not be extinct here. For N_0 large, $N_0/(\lambda\nu_2) \simeq 1/\lambda_c$ indeed represents the characteristic time of pair renewal, i.e. the time after which most of the particle pairs of the system have been renewed, such that we expect that most of the particles come from the same ancestor (and thus belong to the same family).

Comments on the different correlation functions

- $P_2(\mathbf{x}, \mathbf{y}, t)$ is the probability density of pairs of distinct particles, one about $\mathbf{x}$ and the other about $\mathbf{y}$.
- $h(\mathbf{x}, \mathbf{y}, t) = \overline{N}_t\,[\overline{N}_t - 1]\,P_2(\mathbf{x}, \mathbf{y}, t)$ is the density of pairs of distinct particles in the system, with one particle about $\mathbf{x}$ and the other one about $\mathbf{y}$. This quantity is called *pair correlation function* in this chapter.

  $h(\mathbf{x}, \mathbf{y}, t)$ is a bias estimator for $\langle \rho(\mathbf{x}, t)\,\rho(\mathbf{y}, t)\rangle$, which accounts for self-correlations[a]. Note that $h(\mathbf{x}, \mathbf{y}, t)/(\langle \rho(\mathbf{x}, t)\rangle\,\langle \rho(\mathbf{y}, t)\rangle) = h(\mathbf{x}, \mathbf{y}, t)/(n(\mathbf{x}, t)\,n(\mathbf{y}, t))$ is the probability to find two distinct particles, one in $\mathbf{x}$ and one in $\mathbf{y}$, among the population.
- $h(\mathbf{x}, \mathbf{y}, t) - h^{ind}(\mathbf{x}, \mathbf{y}, t)$ is the centered version of $h(x, y, t)$, equivalent to the covariance $Cov(x, y, t)$ without the self-contributions.
- The *centered and normalised pair correlation function*,

$$g(\mathbf{x}, \mathbf{y}, t) = \frac{h(\mathbf{x}, \mathbf{y}, t) - h^{ind}(\mathbf{x}, \mathbf{y}, t)}{n(\mathbf{x}, t)\,n(\mathbf{y}, t)},$$

  is a central quantity in the clustering problem. The common corresponding definition in mathematics is $Cov(\mathbf{x}, \mathbf{y}, t)/(n(\mathbf{x}, t)\,n(\mathbf{y}, t))$ that doesn't take out self-correlations. These two definitions coincide for a large population.

[a] Contributions to correlations due "pairs" formed by particles with themselves.

b. System of finite size surrounded by reflecting boundaries

Let us consider again the one-dimensional fuel rod model introduced in Sec. III.1.1, surrounded by reflecting boundaries[15], and start the system with a uniform distribution of particles $p(x_0) = 1/(2L)$ (see Sec. III.2). The

[15] Note that if the system is infinite (unbounded system), starting with a finite number of particles uniformly distributed over the system (equilibrium configuration) is impossible. For the infinite system, two main cases can be in fact consider: either, an infinite number of particles starting with a uniform distribution, studied by [Houchmandzadeh 2009] (see Sec. III.2.2); or, a finite number N_0 of particles starting all from the same point, considered by [Meyer et al. 1996].

pair correlation function h_c in Eq. (III.126) then simplifies

$$h_c(x,y,t) = \frac{N_0(N_0-1)}{(2L)^2}\, e^{-\lambda_c t} \qquad \text{(III.128)}$$
$$+ \frac{\lambda\nu_2 N_0}{2L}\int_0^t dt_a\, e^{-\lambda_c(t-t_a)}\int_V G_D(x,r_a,t-t_a)\, G_D(y,r_a,t-t_a)\, dr_a\ ,$$
$$h_c(x,y,t) = \frac{N_0(N_0-1)}{(2L)^2}\, e^{-\lambda_c t} + \frac{\lambda\nu_2 N_0}{2L}\int_0^t dt_a\, e^{-\lambda_c(t-t_a)} G_D(x,y,2(t-t_a))\ .$$

Then, replacing the propagator $G_D(x,y,t)$ by its expression for the case of reflecting boundaries, see Eq. (III.67),

$$G_D(x,y,t) = \frac{1}{2L} + \frac{1}{L}\sum_{n=1}^{\infty} a_n(x,y)\, \exp\left(-\frac{n^2 t}{\tau_D}\right)\ , \qquad \text{(III.129)}$$

we obtain, after integration of the constant term:

$$h_c(x,y,t) = \frac{N_0(N_0-1)}{(2L)^2} + \frac{\lambda_c N_0(N_0-1)}{2L^2}\int_0^t dt'\sum_{n=1}^{\infty} a_n(x,y) e^{-(\lambda_c + 2\frac{n^2}{\tau_D})\,t'}\ .$$

We used $\lambda_c = \lambda\nu_2/(N_0-1)$, and the change of variable $t' = t - t_a$ in the second integral. An integration over time yields:

$$h_c(x,y,t) = \frac{N_0(N_0-1)}{(2L)^2}\left[1 + 2\,\frac{\tau_D}{\tau_C}\sum_{n=1}^{\infty} a_n(x,y)\,\frac{1-e^{-\left(\frac{1}{\tau_C}+2\frac{n^2}{\tau_D}\right)t}}{\frac{\tau_D}{\tau_C}+2n^2}\right]\ ,$$

where $\tau_C = 1/\lambda_C$ is the characteristic time of pair renewal, i.e. the time after which most of the particles in the system are descended from the same ancestor. As for large N_0, $\tau_C \simeq \tau_E$, in the following we will keep the notation τ_E instead of τ_C, even though we noted that the interpretation is different. Finally, as $h_c^{ind}(x,y,t) = N_0(N_0-1)/(2L)^2$, the centered and normalised pair correlation function Eq. (III.123) reads

Pair correlation function; reflecting boundaries with control

$$g_c(x,y,t) = 2\,\frac{\tau_D}{\tau_E}\sum_{n=1}^{\infty} a_n(x,y)\,\frac{1-e^{-\left(\frac{1}{\tau_E}+2\frac{n^2}{\tau_D}\right)t}}{\frac{\tau_D}{\tau_E}+2n^2}\ . \qquad \text{(III.130)}$$

Figure III.14 compares this result with the pair correlation function obtained by Monte Carlo simulations at different times t (see Appendix 5 for details concerning the simulations). It shows a good agreement between Monte Carlo simulation and theoretical curves. We observe that $g_c(x, y, t)$ initially develops a peak at $x = y$, as for the case without control, which is a signature of spatial clustering. The pair correlation function $g_c(x = 0, y, t)$ also displays negative correlations close to the boundaries[16] $x = \pm L$. These anti-correlations can be explained by the population control mechanism applied on the total number of particles in the system: positive correlations for $x = y$ (short distances) are compensated by negative correlations at long distances. However, to check if the system actually develop clusters, we must consider the amplitude of g_c: if this amplitude stays close to zero ($\sim$ flat g_c) the fluctuations will remains Poissonian, whereas if it becomes larger than 1 the system will display clusters.

Contrary to the free case (see Eq. III.73), the pair correlation function here does not diverge. Indeed for all time $t \geqslant 0$, Eq. (III.130) is bounded:

$$|g_c(x, y, t)| \leqslant 2\,\frac{\tau_D}{\tau_E}\sum_{n=1}^{\infty}\frac{1}{2n^2} = \frac{\pi^2}{6}\,\frac{\tau_D}{\tau_E}\,. \tag{III.131}$$

As expected, the control applied to the neutron population prevents drastic global fluctuations in the system (associated to the diverging term t/τ_E in Eq. (III.73) for the free case). In particular, for times larger than $\min(\tau_D, \tau_E)$, $g_c(x, y, t)$ converges to an asymptotic spatial shape (black dashed curve in Fig. III.14):

$$g_c^{\infty}(x, y) = 2\,\frac{\tau_D}{\tau_E}\sum_{n=1}^{\infty}\frac{a_n(x, y)}{\dfrac{\tau_D}{\tau_E} + 2n^2}\,, \tag{III.132}$$

where the coefficients $a_n(x, y)$ are given in Eq. (III.68). Its amplitude, $g_c^{\infty}(0, 0) - g_c^{\infty}(0, L)$, is a growing function of the ratio τ_D/τ_E (see Fig. III.14). As the pair correlation function is now converging to an asymptotic function, we intuitively expect a characteristic asymptotic correlation length to emerge from the pair correlation function.

[16] Note that it does not necessarily mean that particles tend to cluster far from the borders, in the center of the box (we have plotted g_c for $x = 0$), but only that if we take one particle in $x = 0$, it is more probable that the other particles around are close to 0 than to $\pm L$. In other words, it only shows that particles tend to get closer to each other (clustering).

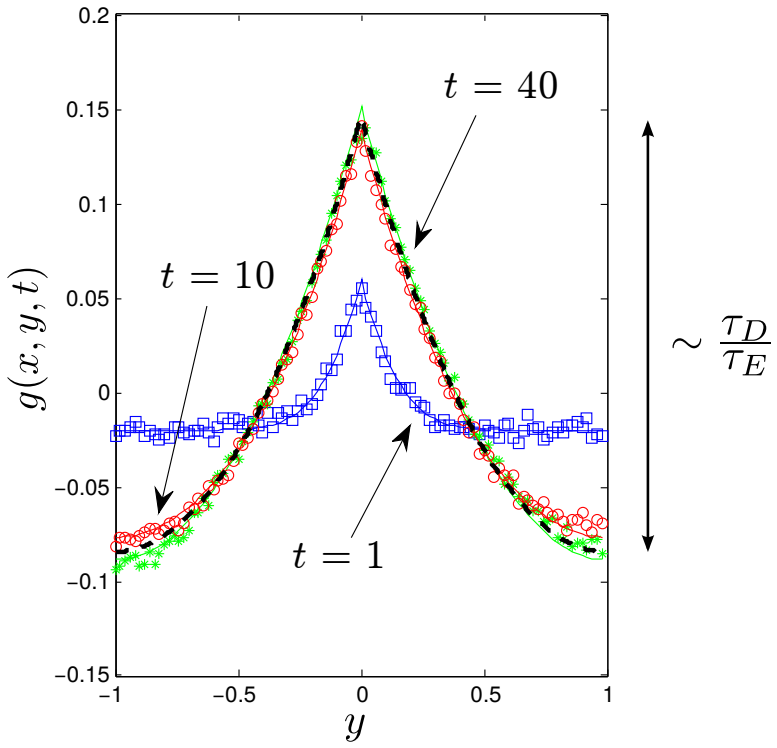

Figure III.14: The normalized and centered pair correlation function $g_c(x = 0, y, t)$ for a collection of $N_0 = 100$ branching Brownian motions at criticality ($\nu_1 = 1$) with diffusion coefficient $D = 0.01$ and birth-death rate $\lambda = 1$ with $\nu_2 = 1$ in a one-dimensional box of half-size $L = 1$. We took $x = 0$ and plotted $g(x, y, t)$ with respect to y at successive times $t = 1$ (blue squares), $t = 10$ (red circles) and $t = 40$ (green stars). Symbols correspond to Monte Carlo simulations with 10^5 ensembles, solid lines to exact solutions Eq. (III.130). Statistical uncertainties are of the order of 10^{-2}. For the case of a system with population control, $g_c(x, y, t)$ initially develops again a peak at $x = y$. Because of particle number conservation, an increased correlation about $x = 0$ implies negative correlations close to the boundaries $y = \pm L$. For times larger than τ_D, $g_c(x, y, t)$ converges to an asymptotic spatial shape $g_c^\infty(x, y, t)$ (see Eq. (III.132)), displayed as a black dashed curve, and whose amplitude is proportional to the ratio τ_D/τ_E.

III.3.4 Average squared distance and typical size of a cluster

Complementary information can be extracted from the pair correlation function by considering the average squared distance, defined by:

$$\langle r^2 \rangle(t) = \int_V \int_V d\mathbf{x} d\mathbf{y} \, |\mathbf{x}-\mathbf{y}|^2 P_2(\mathbf{x},\mathbf{y},t) \, . \tag{III.133}$$

Note that $\langle r^2 \rangle$ can also be defined in the free case, where we can obtain P_2 by renormalising h:

$$P_2(\mathbf{x},\mathbf{y},t) = \frac{h(\mathbf{x},\mathbf{y},t)}{\int_V \int_V d\mathbf{x} d\mathbf{y} h(\mathbf{x},\mathbf{y},t)} \, . \tag{III.134}$$

For an uncorrelated population of neutrons uniformly distributed in a system in dimension d, the ideal average square distance is [Young et al. 2001]:

$$\langle r^2 \rangle_{id} = \frac{1}{V^2} \int_V \int_V d\mathbf{x} d\mathbf{y} \, |\mathbf{x}-\mathbf{y}|^2 = \frac{d}{6} V^{\frac{2}{d}} \, . \tag{III.135}$$

Deviations of the average squared distance from this reference value allow detecting spatial effects due to clustering [Zhang et al. 1990; Meyer et al. 1996]. In the case of a critical one-dimensional system of finite size $[-L, L]$ with reflecting boundaries starting with N_0 uniformly distributed particles, the initial average square distance is equal to the ideal one:

$$\langle r^2 \rangle(t=0) = \langle r^2 \rangle_{id} = \frac{2}{3} L^2, \qquad \text{for } d = 1 \text{ and } V = 2L \, . \tag{III.136}$$

Then $P_2(x,y,t) = h(x,y,t)/N_0/(N_0-1)$, where h is given by Eq. (III.130), and the time evolution of the average square distance can be obtained from Eq. (III.133). The average square distance between particles for the system with population control is displayed in Fig. III.15. At time $t = 0$, the population is uniformly distributed and $\langle r^2 \rangle_c(0) = \langle r^2 \rangle_{id} = \frac{2}{3} L^2$. Immediately afterward, $\langle r^2 \rangle_c(t)$ starts to decrease due to the competition between diffusion and birth-death. For times $t \gg \min(\tau_E, \tau_D)$, $\langle r^2 \rangle_c(t)$ converges to the asymptotic value

$$\langle r^2 \rangle_c^\infty = \lim_{t\to\infty} \langle r^2 \rangle_c(t) = r_0^2 \left[1 - \frac{2}{\pi} \sqrt{\frac{2\tau_P}{\tau_D}} \tanh\left(\frac{\pi}{2} \sqrt{\frac{\tau_D}{2\tau_P}} \right) \right] . \tag{III.137}$$

where $r_0 = \sqrt{4D\tau_E}$ is the average square distance obtained in [Meyer et al. 1996] for a system of infinite size. The result (III.137) thus generalises to confined geometries the results for unbounded domains derived in [Meyer et al. 1996]. Note that, in the limit of extremely large populations,

$$\lim N \to \infty \langle r^2 \rangle_c = \frac{2}{3} L^2 \, . \tag{III.138}$$

and we recover the ideal case.

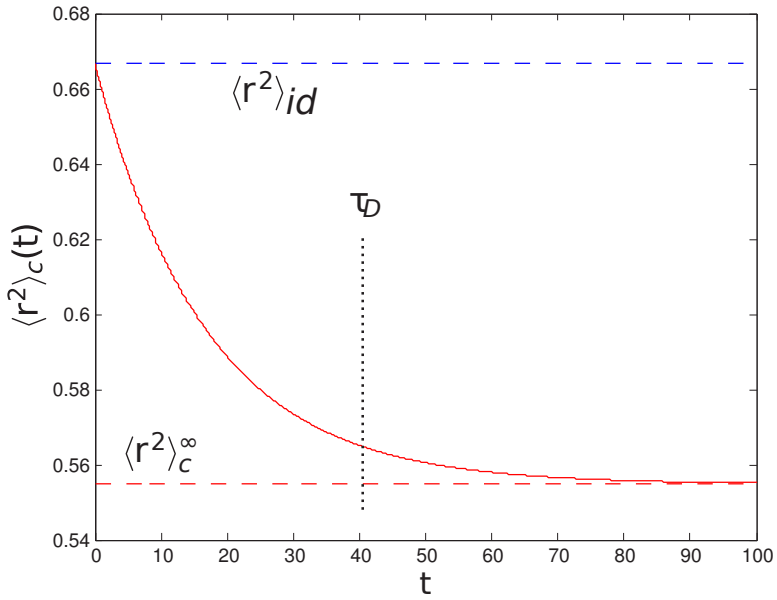

Figure III.15: Time evolution of the average square distance between particles $\langle r^2 \rangle_c(t)$ for the one-dimensional model with $N = 100$ initial neutrons, $\lambda = 1$, $D = 10^{-2}$ and $L = 1$. The red solid line corresponds to the case of population control: at long times, $\langle r^2 \rangle_c(t)$ asymptotically converges to the value $\langle r^2 \rangle_c^\infty$ given in Eq. (III.137) and displayed as a red dashed line.

4 Conclusions and perspectives

So far, clustering phenomena have been mostly analysed in unbounded system of infinite size: either in the thermodynamic limit ($V \to \infty$ and $N \to \infty$, with finite $n_0 = N/V$) [Cox and Griffeath 1985; Houchmandzadeh 2009] or in unbounded domains with a finite number of particles N [Zhang et al. 1990; Meyer et al. 1996]. A realistic description of actual physical systems demands however that the effects due to the finiteness of the viable volume V be explicitly taken into account. In sections III.2.3 and III.2.4, we studied the correlation within a neutron population in a finite size reactor at critical regime. Then in section 3, we included the effects of a population control by imposing that the total number N of neutrons in V is preserved, and investigate the consequences of such constraint on spatial fluctuations. The results presented along this chapter were published in [Dumonteil et al. 2014; Zoia et al. 2014; de Mulatier et al. 2015].

A population of N_0 individuals that can reproduce or die intrinsically undergoes very strong fluctuations of its community size in time. In the

critical case, these fluctuations are responsible for the extinction of the population in the characteristic time $\tau_E = N_0/(\lambda\nu_2)$ (*critical catastrophe*). In the first part of this chapter, coupling diffusion and reproduction processes, we have first observed the presence of two types of fluctuations:

- first, **local fluctuations**, that result from a competition between diffusion and birth/death processes. These fluctuations are responsible for a local particle clustering, as attests the pointed shaped pair-correlation function: whereas reproduction/birth process tends to correlate particles on one point, diffusion tends to enlarge the correlated zone, and thus the size of the cluster.

- then, here as well, **strong global fluctuations** due to the reproduction process. These fluctuations leads to a trivial clustering and, finally to the extinction of the whole population in the characteristic time τ_E.

We then have showed that applying a control on the whole population prevents the trivial death of the population by drastically reducing the global fluctuations. However, clustering due to local fluctuations of the population can still happen, depending on the ratio of two time scale: a diffusion characteristic time $\tau_D = L^2/D$, that characterise the time taken by particles to explore the whole system, and a reproduction characteristic time, $\tau = 1/\lambda_p$, that is the time taken by the system to renewal all its particle pairs (after which the distance between two particles is not due to diffusion from their common father anymore).

As a perspective, it was highlighted in the free case a different behaviour, depending on the dimension of the system, showing that, in higher dimension, diffusion is struggling more to compensate the clustering effect caused by birth and death. It could be then very interesting to understand the dependence in dimension of this phenomenon, in a finite system, and in the presence of population control. Finally, it would be very interesting to understand the effect of delay neutrons on the clustering. Indeed, this neutrons should severely modify the various time scales, and thus lead to different conclusions.

Second part

ANOMALOUS TRANSPORT

CHAPTER IV

OPACITY OF BOUNDED MEDIA

In this chapter we are interested in the occupation statistics of a radiation flow within a region of a medium completely immersed in the flow. In this context, we are focusing on the Cauchy formula, which originally established the mean length travelled by random straight paths crossing a finite domain. Over the last years, this formula has been extended to the class of exponential branching random walks. In this chapter, we first generalise this formula to heterogeneous media with anisotropic scattering. Then we show that this formula holds for non-exponential branching random walks (provided that the walk has a finite mean free path), which presents an interest in the study of transport on disordered media.

Contents

1 OPACITY FORMULAE - MOTIVATION AND STATE OF THE ART

PRECISELY quantifying the flow of radiation, such as neutrons or photons, through a structural material or a living body represents a long-standing problem in physics [Chandrasekhar 1943; Duderstadt and Martin 1979; Case and Zweifel 1967]. It is key to mastering technological issues encompassing the design of nuclear reactors [Bell and Glasstone 1970], light distribution in tissues for medical diagnosis [Tuchin 2007], and radiative heat transfer [Modest 2013]. In transport theory, a fundamental question concerns the occupation statistics of the transported particles within the medium or the body that they flow through (see Chapter II Sec. 2):

- the distribution of the total length l_V travelled through the medium is, for instance, directly proportional to the radiation flux;

- the distribution of the number n_V of collisions performed inside the medium is related to the power density deposited in the traversed region [Duderstadt and Martin 1979; Case and Zweifel 1967].

In this context, one is often called to relate the physical properties of a medium immersed in a radiation flow to the statistics of the random trajectories of the particles flowing through it. Thus, one of the basis formulae in reactor physics, known as the *opacity formula*, gives the opacity of a medium as an estimate of the "size" $\langle L \rangle$ of the traversed region compared to the mean free path λ of the particles flowing through it [Reuss 2012; Duderstadt and Martin 1979; Case and Zweifel 1967]:

Opacity
$$\mathcal{O} = \frac{\langle L \rangle}{\lambda} . \tag{IV.1}$$

If this opacity is large the structure of the medium, and in particular its heterogeneities, will affect the distribution of the flux of particles [Reuss 2012], and conversely, the flow of particles may affect the medium (creating damages for instance). On the other hand, a small opacity means that the medium appears almost transparent to the particles: the flow traverses the medium without interacting with it. In this opacity formula, the size $\langle L \rangle$ of the medium is evaluated from the *Cauchy formula* [Reuss 2012], established by Augustin Cauchy (1789–1857), which relates the mean length of a chord[1] crossing the medium to the geometrical properties of the medium itself – its volume V, its surface S and its dimensionality d [Santaló 2004] (see Fig. IV.1 Left):

Cauchy formula
$$\langle L \rangle_S = \eta_d \frac{V}{S} , \tag{IV.2}$$

[1] It is considered that the mean length of a chord of the medium, i.e. the average distance separating the entrance point from the exit point of a neutron crossing it, is representative of the size of the medium.

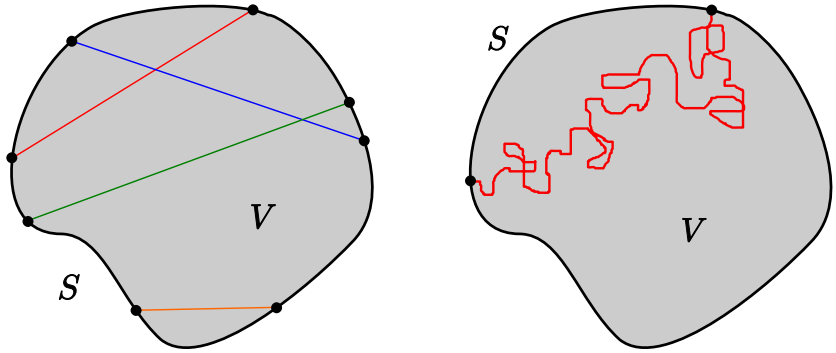

Figure IV.1: Left. Several random chords traversing a two-dimensional domain. **Right.** Purely diffusive random walker crossing the domain, from one point to another point of its surface S.

where η_d is a geometrical constant, depending on the dimension d of the system (for instance $\eta_2 = \pi$ and $\eta_3 = 4$)[2]. The notation $\langle\cdot\rangle_S$ denotes the average over all possible directions and points of entry of the chords on the surface S of the medium.

Within the framework of random walks, the mean chord length $\langle L\rangle_S$ corresponds to the mean length travelled by random straight paths crossing a domain of finite size. In a different context, motivated by the study of animal trajectories in various conditions, Blanco and Fournier [2003] and then Bénichou et al. [2005] have shown that the Cauchy formula (IV.2) holds for walkers starting uniformly from the surface S of the domain and performing exponential Pearson random walks, as illustrated on Fig. IV.1 Right (see also [Bardsley and Dubi 1981; Mazzolo 2004]). Surprisingly enough, the mean total length $\langle L\rangle_S$ travelled by such a walker within a finite domain depends only on the geometrical properties of the traversed domain, and not on the specific details of the walk. Note that here the length L is the ensemble average[3] of the total length l_V travelled by one walker through the domain (see Fig. IV.4):

$$L = \langle l_V \rangle \,, \tag{IV.3}$$

as defined in Chapter II (Eq. (II.34) for $m = 1$). More recently, resorting to the Feynman-Kac formalism (see Chapter II), Zoia et al. [2012a] have generalised the Cauchy formula (IV.2) to branching exponential random

[2]Note that, if the domain considered is non-convex, a straight line crossing the medium may generate several chords. In this case each of them is considered independently and thus contributes independently to $\langle L\rangle_S$ [Mazzolo et al. 2003].

[3]Average over the different realisations of the walk starting from the same point of the surface, with the same direction (see Chapter II).

walks,

$$\langle L\rangle_S = \eta_d \frac{V}{S}\left[1 + \frac{(\nu-1)}{\lambda}\langle L\rangle_V\right], \tag{IV.4}$$

relating the surface average $\langle L\rangle_S$ to the volume averages $\langle L\rangle_V$, which is the mean total length travelled by a walker (and all its descendants) starting uniformly within the volume V, with a random direction (see Fig. IV.2). The constant λ is the mean free path of the walkers, and ν is the mean number of descendants at each collision (see Eq. (I.24)). In particular, when $\nu = 1$, we recover the Cauchy formula (IV.2), such that, even in the presence of branching, the mean length travelled by a walker and its family within a domain depends only on the geometrical properties of the domain. A similar property has been also established for the mean number $N = \langle n_V\rangle$ of collisions performed by a branching exponential random walk within a bounded domain [Zoia et al. 2012a]:

$$\langle N\rangle_S = \eta_d \frac{V}{\lambda S}\left[1 + (\nu-1)\langle N\rangle_V\right], \tag{IV.5}$$

relating the surface average to the volume averages of N. At criticality ($\nu = 1$), the mean number of collisions then becomes:

$$\langle N\rangle_S = \eta_d \frac{V}{\lambda S} = \mathcal{O}, \tag{IV.6}$$

where we recognise here the opacity $\mathcal{O}$ defined in Eq. (IV.1) and Eq. (IV.2). Thus, in case of branching exponential walks at criticality, the opacity $\mathcal{O}$ introduced above exactly corresponds to the mean total number of collisions occurred within the considered domain. In this sense, this latter formula is commonly used in microdosimetry [Zaider and Rossi 1996; Brahme and Kempe 2014; Northum and Guetersloh 2014].

Beyond the application to neutron transport, the use of this invariance property (IV.2) is reported in various fields, such as biology [Blanco and Fournier 2003; Bénichou et al. 2005; Challet et al. 2005; Jeanson et al. 2003, 2005], or radiative transfer [Levitz 2005]. It is intimately connected to the problem of the mean residence time $\langle t\rangle_{S/V}$ of a random walk within the volume V, given, for walkers with finite velocity v, by [Blanco and Fournier 2003; Bénichou et al. 2005; Zoia et al. 2012a]:

$$\langle t\rangle_{S/V} = \frac{\langle L\rangle_{S/V}}{v}. \tag{IV.7}$$

The mean residence time of the walk inside the medium is the mean of the sum of the times spent by the first walker and each of its descendants within the domain, from the entrance of the first walker to the exit of each

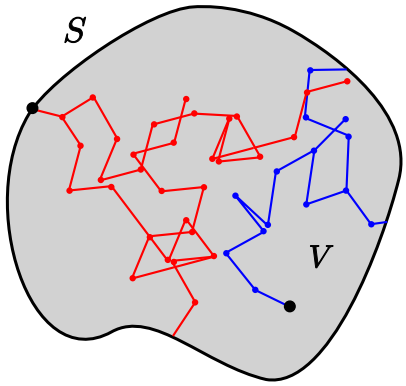

Figure IV.2: Branching random walk, starting from the surface S of the domain (red) or within the volume V of the domain (blue).

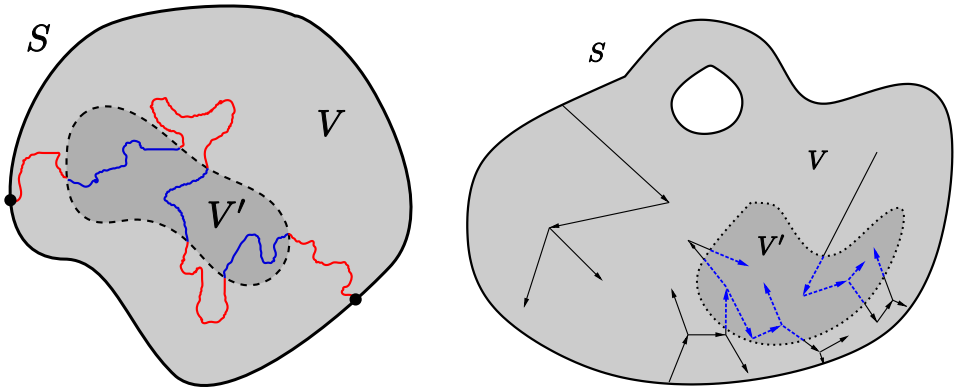

Figure IV.3: Total length travelled (or time spent) by a walk in a subdomain V' (computed on the blue paths) for a purely diffusive walker (Left) and for a branching random walk (Right).

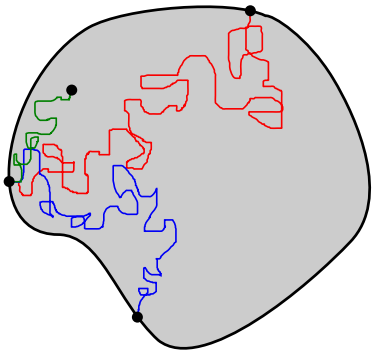

Figure IV.4: Several realisations of a purely diffusive random walk starting from the same phase space position. The ensemble average, appearing for instance in Eq. (IV.3), corresponds to an average over all possible realisations of this walk.

of them [Redner 2001; Weiss 2005][4]. A generalisation of the formulae (IV.2), (IV.4) and (IV.6), has also been carried out concerning the mean total length $\langle L' \rangle_S$ travelled in a subdomain V' of the domain V [Zoia et al. 2012a] (see Fig. IV.3) and the corresponding *mean sojourn time*[5] of a walk in V': $\langle t' \rangle_S = \langle L' \rangle_S / v$ [Bénichou et al. 2005].

Up to now, we have considered only the case of exponential transport of particles. However, exponential transport stems from assuming that the medium is homogeneous and that scattering centres are uncorrelated (see Chapter I). One may wonder if the invariant property (IV.2) and the Cauchy-like formulae (IV.4) and (IV.6) hold in the case of an heterogeneous medium, or in the case of a disordered and strongly heterogeneous medium (containing holes of size comparable to the mean free path of the transported particles, such as within Pebble-bed reactors or Lévy glasses). In this chapter, we will first be interested in a generalisation of the Cauchy-like formulae (IV.4) and (IV.6) to heterogeneous media with anisotropic scattering (sec. 2). Then we will move on to the case of non-exponential branching random walks (sec. 3 and 4), including Lévy branching random walks, which may contribute to the study of transport in strongly heterogeneous and disordered media.

2 CAUCHY FORMULA FOR A NON-STOCHASTIC HETEROGENEOUS MEDIUM

Let us consider a flow of neutrons moving at constant speed v within an inhomogeneous multiplying medium with anisotropic scattering. We assume that the heterogeneities of the medium are fully determined (the medium is not disordered), and that the characteristic length separating scattering centres is small compared to the mean free path of the transported particles (no holes in the medium). The medium can be thus characterised by a total cross section $\Sigma(\mathbf{r})$ at any position $\mathbf{r}$. Note that, for an homogeneous medium, the cross section Σ is constant and corresponds to the inverse of the mean free path: $\Sigma = 1/\lambda$. The scattering is characterised by a scattering kernel $C(\boldsymbol{\omega} \to \boldsymbol{\omega}' \,|\, \mathbf{r})$[6], and the branching process by the mean number of descendants per collision $\nu_1(\mathbf{r})$. Let us now consider a domain $\mathcal{D}$ of volume V and surface S of this medium. We are interested in the mean total length $\langle L \rangle_S$ travelled by a walker starting from the surface S, and all its descendants, within the domain $\mathcal{D}$ until they all exit or have been absorbed.

For this type of system, we have already established in Chapter II the

[4] For a random walk without branching, the mean residence time is equivalent to the first return time (or first exit time), i.e. the time interval between the entry of the particle from the surface S and its first exit through S.

[5] Cumulative time spent in the subdomain V'.

[6] We assume that the scattering kernel C is reversible, and admits an adjoint denoted C^*.

backward equation verified by any moment $L_m = \langle l_V^m \rangle$ (including $L = L_1$) of the total length $l_V(\mathbf{r}_0, \boldsymbol{\omega}_0, t)$ travelled up to a time t by a neutron emitted from a point $\mathbf{r}_0$ with a direction $\boldsymbol{\omega}_0$, and all its descendants, within a volume V of the medium (see Eq. II.48):

$$\begin{aligned}\frac{1}{v}\frac{\partial L_m}{\partial t}(\mathbf{r}_0, \boldsymbol{\omega}_0, t) \;=\; & \underbrace{\boldsymbol{\omega}_0 \cdot \nabla_{\mathbf{r}_0} L_m}_{\text{Transport}} + \underbrace{m\, \mathbb{1}_V(\mathbf{r}_0)\, L_{m-1}}_{\text{Counting term}} \underbrace{-\Sigma(\mathbf{r}_0)\, L_m}_{\text{Loss at collisions}} \\ & + \underbrace{\Sigma(\mathbf{r}_0)\left[\nu_1\, \mathcal{C}^*\left[L_m\right] + \sum_{j=2}^{m} \nu_j \mathcal{B}_{m,j}\left(\mathcal{C}^*\left[L_i\right]\right)\right]}_{\text{Contribution of the descendants at each collision}}, \end{aligned} \tag{IV.8}$$

considering here that particles have a constant speed v. We recall that the average $\langle \cdot \rangle$ corresponds to the ensemble average, i.e. the average over different realisations[7] of the walk starting from $(\mathbf{r}_0, \boldsymbol{\omega}_0)$, as illustrated on Fig. IV.4. On one realisation, the total length $l_V(\mathbf{r}_0, \boldsymbol{\omega}_0)$ travelled within the volume V until the exit or the absorption of all the particles corresponds to the limit of $l_V(\mathbf{r}_0, \boldsymbol{\omega}_0, t)$ when the observation time t goes to infinity:

$$l_V(\mathbf{r}_0, \boldsymbol{\omega}_0) = \lim_{t \to \infty} l_V(\mathbf{r}_0, \boldsymbol{\omega}_0, t)\,. \tag{IV.9}$$

The mean total length $L(\mathbf{r}_0, \boldsymbol{\omega}_0) = \langle l_V \rangle$, and all the other moments $L_m(\mathbf{r}_0, \boldsymbol{\omega}_0)$, then correspond to the stationary solutions of Eq. (IV.8):

$$\begin{aligned} \underbrace{-\boldsymbol{\omega}_0 \cdot \nabla_{\mathbf{r}_0} L_m}_{\text{Transport}} \;=\; & \underbrace{m\, \mathbb{1}_V(\mathbf{r}_0)\, L_{m-1}}_{\text{Counting term}} \underbrace{-\Sigma(\mathbf{r}_0)\, L_m}_{\text{Loss at collisions}} \\ & + \underbrace{\Sigma(\mathbf{r}_0)\left[\nu_1\, \mathcal{C}^*\left[L_m\right] + \sum_{j=2}^{m} \nu_j \mathcal{B}_{m,j}\left(\mathcal{C}^*\left[L_i\right]\right)\right]}_{\text{Contribution of the descendants at each collision}}, \end{aligned} \tag{IV.10}$$

Note that the limit in Eq. (IV.9) is not necessarily finite (the population may keep growing within the domain $\mathcal{D}$ in case of a super-diffusive branching process), such that Eq. (IV.8) may not admit any stationary solution. Intuitively, this condition is satisfied when the particle losses due to absorptions and leakages from the boundaries (exit from the surface S) are larger than the gain due to population growth. This is always the case if $\nu_1 \leqslant 1$ (see Chapter II). When $\nu_1 > 1$, this typically amounts to further requiring that the volume V is below some critical size V_c [Pázsit and Pál 2007] (see Sec. II.3.3.b). In the following we will assume that $V < Vc$.

[7] $l_V(\mathbf{r}_0, \boldsymbol{\omega}_0, t)$ is to the total length travelled during one realisation. It is a stochastic variable (see Sec. II.2.1).

To derive now an equivalent of equation (IV.4), we have to consider two cases.

$\longrightarrow$ First, the walker starts from a random position $\mathbf{r}_0$ uniformly distributed over the volume V, with an isotropic direction $\boldsymbol{\omega}_0 \in \Omega_d$. This leads us to define the volume average $\langle\cdot\rangle_V$, appearing in Eq. (IV.4) [Bénichou et al. 2005; Santaló 2004; Mazzolo 2004]:

$$\langle f(\mathbf{r}_0, \boldsymbol{\omega}_0) \rangle_V = \int_V \frac{d^3\mathbf{r}_0}{V} \int_{\Omega_d} \frac{d^2\boldsymbol{\omega}_0}{\Omega_d} f(\mathbf{r}_0, \boldsymbol{\omega}_0) \,. \tag{IV.11}$$

The normalisation constant Ω_d is the maximum solid angle in a d-dimensional space (corresponding to the area of the surface of a unit d-ball [Mazzolo 2009]):

$$\Omega_d = \int_{Sp_d} d^d\boldsymbol{\omega} = \frac{2\pi^{d/2}}{\Gamma\left(\frac{d}{2}\right)} \tag{IV.12}$$

where $\Gamma(x)$ is the gamma function; for instance $\Omega_2 = 2\pi$, $\Omega_3 = 4\pi$.

$\longrightarrow$ Second, the walker enters the domain $\mathcal{D}$ from its surface S: the entry point $\mathbf{r}_0$ of the walker is uniformly distributed over the surface S, and its direction $\boldsymbol{\omega}_0$ is isotropically distributed and directed inward. This allows precisely defining the surface average appearing in Eq. (IV.4) [Bénichou et al. 2005; Santaló 2004]:

$$\langle f(\mathbf{r}_0, \boldsymbol{\omega}_0) \rangle_S = \oint_S \frac{dS(\mathbf{r}_0)}{S} \int_{\substack{\boldsymbol{\omega}_0 \in \Omega_d \\ \boldsymbol{\omega}_0 \cdot \mathbf{n}_{\mathbf{r}_0} > 0}} \frac{d^2\boldsymbol{\omega}_0}{\alpha_d} \, \boldsymbol{\omega}_0 \cdot \mathbf{n}_{\mathbf{r}_0} \, f(\mathbf{r}_0, \boldsymbol{\omega}_0) \,, \tag{IV.13}$$

where $\mathbf{n}_{\mathbf{r}_0}$ is a unit vector, orthogonal to the surface S in $\mathbf{r}_0$ and directed toward the inside of the domain $\mathcal{D}$[8], and $dS(\mathbf{r}_0)$ is the area of the surface element in the vicinity of $\mathbf{r}_0 \in S$: $\oint_S dS = S$. The integral over $\boldsymbol{\omega}_0$ is such that $\boldsymbol{\omega}_0$ is directed inward, i.e. $\boldsymbol{\omega}_0 \cdot \mathbf{n}_{\mathbf{r}_0} > 0$. The normalisation constant α_d is the mean inward flux of an isotropically distributed unit vector through a unit surface (see Fig. IV.5):

$$\alpha_d = \int_{\substack{\boldsymbol{\omega}_0 \in \Omega_d \\ \boldsymbol{\omega}_0 \cdot \mathbf{n}_{\mathbf{r}_0} > 0}} \boldsymbol{\omega}_0 \cdot \mathbf{n}_{\mathbf{r}_0} \, d^2\boldsymbol{\omega}_0 = \frac{2\pi^{(d-1)/2}}{(d-1)\,\Gamma\left(\frac{d-1}{2}\right)} \,. \tag{IV.14}$$

α_d can also be seen as the volume of a unit $(d-1)$-ball [Mazzolo 2009], and, for instance, $\alpha_2 = 2$ and $\alpha_3 = \pi$.

[8] Customarily, in reactor physics the vector normal to a surface is chosen directed outward (as we did for the surface elementary vector $d^2\mathbf{S}$ in Sec. I.2.1). Here, for convenience, we adopt a different convention.

Following the lines of [Bénichou et al. 2005] and [Zoia et al. 2012a], we apply the volume average (IV.11) to Eq. (IV.10), which yieds:

$$\left\langle L_m \right\rangle_S = \eta_d \frac{V}{S}\Bigg[m \left\langle L_{m-1} \right\rangle_V + \left\langle \Sigma(\mathbf{r}_0)\left(\nu_1(\mathbf{r}_0)\,\mathcal{C}^*\{\cdot\} - 1\right) L_m \right\rangle_V + \left\langle \Sigma(\mathbf{r}_0) \sum_{j=2}^{m} \nu_j \mathcal{B}_{m,j}\left(\mathcal{C}^*\left[L_i\right]\right)\right\rangle_V\Bigg], \quad \text{(IV.15)}$$

where the constant $\eta_d = \Omega_d/\alpha_d$. We have computed the volume average of the transport term by applying the Gauss divergence theorem:

$$\begin{aligned} -\langle\, \boldsymbol{\omega}_0 \cdot \nabla_{\mathbf{r}_0} L_m \,\rangle_V &= -\frac{1}{\Omega_d\, V}\int_{\Omega_d} d^2\boldsymbol{\omega}_0 \int_V d^3\mathbf{r}_0\; \nabla_{\mathbf{r}_0} \cdot \left[\, L_m(\mathbf{r}_0, \boldsymbol{\omega}_0)\; \boldsymbol{\omega}_0 \,\right], \\ &= \frac{1}{\Omega_d\, V}\int_{\Omega_d} d^2\boldsymbol{\omega}_0 \oint_S dS\; (\boldsymbol{\omega}_0 \cdot \mathbf{n}_{\mathbf{r}_0})\; L_m(\mathbf{r}_0, \boldsymbol{\omega}_0)\,. \end{aligned} \quad \text{(IV.16)}$$

As $L_m(\mathbf{r}_0, \boldsymbol{\omega}_0) = 0$ for any $(\mathbf{r}_0, \boldsymbol{\omega}_0)$ such that $\boldsymbol{\omega}_0$ is directed outward, we can reduce the integral over Ω_d in Eq. (IV.16) to the inward direction $\boldsymbol{\omega} \cdot \mathbf{n}_{\mathbf{r}_0} > 0$ (see Fig. IV.5), and we recognise the surface average (IV.13):

$$-\langle\, \boldsymbol{\omega}_0 \cdot \nabla_{\mathbf{r}_0} L_m \,\rangle_V = \frac{\alpha_d\, S}{\Omega_d\, V}\langle\, L_m \,\rangle_S\,. \quad \text{(IV.17)}$$

Let us write each integral of the volume average of the scattering term:

$$\begin{aligned} &\left\langle\, \Sigma(\mathbf{r}_0)\, \nu_1(\mathbf{r}_0)\, \mathcal{C}^*\{L_m\} \,\right\rangle_V \quad \text{(IV.18)} \\ &\quad = \int_V \frac{d^3\mathbf{r}_0}{V} \Sigma(\mathbf{r}_0)\, \nu_1(\mathbf{r}_0) \int_{\Omega_d} \frac{d^2\boldsymbol{\omega}_0}{\Omega_d} \int_{\Omega_d} d^2\boldsymbol{\omega}_0' C^*(\boldsymbol{\omega}_0' \to \boldsymbol{\omega}_0 \,|\, \mathbf{r}_0) L_m(\mathbf{r}_0, \boldsymbol{\omega}_0') \end{aligned}$$

By definition, the adjoint scattering operator $C^*\{\cdot\}$ is related to the scattering $C\{\cdot\}$ by the relation [Reuss 2012]:

$$\langle C\{f\}, g\rangle = \langle f, C^*\{g\}\rangle\,, \quad \text{(IV.19)}$$

where f and g are two square-integrable functions over Ω_d, and $\langle f, g\rangle$ denotes the inner product of f and g[9]. We thus have for f and g real, that

$$\begin{aligned} &\int_{\Omega_d} d^2\boldsymbol{\omega}_0\, f(\boldsymbol{\omega}_0) \int_{\Omega_d} d^2\boldsymbol{\omega}_0'\; C^*(\boldsymbol{\omega}_0' \to \boldsymbol{\omega}_0 \,|\, \mathbf{r}_0) g(\mathbf{r}_0, \boldsymbol{\omega}_0') \\ &\qquad = \int_{\Omega_d} d^2\boldsymbol{\omega}_0 \int_{\Omega_d} d^2\boldsymbol{\omega}_0'\, C(\boldsymbol{\omega}_0 \to \boldsymbol{\omega}_0' \,|\, \mathbf{r}_0) f(\mathbf{r}_0, \boldsymbol{\omega}_0') g(\mathbf{r}_0, \boldsymbol{\omega}_0) \end{aligned} \quad \text{(IV.20)}$$

[9] Let f and g be two real square-integrable functions over Ω_d; the inner product of f and g is given by $\langle\, f, g \,\rangle = \int_{\Omega_d} d\boldsymbol{\omega}\, f(\boldsymbol{\omega})\, g(\boldsymbol{\omega})$.

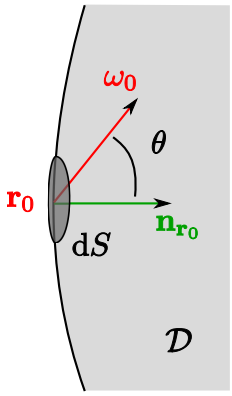

Figure IV.5: Consider a particle emitted from $\mathbf{r}_0$, located on the surface of $\mathcal{D}$, with an isotropic direction ω_0 (over Ω_d). Of these particles, those that are directed toward the inside of $\mathcal{D}$ are the ones considered in the surface average (IV.13) and for the computation of α_d: for a convex domain with a smooth surface, they are such that the angle between ω_0 and $\mathbf{n}_{\mathbf{r}_0}$ is $\theta \leqslant \pi/2$, i.e. $\omega_0 \cdot \mathbf{n}_{\mathbf{r}_0} > 0$.

for all position $\mathbf{r}_0$. Taking $f(\mathbf{r}_0, \omega_0) = 1$ and $g(\mathbf{r}_0, \omega_0) = L_m(\mathbf{r}_0, \omega_0)$, we finally get the relation:

$$\int_{\Omega_d} d^2\omega_0 \int_{\Omega_d} d^2\omega_0' \, C^*(\omega_0' \to \omega_0 \,|\, \mathbf{r}_0) L_m(\mathbf{r}_0, \omega_0') = \int_{\Omega_d} d^2\omega_0 \int_{\Omega_d} d^2\omega_0' \, C(\omega_0 \to \omega_0' \,|\, \mathbf{r}_0) L_m(\mathbf{r}_0, \omega_0) \,, \quad \text{(IV.21)}$$

so that the volume average of the scattering term reads:

$$\left\langle \Sigma(\mathbf{r}_0)\, \nu_1(\mathbf{r}_0)\, \mathcal{C}^*\{L_m\} \right\rangle_V = \int_V \frac{d^3\mathbf{r}_0}{V} \int_{\Omega_d} \frac{d^2\omega_0}{\Omega_d} \Sigma(\mathbf{r}_0)\, \nu_1(\mathbf{r}_0)\, L_m(\mathbf{r}_0, \omega_0) = \left\langle \Sigma(\mathbf{r}_0)\, \nu_1(\mathbf{r}_0)\, L_m(\mathbf{r}_0, \omega_0) \right\rangle_V \quad \text{(IV.22)}$$

We finally obtain the recursive formula,

Inhomogeneous media with anisotropic scattering

$$\left\langle L_m \right\rangle_S = \eta_d \frac{V}{S} \left[m \left\langle L_{m-1} \right\rangle_V + \left\langle \Sigma(\mathbf{r}_0)\, (\nu_1(\mathbf{r}_0) - 1)\, L_m \right\rangle_V + \left\langle \Sigma(\mathbf{r}_0) \sum_{j=2}^{m} \nu_j \mathcal{B}_{m,j}\left(\mathcal{C}^*[L_i]\right) \right\rangle_V \right], \quad \text{(IV.23)}$$

that relates the m-th moment of l_V for walks starting from the surface S to

the lower moments (of l_V, up to m) for walks starting within the volume V. This relation generalises to inhomogeneous media, with anisotropic scattering, the recursive formula of [Zoia et al. 2012a] (see also [Mazzolo 2004; Bénichou et al. 2005]). In particular, for $m = 1$, we generalise Eq. (IV.4):

Inhomogeneous media with anisotropic scattering

$$\langle L \rangle_S = \eta_d \frac{V}{S} \left[1 + \langle \Sigma(\mathbf{r}_0) \left(\nu_1(\mathbf{r}_0) - 1 \right) L \rangle_V \right] . \qquad \text{(IV.24)}$$

We recall that, for an homogeneous medium, jumps are exponentially distributed, with a mean free path $\lambda = 1/\Sigma$, which gives back Eq. (IV.4).

The latter result has been carefully checked with numerical simulations for a piecewise inhomogeneous medium (see Fig. IV.6), for a medium with a continuous variation of the parameter $\nu_1(\mathbf{r}_0)$ (see Fig. IV.7), and for an homogeneous medium with anisotropic scattering. Moreover, for a critical system, such that $\nu_1(\mathbf{r}_0) = 1 \; \forall \mathbf{r}_0 \in \mathcal{D}$, Eq. (IV.24) yields back the Cauchy formula (IV.2), which then holds for inhomogeneous media with anisotropic scattering [Bardsley and Dubi 1981]. To illustrate this point, we have performed a Monte Carlo simulation of a critical branching process in three different cases (see Fig IV.8):

$\longrightarrow$ *black* – an homogeneous medium ($\Sigma = 1$) with isotropic scattering;

$\longrightarrow$ *red*– the piecewise heterogeneous medium illustrated on Fig. IV.6 with $\Sigma_1 = 1$ and $\Sigma_2 = 0.5$ and with isotropic scattering;

$\longrightarrow$ *blue* – an homogeneous medium ($\Sigma = 1$) with anisotropic scattering: at a collision, the direction $\boldsymbol{\omega}'$ of the outgoing particle is given by

$$\boldsymbol{\omega}' = \begin{cases} \text{isotropic} & \text{with probability } 0.5 \\ \boldsymbol{\omega} & \text{else} \end{cases} \qquad \text{(IV.25)}$$

where $\boldsymbol{\omega}$ is the direction of the incoming particle.
See Appendix 5 for details concerning the Monte Carlo simulations.

Using the same strategy for the mean number of collision N, thanks to the Feynman-Kac formalism, it is possible to extend Eq. (IV.6) to non-homogeneous systems with anisotropic scattering, and to find a recursive relation for the moments $N_m = \langle n_V^m \rangle$ equivalent to Eq. (IV.23) [Zoia et al. 2012a]; this generalisation has not been done yet.

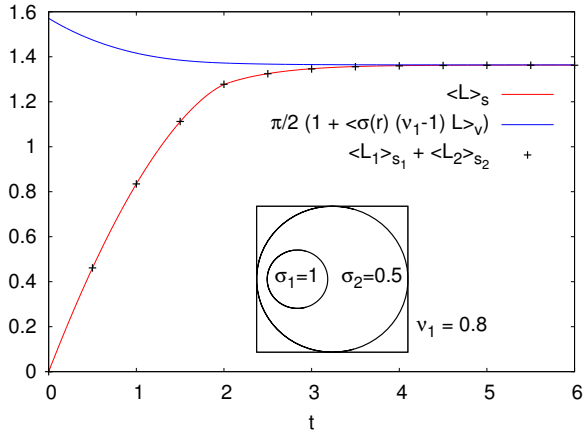

Figure IV.6: Monte Carlo simulations of the time evolution of the mean total length travelled by a branching exponential random walk in a disk of unit radius. The considered medium is illustrated in the inset: a piecewise inhomogeneous medium, composed of a homogeneous disk of radius 0.2 and cross section $\Sigma_1 = 1$ included in a unit and uniform disk of cross section $\Sigma_2 = 0.5$. The parameter ν_1 is constant. The figure compares the lhs to the rhs of Eq. (IV.24), with $\eta_2 V/S = \pi/2$ for a unit disk. Averages are obtained over 10^7 realisations of the system (10^7 particles starting uniformly from the surface S, or within the volume V), so that the statistical uncertainties are of the order of 10^{-3}.

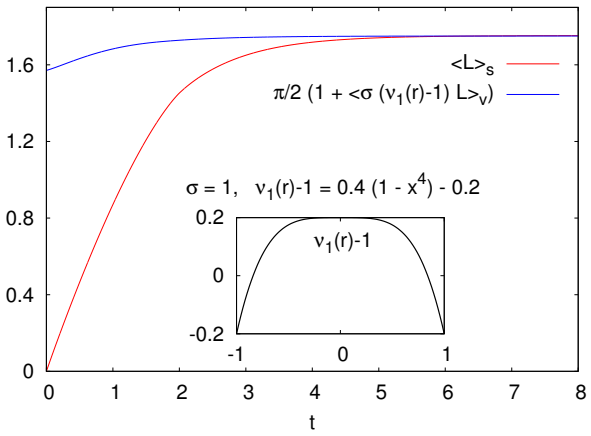

Figure IV.7: Monte Carlo simulations of the time evolution of the mean total length travelled by a branching exponential random walk in a disk of unit radius ($d = 2$ and $\eta_2 V/S = \pi/2$) and of constant cross section $\Sigma = 1$. The branching parameter ν_1 is chosen such that the process is surcritical in the center of the disk and subcritical close to the borders (see the profile of $\nu_1(\mathbf{r}) - 1$ in inset). The figure compares the lhs to the rhs of Eq. (IV.24), with $\eta_2 V/S = \pi/2$ for a unit disk: when the stationary state is reached, the two curves collapse, which is in agreement with Eq. (IV.24). Averages are obtained over 10^7 realisations of the system (10^7 particles starting uniformly from the surface S, or within the volume V), so that the statistical uncertainties are of the order of 10^{-3}.

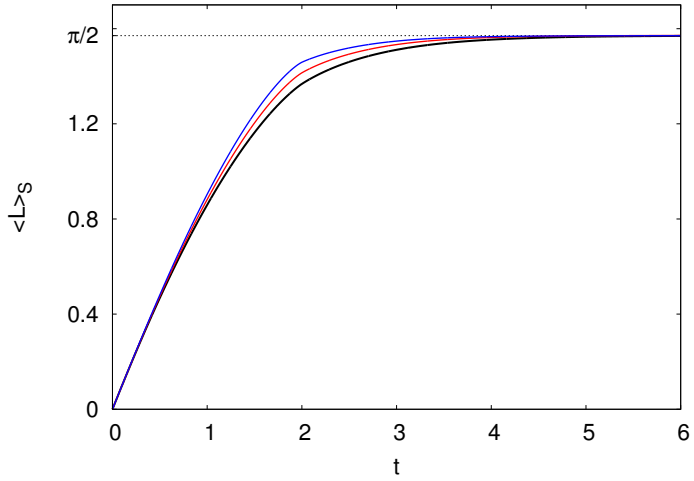

Figure IV.8: Monte Carlo simulations of the time evolution of the mean total length travelled by a branching exponential random walk, at criticality, in a disk of unit radius ($\mathrm{d} = 2$ and $\eta_2\, V/S = \pi/2$). Three cases are considered: an homogeneous medium with isotropic scattering (black curve), a piecewise heterogeneous medium with isotropic scattering (red curve), and an homogeneous medium with the anisotropic scattering (blue curve). At the stationary states, the three curves converge to the constant $\pi/2$, which is in agreement with the Cauchy property Eq. (IV.2). The Monte Carlo simulations have been performed using 10^7 particles starting uniformly from the surface S with uniform directions (directed inward the domain V), and the statistical uncertainties are in the order of 10^{-3}.

3 A Universal Property of Branching Random Walks in Confined Geometries

The results derived in this section have been published in collaboration with Alain Mazzolo and Andrea Zoia in [De Mulatier et al. 2014].

IV.3.1 General Setup and Hypothesis

Consider particles moving at constant speed and performing jumps of random length s distributed according to the probability density function $T(s)$ that is independent on the position and the direction of the walker. Upon collisions, each walker gives rise to k descendants with probability p_k, where the mean number of descendants $\nu = \sum_k k p_k$ is a parameter of the system (see Sec. I.1.2). The directions $\boldsymbol{\omega}$ then taken by the descendants are assumed to be isotropically distributed over Ω_d, where

$$\Omega_d = \frac{2\pi^{d/2}}{\Gamma\left(\frac{d}{2}\right)}, \tag{IV.26}$$

is the surface of the unit $(d-1)$-sphere. Each descendant then behaves independently as the progenitor particle, thus resulting in a ramified structure for the stochastic paths. Moreover we will assume the pdf of the jump lengths $T(s)$ to have a finite mean λ:

$$\lambda = \int_0^{+\infty} s\, T(s)\, ds, \tag{IV.27}$$

which corresponds to the mean free path of the walkers. This definition encompasses a large class of random walks[10]. As a particular case, when T is exponential, we recover the class of branching exponential walks, for which the mean free path is inversely proportional to the cross-section, $\lambda = 1/\Sigma$ (see Sec. I.1.2). If T is a *Levy-stable law* instead, its asymptotic behaviour is of the form [Nolan 2012]

$$T(s) \sim \frac{1}{|s|^{\alpha+1}}, \qquad \text{when } s \to \infty, \tag{IV.28}$$

where $\alpha \in (0,2)$ is a parameter characterising the law, such that the mean of $T(s)$ is finite for $\alpha > 1$.

Consider now a domain of finite volume V and regular surface S immersed in the radiation flow described above at stationary state (stationary flow). Trajectories are observed from the entrance of a single particle through S until the disappearance of the particle and all its descendants by

[10] In the absence of branching, this type of walk is called *Pearson random walk*.

either absorption inside V or escape through S (see fig. IV.10). Supposing that the flow of particles is stationary, we assume that the walker will enter the domain with a uniform distribution of entry point $\mathbf{r}_0$ on the surface S and an isotropic distribution of incident directions $\boldsymbol{\omega}_0$ [Blanco and Fournier 2003, 2006]. Thus, Eq. (IV.13) is still relevant to average over all entry positions and directions of the walkers coming, now, from outside the domain (previously, the walkers were considered to start directly on the surface S).

IV.3.2 Integral Equations

a. Integral transport equations

We are interested in characterising the mean total number of collisions N performed and the mean total length L travelled by a particle and all its descendants within V, and our aim is to establish an equation that the relates $\langle L/N\rangle_S$ to $\langle L/N\rangle_V$ in case of non-exponential branching random walks. The idea is to use one of the equations that govern neutron transport (see Chapter 1 and 2), as we did in the previous section. However, the Boltzmann equation (I.55) and the Feynman-Kac backward equation (II.48) are both established for transport, with a transport kernel of the form (I.10) (see Sec. I.1.2)

$$T(s) = \Sigma(s)\,\exp\left[-\int_0^s \Sigma(s')\,ds'\right] \qquad \text{for } s > 0\,, \tag{IV.29}$$

which yields the transport operator $\boldsymbol{\omega}\cdot\nabla\{\cdot\}$ for these two differential transport equations. As the purpose is to work with any type of transport pdf $T(s)$, these equations can not be used here. The integral equations (I.83) and (I.84) can instead be obtained directly from a neutron balance, using the physical arguments given in Sec. I.2.4.b:

$$\varphi(\mathbf{r},\boldsymbol{\omega},v,t) = \int_0^{s_0} \underbrace{U(s|\mathbf{r},\boldsymbol{\omega},v)}_{\substack{\text{probability to have}\\ \text{no collision between}\\ \mathbf{r}-s\boldsymbol{\omega} \text{ and } \mathbf{r}}} \underbrace{\chi\left(\mathbf{r}-s\boldsymbol{\omega},\boldsymbol{\omega},v,t-\frac{s}{v}\right)ds}_{\substack{\text{flux of particles emitted}\\ \text{about } \mathbf{r}-s\boldsymbol{\omega}\\ \text{in the direction } \boldsymbol{\omega}}} + \varphi_1\,, \tag{IV.30}$$

and

$$\psi(\mathbf{r},\boldsymbol{\omega},v,t) = \int_0^{s_0} \underbrace{ds\,T(s|\mathbf{r},\boldsymbol{\omega},v)}_{\substack{\text{probability to encounter}\\ \text{a collision about } \mathbf{r}\\ \text{(after travelling a distance } s\text{)}}} \underbrace{\chi\left(\mathbf{r}-s\boldsymbol{\omega},\boldsymbol{\omega},v,t-\frac{s}{v}\right)}_{\substack{\text{rate density of particles}\\ \text{emitted about } \mathbf{r}-s\boldsymbol{\omega}\\ \text{in the direction } \boldsymbol{\omega}}} + \psi_1\,, \tag{IV.31}$$

where $\varphi_1(\mathbf{r}, \boldsymbol{\omega}, v, t)$ is the *uncollided flux*[11] defined in Eq. (I.88) and $\psi_1(\mathbf{r}, \boldsymbol{\omega}, v, t)$ the *uncollided collision rate density* defined in Eq. (I.87). The only condition is that the process has to be Markovian at each collision, which is the case for the walks considered here (branching Pearson random walks) whatever the form of $T(s)$. These two integral transport equations for the collision rate density and the flux thus hold true in the case of non-exponential walks.

To work with these equations in the stationary state, we introduce two quantities. We define the *collision density* $\psi(\mathbf{r}, \boldsymbol{\omega}|\mathbf{r}_0, \boldsymbol{\omega}_0)$ so that

$$N(\mathbf{r}_0, \boldsymbol{\omega}_0) = \int_V d\mathbf{r} \int_{\Omega_d} d\boldsymbol{\omega}\, \psi(\mathbf{r}, \boldsymbol{\omega}|\mathbf{r}_0, \boldsymbol{\omega}_0) \tag{IV.32}$$

is the average number of particles having a collision within V, for a single walker starting from $\mathbf{r}_0$ in direction $\boldsymbol{\omega}_0$ [Case and Zweifel 1967]. The collision density thus corresponds to the time integral of the collision rate density $\psi(\mathbf{r}, \boldsymbol{\omega}, t|\mathbf{r}_0, \boldsymbol{\omega}_0)$[12]:

$$\psi(\mathbf{r}, \boldsymbol{\omega}|\mathbf{r}_0, \boldsymbol{\omega}_0) = \int_0^{+\infty} \psi(\mathbf{r}, \boldsymbol{\omega}, t|\mathbf{r}_0, \boldsymbol{\omega}_0) dt\,. \tag{IV.33}$$

We then define the *length density* $\varphi(\mathbf{r}, \boldsymbol{\omega}|\mathbf{r}_0, \boldsymbol{\omega}_0)$ so that

$$L(\mathbf{r}_0, \boldsymbol{\omega}_0) = \int_V d\mathbf{r} \int_{\Omega_d} d\boldsymbol{\omega}\, \varphi(\mathbf{r}, \boldsymbol{\omega}|\mathbf{r}_0, \boldsymbol{\omega}_0) \tag{IV.34}$$

is the average length travelled in V, for a single walker starting from $\mathbf{r}_0$ in direction $\boldsymbol{\omega}_0$ [Case and Zweifel 1967]. The length density corresponds to the integral of the neutron flux over time[13]:

$$\varphi(\mathbf{r}, \boldsymbol{\omega}|\mathbf{r}_0, \boldsymbol{\omega}_0) = \int_0^{+\infty} \varphi(\mathbf{r}, \boldsymbol{\omega}, t|\mathbf{r}_0, \boldsymbol{\omega}_0)\, dt\,. \tag{IV.35}$$

For a stationary flow[14], with constant speed, the collision density ψ is thus related to the *outgoing collision density* χ through the integral equation:

$$\psi(\mathbf{r}, \boldsymbol{\omega}) = \int_0^{u(\mathbf{r},\boldsymbol{\omega})} \underbrace{ds\, T(s)}_{\substack{\text{probability to undergo} \\ \text{a collision about } \mathbf{r} \\ \text{(after travelling a distance } s\text{)}}} \underbrace{\chi(\mathbf{r} - s\boldsymbol{\omega}, \boldsymbol{\omega})}_{\substack{\text{density of particles} \\ \text{leaving a collision about } \mathbf{r}-s\boldsymbol{\omega} \\ \text{in the direction } \boldsymbol{\omega}}} + \psi_1\,, \tag{IV.36}$$

[11] The *uncollided flux* represents the contribution to the angular flux due to particles that have not undergone collisions since they were emitted (from the surface S or within the volume V).

[12] Such that Eq. (IV.32) and (II.66) are consistent, N being the mean number of collisions $\langle n_V \rangle$ defined in Sec. II.3.2.

[13] Such that Eq. (IV.34) and (II.32) are consistent, L being the mean length travelled in V, $\langle l_V \rangle$, defined in Sec. II.2.1.

[14] Eq. (I.86) is integrated over time to give Eq. (IV.36), where the outgoing collision density corresponds to the time integral of the outgoing collision rate density.

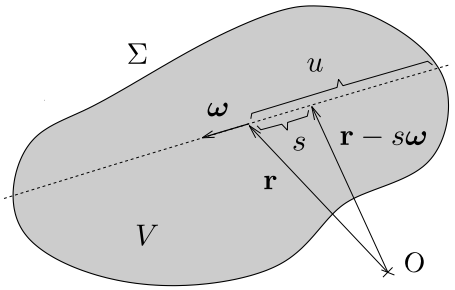

Figure IV.9: A two-dimensional illustration of the coordinate s and the distance $u = u(\mathbf{r}, \boldsymbol{\omega})$ from the point $\mathbf{r}$ to the surface S in the direction given by $-\boldsymbol{\omega}$.

where $\psi_1(\mathbf{r}, \boldsymbol{\omega}) = \int_0 \psi_1(\mathbf{r}, \boldsymbol{\omega}, t)dt$ is the *first-collision density*, and $T(s|\mathbf{r}, \boldsymbol{\omega}, v)$ has been replaced by $T(s)$ assuming that the background medium is homogeneous and isotropic, and that particles evolve at constant speed. The upper limit $u(\mathbf{r}, \boldsymbol{\omega})$ of the integral accounts for the boundaries of the finite medium (see Sec. I.2.4): it is the distance between the position $\mathbf{r}$ inside the domain and the surface S in the direction of $(-\boldsymbol{\omega})$ (see Fig. IV.9). The corresponding equation for the length density φ (integration of Eq. (I.83) over time), is then:

$$\varphi(\mathbf{r}, \boldsymbol{\omega}) = \int_0^{u(\mathbf{r},\boldsymbol{\omega})} \underbrace{U(s)}_{\substack{\text{probability to undergo} \\ \text{a collision about } \mathbf{r} \\ \text{(after travelling a distance } s\text{)}}} \underbrace{\chi(\mathbf{r} - s\boldsymbol{\omega}, \boldsymbol{\omega})}_{\substack{\text{density of particles} \\ \text{leaving a collision about } \mathbf{r}-s\boldsymbol{\omega} \\ \text{in the direction } \boldsymbol{\omega}}} ds + \varphi_1 , \quad \text{(IV.37)}$$

where U is the marginal probability that no collision occurs between $\mathbf{r} - s\,\boldsymbol{\omega}$ and $\mathbf{r}$, and $\varphi_1(\mathbf{r}, \boldsymbol{\omega}) = \int_0^\infty \varphi_1(\mathbf{r}, \boldsymbol{\omega}, t)$ is the *first-length density*.

For a markovian process (such as the neutron transport described in Chapter I) we have seen that the collision density is proportional to the length density: $\psi(\mathbf{r}, \boldsymbol{\omega}) = \Sigma\varphi(\mathbf{r}, \boldsymbol{\omega})$ (see Sec. I.1.2). In the case of exponential flight (for which $\Sigma = 1/\lambda$), this relation leads to the natural result: $\psi(\mathbf{r}, \boldsymbol{\omega}) = \varphi(\mathbf{r}, \boldsymbol{\omega})/\lambda$; the mean number of collisions in an volume element about $(\mathbf{r}, \boldsymbol{\omega})$ is equal to the mean length travelled in this volume, divided by the mean inter-collision distance (mean free path). This relation is counter-intuitively not valid in the general case of non-exponential jumps. This relation is indeed a consequence of the Markovian property of exponential walks, and will be discussed more in detail in section IV.3.4. For this reason, equations (IV.37) and (IV.36) for φ and ψ must be established separately.

b. Stationary state and first jump within the domain

To go further, we need to characterise ψ_1 and φ_1. Up to now, we have discussed only the case of walkers starting from the surface S of the domain $\mathcal{D}$. In this case, or if the source $Q(\mathbf{r},\boldsymbol{\omega})$ is located within the domain $\mathcal{D}$, the densities ψ_1 and φ_1 are given by Eq. (I.87) and Eq. (I.88):

$$\begin{cases} \varphi_1(\mathbf{r},\boldsymbol{\omega}) &= \displaystyle\int_0^{u(\mathbf{r},\boldsymbol{\omega})} U(s)\, Q(\mathbf{r}-s\boldsymbol{\omega},\boldsymbol{\omega})\, ds \\ \psi_1(\mathbf{r},\boldsymbol{\omega}) &= \displaystyle\int_0^{u(\mathbf{r},\boldsymbol{\omega})} T(s)\, Q(\mathbf{r}-s\boldsymbol{\omega},\boldsymbol{\omega})\, ds\,, \end{cases} \tag{IV.38}$$

which respectively corresponds to the length and the collision density resulting from the transport of the source $Q(\mathbf{r},\boldsymbol{\omega})$ until the first collision. However, implementing this expressions in Eq.(IV.36) and (IV.37), and taking the surface average Eq.(IV.13) do not lead to the Cauchy-like formulae. Recently, Mazzolo [2009] has shown, in the context of exponential random walks, that Cauchy's property (IV.2) stays valid for a domain immersed in a stationary flow of radiation, such that particles enter the domain from outside, and does not necessarily start from the surface. This was assumed to be the general conditions for the Cauchy formula to hold [Blanco and Fournier 2003; Mazzolo 2009]. However, the length of the first jump performed within the domain, by an exponential walker entering through the surface (from outside) is also exponentially distributed, such as the other jumps of the walk [Mazzolo 2009]. Thus, the two cases – walker starting from the surface and walker coming from outside in case of a stationary flow – can not be distinguished for exponential Pearson random walks. Naturally, this result also extend to branching exponential walks (that also have exponentially distributed jump lengths).

Regarding the case of non-exponential random walk; we consider now that the domain $\mathcal{D}$ is immersed in a stationary flow of walkers: particles entering from outside can cross the surface without undergoing a collision on it (the surface is transparent). Therefore the distance r travelled by the walker from the surface to its first collision inside $\mathcal{D}$ is not necessarily given by the jumps pdf $T(r)$ (see Fig. IV.10). We denote by $H(r)$ the pdf of this distance r (length of a first jump within $\mathcal{D}$ from the surface). Then, by definition, ψ_1 will be related to the surface source by

$$\psi_1(\mathbf{r},\boldsymbol{\omega}) = \int_0^{+\infty} H(s) Q_S(\mathbf{r}-s\boldsymbol{\omega},\boldsymbol{\omega})\, ds\,, \tag{IV.39}$$

and the density φ_1 is similarly given by

$$\varphi_1(\mathbf{r},\boldsymbol{\omega}) = \int_0^{+\infty} U_H(s) Q_S(\mathbf{r}-s\boldsymbol{\omega},\boldsymbol{\omega})\, ds\,, \tag{IV.40}$$

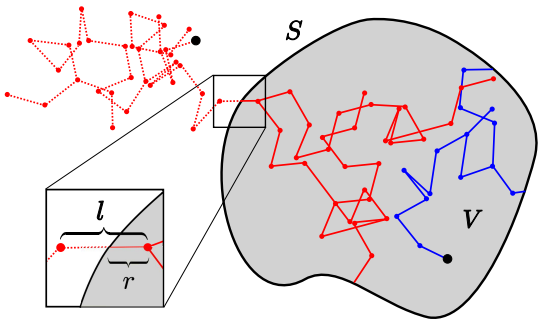

Figure IV.10: Trajectories entering the body through the surface S (red) and trajectories born inside the body (blue) for a branching Pearson random walk with jumps of constant size. Source points are marked as black dots. The inset displays the distinct behaviour of the first jump across S for particles coming from outside in the case of walks with constant jumps: the first jump is distributed according to $H(r) = \mathrm{uni}(0, a)$, whereas the distance between two collisions is constant, $T(l) = \delta(l - a)$.

where
$$U_H(s) = \int_s^{+\infty} H(\ell)\,\mathrm{d}\ell = 1 - \int_0^s H(\ell)\,\mathrm{d}\ell\,, \tag{IV.41}$$
is the marginal probability that a particle entering $\mathcal{D}$ has not yet encounter any collisions after travelling a distance s from the surface (see Sec. I.1.2).

The final ingredient needed to fully characterise the particle inflow through the surface S is the probability density $H(r)$ of the first jump length (see Fig. IV.10). Since walkers enter $\mathcal{D}$ from outside, they have performed a jump (from outside) of total length $\ell \geqslant r$. As a consequence, $H(r)$ must be proportional to the probability that the jump from outside V is larger than r, namely, $H(r) \propto \int_r^\infty T(l)\mathrm{d}l$. By imposing normalisation $\int_0^{+\infty} H(r)\mathrm{d}r = 1$ and using $\lambda = \int_0^\infty \mathrm{d}r \int_r^\infty T(l)\mathrm{d}l$, we recover the first jump length density, initially introduced by Mazzolo [2004, 2009]
$$H(r) = \frac{1}{\lambda} \int_r^{+\infty} T(l)\,\mathrm{d}l\,. \tag{IV.42}$$
Observe that we require λ to be finite in order for $h(r)$ to be properly defined. For exponential flights, we have in particular
$$H(r) = T(r) = \frac{1}{\lambda} \exp\left(-\frac{r}{\lambda}\right)\,, \tag{IV.43}$$
which is the signature of the Markovian nature of this process: trajectories crossing S have no memory of their past history, so that the first jump dis-

tribution does not differ from the others. One can stop an exponential flight an restart it without worrying about what happened before the stop.

c. Surface and volume averages

Surface Source – The contribution to ψ_1 and φ_1 due to particles generated outside the domain V and entering through its surface are given by equations (IV.36) and (IV.37). Let us focus first on the first collision density ψ_1. We have seen in Eq. (I.97) that the contribution due to a surface source can be rewritten, in the stationary case,

$$\psi_1(\mathbf{r},\boldsymbol{\omega}) = H((\mathbf{r}-\mathbf{r}_S)\cdot\boldsymbol{\omega})\,\Lambda_S(\mathbf{r}_S,\boldsymbol{\omega})\,. \tag{IV.44}$$

using the definition $Q_S(\mathbf{r},\boldsymbol{\omega}) = \Lambda_S(\mathbf{r},\boldsymbol{\omega})\,\mathbb{1}_S(\mathbf{r})$ for the surface source in Eq. (IV.39). Applying now the surface average (IV.13) to this expression of ψ_1, with $\Lambda_S(\mathbf{r},\boldsymbol{\omega}) = \delta_3(\mathbf{r}-\mathbf{r}_S)\,\delta_2(\boldsymbol{\omega}-\boldsymbol{\omega}_S)$, we obtain:

$$\begin{aligned}
\langle\psi_1(\mathbf{r},\boldsymbol{\omega})\rangle_S &= \int_S \frac{dS(\mathbf{r}_S)}{S}\int_{\Omega_d}\frac{d\boldsymbol{\omega}_S}{\alpha_d}\,\boldsymbol{\omega}_S\cdot\mathbf{n}_{\mathbf{r}_S}\,H((\mathbf{r}-\mathbf{r}_S)\cdot\boldsymbol{\omega})\,\delta(\boldsymbol{\omega}-\boldsymbol{\omega}_S)\,,\\
&= \frac{1}{S\,\alpha_d}\int_S dS(\mathbf{r}_S)\;\mathbf{n}_{\mathbf{r}_S}\cdot\boldsymbol{\omega}\;H((\mathbf{r}-\mathbf{r}_S)\cdot\boldsymbol{\omega})\,, &\text{(IV.45)}\\
&= -\frac{1}{S\,\alpha_d}\int_V d^3\mathbf{r}_V\,\nabla_{\mathbf{r}_V}\cdot\Big[\,H((\mathbf{r}-\mathbf{r}_V)\cdot\boldsymbol{\omega})\,\boldsymbol{\omega}\,\Big] &\text{(IV.46)}
\end{aligned}$$

where we used the Gauss divergence theorem, recalling that $\mathbf{n}_{\mathbf{r}_S}$ is directed inward. This last integral can be explicitly computed by observing that $\nabla_{\mathbf{r}_V}$ can be replaced by a single derivation along the line defined by the fixed position $\mathbf{r}$ and the fixed direction $\boldsymbol{\omega}$ (see Fig. IV.10), which yields $-H(u)$ A similar derivation can be done for the first length density φ_1, replacing $H(r)$ by $U_H(s)$. We finally obtain:

$$\langle\psi_1(\mathbf{r},\boldsymbol{\omega})\rangle_S = \frac{1}{S\,\alpha_d}\,H\big[u(\mathbf{r},\boldsymbol{\omega})\big] \tag{IV.47}$$

and

$$\langle\varphi_1(\mathbf{r},\boldsymbol{\omega})\rangle_S = \frac{1}{S\,\alpha_d}\,U_H\big[u(\mathbf{r},\boldsymbol{\omega})\big] = \frac{1}{S\,\alpha_d}\left[1-\int_0^{u(\mathbf{r},\boldsymbol{\omega})}H(s)ds\right] \tag{IV.48}$$

by definition of the complementary cumulative U_H of H.

Volume source – We consider now the trajectories of particles born within the $\mathcal{D}$. In this case, particles are transported from the source to their first collision with the usual jump pdf T, so that φ_1 and ψ_1 are given by equation (IV.38). Applying the volume average (IV.11) to ψ_1 and to φ_1, with the

volume source $Q(\mathbf{r},\boldsymbol{\omega}) = \mathbb{1}_V(\mathbf{r})\,\delta_3(\mathbf{r}-\mathbf{r}_V)\,\delta_2(\boldsymbol{\omega}-\boldsymbol{\omega}_V)$, directly yields:

$$\langle \psi_1(\mathbf{r},\boldsymbol{\omega})\rangle_V = \frac{1}{V\,\Omega_d}\int_0^{u(\mathbf{r},\boldsymbol{\omega})} T(s)\,ds\,, \tag{IV.49}$$

$$\langle \phi_1(\mathbf{r},\boldsymbol{\omega})\rangle_V = \frac{1}{V\,\Omega_d}\int_0^{u(\mathbf{r},\boldsymbol{\omega})} U_T(s)\,ds = \frac{\lambda}{V\,\Omega_d}\int_0^{u(\mathbf{r},\boldsymbol{\omega})} H(s)\,ds\,, \tag{IV.50}$$

using $U_T(s) = \int_s^{+\infty} T(\ell)d\ell = \lambda\,H(s)$ (see Eq. (IV.42)).

Integral equations with a volume source or a surface source – Finally applying respectively the surface average and the source average to the transport equation (IV.37), we obtain local integral equations for the length and the collision density:

Integral Equations

for the Collision Density

$$\begin{cases} \langle\,\psi\,\rangle_S(\mathbf{r},\boldsymbol{\omega}) - \dfrac{1}{\lambda\alpha_d S} = \displaystyle\int_0^u \left[\langle\,\chi\,\rangle_S(\mathbf{r}-s\boldsymbol{\omega}) - \frac{1}{\lambda\alpha_d S}\right] T(s)\,ds, & \text{(IV.51)} \\[2ex] \langle\,\psi\,\rangle_V(\mathbf{r},\boldsymbol{\omega}) = \displaystyle\int_0^u \left[\langle\,\chi\,\rangle_V(\mathbf{r}-s\boldsymbol{\omega}) + \frac{1}{V\Omega_d}\right] T(s)\,ds. & \text{(IV.52)} \end{cases}$$

for the Length Density

$$\begin{cases} \langle\,\varphi\,\rangle_S(\mathbf{r},\boldsymbol{\omega}) - \dfrac{1}{\alpha_d S} = \displaystyle\int_0^u \left[\lambda\,\langle\,\chi\,\rangle_S(\mathbf{r}-s\boldsymbol{\omega}) - \frac{1}{\alpha_d S}\right] H(s)\,ds, & \text{(IV.53)} \\[2ex] \langle\,\varphi\,\rangle_V(\mathbf{r},\boldsymbol{\omega}) = \displaystyle\int_0^u \left[\langle\,\chi\,\rangle_V(\mathbf{r}-s\boldsymbol{\omega}) + \frac{1}{V\Omega_d}\right] \lambda H(s)\,ds. & \text{(IV.54)} \end{cases}$$

χ is the outgoing collision density

$$\chi(\mathbf{r}|\mathbf{r}_0,\boldsymbol{\omega}_0) = \nu\int_{\Omega_d}\frac{d\boldsymbol{\omega}'}{\Omega_d}\psi(\mathbf{r},\boldsymbol{\omega}'|\mathbf{r}_0,\boldsymbol{\omega}_0)$$

IV.3.3 A universal and local version of the Cauchy formulae

a. Results

Collision density – Let us start first with Eq. (IV.51) and rewrite it, replacing the expression of χ:

$$\lambda\alpha_d S\left\langle \psi \right\rangle_S(\mathbf{r},\boldsymbol{\omega}) - 1 = \int_0^u \left[\nu \int_{\Omega_d} \frac{d\boldsymbol{\omega}'}{\Omega_d} \lambda\alpha_d S\left\langle \psi \right\rangle_S(\mathbf{r}-s\boldsymbol{\omega}) - 1 \right] T(s)\, ds\,. \tag{IV.55}$$

From inspection, this equation can be recast as a system of two integral equations:

$$\begin{cases} F_S(\mathbf{r},\boldsymbol{\omega}) &= \displaystyle\int_0^u \Big[\nu - 1 + G_S(\mathbf{r}-s\boldsymbol{\omega})\Big]\, T(s)\, ds\,, \\ G_S(\mathbf{r},\boldsymbol{\omega}) &= \displaystyle\nu \int_{\Omega_d} \frac{d\boldsymbol{\omega}'}{\Omega_d} F_S(\mathbf{r},\boldsymbol{\omega}')\,, \end{cases} \tag{IV.56}$$

where $F_S(\mathbf{r},\boldsymbol{\omega}) = \lambda\alpha_d S\left\langle \psi \right\rangle_S(\mathbf{r},\boldsymbol{\omega}) - 1$. Similarly, we rewrite Eq. (IV.52), multiplying both side by $(\nu-1)\,V\Omega_d$,

$$(\nu-1)\,V\Omega_d\left\langle \psi \right\rangle_V(\mathbf{r},\boldsymbol{\omega}) = \int_0^u \left[\nu \int_{\Omega_d} \frac{d\boldsymbol{\omega}'}{\Omega_d} (\nu-1)\,V\Omega_d \left\langle \psi \right\rangle_V(\mathbf{r}-s\boldsymbol{\omega}) + (\nu-1)\right] T(s)\, ds, \tag{IV.57}$$

and reformulate the equation in the same system of two integral equations Eq. (IV.56), where F_S is now replaced by $F_V(\mathbf{r},\boldsymbol{\omega}) = (\nu-1)\,V\Omega_d\left\langle \psi \right\rangle_V(\mathbf{r},\boldsymbol{\omega})$. A general form for the analytical solution of this system cannot be obtained, however it can be shown that its solution is unique [Feller 2008]: $F_V(\mathbf{r},\boldsymbol{\omega}) = F_S(\mathbf{r},\boldsymbol{\omega})$ for all $(\mathbf{r},\boldsymbol{\omega})$ in the domain $\mathcal{D}$. It follows a local version of a Cauchy-like formula for the collision density:

Collision density

$$\lambda\alpha_d S\left\langle \psi \right\rangle_S(\mathbf{r},\boldsymbol{\omega}) = 1 + (\nu-1)\,V\Omega_d\left\langle \psi \right\rangle_V(\mathbf{r},\boldsymbol{\omega})\,. \tag{IV.58}$$

Finally, setting $\eta_d = \Omega_d/\alpha_d$ and integrating uniformly over the volume V and all the directions in the solid angle Ω_d, leads to the usual Cauchy-like formula for the mean number of collisions in V

Total number of collisions

$$\left\langle N \right\rangle_S = \eta_d \frac{V}{\lambda S}\Big[1 + (\nu-1)\left\langle N \right\rangle_V\Big]\,, \tag{IV.59}$$

that we have shown now as being valid for general branching Pearson random walk.

Travelled length – The integrals involving the outgoing collision densities $\langle \chi \rangle_{S/V}$ appearing on the right-hand side of Eq. (IV.53) and (IV.54) can be simplified by resorting to Eq. (IV.51) and (IV.52), respectively. Then, combining these two equations, the surface average $\langle \varphi \rangle_S$ can be directly written in terms of the volume average $\langle \varphi \rangle_V$, from which stems the identity

Length density

$$\lambda \alpha_d S \langle \varphi \rangle_S(\mathbf{r}, \boldsymbol{\omega}) = \lambda + (\nu - 1) V \Omega_d \langle \varphi \rangle_V(\mathbf{r}, \boldsymbol{\omega}) \,. \tag{IV.60}$$

Finally, an integration over the volume V and the directions given by Ω_d yields a Cauchy-like formula for the mean total length travelled in the domain V:

Total travelled length

$$\langle L \rangle_S = \eta_d \frac{V}{S} \left[1 + \frac{(\nu - 1)}{\lambda} \langle L \rangle_V \right] . \tag{IV.61}$$

Comment – The results obtained in Eq. (IV.58) and (IV.60) are local properties of branching Pearson random walks which are valid at any point $(\mathbf{r}, \boldsymbol{\omega})$ of the phase space, and thus represent stronger results than Eq. (IV.59) and (IV.61). In particular, when $\nu = 1$, the surface averages of length angular density and of the collision angular density become constant over the domain $\mathcal{D}$,

$$\langle \psi \rangle_S(\mathbf{r}, \boldsymbol{\omega}) = \frac{1}{\lambda \alpha_d S} \qquad \text{and} \qquad \langle \varphi \rangle_S(\mathbf{r}, \boldsymbol{\omega}) = \frac{1}{\alpha_d S} \,. \tag{IV.62}$$

For the average angular flux the constant is a purely geometrical quantity, independent of the specific details of the underlying random walk.

b. Comparison with numerical simulation

To illustrate the Cauchy-like formula for the mean travelled length, Eq. (IV.61), Fig. IV.11 compares several examples based on Monte Carlo simulation: the solid lines correspond to the surface average on the lhs of the formula and the dashed lines to its rhs. The simulations follow the evolution in time of the mean total length travelled in a disk of unit radius by a walker and all its descendants, evolving at constant speed $v = 1$ with jump lengths of different type:

Constant jumps $$T(\ell) = \delta(\ell - 1) \,, \tag{IV.63}$$

Exponential jumps $$T(\ell) = \exp(-\ell) \,, \tag{IV.64}$$

Power-law distributed jumps $$T(\ell) = \begin{cases} 0 & \text{for } \ell \leqslant \left(\frac{a}{\alpha}\right)^{1/\alpha} \\ \frac{a}{\ell^{\alpha+1}} & \text{else} \end{cases} \tag{IV.65}$$

where we took the *stability parameter* $\alpha = 1.1$ and the *amplitude parameter* is such that $a = \alpha^{1-\alpha}(\alpha-1)^{\alpha}\lambda^{\alpha}$. See Appendix 5 for details concerning the Monte Carlo simulations, and Appendix A.4.3 for information about the sampling of exponential and power-law distributed random variables. For long observation times, each pair of solid and dash lines converge to the same value, which is in agreement with equation (IV.61). In particular, for $\nu = 1$ this value is independent of the jump distribution and is given by $\eta_2 V/S = \pi/2$.

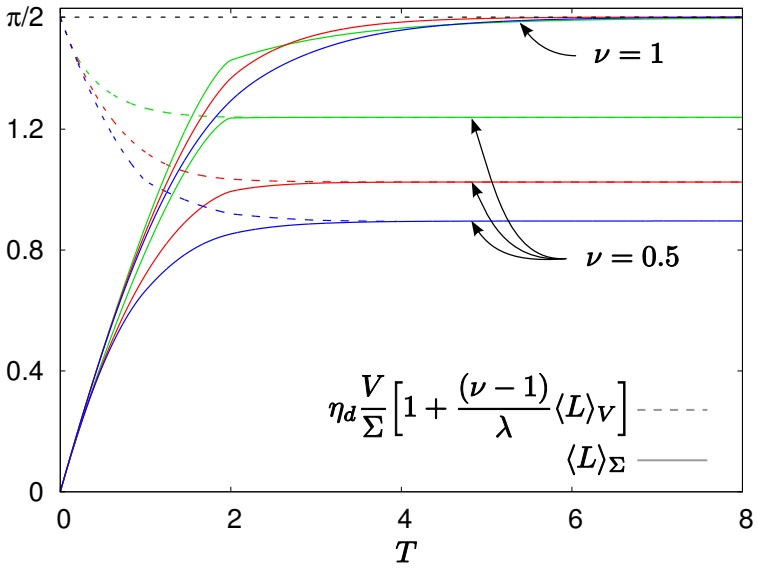

Figure IV.11: Monte Carlo simulations of the time evolution of the total length travelled in a disk of unit radius ($d = 2$ and $\eta_2 V/S = \pi/2$) by a branching Pearson random walk with constant jumps (blue), exponential jumps (red) and power-law distributed jumps (green). Averages are obtained over 10^7 realisations of the system (10^7 particles starting uniformly from the surface S, or within the volume V), so that the statistical uncertainties are of the order of 10^{-3}.

IV.3.4 Ensuing results

a. Relation between collision density and length density

Previously, we mentioned the non-generality of the relation

$$\psi(\mathbf{r},\boldsymbol{\omega}) = \varphi(\mathbf{r},\boldsymbol{\omega})/\lambda\,, \tag{IV.66}$$

valid for exponential (branching) random walks. This relation is in fact a property of Markovian transport, and is therefore commonly used in transport theory of neutrons and photons. However, modelling the transport of particles by an other type of random walk does not necessarily keep the markovianity of the process, and in the general case of non-exponential walks, the relation (IV.66) does not hold.

Volume and surface terms can be separately singled out by algebraic manipulations of Eq. (IV.53), (IV.51), (IV.54) and (IV.52). For the volume terms, we have

$$\begin{aligned}\Omega_d V\left[\,\langle\varphi\rangle_V(\mathbf{r},\boldsymbol{\omega}) - \lambda\langle\psi\,\rangle_V(\mathbf{r},\boldsymbol{\omega})\,\right] = \\ \lambda\int_0^u \left[\,\Omega_d V\,\langle\chi\rangle_V(\mathbf{r}-s\,\boldsymbol{\omega})+1\,\right]\left[H(s)-T(s)\right]ds.\end{aligned} \tag{IV.67}$$

The quantity $1+V\Omega_d\langle\chi\rangle_V$ is positive, so that $\langle\varphi\rangle_V - \lambda\langle\psi\rangle_V$ vanishes only if $H(s) = T(s)$ for any s (i.e. for exponential jumps $T(s) = \exp(-s/\lambda)/\lambda$). It thus follows that the local relation $\langle\varphi\rangle_V(\mathbf{r},\boldsymbol{\omega}) = \lambda\langle\psi\rangle_V(\mathbf{r},\boldsymbol{\omega})$, whence also $\langle L\rangle_V = \lambda\langle N\rangle_V$, demands the Markov property of exponential random walks. For the surface terms, we have

$$\begin{aligned}\alpha_d S\left[\,\langle\varphi\rangle_S(\mathbf{r},\boldsymbol{\omega}) - \lambda\langle\psi\rangle_S(\mathbf{r},\boldsymbol{\omega})\,\right] = \\ \int_0^u \left[\,\lambda\alpha_d S\,\langle\chi\rangle_S(\mathbf{r}-s\,\boldsymbol{\omega})-1\,\right]\left[H(s)-T(s)\right]ds.\end{aligned} \tag{IV.68}$$

The right hand side of this equation vanishes when $H(s) = T(s)$ for any s (i.e., for exponential random walks), or more generally for any class of branching Pearson walks when $\nu = 1$, thanks to the local Cauchy property $\langle\chi\rangle_S(\mathbf{r}) = 1/(\lambda\alpha_d S)$ (see Eq. (IV.62), and $\langle\chi\rangle_S(\mathbf{r}) = \int_{\Omega_d}\langle\psi\rangle_S(\mathbf{r},\boldsymbol{\omega})d\boldsymbol{\omega}$). In either case, we obtain the simple local relation $\langle\varphi\rangle_S(\mathbf{r},\boldsymbol{\omega}) = \lambda\langle\psi\rangle_S(\mathbf{r},\boldsymbol{\omega})$, from which stems also $\langle L\rangle_S = \lambda\langle N\rangle_S$.

b. Excursion in a sub-domain

It is interesting to consider the occupation statistics – mean travelled length or mean sojourn time – of the walk in a sub-domain V' included in V (see Fig. IV.12). In this context, several investigations have been already carried out for Brownian motion (with or without branching), Pearson random

walks or branching exponential walks in various fields [Grebenkov 2007; Agmon 2010; Berezhkovskii et al. 1998; Sawyer and Fleischman 1979; Cox and Griffeath 1985; Bénichou et al. 2005; Zoia et al. 2012a]. Let us consider a walker emitted within the domain V or entering through its surface: this walker and its descendants can enter the sub-domain V', reproduce or die inside, or escape and possibly re-enter it, and so on. The mean total length thus travelled in V' by the first particles and all its descendants, until the disappearance of all of them by absorption or escape through S, is given by:

$$L'(\mathbf{r}_0, \boldsymbol{\omega}_0) = \int_{V'} d^3\mathbf{r} \int_{\Omega_d} d^2\boldsymbol{\omega}\, \varphi(\mathbf{r}, \boldsymbol{\omega} | \mathbf{r}_0, \boldsymbol{\omega}_0) \tag{IV.69}$$

The relation between the volume and the surface average of this quantity is straightforward from the local Cauchy-like equation (IV.60). An integration over the volume V' and the directions given by Ω_d yields:

$$\langle L' \rangle_S = \eta_d \frac{V}{S} \left[\frac{V'}{V} + \frac{(\nu - 1)}{\lambda} \langle L' \rangle_V \right]. \tag{IV.70}$$

Previously established for branching exponential walks [Zoia et al. 2012a], this relation remains thus valid for any type of branching Pearson random walks with finite mean free path and constant speed. This is a consequence of the local Cauchy-like equation.

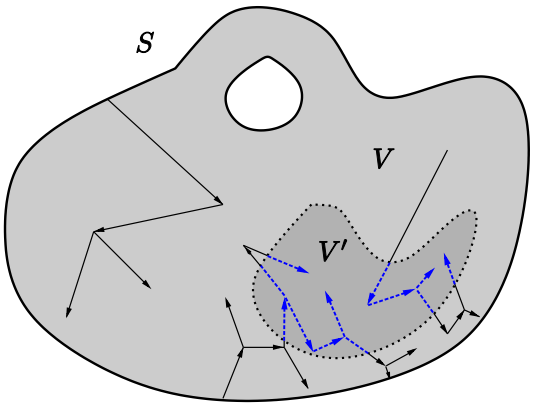

Figure IV.12: Figure adapted from [Zoia et al. 2012a]. The figure displays trajectories starting within the volume V or from its surface. In this section we are interested in the occupation statistics, i.e., in the statistics of length travelled or of the time spent by these walkers within a region V' of the domain V (portion of the paths in blue dashed lines).

In particular, for a critical system ($\nu = 1$), it follows that the ratio of the

mean length travelled in V' and the one travelled in V is simply

$$\frac{\langle L' \rangle_S}{\langle L \rangle_S} = \frac{V'}{V}, \tag{IV.71}$$

just as the ratio of the mean number of collisions in V' and the one in V, obtained from Eq. (IV.62):

$$\frac{\langle N' \rangle_S}{\langle N \rangle_S} = \frac{V'}{V}. \tag{IV.72}$$

This property has been previously shown for branching exponential walks [Zoia et al. 2012a], and can be seen as an ergodic property of the system [Bénichou et al. 2005].

c. General boundary conditions

So far, we have assumed that the surface of the body is transparent to the incoming radiation. Each re-entry from the surface (if any) is taken into account as a new trajectory, which formally corresponds to imposing absorbing boundary conditions on S. This is coherent with the definition given for chords traversing non-convex bodies [Mazzolo et al. 2003] and ensures the validity of the previous results for convex as well as non-convex domains. More generally, we might consider mixed boundary conditions, the surface S being composed of an arbitrary combination of reflecting portions S_r and absorbing portions S_a. Trajectories can enter the body (and escape) only through S_a. Collisions on S_r can be indifferently modelled by assuming that the inward direction angle equals the outward direction angle (perfect reflection), or that the surface acts an isotropic diffuser [Bénichou et al. 2005]. In either case, by following the same strategy as above, it can be shown that any of these boundary conditions can be straightforwardly taken into account in formulae (IV.4) and (IV.6) by replacing the term S by S_a [Bénichou et al. 2005],

$$\langle L \rangle_S = \eta_d \frac{V}{S_a} \left[1 + \frac{(\nu - 1)}{\lambda} \langle L \rangle_V \right]. \tag{IV.73}$$

which further extends the applicability of our results to mixed boundary conditions.

4 GEOMETRICAL PROOF FOR PEARSON RANDOM WALK

IV.4.1 Introduction

The main development proposed in this section has been published in collaboration with Alain Mazzolo and Andrea Zoia in [Mazzolo et al. 2014],

where we have restricted our attention to diffusive Pearson random walks without branching. In particular, starting from the Cauchy formula for the mean number of collisions performed by a Pearson random walk in the domain V (see the previous section):

$$\langle N \rangle_S = \frac{\eta_d V}{\lambda S}, \tag{IV.74}$$

we have proposed an original proof, based on geometrical arguments alone, of the Cauchy formula for the length travelled by a purely diffusive particle in the domain V, namely

$$\langle L \rangle_S = \frac{\eta_d V}{S}. \tag{IV.75}$$

In this section, we are interested in analysing the geometrical origin of the non trivial relation between $\langle L \rangle_S$ and $\langle N \rangle_S$:

$$\langle L \rangle_S = \lambda \langle N \rangle_S. \tag{IV.76}$$

Indeed, we have just seen (Sec. 3.a.), that this property, known for exponential walks as a consequence of their markovianity [Mazzolo 2009; Zoia et al. 2012a], can be surprisingly extended to any type of Pearson random walk, provided that they have a finite mean free path λ. For non-exponential walks the geometrical origin of this relation is not trivial due to the fact that the first and last jumps in the domain are not following the same law than the others. In fact, from a purely geometrical point of view, even for exponential jumps relation (IV.76) is not obvious at all, as naively counting the number of collisions would lead to a relation of the form $\langle L \rangle_S = \lambda (\langle N \rangle_S + 1)$.

In the previous section, results Eq. (IV.74) and (IV.75) were demonstrated separately. Here, assuming that the Cauchy formula Eq. (IV.75) holds true for any type of Pearson random walk (which was shown in the last section), we would like to show how the identity Eq. (IV.76) then arises from purely geometrical considerations.

IV.4.2 Geometrical proof

Consider a purely diffusive Pearson random walker, whose jump lengths are distributed according to an arbitrary pdf $t(s)$, provided that it admits a finite mean λ. We assume that the hypotheses stated in section IV.3.1, concerning the equilibrium state, the constant speed and the finite mean free path λ, still hold here, such that the pdf

$$h(r) = \frac{1}{\lambda} \int_r^{+\infty} t(s)\, ds. \tag{IV.77}$$

yields the first jump length r performed inside V by a walker entering the domain through its surface (see Fig. IV.10).

To go further, we have to introduce new notations. Let P_n be the probability that a trajectory entering the domain V performs exactly n collisions inside it. Then, by definition,

$$\langle N \rangle_S = \sum_{n=1}^{\infty} n P_n . \tag{IV.78}$$

In particular P_0 is the probability that the trajectory through the domain V is a straight line, i.e. a *chord*: the stochastic path undergoes zero collisions in V as illustrated in Fig. IV.13. Since trajectories performing exactly n collisions within the domain form a complete set of disjoint events, their mean length $\langle L \rangle_S$ can be decomposed in the following sum

$$\langle L \rangle_S = \sum_{n=0}^{\infty} P_n \langle L_n \rangle_S, \tag{IV.79}$$

where $\langle L_n \rangle_S$ is the mean length travelled by the paths constrained to have performed exactly n collisions inside V. As shown in Fig. IV.13, each stochastic trajectory consists of a series of segments that can be of three different types:

- the ones that are crossing the domain from one point of the surface to the other (random chords, in blue), whose length $\tilde{c}$ is a random variable associated with the pdf $\tilde{F}(\tilde{c})$;
- the ones (in green) that are entering or leaving the domain from its surface, whose lengths $\tilde{r}$ are random, following the pdf $\tilde{H}(\tilde{r})$;
- the ones (in orange) that are entirely contained within the volume V, whose random lengths $\tilde{s}$ are distributed according to $\tilde{T}(\tilde{s})$.

At a first sight, the pdf $\tilde{T}$, $\tilde{H}$ and $\tilde{F}$ may look very similar to the pdf t, h and f. However, the subtle difference between these quantities is one of the key aspects of the problem. As defined above, the length of a jump starting from the inside of the domain is given by $t(s)$, independently on whether the jump stays inside or gets outside of the domain. On the other hand, the pdf $\tilde{T}$ gives the length of a jump starting within the domain and actually staying inside it until it finishes (see Fig. IV.14). In other words $\tilde{T}$ defines the length of jumps constrained to stay inside the domain. In the same way, $h(r)$ gives the length of jumps starting from the surface (coming from outside) without considering whether or not they finish within the domain, whereas $\tilde{H}(r)$ gives the length of jumps starting from the surface

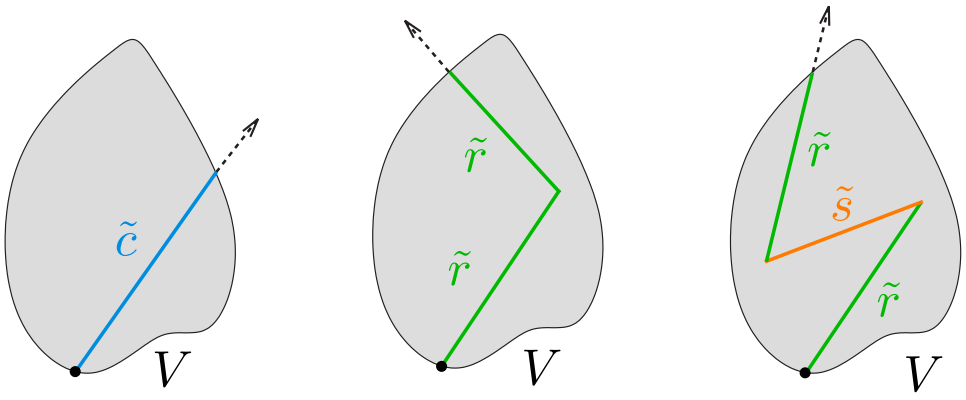

Figure IV.13: A schematic representation of trajectories having $0, 1, 2$ collisions inside V and their associated lengths. Each of these trajectories happens respectively with probability P_0, P_1 and P_2.

and constrained to finish inside the domain. Thus the new pdfs (with the tilde sign) take additionally into account the finite size of the domain, i.e. the presence of boundaries.

Using the notations introduced above, we can develop the mean length $\langle L_n \rangle_S$ of a path within the domain V,

– knowing that it has undergone 0 collision:

$$\langle L_0 \rangle_S = \langle \tilde{c} \rangle ; \tag{IV.80}$$

– knowing that it has undergone exactly $n \geqslant 1$ collisions:

$$\langle L_n \rangle_S = 2 \langle \tilde{r} \rangle + (n-1) \langle \tilde{s} \rangle . \tag{IV.81}$$

Replacing these expressions in Eq. (IV.79) then leads to

$$\langle L \rangle_S = \langle \tilde{c} \rangle P_0 + 2 \langle \tilde{r} \rangle \sum_{n=1}^{\infty} P_n + \langle \tilde{s} \rangle \sum_{n=1}^{\infty} (n-1) P_n , \tag{IV.82}$$

and, using the normalisation $\sum_{n=0}^{\infty} P_n = 1$ and the definition Eq. (IV.78), it follows

$$\langle L \rangle_S = \langle \tilde{c} \rangle P_0 + 2 \langle \tilde{r} \rangle (1 - P_0) + \langle \tilde{s} \rangle \big[\langle N \rangle_S - (1 - P_0) \big] . \tag{IV.83}$$

We now have to explicitly compute each term appearing in this equation, namely, P_0, $\langle \tilde{c} \rangle$, $\langle \tilde{r} \rangle$ and $\langle \tilde{s} \rangle$.

The probability P_0 is the probability that a path does not undergo any collision while going through the domain V. In other words, it is the probability that the length r of the first jump inside V is actually larger than the length c of the supported chord (see Fig. IV.15):

$$P_0 = \text{Prob}[r \geqslant c] \tag{IV.84}$$

$$P_0 = \int_0^\infty \mathrm{d}c\, f(c) \int_c^\infty \mathrm{d}r\, h(r) = \int_0^\infty \mathrm{d}r\, h(r) \int_0^r \mathrm{d}c\, f(c)\,. \tag{IV.85}$$

Mean length of the constrained chord $\langle\, \tilde{c}\,\rangle$ Shown in Fig. IV.15, the conditional pdf $\tilde{F}(\tilde{c})$ of sampling directly a chord at the first jump from the surface is proportional to the probability density of chords $f(c)$ (unconstrained chords of length c), multiplied by the probability that this first jump is longer than the chord, i.e.

$$\tilde{F}(\tilde{c}) \propto \underbrace{f(\tilde{c})}_{\text{chord length pdf}} \underbrace{\int_{\tilde{c}}^{+\infty} \mathrm{d}r\, h(r)}_{\text{prob. first jump longer than } \tilde{c}}\,. \tag{IV.86}$$

from which follows the mean length of a constrained chord

$$\langle\, \tilde{c}\,\rangle = \frac{1}{P_0} \int_0^\infty \mathrm{d}c\, c\, f(c) \int_c^\infty \mathrm{d}r\, h(r) = \frac{1}{P_0} \int_0^\infty \mathrm{d}r\, h(r) \int_0^r \mathrm{d}c\, c\, f(c)\,, \tag{IV.87}$$

observing that the normalisation factor of $\tilde{F}$ in Eq. (IV.86) is actually $1/P_0$ (which can be expected from the definition of P_0).

Mean length of the first/last constrained jump $\langle\, \tilde{r}\,\rangle$ As illustrated in Fig. IV.16a, the pdf of the first jump starting from the surface and arriving inside V corresponds to the first jump probability density $h(r)$, conditioned to jumps of length $\tilde{r}$ shorter than the supporting chord, $\tilde{r} \leqslant c$:

$$\tilde{H}(\tilde{r}) = \frac{h(\tilde{r}) \displaystyle\int_{\tilde{r}}^{+\infty} \mathrm{d}c\, f(c)}{\displaystyle\int_0^\infty \mathrm{d}\tilde{r}\, h(\tilde{r}) \int_{\tilde{r}}^\infty \mathrm{d}c\, f(c)}\,. \tag{IV.88}$$

Using Eq. (IV.85), the denominator of $\tilde{H}$ can be written in term of P_0:

$$\begin{aligned} \int_0^\infty \mathrm{d}\tilde{r}\, h(\tilde{r}) \int_{\tilde{r}}^\infty \mathrm{d}c\, f(c) &= \int_0^\infty \mathrm{d}\tilde{r}\, h(\tilde{r}) \left[1 - \int_0^{\tilde{r}} \mathrm{d}c\, f(c)\right] \\ &= 1 - P_0\,. \end{aligned} \tag{IV.89}$$

Moreover, to simplify the notations, we introduce the ray[15] pdf, related to the chord length pdf by [Dixmier 1978]

$$w(r) = \frac{1}{\langle c \rangle} \int_r^\infty dc\, f(c)\,. \tag{IV.90}$$

where $\langle c \rangle = \int_r^\infty c\, f(c)\, dc$ is the mean chord length: $\langle c \rangle = \eta_d\, V/S$. The pdf of the first/last jump then takes the compact form

$$\tilde{H}(\tilde{r}) = \frac{\langle c \rangle\, h(\tilde{r})\, w(\tilde{r})}{1 - P_0}\,, \tag{IV.91}$$

and the mean length of the first or the last constrained jump is finally:

$$\langle \tilde{r} \rangle = \frac{\langle c \rangle}{1 - P_0} \int_0^\infty dr\, r\, h(r)\, w(r)\,. \tag{IV.92}$$

Remark

In principle, we should distinguish the segments entering the domain (first jump inside V), from those leaving the domain (last jump), with distinct random length $\tilde{r}_{in}$ and $\tilde{r}_{out}$, associated to the respective pdf $\tilde{H}_{in}$ and $\tilde{H}_{out}$. However it is possible to show that these pdf are in fact identical [Mazzolo 2004; Mazzolo et al. 2014].

Mean length of a jump constrained within the domain $\langle \tilde{s} \rangle$ Illustrated in Fig. IV.16b, the conditional probability density of performing a jump of length s entirely included within the domain V is proportional to the density $t(s)$ (of performing a jump of length s starting inside V), times the probability that the length of this jump is smaller than the supported ray. The latter probability being equal to $\int_s^\infty dr\, w(r)$, we obtain, after normalisation:

$$\tilde{T}(s) = \frac{t(s) \displaystyle\int_x^\infty dr\, w(r)}{\displaystyle\int_0^\infty ds\, t(s) \int_s^\infty dr\, w(r)}\,. \tag{IV.93}$$

The denominator can be expended using successively the definition of the pdf $h(r)$ in Eq. (IV.77) and the definition of the pdf $w(r)$ in Eq. (IV.90):

$$\begin{aligned}\int_0^\infty ds\, t(s) \int_s^\infty dr\, w(r) = \int_0^\infty dr\, w(r) \int_0^r ds\, t(s) &= 1 - \lambda \int_0^\infty dr\, w(r)\, h(r)\,,\\ &= 1 - \frac{\lambda}{\langle c \rangle} \int_0^\infty dr\, h(r) \int_r^\infty dc\, f(c)\,,\\ &= 1 - \frac{\lambda}{\langle c \rangle}(1 - P_0)\,,\end{aligned} \tag{IV.94}$$

[15] A ray of length r is defined by the distance of a point inside V to the frontier ∂V of V (see Fig. IV.16b).

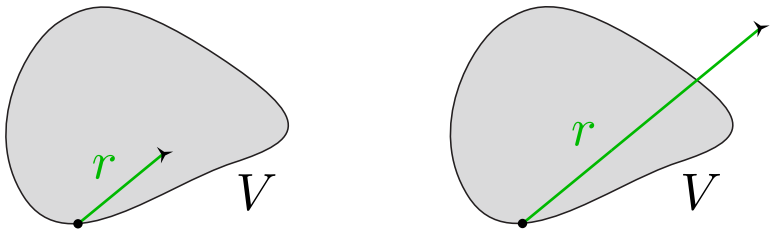

Figure IV.14: $\tilde{\mathrm{H}}$ samples jumps inside V starting from the surface and arriving within V, as the one illustrated on the left panel, whereas $\mathrm{h}(\mathrm{r})$ samples jumps entering the domain from the surface no matter where the jump while end up (jumps on the left and on the right panel).

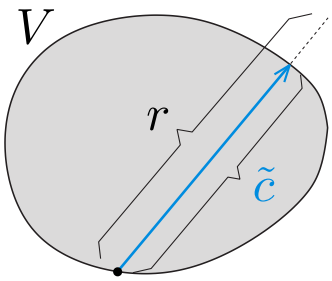

Figure IV.15: A path from the surface performs a chord of V, under the condition that its first jump since the surface (sampled with $\mathrm{h}(\mathrm{r})$) is longer than the chord itself.

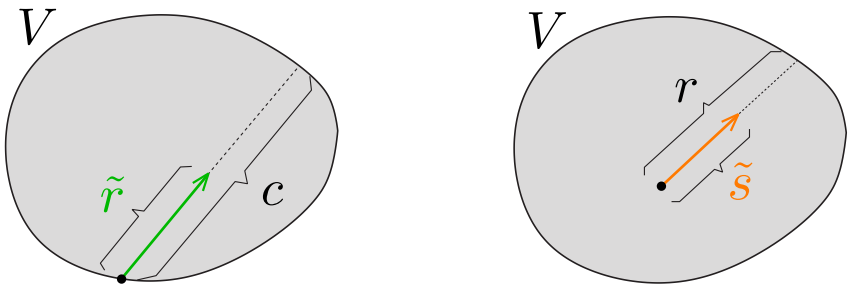

(a) **(b)**

Figure IV.16: **(a)** First jumps inside V (green) are smaller than the supported chords.
(b) Jumps entirely contained in V (orange) must be shorter than the supported ray, whose length is given by $w(\mathrm{r})$.

recalling Eq. (IV.89), which makes use of the definition of P_0. Therefore, the mean length of a jump constrained to stay within the domain V is

$$\langle \tilde{s} \rangle = \frac{\langle c \rangle \int_0^\infty ds\ s\, t(s) \int_s^\infty dr\, w(r)}{\langle c \rangle - \lambda (1 - P_0)} . \tag{IV.95}$$

The numerator on the right hand side (rhs) of this equation can be rearranged as:

$$\int_0^\infty ds\, t(s)\, s \int_s^\infty dr\, w(r) = \lambda - A , \tag{IV.96}$$

$$\text{where} \qquad A = \int_0^\infty ds\, t(s)\, s \int_0^s dr\, w(r) . \tag{IV.97}$$

In Appendix 3, we show that

$$A = \lambda \left[\frac{1}{\langle c \rangle} \int_0^\infty dr\, h(r) \int_0^r dc\ c\, f(c) + 2 \int_0^\infty dr\, r\, h(r)\, w(r) \right] . \tag{IV.98}$$

where it is possible to recognise $\langle \tilde{r} \rangle$ and $\langle \tilde{c} \rangle$ from Eq. (IV.92) and Eq. (IV.87), which consequently yields

$$\langle \tilde{s} \rangle = \frac{\lambda}{\langle c \rangle - \lambda (1 - P_0)} \left[\langle c \rangle - P_0 \langle \tilde{c} \rangle - 2 (1 - P_0) \langle \tilde{r} \rangle \right] . \tag{IV.99}$$

Final result Finally, replacing this last expression of $\langle \tilde{s} \rangle$ in Eq. (IV.83) and using the Cauchy formula $\langle L \rangle_S = \langle c \rangle$, it follows:

$$\langle \tilde{s} \rangle \left[\langle N \rangle_S - (1 - P_0) \right] = \langle L \rangle_S - P_0 \langle \tilde{c} \rangle - 2 (1 - P_0) \langle \tilde{r} \rangle , \tag{IV.100}$$

$$\lambda \left[\langle N \rangle_S - (1 - P_0) \right] = \langle L \rangle_S - \lambda (1 - P_0) , \tag{IV.101}$$

which yields the final result

$$\langle N \rangle_S = \frac{\langle L \rangle_S}{\lambda} = \frac{\langle c \rangle}{\lambda} . \tag{IV.102}$$

5 General Conclusion and Perspectives

Universal property In this chapter, we have shown that the Cauchy property IV.2

$$\langle L \rangle_S = \eta_d \frac{V}{S} , \tag{IV.103}$$

surprisingly generalises to a very broad class of stochastic processes, and thus exhibits a universal character. The property holds for any type of Pearson random walk, or branching Pearson random walk at criticality (provided that walkers have a finite mean free path). We have also seen that

the property is still valid for an inhomogeneous medium (provided that the heterogeneities are not strong) with anisotropic scattering. For each of these cases, the mean total length $\langle L \rangle_S$ travelled by a walk within a finite domain, if entering through its surface S, thus depends only on the geometrical properties of the traversed domain, and not on the specific details of the walk.

Local Formulae More generally, we have shown that Cauchy-like formula Eq. (IV.4) and (IV.6) carry over to any type of branching Pearson random walk with a finite mean free path and a constant speed. These formulae result in fact from a stronger property, valid at any point $(\mathbf{r}, \boldsymbol{\omega})$ within the domain $\mathcal{D}$:

Results

For the collision density $\psi(\mathbf{r}, \boldsymbol{\omega})$

$$\lambda \alpha_d S \langle \psi \rangle_S (\mathbf{r}, \boldsymbol{\omega}) = 1 + (\nu - 1) V \Omega_d \langle \psi \rangle_V (\mathbf{r}, \boldsymbol{\omega}) . \tag{IV.104}$$

For the length density $\varphi(\mathbf{r}, \boldsymbol{\omega})$

$$\lambda \alpha_d S \langle \varphi \rangle_S (\mathbf{r}, \boldsymbol{\omega}) = \lambda + (\nu - 1) V \Omega_d \langle \varphi \rangle_V (\mathbf{r}, \boldsymbol{\omega}) . \tag{IV.105}$$

Another direct consequence of these equations is the ergodic-type property

$$\frac{\langle L' \rangle_S}{\langle L \rangle_S} = \frac{\langle N' \rangle_S}{\langle N \rangle_S} = \frac{V'}{V} . \tag{IV.106}$$

valid for any sub-domain $V' \in V$.

Steady State Furthermore, we have shown that the Cauchy-like formulae in fact hold for systems immersed in a radiation flow at stationary state (and not for systems where all particles start from the surface of the domain).

To conclude, formulae (IV.104) and (IV.105) are valid for non-exponential branching random walks, and may thus contribute to the investigation of non-exponential radiation transport and, in particular, to transport in strongly heterogeneous and disordered media [Pierrat et al. 2014]. Moreover, the proposed formalism may also apply to animal search strategies [Blanco and Fournier 2003; Bénichou et al. 2005] in the presence of non-exponential displacements [Bénichou et al. 2011; Zaburdaev et al. 2015; Viswanathan et al. 1996].

CHAPTER V

ASYMMETRIC LÉVY FLIGHTS IN THE PRESENCE OF ABSORBING BOUNDARIES

In this chapter we are interested in semi-confined asymmetric Lévy flights in the presence of absorbing boundaries. We will study the exponent θ of the survival probability of these flights in presence of boundaries. We will also discuss the asymptotic behaviour of the flight propagator (pdf of the walker positions) after a long time, i.e. the probability density to find a walker far from the boundaries after a large number of steps.

Contents

CONSIDER a one-dimensional asymmetric random walk whose jumps are identical, independent and drawn from a distribution displaying asymmetric power-law tails. In the absence of boundaries and after a large number of steps, the probability density function of the walker positions converges to an asymmetric Lévy stable law whose full characterisation is known from the generalised central limit theorem. Much less is known when the walker is confined, or partially confined, in a region of the space. In this chapter we will be interested to semi-confined walkers in the presence of absorbing boundaries. We will first focus on their survival probability (Sec. V.2.1) and then attempt to characterise the probability density function of the walker positions (Sec. V.2.2). Finally, we will try to generalise our results for the pdf of the walker positions in higher dimension (Sec. 3).

At the beginning of the anomalous transport part, we have argued that anomalous diffusion is not easy to study, especially in confined geometry, and in general in the presence of any boundary, where very few results are already known. To illustrate this point, in this chapter we will focus on semi-confined asymmetric Lévy flights (the domain where the flight evolves is still open) in presence of absorbing boundaries. The work discussed here was done in collaboration with Grégory Schehr and Alberto Rosso, and has been published in [De Mulatier et al. 2013].

1 FREE WALKER

Let us consider a one-dimensional random walker, in discrete time, moving on a continuous line. Its position x_n after n steps evolves, for $n \geqslant 1$ according to

$$x_n = x_{n-1} + \eta_n \,, \tag{V.1}$$

starting from $x_0 = 0$. The random jumps variables η_i are independent and identically distributed (i.i.d.) according to a probability density function (pdf) $\xi(\eta)$ displaying power law tails, asymmetric for $\gamma \neq 1$:

$$\xi(\eta) \sim \begin{cases} \dfrac{c}{\eta^{1+\alpha}} \,, \ \eta \to +\infty \,, \\ \dfrac{c/\gamma}{|\eta|^{1+\alpha}} \,, \ \eta \to -\infty \,, \end{cases} \tag{V.2}$$

where c is a positive amplitude parameter and α is a positive number in the interval $(0, 2)$ (see also Appendix A.4.3). In this case, the random walk exhibits a super-diffusive behaviour. Furthermore it is *Markovian* between each step, and in the large n limit the process converge to the so-called

Lévy flight. The pdf of the walker position x_n then exhibits a strong universal behaviour, depending on very few characteristics of the initial jump distribution $\xi(\eta)$:

- its *location* μ (corresponding to the mean $\mu = \langle\eta\rangle$ if $1 < \alpha < 2$);
- and the characteristics of its tail: the index α, the constant c and the parameter γ.

Remark Note that for $\alpha \geqslant 2$, we know from the central limit theorem that only the bulk of the jump distribution $\xi(\eta)$ matters through its mean $\mu = \langle\eta\rangle$ and its variance $\sigma^2 = \langle\eta^2\rangle - \langle\eta\rangle^2$. However, for $1 < \alpha < 2$, the variance is not defined and the pdf depends on μ, but also on the tails of the jump distribution. For $0 < \alpha < 1$, the mean is not defined, however we can still define μ as the location of the distribution, and the previous statements remain valid.
One striking feature of Lévy flights (and of process governed by Power-law distribution in general) is that their statistical behaviour is dominated by few rare very large events (jumps), whose occurrence is thus governed by the tail of the distribution.

Power-law distributions and Lévy flights

Power-law distributions, satisfying Eq. (V.2), were initially studied in the early 1960s in economics [Pareto 1964] and financial theory [Mandelbrot 1963]. Later, these processes became very common in physics [Shlesinger et al. 1995], where they have found many applications, encompassing random matrices [Biroli et al. 2007; Majumdar et al. 2013], disordered systems [Bouchaud and Georges 1990], photons in hot atomic vapors [Mercadier et al. 2009], gene regulation [Lomholt et al. 2005] and many others. Often the applications of Lévy flights are restricted to the symmetric case when $\gamma = 1$. However, recently the asymmetric Lévy flights have found applications in search problems [Koren et al. 2007a] and finance [Podobnik et al. 2011]. Diffusion in asymmetric disordered potential was recently considered in connection with the ratchet effect [Gradenigo et al. 2010].

To study the large n behaviour it is useful to write the walker position after n steps in the scaling form [Feller 1968; Hughes 1996; Metzler and Klafter 2000]:

$$x_n = \mu n + y\, n^{1/\alpha} . \tag{V.3}$$

Then when $n \to \infty$, the fluctuations of the variable y are described by a pdf which is independent of n and of the details of $\xi(\eta)$, except for the index α, the constant c and the parameter γ, as mentioned above. More precisely, in

absence of any boundary and for a large number of steps, the Generalised Central Limit Theorem (GTCL) ensures that the pdf of y converges to the skewed *α-stable distribution*, $R(y)$, which is defined through its characteristic function [Samoradnitsky and Taqqu 1994; Weron 1996]:

characteristic function
$$\psi(t) = \int_{-\infty}^{+\infty} dy\, R(y) e^{iyt} \tag{V.4}$$

$$\psi(t) = \begin{cases} \exp\left[-|at|^{\alpha}\left(1 - i\,\beta\,\mathrm{sgn}(t)\tan(\pi\alpha/2)\right)\right] & \text{if } \alpha \neq 1\,, \\ \exp\left[-|at|\left(1 + \dfrac{2i}{\pi}\,\beta\,\mathrm{sgn}(t)\ln|t|\right)\right] & \text{if } \alpha = 1\,. \end{cases} \tag{V.5}$$

The parameter $\alpha \in (0,2)$ is called the *stability index*, $\beta \in [-1,+1]$ is the *skewness parameter* describing the asymmetry of $R(y)$ (i.e. the property that $\gamma \neq 1$), $a > 0$ is the *d*escribing the width of the distribution, and $\mathrm{sgn}(t)$ denotes the sign of t.

Examples

Three particular cases can be expressed in terms of elementary functions, as can be seen by inspection of the characteristic function: the Gaussian distribution for $\alpha = 2$ (fast-decaying distribution), the Cauchy distribution for $\alpha = 1$ and $\beta = 0$ (fat-tailed but still symmetric distribution), and the Lévy distribution for $\alpha = 1/2$ and $\beta = 1$ (fat-tailed and totally asymmetric distribution) (see Appendix A.4.3 for their analytical expressions). Figure V.1 shows the three distributions (left panel) and a comparison of their tails in log-log scale (right panel).

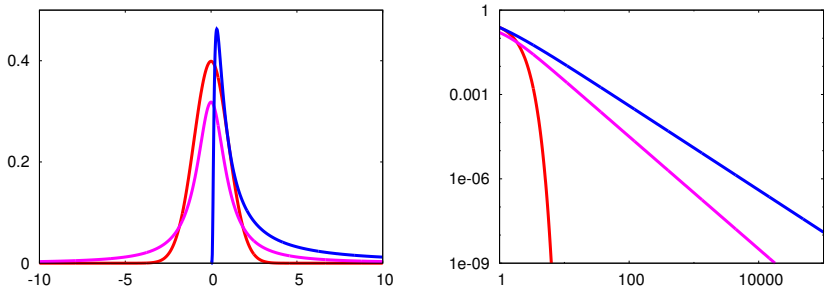

Figure V.1: Gaussian distribution (red), Cauchy distribution (pink) and Lévy distribution (blue).

For general values of α and β, the Fourier transform of Eq. (V.5) is no easy to compute and $R(y)$ can not be expressed in terms of elementary functions. However, the asymptotic exact expansion of $R(y)$, valid for any value of

$\alpha < 2$, is known [Hughes 1996]:

$$R(y) \underset{|y|\to\infty}{\sim} \frac{1}{\pi|y|}\sum_{k=1}^{\infty}\frac{a^{\alpha k}\,(1+\beta\,\mathrm{sgn}(y))^k \sin\left(\frac{\alpha k\pi}{2}\right)\Gamma(\alpha k+1)\,(-1)^{k+1}}{k!\,|y|^{\alpha k}}\,, \tag{V.6}$$

which gives in the first order

$$R(y) \underset{|y|\infty}{\sim} \frac{a^{\alpha}\sin\left(\frac{\alpha\pi}{2}\right)\Gamma(\alpha+1)\;(1+\beta\,\mathrm{sgn}(y))}{\pi|y|^{\alpha+1}}\,. \tag{V.7}$$

We observe that $R(y)$ inherits the power law tails $\propto |y|^{-\alpha-1}$ of the jump distribution $\xi(\eta)$ define in Eq. (V.2). Furthermore, as a consequence of the GTCL, the amplitude of the right and the left tails of $R(y)$ are both equal to the corresponding amplitudes of $\xi(\eta)$, namely c and c/γ [Hughes 1996]. Thus,

$$R(y) \underset{|y|\infty}{\sim} \xi(y)\,; \quad R(y) \sim \begin{cases} \dfrac{c}{y^{1+\alpha}}\,, & y \to +\infty\,, \\ \dfrac{c/\gamma}{|y|^{1+\alpha}}\,, & y \to -\infty\,. \end{cases} \tag{V.8}$$

and the parameters c and γ can be related to a and β via

$$c = \frac{a^{\alpha}\,\sin\left(\frac{\alpha\pi}{2}\right)\Gamma(\alpha+1)}{\pi}\,(1+\beta) \qquad \text{and} \qquad \gamma = \frac{1+\beta}{1-\beta}\,. \tag{V.9}$$

An illustration of this property of the tails is shown on Fig. V.2, using data from numerical simulations. Much less is known in the presence of boundaries, which is the focus of the present chapter, first for a one dimension random walker, then for a walker in higher dimensionality. As a process for which $\mu \neq 0$ can be reformulated as a "standard" process ($\mu = 0$) by a translation of the x-coordinate (see Eq. (V.3)), we will directly focus on the latter case, for which the rescaled variable describing the walker position after a large number of steps n, Eq. (V.3), becomes:

$$y = \frac{x_n}{n^{1/\alpha}}\,. \tag{V.10}$$

Propagator of a free Lévy particle – Consider a particle starting at $x(0) = 0$ and performing a free Lévy flight up to n steps. Using the previous rescaling, we can rewrite the *propagator* $P(x,n)$ of this walker, i.e. the probability density to find the particle in x after n steps [1]:

$$P(x,n) = \frac{1}{n^{1/\alpha}} R\left(y = \frac{x}{n^{1/\alpha}}\right)\,. \tag{V.11}$$

[1] $P(x,n)dx = R(y)dy$ in the large n regime.

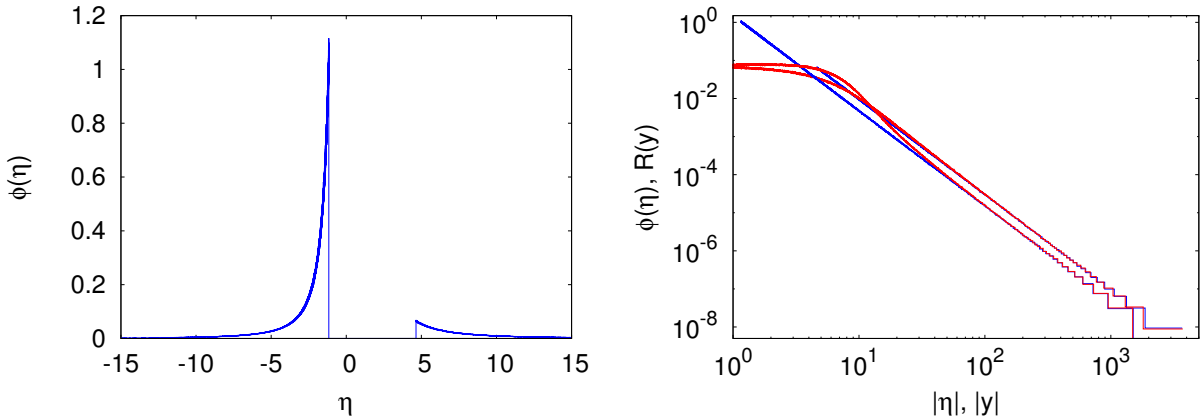

Figure V.2: Histograms are computed from numerical simulations, using a sample of 10^8 walkers. Sec. V.2.3 and Appendix A.4.3 give more details about the simulations. **Left**: The jump pdf chosen for the simulation: an asymmetric Pareto distribution for which $\alpha = 3/2$, $\gamma = 2$ and $c = 3$. **Right**: We simulate Lévy flights, using the jump distribution shown in the left panel. This figure compares the respective left and right tails in log-scale of the original jump distribution (blue) and the resulting pdf $R(y)$ for the Lévy flight (red) after $n = 1000$ steps. The tails of the jump distribution coincides with the tails of $R(y)$, so that the two pdf exhibit exactly the same asymptotic behaviour.

2 ONE DIMENSIONAL LÉVY FLIGHT WITH AN ABSORBING BOUNDARY AT THE ORIGIN

We consider the same walker, starting from $x_0 = 0$ and moving as defined in Eq. (V.1), adding now an absorbing wall on the negative half-line: if at a certain time n the walker position becomes negative ($x_n < 0$) the walker is absorbed and its walk finishes, as illustrated on Fig. (V.3).

An important property characterising this type of random walk is the *survival probability* of the walker, also named *persistence* [Majumdar 1999; Bray et al. 2013], defined as the probability that the walker, starting from $x_0 = 0$, is still "alive" after n steps (see also Sec. II.3.3.b):

$$q(n) = \text{Prob.}[\, x_n \geqslant 0, \cdots, x_1 \geqslant 0 \,|\, x_0 = 0 \,] \,. \tag{V.12}$$

Necessarily, for all $n > 0$, $q(n) < 1$ must be smaller than 1. Furthermore, it is known that if the domain where the walker evolved is closed (which is not the case here), $q(n)$ decreases exponentially, whereas if the domain is

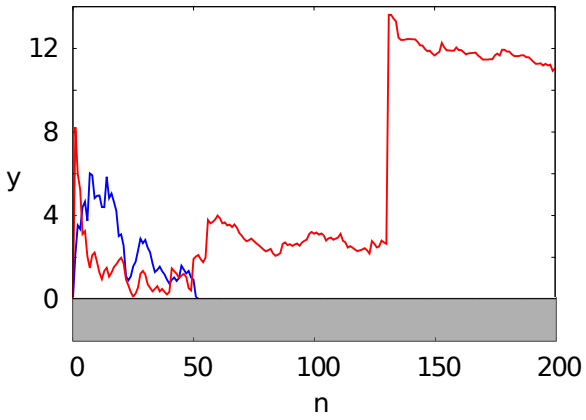

Figure V.3: Numerical simulation with $\alpha = 3/2$ and $\gamma = 1$: evolution in time n (number of steps) of the rescaled position y of two one-dimensional Lévy walkers in the presence of an absorbing boundary on the negative half-line (grey area). The blue walker has been absorbed, whereas the red one is still alive after $n = 200$ steps.

open (like here), $q(n)$ decays algebraically:

$$q(n) \underset{n\to\infty}{\propto} n^{-\theta}. \tag{V.13}$$

The *persistence exponent* θ appearing here is expected to depend explicitly on α and β: $\theta(\alpha, \beta)$. However deriving the analytical expression of θ is not simple, even in the symmetric case ($\beta = 0$), in particular because the method of image fails for Lévy flights, due to the presence of non-local jumps [Chechkin et al. 2003]. The first subsection of this part concerns the exact computation of this exponent, using a generalised version of the Sparre Andersen theorem [Andersen 1954].

Next we focus on the pdf of the rescaled variable y, defined in Eq. (V.10), in the case where the walker is confined on the semi-axis $[0, +\infty)$ (Fig. V.3), namely $R_+(y)$. Just like $R(y)$, far from the boundary $R_+(y)$ displays the same algebraic decay as the original jump distribution $\xi(\eta)$ (i.e. $\propto y^{-1-\alpha}$) [Zumofen and Klafter 1995], but with a different amplitude c_+ instead of c. In section V.2.2, we compute the exact value of the amplitude c_+ and show that it is related to the corresponding persistence exponent θ defined in Eq. (V.13):

$$R_+(y) \underset{+\infty}{\sim} \frac{c_+}{y^{1+\alpha}}, \qquad \text{where } c_+ = \frac{c}{1-\theta}. \tag{V.14}$$

V.2.1 Survival Probability and Persistence Exponent

Given the asymmetry of the jump distribution, it is in fact interesting to introduce two distinct survival probabilities $q_+(n)$ and $q_-(n)$ defined as

$$q_+(n) = q(n) = \text{Prob.}[x_n \geqslant 0, \cdots, x_1 \geqslant 0 \,|\, x_0 = 0]\,, \tag{V.15}$$

$$q_-(n) = \text{Prob.}[x_n \leqslant 0, \cdots, x_1 \leqslant 0 \,|\, x_0 = 0]\,. \tag{V.16}$$

Of course if the jump distribution is symmetric, $\xi(\eta) = \xi(-\eta)$ and then $q_+(n) = q_-(n)$. However, these two persistences must be distinct in the more general case of an asymmetric distribution. For large n, $q_+(n)$ and $q_-(n)$ decay algebraically with two distinct persistence exponents $\theta_+ \neq \theta_-$,

Asymptotic behaviour of the survival probabilities

$$q_+(n) \underset{n\to\infty}{\propto} n^{-\theta_+} \qquad \text{and} \qquad q_-(n) \underset{n\to\infty}{\propto} n^{-\theta_-}\,, \tag{V.17}$$

where the exponents $\theta\pm$ are expected to depend explicitly on α and β, $\theta_\pm \equiv \theta_\pm(\alpha,\beta)$. The exponents θ_+ and θ_- for the asymmetric case have been already study in the physics literature in [Koren et al. 2007a,b; Dybiec et al. 2007]. In particular, their expressions were obtained in [Baldassarri et al. 1999] in the different context of generalised persistence for spin models. In this section we give the details of a derivation specific to random walks on a half-line.

The survival probabilities $q_+(n)$ and $q_-(n)$ can be computed using the (generalised) Sparre-Andersen theorem [Andersen 1954] which yields explicit expressions for their generating functions, $\tilde{q}_\pm(s) = \sum_{n=0}^{\infty} q_\pm(n)\, s^n$:

$$\tilde{q}_+(s) = \exp\left[\sum_{n=1}^{\infty} \frac{p_n^+}{n}\, s^n\right], \qquad \text{where } p_n^+ = \text{Prob.}\,[x_n \geqslant 0]\,, \tag{V.18}$$

$$\tilde{q}_-(s) = \exp\left[\sum_{n=1}^{\infty} \frac{p_n^-}{n}\, s^n\right], \qquad \text{where } p_n^- = \text{Prob.}\,[x_n \leqslant 0]\,.$$

In particular, in the symmetric case ($\beta = 0$), $p_n^+ = p_n^- = 1/2$ and, using $\sum_{n\geqslant 1} s^n/n = -\ln(1-s)$ yields

$$\tilde{q}_+(s) = \tilde{q}_-(s) = \frac{1}{\sqrt{1-s}}\,. \tag{V.19}$$

$$\text{Hence} \qquad q_+(n) = q_-(n) = \binom{2n}{n}\frac{1}{2^{2n}} \underset{n\to\infty}{\sim} \frac{1}{\sqrt{\pi n}}\,, \tag{V.20}$$

such that, in the symmetric case, $\theta_\pm = 1/2$, independently of the jump distribution. In the asymmetric case, $\beta \neq 0$, the situation is slightly more

complicated and we focus now on $q_+(n)$. Its large n behaviour can be obtained by analysing the behaviour of its generating function when $s \to 1$. In the right hand side of Eq. (V.18), the series in the argument of the exponential is dominated, when $s \to 1$, by the large n terms. In this regime, the scaling form in Eq. (V.10) is valid, and the probability p_n^+ to find the particle on the positive half-line after a large number of steps converges to

$$p_n^+ = \int_0^\infty P(x,n)dx \underset{n\infty}{\longrightarrow} \int_0^\infty R(y)dy\,, \tag{V.21}$$

which implies that

$$\sum_{n=1}^{\infty} \frac{p_n^+}{n} s^n \underset{s\to 1}{\sim} -\rho \ln(1-s)\,, \quad \text{where we set } \rho = \int_0^\infty R(y)dy\,. \tag{V.22}$$

Therefore, from the Sparre Andersen theorem (V.18) and the above asymptotic result (V.22), we get $\tilde{q}_+(s) \sim (1-s)^{-\rho}$, and, from standard Tauberian theorem,

$$q_+(n) \underset{n\infty}{\sim} \frac{1}{\Gamma(\rho)} n^{-\theta_+}\,, \text{ where } \theta_+ = 1-\rho\,. \tag{V.23}$$

Similarly, we can show that $q_-(n) \sim n^{-\theta_-}/\Gamma(1-\rho)$ where $\theta_- = \rho$. Finally, using the expression of the characteristic function of $R(y)$ given in Eq. (V.5) it is possible to compute explicitly ρ (which is sometimes known under the name of the Zolotarev integrand) [Zolotarev 1986]

$$\rho = \int_0^\infty R(y)dy = \frac{1}{2} + \frac{1}{\pi\alpha}\arctan\left[\beta \tan\left(\frac{\pi\alpha}{2}\right)\right]\,, \text{ for } \alpha \neq 1\,. \tag{V.24}$$

Thus, using from Eq. (V.23),

$$\theta_+ = 1-\rho = \int_{-\infty}^0 R(y)dy\,, \tag{V.25}$$

and $\theta_- = \rho$, we obtain the exact results for the persistence exponents in the case $\alpha \neq 1$:

Persistence exponents for $\alpha \neq 1$

$$\theta_+ = \frac{1}{2} - \frac{1}{\pi\alpha}\arctan\left(\beta \tan\left(\frac{\pi\alpha}{2}\right)\right)\,, \tag{V.26}$$

$$\theta_- = 1-\theta_+ = \frac{1}{2} + \frac{1}{\pi\alpha}\arctan\left(\beta \tan\left(\frac{\pi\alpha}{2}\right)\right)\,. \tag{V.27}$$

Of course, for $\rho = 1/2$, one recovers the standard result of Sparre Andersen Eq. (V.20) [Anderson 1953]. For $\alpha = 1$, the exponent θ_+ can be evaluated

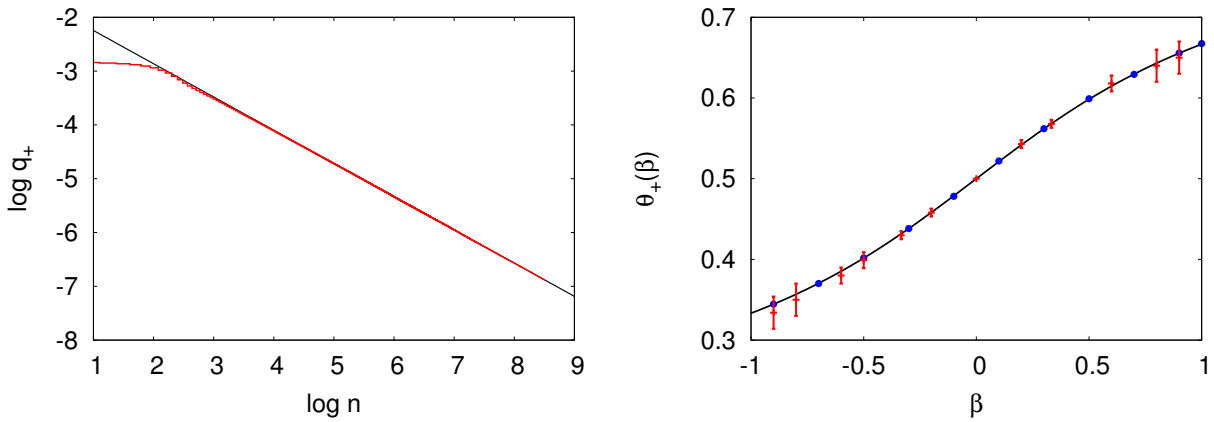

Figure V.4: **Left**: Survival probability of an asymmetric Lévy flight (with $\alpha = 3/2$, $\gamma = 4$, $c = 3$ and $n = 5000$) constrained on the positive half axis (log-log plot). The survival probability was computed performing 10^7 walks. A linear fit of its tail (black line) gives us $\theta_+ = 0.62 \pm 0.01$. **Right**: Plot of the persistence exponent θ_+ as a function of $\beta = (\gamma - 1)/(\gamma + 1)$, from the data given in Table V.1 (here $\alpha = 3/2$). The red marks are the numerical estimates of θ_+ extracted from the algebraic decay of $q_+(n)$ while the solid curve is our exact analytical result Eq. (V.26). The blue dots correspond to numerical estimates of $1 - \rho$.

γ	β	numerical θ_+	exact θ_+	numerical $1-\rho$
$1/19$	-0.9	0.33 ± 0.02	$0.344\ldots$	0.3445
$1/9$	-0.8	0.35 ± 0.02	$0.357\ldots$	0.3566
$1/4$	-0.6	0.38 ± 0.01	$0.385\ldots$	0.3851
$1/3$	-0.5	0.40 ± 0.01	$0.402\ldots$	0.4018
$1/2$	$-1/3$	0.430 ± 0.005	$0.4317\ldots$	
$2/3$	-0.2	0.458 ± 0.005	$0.4581\ldots$	0.4584
1	0	0.5	0.5	0.500
$3/2$	0.2	0.543 ± 0.005	$0.5419\ldots$	0.5412
2	$1/3$	0.568 ± 0.005	$0.5683\ldots$	
4	0.6	0.62 ± 0.01	$0.615\ldots$	0.6143
9	0.8	0.64 ± 0.02	$0.643\ldots$	0.6428
19	0.9	0.65 ± 0.02	$0.656\ldots$	0.6558

Table V.1: Summary of our numerical estimates for θ_+ extracted from the algebraic decay of the persistence probability, compared to the exact values calculated from Eq. (V.26) and displayed up to the third or fourth digit. We also added the numerical estimates of $1-\rho$. The uncertainty on the numerical values of θ_+ given in the table have been estimated by varying the fitting parameters (mainly the fitting range), and by evaluating the corresponding variations in the slope of the fit.

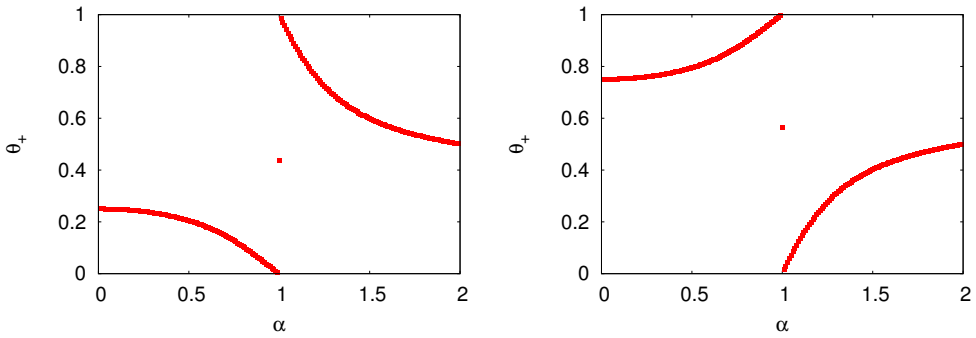

Figure V.5: **Left:** Plot of $\theta_+(\alpha, \beta = 1/2)$ given in Eq. (V.26). **Right:** Plot of $\theta_+(\alpha, \beta = -1/2)$ given in Eq. (V.26). For $\alpha = 1$, the values have been evaluated numerically from Eq. (V.25) and (V.5).

numerically thanks to the integral of Eq. (V.25) and the definition Eq. (V.5). Fig. V.5 shows a plot of the exact formula of $\theta_+(\alpha, \beta)$ for $\beta = 1/2$ (left) and $\beta = -1/2$ (right), given in Eq. (V.26) for $\alpha \neq 1$. In both cases, we observe that θ_+ exhibits a discontinuity at $\alpha = 1$. This discontinuity can be traced back to the discontinuous behaviour of the Lévy stable distribution itself in Eq. (V.5), for $\beta \neq 0$ as α crosses the value $\alpha = 1$. Note that a similar discontinuous behaviour, for $\alpha = 1$, was also observed in the numerical estimate of the mean first passage time of skewed Lévy flights in bounded domains [Dybiec et al. 2006].

Note that if the jump distribution $\xi(\eta)$ is itself a stable law, then $\xi(\eta) = R(\eta)$ and $p_n^+ = \rho$ for all n (not only in the asymptotic large n limit), such that $\tilde{q}_+(s) = (1-s)^{-\rho}$ and in this case $q_+(n)$ can be computed exactly for all n (see also [Aurzada and Simon 2012]):

$$q_+(n) = \frac{\Gamma(n+\rho)}{n!\,\Gamma(\rho)}\,, \quad \text{for } \xi(\eta) = R(\eta)\,. \tag{V.28}$$

V.2.2 Tail of the Propagator

We are now interested in the asymptotic behaviour of the distribution of the rescaled position $y = x_n/n^{1/\alpha}$ of the walker given that it has survived up to time n, namely $R_+(y)$. For this purpose it is useful to introduce the probability to find a free particle in $x > M$ after n steps

$$F(M, n) = \int_0^M P(x, n)\,dx\,, \tag{V.29}$$

and the probability to find the constrained particle in $x > M$ after n steps

$$F_+(M,n) = \int_0^M P_+(x,n)\,dx\,, \tag{V.30}$$

where M is a positive number, and $P_+(x,n)$ is the propagator of the constrained walkers (the pdf to find a constrained walker in x after n steps). The probability function F and F_+ are the cumulative functions of the pdf P and P_+. Thanks to the scaling $y = x_n/n^{1/\alpha}$, these probabilities can be expressed using R and R_+ as

$$F\,(M,n) = \int_M^\infty \frac{dx}{n^{1/\alpha}}\,R\left(\frac{x}{n^{1/\alpha}}\right) \;= \int_{M/n^{1/\alpha}}^\infty dy\,R(y)\,, \tag{V.31}$$

$$F_+(M,n) = \int_M^\infty \frac{dx}{n^{1/\alpha}}\,R_+\left(\frac{x}{n^{1/\alpha}}\right) = \int_{M/n^{1/\alpha}}^\infty dy\,R_+(y)\,.$$

We are interested in the behaviour of $F(M,n)$ and $F_+(M,n)$ when $M/n^{1/\alpha} \gg 1$, so that we can use the asymptotic behaviours of $R(y)$ and $R_+(y)$ to evaluate the integrals in Eq. (V.31):

$$R(y) \underset{+\infty}{\sim} \frac{c}{y^{\alpha+1}} \qquad \text{and} \qquad R_+(y) \underset{+\infty}{\sim} \frac{c_+}{y^{\alpha+1}}\,. \tag{V.32}$$

We obtain the asymptotic behaviour of $F(M,n)$ and $F_+(M,n)$ in the limit of large $M/n^{1/\alpha}$ ($M \gg n^{1/\alpha} \gg 1$),

$$F(M,n) \underset{M\gg n^{1/\alpha}\gg 1}{\sim} \frac{n}{\alpha}\frac{c}{M^\alpha} \qquad \text{and} \qquad F_+(M,n) \underset{M\gg n^{1/\alpha}\gg 1}{\sim} \frac{n}{\alpha}\frac{c_+}{M^\alpha}\,. \tag{V.33}$$

Therefore we get

$$\lim_{n\to\infty}\lim_{M\to\infty}\frac{F_+(M,n)}{F\,(M,n)} = \frac{c_+}{c}\,. \tag{V.34}$$

To compute the right hand side of this equation, we write can formally write

$$F(M,n) = \text{Prob.}\big[\,x(n) > M\,\big]\,, \tag{V.35}$$

$$\text{and} \quad F_+(M,n) = \quad \text{Prob.}\big[\,x(n) > M \mid \forall n' \in [0,n],\, x(n') > 0\,\big]\,, \tag{V.36}$$

where we denote by $\text{Prob.}(A|B)$ the condition probability of A given B. Using then Bayes' formula [2] for Eq. (V.36) yields

$$F_+(M,n) = \frac{\text{Prob.}\big[\,x(n) > M\,\big]}{\text{Prob.}\big[\forall n' \in [0,n],\, x(n') > 0\big]}\text{Prob.}\big[\forall n' \in [0,n],\, x(n') > 0 \,|\, x(n) > M\big]\,. \tag{V.37}$$

[2] $\text{Prob.}(A|B) = \text{Prob.}(B|A)\text{Prob.}(A)/\text{Prob.}(B)$

Here we recognise in the numerator the probability $F(M,n)$ given in Eq. (V.35), and, in the denominator, the survival probability

$$q_+(n) = \text{Prob.}\big[\,\forall n' \in [0,n],\, x(n') > 0\,\big]\,. \tag{V.38}$$

Working hypothesis – To evaluate then, in the limit of large M, the probability $\text{Prob.}[\forall n' \in [0,n],\, x(n') > 0\,|\,x(n) > M]$, we assume that the trajectories such that $x(n) > M$ are characterised by a single jump larger than M which happens at a step n_1 which may occur at any time in the interval $[0,n]$, hence $\eta(n_1) > M$. Thus, after this big jump the particle stays above 0 with a probability 1 as it is already far away from the origin. This argument, namely that trajectories are dominated by a single large jump, holds only for jump distributions with heavy tails ($\alpha < 2$), and thus does not apply to standard random walks, which converge to Brownian motion.
Within this hypothesis we obtain, using the definition of a conditional probability, $\text{Prob.}(A|B) = \text{Prob.}(A \cap B)/\text{Prob.}(B)$,

$$\text{Prob.}[\forall n' \in [0,n],\, x(n') > 0\,|\,x(n) > M] \underset{M\infty}{\sim} \frac{\displaystyle\sum_{n_1=0}^{n} q_+(n_1)\ \text{Prob.}[\eta(n_1) > M]}{\displaystyle\sum_{n_1=0}^{n} \text{Prob.}[\,\eta(n_1) > M\,]}\,. \tag{V.39}$$

As the jump variables are i.i.d., $\text{Prob.}[\,\eta(n_1) > M\,]$ is independent of n_1, and we obtain in the large M limit:

$$\lim_{n\to\infty}\lim_{M\to\infty}\frac{F_+(M,n)}{F\,(M,n)} = \lim_{n\to\infty}\frac{\displaystyle\sum_{n_1=0}^{n} q_+(n_1)}{n\,q_+(n)}\,. \tag{V.40}$$

For sufficiently large values of n_1, we can replace $q_+(n_1)$ by its expression Eq. (V.17) in the sum we obtain the Riemann series:

$$\sum_{n_1=0}^{n} q_+(n_1) \underset{n\infty}{\sim} \sum_{n_1=1}^{n} n_1^{-\theta_+}\,. \tag{V.41}$$

For constrained one dimensional Lévy flights, the persistence exponent given by Eq. (V.25) is always strictly smaller than 1: $\theta_+ < 1$. As a consequence the Riemann series (V.41) is diverging for large n, behaving as:

$$\text{for } \theta_+ < 1, \qquad \sum_{n_1=1}^{n} n_1^{-\theta_+} \underset{n\infty}{\sim} \frac{n^{(1-\theta_+)}}{1-\theta_+}\,. \tag{V.42}$$

We thus get,

$$\lim_{n\to\infty}\lim_{M\to\infty}\frac{F_+(M,n)}{F(M,n)}=\frac{1}{1-\theta_+}\,, \tag{V.43}$$

which finally leads, with Eq. (V.34), to the general result in one dimension Eq. (V.14):

Asymptotic behaviour of $R_+(y)$

$$R_+(y)\underset{+\infty}{\sim}\frac{c_+}{y^{1+\alpha}},\qquad \text{where}\ \ c_+=\frac{c}{1-\theta}\,. \tag{V.44}$$

This result is in agreement with the previous prediction $c_+ = 2\,c$ valid only for symmetric Lévy flights (where $\beta = 0$ and $\theta = 1/2$). In this case, this result was first obtained in [García-García et al. 2012] using a perturbative expansion around $\alpha = 2$ [Zoia et al. 2007], and confirmed by an exact calculation valid for any α in [Wergen et al. 2012].

V.2.3 Details of the numerical simulation details

The purpose of this section is to clarify the methods used to handle the numerical simulations.

Jump distribution To verify the predictions for the persistence exponent (Sec. V.2.1) and the tail of the constrained propagator (Sec. V.2.2), we have simulated numerically the random walk defined in Eq. (V.1), whose jumps are given by a power-law distribution (i.e. verifying Eq. (V.2)) with location $\mu = 0$. For this purpose we have chosen a Pareto distribution (see the left panel of Fig. V.2) to sample the jump length η. This distribution is defined for a positive parameter α by (see also Appendix A.4.3)

$$\xi(\eta)=\begin{cases}\dfrac{c}{\eta^{\alpha+1}} & \text{for } \eta > b_+\,,\\[2ex] \dfrac{c/\gamma}{|\eta|^{\alpha+1}} & \text{for } \eta < -b_-\,,\\[2ex] 0 & \text{otherwise}\,.\end{cases} \tag{V.45}$$

The distribution must be normalised and we choose to set its location $\mu = 0$. These two conditions thus fix the parameters b_- and b_+:

$$(b_-)^\alpha=\frac{c\,(1+\gamma^{\frac{1}{1-\alpha}})}{\alpha\,\gamma}\qquad\text{and}\qquad (b_+)^\alpha=\frac{c\,(1+\gamma^{1-\alpha})}{\alpha}\,. \tag{V.46}$$

The Pareto distribution is a fat-tailed distribution, and for α in $(0,2)$ the process converges to a skewed Lévy stable process with stability index α,

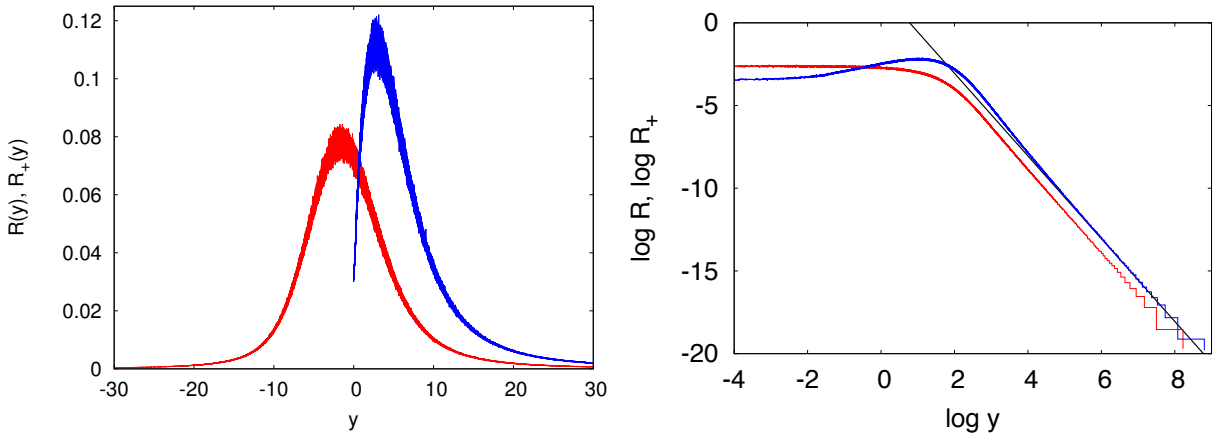

Figure V.6: Pdf of the rescaled variable y for Lévy flights with $\alpha = 3/2$, $\gamma = 2$, $c = 3$ and $n = 1000$ steps (sample of 10^8 walkers), in presence and in absence of an absorbing boundary on the negative half-axis, respectively $R_+(y)$ (red) and $R(y)$ (blue). $R_+(y)$ is compared to its expected asymptotic behaviour $R_+^{\mathrm{exp}}(y)$ (black line) given in Eq. (V.51).

γ	β	numerical c_+/c	exact c_+/c
$1/19$	-0.9	1.52 ± 0.05	$1.526\ldots$
$1/9$	-0.8	1.53 ± 0.03	$1.555\ldots$
$1/4$	-0.6	1.61 ± 0.03	$1.627\ldots$
$1/2$	$-1/3$	1.75 ± 0.03	$1.760\ldots$
1	0	2	2
2	$1/3$	2.34 ± 0.05	$2.316\ldots$
4	0.6	2.6 ± 0.1	$2.595\ldots$
9	0.8	3.0 ± 0.5	$2.803\ldots$
19	0.9	3.3 ± 0.5	$2.903\ldots$

Table V.2: Summary of our numerical estimates for c_+/c, extracted from the algebraic tail of the constrained propagator $R_+(y)$ and compared to the value expected from the theory:
$$\frac{c_+}{c} = \frac{1}{1-\theta_+}.$$
We took the exact value of θ_+ in Eq. (V.26); the values in the fourth column are exact and are provided up to the fourth digit.

skewness parameter β and a scale parameter a, related to the parameter γ and c of the Pareto jump distribution by Eq. (V.9) (see Fig. V.2).

To sample random variables η according to a Pareto distribution we can use a direct sampling method [Krauth 2006]. The Pareto distribution presents in fact the advantage to be easier and faster to sample than a stable law (see Appendix A.4.3). In practice, at each step, the walker makes a positive jump with a probability π_+

$$\pi_+ = \int_{b_+}^{+\infty} d\eta \, \phi(\eta) \,, \tag{V.47}$$

and a negative jump with a probability $1-\pi_+$. The amplitude of this jump is then given by [Krauth 2006]

$$\eta = \begin{cases} \left[\text{rand}\,(0,\, {b_+}^{-\alpha})\right]^{-\frac{1}{\alpha}} & \text{with probability } \pi_+ \,, \\ -\left[\text{rand}\,(0,\, {b_-}^{-\alpha})\right]^{-\frac{1}{\alpha}} & \text{with probability } 1-\pi_+ \,, \end{cases} \tag{V.48}$$

where $\text{rand}\,(x,y)$ is a random number drawn randomly from a uniform distribution in the interval (x,y).

Survival probability In order to compute the survival probability $q_+(n)$ defined in Eq. (V.15), we generated a large number of independent Lévy walkers, evolving via Eq. (V.1) with the Pareto jump distribution of Eq. (V.45). We then computed the fraction of walkers which remained on the positive axis until step n, which, for a large number of samples (walkers), converges to the probability that a walker survives until step n, $q^+(n)$. Fig. V.4 Left shows a plot of q^+ as function of n in log-log scale for $\alpha = 3/2$ and $\gamma = 4$ (corresponding to $\beta = 3/5$): we can observe that $q^+(n)$ exhibits an algebraic decay, which is in agreement with Eq. (V.17), $q^+ \propto n^{-\theta_+}$. A linear fit of the asymptote of $q^+(n)$ in log-log scale thus provides the numerical estimate of the exponent θ_+.

Using this procedure, we have measured the persistence exponent θ_+ for different values of asymmetry γ of the jump distribution[3] in the case $\alpha = 3/2$. These measurements are reported in Table V.1, where they are compared to the theoretical values of θ_+ coming from Eq. (V.26). Each curve $q^+(n)$ has been realised from a sample of 10^7 walkers. Fig. V.4 Right then shows a very good agreement between the numerical estimates of θ_+ (red marks with error bars on the value of θ_+) and its predicted values from Eq. (V.26) (solid line). Finally, a linear fit of the numerical results of θ_+ for small β, $\theta_+(\beta) = C\beta + D + o(\beta^2)$, gives $C = 0.200 \pm 0.006$ and

[3] We recall that $\beta = (\gamma-1)/(\gamma+1)$.

$D = 0.497 \pm 0.005$, which matches perfectly the asymptotic expansion for small β of the function $\theta_+(\beta)$ in Eq. (V.26).

Finally we also computed numerically ρ: from its definition in Eq. (V.22), ρ is the probability that a Lévy walker is on the right half-axis after a large number of steps. In other words it is the probability that a jump sampled directly from the stable distribution $R(y)$ is positive. This probability can be easily computed from a Monte Carlo simulation: we sample directly jumps from the stable distribution $R(y)$ with identical parameter α, β, c and μ than the initial jump distributions $\xi(\eta)$ (see Appendix A.4.3); we then count the ratio of jumps that are positive. Numerical estimates of ρ for $\alpha = 3/2$, $c = 1$ and $\mu = 0$ are shown as blue dots on Fig. V.4 Right. These values are consistent with the results Eq. (V.25) and (V.26):

$$\theta_+ = 1 - \rho = \frac{1}{2} - \frac{1}{\pi\alpha} \arctan\left(\beta \tan\left(\frac{\pi\alpha}{2}\right)\right), \quad \text{for } \alpha \neq 1\,. \tag{V.49}$$

Tail of the propagator We first check that our numerical procedure (V.1) and (V.45) yields back the correct free propagator $R(y)$ before we compute the constrained one, $R_+(y)$.

Free Lévy walkers – We construct a large number of independent Lévy walks evolving via Eqs. (V.1) and (V.45). For each random walk we record the final position x_n after n steps, and compute the normalised histogram of the corresponding rescaled variable $y = x_n/n^{1/\alpha}$. With a sufficiently large number of walkers, this histogram converges to probability density function of y. According to the Generalised Central Limit Theorem, for a large number of steps n, the probability density of y converges to the stable distribution $R(y)$ whose asymptotic expansion is:

$$R(y) \to \begin{cases} \dfrac{c}{y^{1+\alpha}} + \mathcal{O}\left(\dfrac{1}{y^{1+2\alpha}}\right), & \text{if } y > 0\,, \\ \dfrac{c/\gamma}{|y|^{1+\alpha}} + \mathcal{O}\left(\dfrac{1}{|y|^{1+2\alpha}}\right), & \text{if } y < 0\,. \end{cases} \tag{V.50}$$

Our numerical simulations are consistent with this result: in Fig. V.2 Right, the right and left tails of $R(y)$ coincide with the tails of the jump pdf $\xi(\eta)$ for large values of y and η (see Eq. V.8).

Constrained Lévy walkers – We now consider a one-dimensional random walk constrained to stay positive (Fig. V.3). If the particle has survived on the positive semi-axis up to step n, we record its final position x_n. Then we construct the normalised histogram of the rescaled final positions ($y = x_n/n^{1/\alpha}$), which converges to the pdf $R_+(y)$ from a large number of

such constrained walks. In Fig. V.6 Right, a plot of $R(y)$ and $R_+(y)$ (which is defined only for positive y) in log-log scale shows that these two functions have the same asymptotic behaviour, even though $R_+(y)$ is shifted with respect to $R(y)$. This confirms that R and R_+ both decay as $\propto y^{-\alpha-1}$ for large y [Zumofen and Klafter 1995], but with different amplitudes, $c_+ \neq c$.

Fig. V.6 compares, in log-log scale, the tail of R_+ (red curve) to the asymptotic behaviour $R_+^{\rm exp}$ expected from the theory and given by Eq. (V.14), in the case $\alpha = 3/2$ and $\gamma = 2$:

$$R_+(y) \underset{y\to+\infty}{\sim} \frac{c_+}{y^{5/2}} \qquad\qquad R_+^{\rm exp}(y) \underset{y\to+\infty}{\sim} \frac{c}{1-\theta_+}\,\frac{1}{y^{5/2}}\,. \tag{V.51}$$

This expected tail fit very well $R_+(y)$ when y becomes large, which is consistent with the relation (V.14) for asymmetric cases in one dimension. A more precise comparison can be made from the evaluation of c_+ by fitting the algebraic tail of $R_+(y)$, which yields $c_+/c = 2.34 \pm 0.05$ while our exact result predicts $1/(1-\theta_+) \simeq 2.316\ldots$ (taking the exact value of $\theta_+ = 0.5683\ldots$). We have carried out simulations for different values of β and extracted the amplitude c_+ of the tail. In Table V.2 we compare these estimates of c_+ with the values of $1/(1-\theta_+)$. This comparison gives a good support to our heuristic argument (that the process is governed by one large jump (rare and large event)) leading to the relation in Eq. (V.14).

3 Two dimensional Lévy flights in the presence of absorbing boundaries

V.3.1 General setup

There exists two common ways to build Lévy flights in a two dimensional space. One is the *Pearson random walk* that was introduced in Chapter 1: at each time step the walker is given a new direction $\boldsymbol{\omega}_n$ and a new jump length η_n. Its position $\mathbf{r}_{n+1}$ after $n+1$ steps is thus given by:

$$\mathbf{r}_{n+1} = \mathbf{r}_n + \eta_n\,\boldsymbol{\omega}_n\,, \tag{V.52}$$

where the directions $\boldsymbol{\omega}_n$ are independent and isotropically distributed over all possible directions in the plane and the random jump variables η_n are independent and identically distributed according to a power-law probability density function $\xi(\eta)$, i.e. verifying Eq. (V.2). An interesting property of this definition is that the statistical properties of the walk are invariant under rotation. Fig. V.7 displays one realisation of a Pearson Lévy flight. Observe that the few very large jumps can occur in any direction. The second way is a direct generalisation of the 1-dimensional walker (1d-walker) defined in Eq. (V.1), resulting from two 1d-walkers evolving respectively

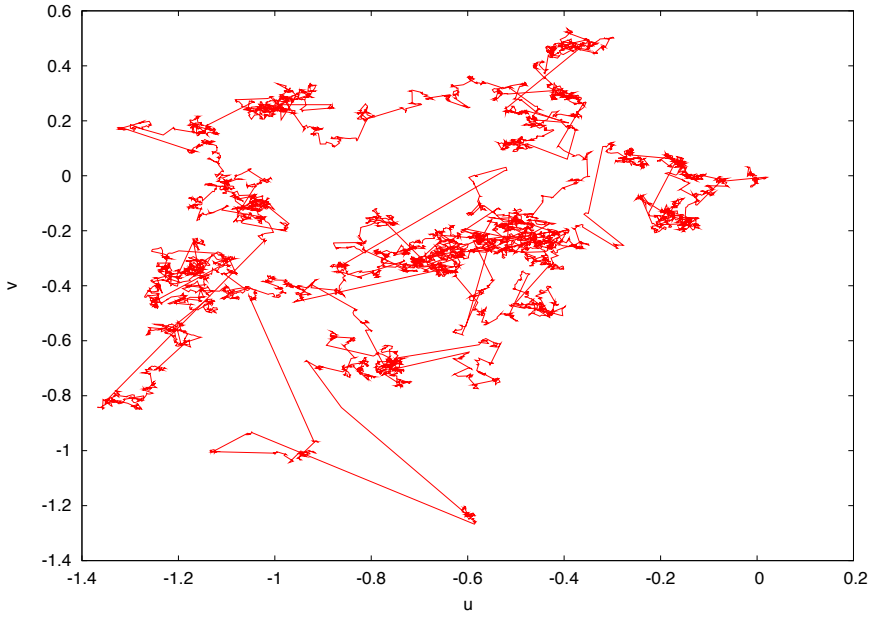

Figure V.7: Free 2d-Lévy flight of 10^4 steps, using the Pearson random walks with power-law distributed jumps ($\alpha = 3/2$, $\gamma = 1$, $c = 1$ and $\mu = 0$). The coordinates u and v have been rescaled using Eq. (V.56).

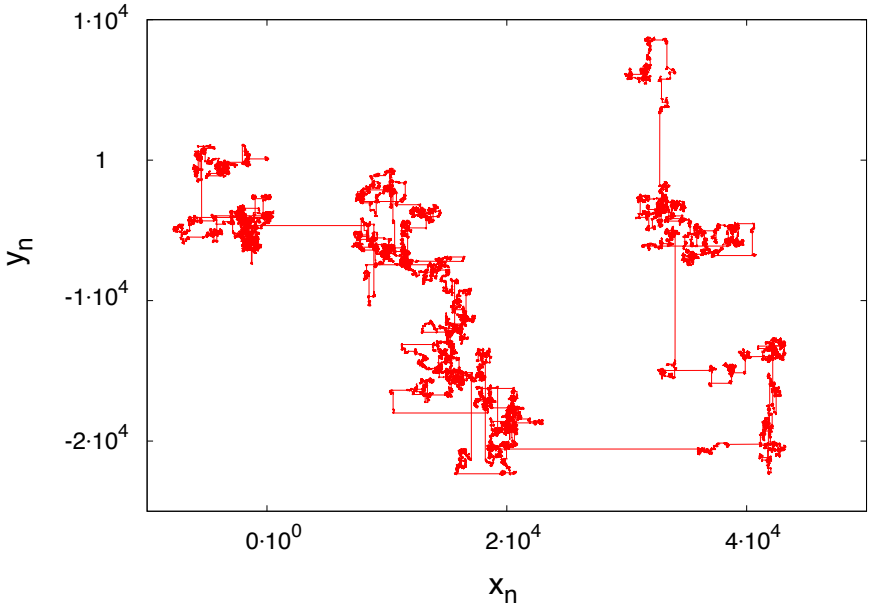

Figure V.8: Free 2d-Lévy flight of 10^6 steps, evolving according to (V.56) with power-law distributed jumps ($\alpha = 3/2$, $\gamma = 1$, $c = 1$ and $\mu = 0$).

along the axis x and the axis y. The position of the 2d-walker after n steps, $\vec{r}_n = x_n\,\vec{e_x} + z_n\,\vec{e_z}$, then evolves according to

$$\text{for } n \geqslant 1, \qquad \begin{cases} x_n = x_{n-1} + \eta_n^x \,, \\ \\ z_n = z_{n-1} + \eta_n^z \,, \end{cases} \tag{V.53}$$

starting from $\vec{r}_0 = \vec{0}$ at initial time. The jumps $\eta_1^{x,z}, \eta_2^{x,z}, \ldots, \eta_n^{x,z}$ are independent and identical random variables, distributed according to a power-law distribution, i.e. verifying Eq. (V.2). Note that for a Brownian walker these two definitions are equivalent. Fig. V.8 displays one realisation of such a Lévy flight, where we can observe that the few very large jumps occur only in two directions, along x or along z. Due to the definition of the walk Eq. (V.53), a long jump in another direction would imply that two very long jumps (one along x and one along z) have occurred exactly at the same time step, which is very unlikely.

Thanks to the "long jump anisotropy", with two preferred directions for the long jumps, it is possible to generalise the previous result, Eq. (V.14), to this second type of 2-dimensional Lévy walkers when the domain $\mathcal{D}$ is open in one of these two directions. Note however that in dimension higher than one, the persistence exponent θ of the walk can be larger than 1. In this case, the Riemann series in Eq. (V.42) would be convergent and would converge to the Riemann Zeta function (analytic for $\theta > 1$):

$$\text{for } \theta > 1, \qquad \sum_{n_1=1}^{n} n_1^{-\theta} \underset{n\infty}{\sim} \zeta(\theta)\,, \tag{V.54}$$

such that the ratio Eq. (V.43) depends on n

$$\frac{F_+(M,n)}{F(M,n)} \underset{\substack{n\infty \\ M\infty}}{\sim} \zeta(\theta)\,\left(\frac{n}{M^\alpha}\right)^{\theta-1}\,, \quad \text{for } \theta > 1, \tag{V.55}$$

assuming that the scaling Eq. (V.10) still holds. This suggests that the algebraic decay of the pdf of the constraint walker could be different from the one of the free walker. Therefore, a generalisation of the result Eq. (V.44) in higher dimension has to be done carefully.

Consider a two-dimensional Lévy random walker defined by (V.53); the jumps along x or z are independent and distributed according to the same power law-distribution (V.2), of parameters α, β and c (we choose $\mu = 0$). We denote by u and w the rescaled variables:

$$u = \frac{x_n}{n^{1/\alpha}} \qquad , \qquad w = \frac{z_n}{n^{1/\alpha}}\,, \text{ with } \qquad \vec{y} = (u, w)\,. \tag{V.56}$$

In absence of boundaries, the pdf of the rescaled variable $\vec{y}$ is easily obtained as the two components x_n and z_n are two independent one-dimensional Lévy walkers:

$$R_2(\vec{y}) = R(u)\, R(w)\,, \tag{V.57}$$

where $R(u)$ is the α-stable distribution (V.4) of parameter α, β and c. In the following, we will consider two cases for the constraint Lévy flight: the domain $\mathcal{D}$ is open in the direction of the long jumps, i.e. along x or z – see Fig. V.9 (a) and (b); the domain $\mathcal{D}$ is open in an other direction – see Fig. V.9 (c) and (d). We denote by $q_{\mathcal{D}}(n)$ the survival probability of a walker in the domain $\mathcal{D}$ after n steps, i.e. the fraction of walkers which stay inside the domain $\mathcal{D}$ up to step n, and by $\theta_{\mathcal{D}}$ its exponent. Analogously to the one-dimensional case Eq. (V.17), when the number of jumps $n \to \infty$,

$$q_{\mathcal{D}}(n) \underset{n\to\infty}{\propto} n^{-\theta_{\mathcal{D}}} \tag{V.58}$$

(while there exists no exact result for $\theta_{\mathcal{D}}$).

V.3.2 Domain $\mathcal{D}$ open along x or z

Let us start with the first case, where $\mathcal{D}$ is open in the direction of the axis x (Fig. V.9a and V.9b). Just like for the one dimensional case, we can assume that walkers that are far from the boundaries after a large number of steps n have performed one long jump in the direction of the axis x. By closely following the lines of Sec. V.2.2, we can then predict that, far from the boundaries, the pdf $R_{2,\mathcal{D}}(\vec{y})$ behaves like the pdf $R_2(\vec{y})$ in absence of boundaries with the universal ratio:

$$\frac{R_{2,\mathcal{D}}(\vec{y})}{R_2(\vec{y})} \underset{d(\vec{y},\partial\mathcal{D})\to\infty}{\longrightarrow} \frac{1}{1-\theta_{\mathcal{D}}}\,, \tag{V.59}$$

where $d(\vec{y}, \partial\mathcal{D})$ denotes the distance between the point located at $\vec{y}$ and the boundary of $\mathcal{D}$.

a. Simple case

In the limit case (a) depicted on Fig. V.9a, for instance, u and w are not correlated, such that we recover exactly the one-dimensional case:

$$\forall u \geqslant 0,\ \forall w, \qquad R_{2,\mathcal{D}}(u,w) = R_+(u)\, R(w)\,, \tag{V.60}$$

$$\text{and} \qquad \forall n, \qquad q_{\mathcal{D}}(n) = q_+(n), \qquad \text{such that } \theta_{\mathcal{D}} = \theta_+\,, \tag{V.61}$$

where $R_+(u)$ and $q_+(n)$ are respectively the pdf and the persistence of the constrained Lévy walker (see sec. 2). Here, the condition "far from the boundaries" can be realised by taking the limit $u \to +\infty$ for any values of

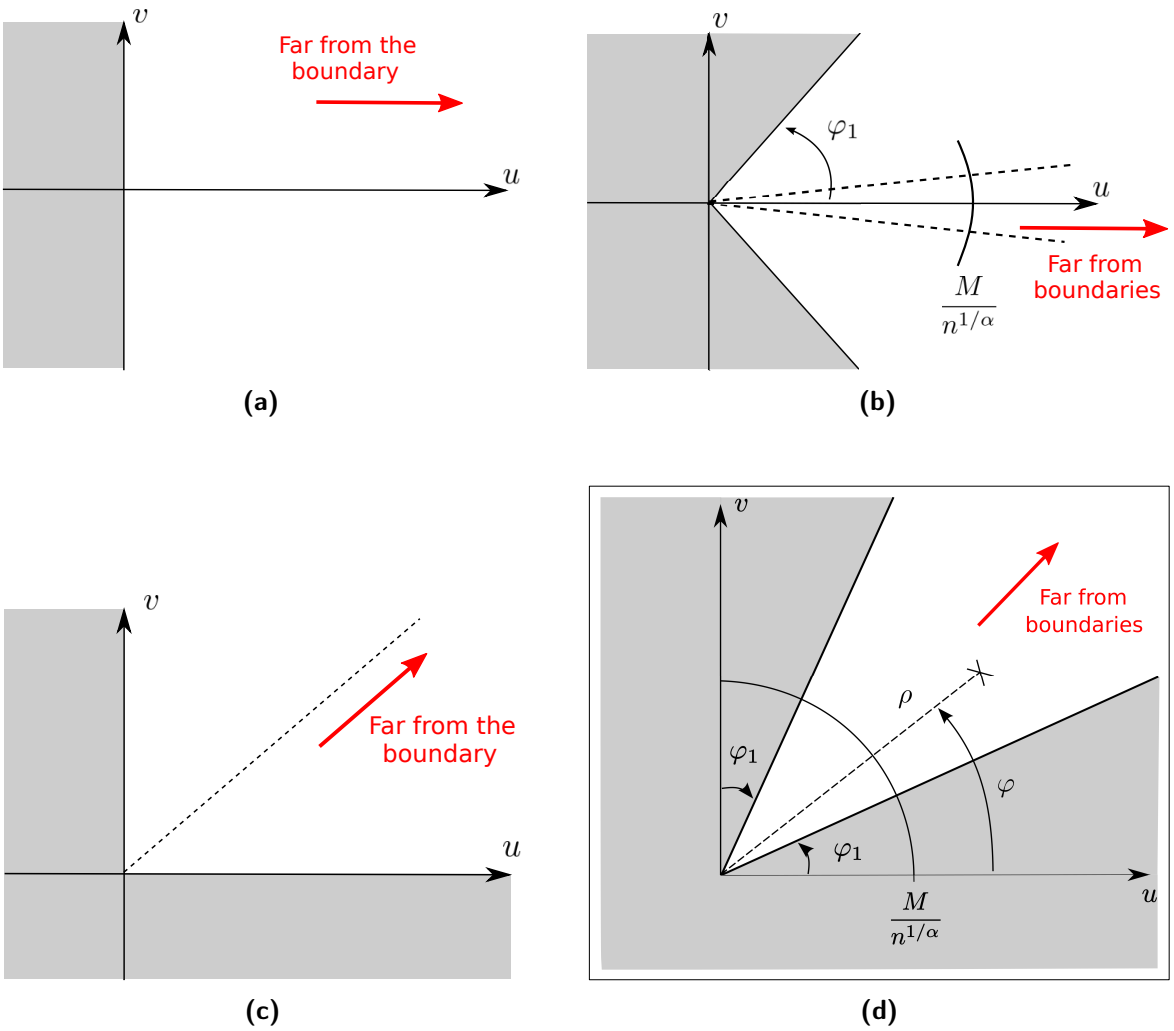

Figure V.9: Schematic representation of the different geometries considered for the boundaries.

w. Using the results for the one-dimensional case Eq. (V.8) and (V.44), we have

$$R_{2,\mathcal{D}}(u,w) \underset{u\infty}{\sim} \frac{c\,R(y)}{(1-\theta_+)\,u^{\alpha+1}} \qquad \text{and} \qquad R_2(u,w) \underset{u\infty}{\sim} \frac{c\,R(y)}{u^{\alpha+1}}\,, \tag{V.62}$$

which finally leads to the result (V.59), as $\theta_+ = \theta_{\mathcal{D}}$ here.

b. General case

In the general case, the open domain $\mathcal{D}$ is defined as (see Fig. V.9b)

$$-\varphi_1 \leqslant \arctan(u/w) \leqslant \varphi_1\,.$$

In this case, the positions x_n and z_n of a walker after n steps are correlated by the presence of the boundaries. For the following, we will use the polar coordinate for the walker position:

$$\begin{cases} \rho &= \sqrt{u^2+w^2} \\ \varphi &= \arctan\left(\dfrac{u}{w}\right)\,. \end{cases} \tag{V.63}$$

The condition "far from the boundaries" can be realised by considering walkers that are in a small wedge $-\epsilon \leqslant \varphi \leqslant \epsilon$ with $\epsilon \ll 1$ (see dash lines on Fig. V.9b), and far from the origin, $\rho \geqslant \tilde{M}$ with $\tilde{M} = M/n^{1/\alpha} \gg 1$. We call $\mathcal{D}_{\epsilon,\tilde{M}}$ the domain thus defined. In this case, we can first define the cumulative $F_\epsilon(\tilde{M})$, as the probability to find a free walker in the small domain defined above[4]:

$$F_\epsilon(\tilde{M}) = \int_{\tilde{M}}^{+\infty} d\rho \int_{-\epsilon}^{+\epsilon} d\varphi\, \rho\, R_2(\rho,\varphi)\,. \tag{V.64}$$

In the presence of boundaries, the probability to find a walker in this small domain is denoted $F_{\epsilon,\mathcal{D}}(\tilde{M})$. It corresponds to the probability to find a walker "far from the boundaries". Let us first compute $F_\epsilon(\tilde{M})$. For $\epsilon \ll 1$, for all $\varphi < \epsilon$,

$$\begin{cases} u = \rho\cos(\varphi) = \rho + o(\varphi) \\ w = \rho\sin(\varphi) = \rho\varphi + o(\varphi) \end{cases} \tag{V.65}$$

and using that $R_2(\rho,\varphi)\rho\,d\rho\,d\varphi = R(u)R(w)\,du\,dw$, we obtain for $\epsilon \ll 1$,

$$F_\epsilon(\tilde{M}) \;=\; \int_{\tilde{M}}^{+\infty} d\rho\,\rho\,R(\rho) \int_{-\epsilon}^{+\epsilon} R(\rho\,\varphi)\,d\varphi \;=\; \int_{\tilde{M}}^{+\infty} d\rho\,R(\rho) \int_{-\rho\epsilon}^{+\rho\epsilon} R(\varphi')\,d\varphi'\,.$$

[4]Numerically, $F_\epsilon(\tilde{M}) = \frac{N_\epsilon(\rho\geqslant\tilde{M})}{N_{tot}}$, where $N_\epsilon(\rho \geqslant \tilde{M})$ is the number of walkers in the small wedge $-\epsilon \leqslant \varphi \leqslant \epsilon$ verifying $\rho \geqslant \tilde{M}$, and N_{tot} the total number of walkers.

Furthermore, for all $\epsilon \ll 1$, ϵ fixed,

$$\lim_{\rho\to\infty} \int_{-\rho\epsilon}^{+\rho\epsilon} R(\varphi')\, d\varphi' = 1\,, \tag{V.66}$$

as $R(\varphi')$ is normalised. Hence, for $\tilde{M}$ such that $\tilde{M} \gg 1/\epsilon \gg 1$,

$$F_\epsilon(\tilde{M}) \underset{\tilde{M}\infty}{\sim} \int_{\tilde{M}}^{+\infty} \frac{c}{\rho^{\alpha+1}}\, d\rho \qquad \Longrightarrow \qquad F_\epsilon(\tilde{M}) \underset{\tilde{M}\infty}{\sim} \frac{c}{\alpha\, \tilde{M}^\alpha}\,. \tag{V.67}$$

For $\tilde{M} \gg 1/\epsilon$, the cumulative $F_\epsilon(\tilde{M})$ does not depend on ϵ. Note that, assuming that a free walker, found in the domain $\mathcal{D}_{\epsilon,\tilde{M}}$ with $\tilde{M} \gg 1$ after a large number of steps n, has performed one large jump in the direction of $+x$ at a time step $n_1 \leqslant n$, we can write

$$F_\epsilon(M,n) = \text{Prob.}[x_n > M] \underset{n,M\infty}{\sim} \sum_{n_1=1}^{n} \text{Prob.}[\eta_x(n_1) > M] \sim n\, \text{Prob.}[\eta_x > M]\,,$$

as jumps are independent and identically distributed. Computing the probability

$$\text{Prob.}[\eta_x > M] = \int_M^{+\infty} \xi(\eta_x) d\eta_x \underset{M\infty}{\sim} \frac{c}{\alpha\, M^\alpha}\,, \tag{V.68}$$

we finally recover the result (V.67): the behaviour of the tail of F is dominated by large events. We now use this large jump hypothesis for the constraint walker, and assume that after performing a large jump along x at a time step n_1 the walker will stay alive with probability 1 (same working hypothesis than for the one-dimensional walker). By definition,

$$F_{\epsilon,\mathcal{D}}(M,n) = \text{Prob.}\big[\,(x_n,z_n) \in \mathcal{D}_{\epsilon,M}\,|\,\forall n' \in [0,n], (x_n,z_n) \in \mathcal{D}\,\big]\,.$$

Within the above working hypothesis, and using the definition of a conditional probability, $\text{Prob.}(A|B) = \text{Prob.}(A \cap B)/\text{Prob.}(B)$, we obtain

$$F_{\epsilon,\mathcal{D}}(M,n) \underset{n,M\infty}{\sim} \frac{\sum_{n_1=1}^{n} q_{\mathcal{D}}(n_1)\, \text{Prob.}[\eta_x(n_1) > M]}{q_{\mathcal{D}}(n)}\,,$$

where $q_{\mathcal{D}}(n) = \text{Prob.}\big[\,\forall n' \in [0,n], (x_n,z_n) \in \mathcal{D}\,\big]$. As the jump variables are i.i.d., $\text{Prob.}[\eta_x(n_1) > M]$ is independent of n_1, and is given by Eq. (V.68). For n large, we can replace $q_{\mathcal{D}}(n)$ by its expression (V.58) in the sum, and we obtain again the Riemann series (V.41) found for the one-dimensional case. For $\theta_{\mathcal{D}} < 1$ this series is diverging as (V.42), such that,

$$\text{For } \theta_{\mathcal{D}} < 1\,, \qquad F_{\epsilon,\mathcal{D}}(\tilde{M}) \underset{\tilde{M}\infty}{\sim} \frac{c}{(1-\theta_{\mathcal{D}})\alpha\, \tilde{M}^\alpha}\,, \tag{V.69}$$

which finally yields, with Eq. (V.67), the result (V.59) in the case $\theta_D < 1$.

Concerning the condition $\theta_{\mathcal{D}} < 1$ – There is currently no theoretical result for $\theta_{\mathcal{D}}$ in the two-dimensional case, so that we can not be sure that θ_D is always smaller than 1. As the survival probability of walkers decreases when the opening angle $2\varphi_1$ is reduced, we must have $\theta_{\mathcal{D}} \geqslant \theta_+$ (persistence exponent for $\varphi_1 = \pi/2$ – case (a)), which is all the information we have concerning $\theta_{\mathcal{D}}$. As done for the one-dimensional case, we obtained numerical estimates for $\theta_{\mathcal{D}}$ from the algebraic decay of $q_{\mathcal{D}}$ for different values of the parameter α, β and φ. We then observed that $\theta_{\mathcal{D}}$ may be always smaller than 1 in this case, which were also consistent with the measurements of the amplitude of the tail of $F_{\epsilon,\mathcal{D}}(\tilde{M})$. This observation would need to be confirmed by a theoretical result.

c. Numerical simulation for a two-dimensional system

Fig. V.10 shows one realisation of a Lévy flight in absence (Left) and in presence (Right) of boundaries. Jumps are sampled from the Pareto distribution (V.45) with the parameter $\alpha = 3/2$, $\gamma = 1$, and $c = 1$. We consider as open domain $\mathcal{D}$ the wedge depicted in the right panel of Fig. V.10 and defined by $-\pi/3 \leqslant \operatorname{atan}(z/x) \leqslant \pi/3$. The fraction of walks which stay inside $\mathcal{D}$ after n steps defines the survival probability $q_{\mathcal{D}}(n)$ which we compute numerically (see the left panel of Fig. V.11). The persistence exponent extracted from our data is $\theta_{\mathcal{D}} = 0.73 \pm 0.01$.

In this geometry, our result (V.59) implies in particular that

$$\frac{R_{2,\mathcal{D}}(u,w)}{R_2(u,w)} \underset{u\to\infty}{\longrightarrow} \frac{1}{1-\theta_{\mathcal{D}}} , \tag{V.70}$$

(we could also consider a small wedge of opening angle ϵ). In practice, we compute the quantities $R_2(u, w = 0)$ and $R_{2,\mathcal{D}}(u, w = 0)$ via $N_\epsilon(u)$, i.e. the number of points inside the rectangle $[u, u + \Delta u] \times [-\epsilon/n^{1/\alpha}, \epsilon/n^{1/\alpha}]$, with ϵ and Δu small (see the right panel of Fig. V.10). In the absence of boundaries, we have that

$$R_2(u,0) = \lim_{\epsilon,\Delta u\to 0} \frac{N_\epsilon(u)}{2\epsilon\Delta u} = R(0)R(u) , \tag{V.71}$$

which behaves, for large u, as

$$R_2(u,0) \underset{\infty}{\sim} \frac{cR(0)}{u^{1+\alpha}} , \qquad R(0) = \frac{\Gamma(1+\alpha^{-1})}{a\pi} , \tag{V.72}$$

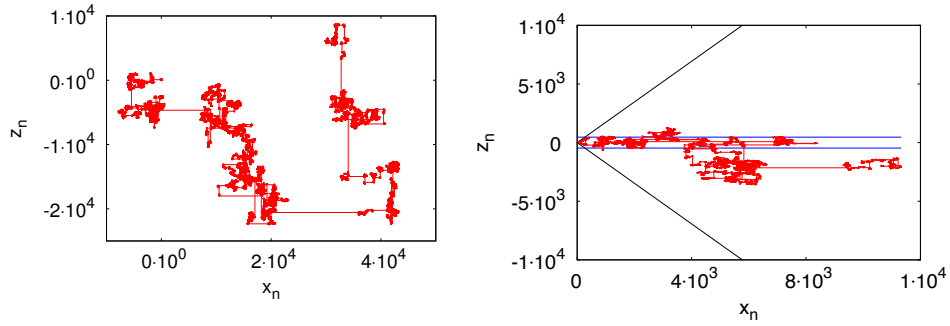

Figure V.10: $\alpha = 3/2$, $\gamma = 1$ and $c = 1$. **Left**: Free Lévy walker of 10^6 steps in a two-dimensional space, evolving according to (V.53). **Right**: A two-dimensional walk in the presence of the absorbing wedge (black). The blue lines delimit the stripe of width 2ϵ used to compute $R_2(u,0)$ and $R_{2,\mathcal{D}}(u,0)$ (V.71).

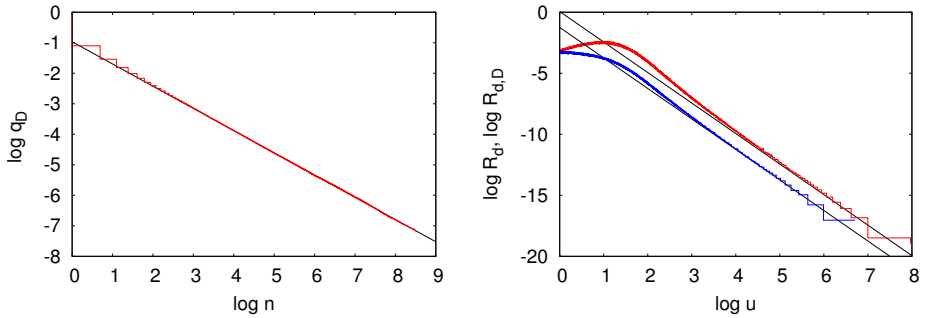

Figure V.11: Two-dimensional Lévy flights (V.56) with $\alpha = 3/2$, $\gamma = 1$ and $c = 1$ and $n = 5000$ steps (10^7 samples). **Left**: Survival probability in the wedged domain $q_{\mathcal{D}}(n)$ (red). A fit of the tail yields $q_{\mathcal{D}}(n) \sim n^{-\theta_{\mathcal{D}}}$ with $\theta_{\mathcal{D}} = 0.73 \pm 0.01$. **Right**: Comparison of the PDF of the rescaled variable in the presence, $R_{2,\mathcal{D}}(u,0)$ (red), and in the absence, $R_2(u,0)$ (blue), of the absorbing wedge. The tails are in good agreement with our conjecture (V.70).

where a and c are related via Eq. (V.9). In particular, in our simulations with $\alpha = 3/2$ and $c = 1$ we have

$$R_2(u,0) \sim \frac{c^*}{u^{5/2}}\,, \qquad c^* = \left(\frac{4\sqrt{2\pi}}{3}\right)^{2/3}\,. \tag{V.73}$$

This relation has been checked numerically, as shown in the right panel of Fig. V.11. Repeating the same numerical procedure in presence of the edge, we obtain $R_{2,\mathcal{D}}(u,0)$ as shown in the right panel of Fig. V.11. The tail is in good agreement with our prediction $R_{2,\mathcal{D}}(u,0) \sim [c^*/(1-\theta_{\mathcal{D}})]u^{-1-\alpha}$, which confirms the validity of the result (V.59).

d. Generalisation to higher dimensions

More generally, for a system of any dimension d, open in one of the directions where walkers are more likely to perform long jumps (see Fig. V.9a and V.9b), we can generalise the "one long jump" argument used for the 1d- and the 2d-cases. We thus predict that far from the boundaries, the pdf $R_{2,\mathcal{D}}(\vec{y})$ behaves like the pdf $R_2(\vec{y})$ in absence of boundaries with the universal ratio:

Asymptotic behaviour of $R_{d,\mathcal{D}}$

$$\frac{R_{d,\mathcal{D}}(\vec{y})}{R_d(\vec{y})} \underset{d(\vec{y},\partial\mathcal{D})\to\infty}{\longrightarrow} \frac{1}{1-\theta_{\mathcal{D}}}\,, \qquad \text{assuming that } \theta_{\mathcal{D}} < 1\,, \tag{V.74}$$

where $d(\vec{y},\partial\mathcal{D})$ denotes the distance between the point located at $\vec{y}$ and the boundary of $\mathcal{D}$.

V.3.3 Domain $\mathcal{D}$ open in an other direction

Let us consider now the case where $\mathcal{D}$ is open in an other direction than the two axes x or z (see Fig. V.9c and V.9d). Here we can no more assume that a walker that is found far from the boundary after a large number of steps has performed one long jump along x or z that would have brought him far from the boundaries. Indeed, to arrive in this situation a walker would have, at least, performed two long jumps, one along x and one along z, simultaneously or not.

a. Simple case

In the limit case (c) depicted on Fig. V.9c, the rescaled positions of the walker, u and w, are not correlated, such that u and w corresponds to two one-dimensional constraint walkers:

$$\forall u \geqslant 0,\ \forall w \geqslant 0, \qquad R_{2,\mathcal{D}}(u,w) = R_+(u)\,R_+(w)\,, \tag{V.75}$$

$$\text{and} \qquad \forall n, \qquad q_{\mathcal{D}}(n) = [q_+(n)]^2, \qquad \text{such that } \theta_{\mathcal{D}} = 2\theta_+ \,, \tag{V.76}$$

where $R_+(u)$ and $q_+(n)$ are respectively the pdf and the persistence of the corresponding constrained one-dimensional Lévy walker (see sec. 2). Here, the condition "far from the boundaries" can be realised by resorting to the polar coordinate (V.63) and taking the limit $\rho \to +\infty$ in the direction of $\varphi = \pi/4$, as illustrated in Fig. V.9c. In this direction, we have, using the results for the one-dimensional case Eq. (V.8) and (V.44),

$$R_2\Big(\rho, \varphi = \frac{\pi}{4}\Big) = R(\rho\cos\varphi)\, R(\rho\sin\varphi) \underset{\rho\infty}{\sim} \frac{2^{\alpha+1}\, c^2}{\rho^{2(\alpha+1)}} \,,$$

$$R_{2,\mathcal{D}}\Big(\rho, \varphi = \frac{\pi}{4}\Big) = R_+(\rho\cos\varphi)\, R_+(\rho\sin\varphi) \underset{\rho\infty}{\sim} 2^{\alpha+1} \frac{c^2}{(1-\theta_+)^2\, \rho^{2(\alpha+1)}} \,.$$

We finally obtain in this case the ratio:

$$\frac{R_{2,\mathcal{D}}(\rho, \pi/4)}{R_2(\rho, \pi/4)} \underset{\rho\to\infty}{\longrightarrow} \frac{1}{(1-\theta_+)^2} = \frac{1}{\left(1 - \dfrac{\theta_{\mathcal{D}}}{2}\right)^2} \,, \tag{V.77}$$

which is different from the result (V.74).

b. General case

In the general case (d) (see Fig. V.9d), a generalisation of the long jump argument would be more complex. For large opening angle of $\mathcal{D}$ (φ_1 small), we can expect walkers to perform two large jumps (one along x and one along z) to go far from the boundaries (as for the limit case $\varphi_1 = 0$). For a small opening angle (φ_1 closer to $\pi/4$), we can expect walkers to perform one long jump in the direction $\varphi = \pi/4$, i.e. two simultaneous jumps respectively along x and z, to go far from the boundaries. For intermediate opening angles, we then may expect an overlap between these two limit cases.

This last part of the work, is still in progress, in collaboration with P.K. Mohanty, G. Schehr and A. Rosso. Beyond the theory, one of the main difficulties for this problem concerns the numerical simulations: due to the two preferred directions for the large jumps (see Fig. V.8), walkers surviving after a large number of steps in the case illustrated on Fig. V.9d are rare, and it is difficult to generate numerically enough statistics.

4 Conclusion

To conclude, we have studied, in this chapter, the problem of asymmetric Lévy flights in presence of absorbing boundaries. In the one dimensional

case we have computed the persistence exponents θ_+ and θ_- for walkers constrained to stay in the semi-positive or semi-negative axis. These exponents are useful to characterise the statistical behaviour of various observables including, for instance, the sequence of records for the walker position [Majumdar et al. 2012]. In particular, the exponent θ_+ for asymmetric Lévy flight was shown to be related to the exponent of the survival probability of the random walk performed by the random variable $a = m_1 - m_2$, where m_1 and m_2 are the current maximum of two independent Brownian particles (with two different diffusion coefficients) [Randon-Furling 2014]. Our main results concern the statistics of the walker positions in a semi-bounded domain. Far from the boundaries the pdf of the walker positions has the same algebraic decay as the original jump distribution: here we have computed with heuristic arguments and numerical simulations the amplitude of this decay. This last result strongly relies on the property that the statistics of this random walk is dominated by rare and large events and thus does not hold for the more familiar Brownian walkers.

RANDOM WALKS ON QUENCHED DISORDERED MEDIA AND OPEN PROBLEM

Let us conclude our discussion on anomalous transport by going back to the initial motivation (see Sec. I.3.2): the study of the neutron or photon transport in strongly heterogeneous and disordered media, such as pebble-bed reactors or Lévy glasses. Up to now, we have considered that this transport can be modelled by (branching) Lévy walks. Experimentally the stable parameter α of the jump distribution can be estimated from measurements of mean square displacement or mean first-passage time (transmission), as proposed in [Davis and Marshak 1997; Barthelemy et al. 2008] for photon transport. Concerning neutron transport, these methods should be generalised to random walks in the presence of branching.

However, an important aspect of this type of transport is the role of *quenched* disorder: the strong heterogeneities of the medium are fixed, and thus induce correlations between lengths and directions of subsequent jumps. These correlations, completely neglected in the Lévy walk approach, have been shown to counteract the increase of diffusivity due to the long jumps [Svensson et al. 2014]. In particular, several works have shown that correlations dominate transport in one-dimensional systems [Beenakker et al. 2009; Burioni et al. 2010; Vezzani et al. 2011], while their effects becomes less significant for Lévy glasses in higher dimensionality[5] [Barthelemy et al. 2010].

The general study of the anomalous transport in disordered medium goes beyond the scope of this thesis. In particular, a first problem that remains open concerns random walks in one-dimensional quenched disordered systems. Following the lines of [Beenakker et al. 2009; Bernabó et al. 2014], we consider a ballistic random walker, with constant speed v, evolving on a one-dimensional chain of barriers with power-law spacing

[5] This does not hold for perfectly self-similar systems [Buonsante et al. 2011; Groth et al. 2012].

distribution (see Fig. V.12):

$$\eta(\ell) \sim \frac{c}{\ell^{\alpha+1}} \qquad \text{when } \ell \to +\infty \tag{V.78}$$

where c is an amplitude parameter, and the power-law exponent $\alpha \in (0, 2)$ characterises the stability of the distribution. The locations of the barriers are fixed in time. At each barrier the walker can change its direction with

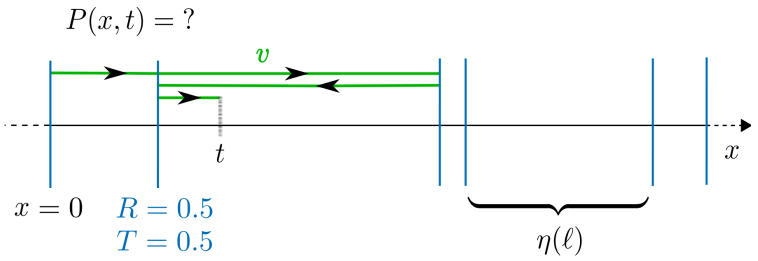

Figure V.12: Ballistic random walker on a one-dimensional quenched disordered system.

probability $R = 1/2$, or continue in the same direction with the transfer probability $T = 1/2$. Between barriers, the walker cannot change its direction, and is thus forced to go straight. Consider now a walker starting at time $t = 0$ from a position $x = 0$ located on a barrier; what is the probability density function to find the walker at a position x at time $t > 0$, namely the propagator of the walk, $P(x, t)$?

First, we expect the propagator to inherit the power-law property of the inter-barrier distances ℓ, such that the walk will exhibit a super-diffusive behaviour, as observed in Lévy glasses, and could be described in terms of Lévy walks. On the other hand, the jumps of the walker are highly correlated: when the walker is reflected on a barrier, it is forced to go back to the previous barrier, and thus sees exactly the same landscape. By contrast, a "classical" random walk, such as an exponential random walk or a Lévy walk, evolves in a background material where the locations of the scattering centres (analogous to the barriers in the model above) constantly change, as each new jump is sampled independently from the others.

This space and time dependent problem has not been solved yet: while the pdf η describes the disorder, the propagator $P(x, t)$ would be the quantity needed to fully characterise the transport phenomenon.

Conclusion

The thesis was oriented along two main axes: the study of the fluctuations of the neutron population within a nuclear reactor, and in particular, the clustering phenomenon [Dumonteil et al. 2014], and the understanding of anomalous transport of neutrons that can be observed in disordered and strongly heterogeneous media, such as pebble-bed reactors.

In the first part of the thesis, we have seen that the process of neutron reproduction (fission) and death (sterile capture) can lead to strong fluctuations of the neutron population. To study these fluctuations in the context of reactor physics, we have derived, thanks to the Feynman-Kac formalism, backward equations for each moment of two key observables: the total length travelled and the total number of collisions performed by walkers in a considered region of the system. The first moment of these two quantities indeed corresponds to the track-length estimator and the collision estimator, central to Monte Carlo simulations of nuclear reactors, and which are respectively related to the neutron flux and reaction rate within the system. For these equations the contribution of the thesis concerns the extension to heterogeneous media with anisotropic scattering [SNA-MC 2013]. The dependence of these equations on energy may be studied more in detail. For applications in reactor physics, an important effort should be now done in the direction of taking into account delayed neutrons, which would require to develop coupled backward equations, for the neutrons and for the precursors.

More generally, the Feynman-Kac formalism allows to go beyond the Boltzmann equation (that describes only the mean behaviour of the system), to study the fluctuations of any observable of the system. In particular, we derived the backward evolution equation for the pair-correlation function between neutrons, that is a key quantity for the understanding of the clustering phenomenon. Solving this equation in a finite medium, surrounded by absorbing or reflecting boundaries, we studied the impact of confined geometries on the clustering phenomenon. We thus observed that the impact of the confined geometry is characterised by a competition between two physical phenomena: the pair-reproduction process that cor-

relates particles of the same family, tends to create clusters, and that will also leads the whole population to extinction in a characteristic time τ_E, and the diffusion process that mix particles over the system and thus tend to counteract the clustering effect on characteristic time τ_D. For $\tau_D < \tau_E$, the system will initially develop a clustering govern by the competition between this two phenomena, but will finally goes to extinction in τ_E (*Critical catastrophe*). We thus highlighted two types of fluctuations: local fluctuations resulting from the competition between birth/death process and diffusion leading to a clustering that can be characterised by a the ratio τ_D/τ_E, and global fluctuations that lead to a trivial clustering and to the extinction of the population [Zoia et al. 2014]. Then adding a control on the whole population (feedback that keep the total population constant) allowed us to prevent the extinction of the system (global fluctuations), and thus focus on the local fluctuations and the clustering thus "stabilised". The characteristic time τ_E can be seen now as the characteristic time of the pair-reproduction process. We then observed that the stabilised size of the clusters depend on the ratio τ_E/τ_D, i.e. on the competition between reproduction that reduces it and diffusion that increases it, and explicitly computed this size [de Mulatier et al. 2015]. So far, we have considered Brownian branching particles. In the context of neutron transport, it would be interesting to consider now a more realistic approach, including in particular exponential displacements, heterogeneities and the energy dependencies. More particularly, in the context of nuclear reactor physics, it could be interesting to study the impact of delayed neutrons that will introduce a new time scale in the system. On another aspect, as the system was started from an equilibrium configuration of particles, and naturally move to this clustered state, we may now wonder how these clusters behave in the system: could we observe an equilibrium configuration of clusters?

In the second part of the thesis, we were interested in non-exponential transport of particles, initially motivated by the problem of transport in strongly heterogeneous and disordered media. We first focused on a property, known as *Cauchy formula*, that characterises branching exponential random walks at criticality: the mean length travelled by such a walk through a finite domain depends only on the geometrical properties of the domain, its finite volume V, its surface S and a dimensionality-dependent constant η_d

$$\langle L \rangle_S = \eta_d V/S \,. \tag{V.79}$$

In Chapter IV, we first showed that this property holds for transport in media with mild heterogeneities, and with anisotropic scattering [SNA-MC 2013]. We then proved that the property surprisingly generalises to any type of Pearson random walk and branching random walk at criticality, provided that walkers have a finite mean free path [Mazzolo et al. 2014;

De Mulatier et al. 2014]. The Cauchy property (V.79) thus displays a universal character: the mean total length travelled by a walk within a finite domain, if entering through its surface S, depends only on the geometrical properties of the traversed domain, and not on the specific details of the walk. Under the same conditions, we showed that the generalised Cauchy-like formulae (IV.4) and (IV.6) for branching random walks also remain valid for non-exponential transport. In fact the result is much stronger: these properties admit a local formulation (Eq. (IV.105) and (IV.104)) valid at any point of the considered domain [De Mulatier et al. 2014].

In the last chapter, we were interested in the issue of (asymmetric) Lévy flights in a semi-open domain, in presence of absorbing boundaries. In particular, we computed the persistence exponents θ_+ and θ_- for walkers constrained to stay in the semi-positive or semi-negative axis, in the one dimensional case. This exponent is not know yet in higher dimension. Our main results concern the statistics of the walker positions in a semi-bounded domain, i.e. the propagator of the walk. Far from the boundaries this propagator has the same algebraic decay as the original jump distribution: here we have computed with heuristic arguments and numerical simulations the amplitude of this decay. This work was carried out for one-dimensional cases, and in higher dimension when the domain is open in the direction of the large jumps. The generalisation to other cases is still in progress. This last result strongly relies on the property that the statistics of Lévy flights are dominated by rare and large jumps [De Mulatier et al. 2013].

In general, concerning non-exponential transport, we propose two perspectives for future developments. First, assuming that neutron transport in strongly heterogeneous and disordered media, such as pebble-bed reactors, can be modeled effectively by *branching* Lévy walks, how do we estimate the stable exponent α of the jumps distribution from experimental data? Second, as one important aspect of this type of transport is the role of *quenched* heterogeneities: are Lévy walks really a good model for these systems? What is the propagator of the walk?

One of the interesting aspect of the work presented here is that problems are treated in the presence of boundaries. Indeed, even though real systems are finite (confined geometries), most of previously existing results concern infinite systems. The results derived along the thesis have led to the publication of 6 peer-reviewed articles, and may apply more broadly to physical and biological systems with diffusion, reproduction and death.

Appendix

APPENDIX A

APPENDIX AND NUMERICAL TOOLS

Contents

1 ARBOGAST'S FORMULA [ARBOGAST 1800] FAÀ DI BRUNO FORMULA [FAÀ DI BRUNO 1855]

Derivatives of compositions involving differentiable functions can be found using the chain rule, $(f \circ g(x))' = (f' \circ g)(x)\, g'(x)$. Higher derivatives of such functions are given by Faà di Bruno's formula [Pitman 2006].

The most well-known form of Faà di Bruno formula gives [Craik 2005]

$$\frac{\partial^m}{\partial s^m}\left[f \circ g(x)\right] = \sum_{k=1}^{m} f^{(k)} \circ g(x)\, \mathcal{B}_{m,k}\left[g'(x), \cdots, g^{(m-k+1)}(x)\right], \tag{A.1}$$

where $\mathcal{B}_{m,k}[x_1, \cdots, x_{m-k+1}]$ are the Bell polynomials, defined as [Bell 1927; Comtet 1974; Pitman 2006]:

$$\mathcal{B}_{m,k}[x_1, \cdots, x_{m-k+1}] = \sum_{\substack{i_1+i_2+\cdots=k \\ i_1+2\,i_2+\cdots=m}} \frac{m!}{i_1!\; i_2! \cdots} \left(\frac{x_1}{1!}\right)^{i_1} \left(\frac{x_2}{2!}\right)^{i_2} \cdots \tag{A.2}$$

In particular, for all $m \geqslant 1$,

$$\begin{cases} \mathcal{B}_{m,1}[x_1, \cdots, x_{m-k+1}] = x_m \\ \mathcal{B}_{m,m}[x_1, \cdots, x_{m-k+1}] = x_1^m \end{cases} \tag{A.3}$$

For the sake of simplicity of the notation, in the thesis, $\mathcal{B}_{m,k}[x_1, \cdots, x_{m-k+1}]$ is denoted by $\mathcal{B}_{m,k}[x_i]$, where the index i implicitly include the all family $\{x_i\}_{i,\, 1 \leqslant i \leqslant m-k+1}$.

Let us apply this formula to the calculation of the m-th derivative of the composite functions needed in Sec. II.2.2.d. $G \circ \mathcal{C}^*[Q_t](s|\mathbf{r}_0, \mathbf{v}_0)$, evaluated at $s = 0$:

$$\begin{aligned} \frac{\partial^m}{\partial s^m}\left[G \circ \mathcal{C}^*[Q_t](s)\right]_{s=0} = \sum_{k=1}^{m} G^{(k)} \circ \mathcal{C}^*[Q_t](0) \\ \times\, \mathcal{B}_{m,k}\left[\mathcal{C}^*\left[Q_t'(0)\right], \cdots, \mathcal{C}^*\left[Q_t^{(m-k+1)}(0)\right]\right], \end{aligned} \tag{A.4}$$

$\mathcal{C}^*$ being a linear form (see Eq. (II.43)). By definition of the moment generating function $Q_t(s|\mathbf{r}_0, \mathbf{v}_0)$, the values of $Q_t(s|\mathbf{r}_0, \mathbf{v}_0)$ and its derivatives evaluated at $s = 0$ for all point $\mathbf{r}_0, \mathbf{v}_0$ of the phase space are:

$$L_m(\mathbf{r}_0, \mathbf{v}_0, t) = (-1)^m \left.\frac{\partial^m Q_t(s|\mathbf{r}_0, \mathbf{v}_0)}{\partial\, s^m}\right|_{s=0}. \tag{A.5}$$

Furthermore, the multiple derivatives of generating function of the number of descendants $G(z) = \sum_k p_k z^k$, evaluated at $\mathcal{C}^*[Q_t](0) = 1$ are:

$$\begin{cases} G[1] & = \sum_i p_i = 1 \\ G'[1] & = \sum_i i\, p_i = \nu_1 \\ G^{(2)}[1] & = \sum_i i(i-1)\, p_i = \nu_2 \\ & \cdots \\ G^{(k)}[1] & = \sum_i i(i-1)\cdots(i-k+1)\, p_i = \nu_k \end{cases} \tag{A.6}$$

where ν_k are the falling factorial moment of the number of particles emitted at a collision. Thus, Eq. (A.4) successively becomes

$$\begin{aligned} \frac{\partial^m}{\partial s^m}\Big[G \circ \mathcal{C}^*[Q_t](s)\Big]_{s=0} &= \sum_{k=1}^{m} \nu_k\, \mathcal{B}_{m,k}\Big[-\mathcal{C}^*\big[L\big], \cdots, (-1)^{(m-k+1)}\mathcal{C}^*\big[L_{(m-k+1)}\big]\Big], \\ &= (-1)^m \sum_{k=1}^{m} \nu_k\, \mathcal{B}_{m,k}\Big[\mathcal{C}^*\big[L\big], \cdots, \mathcal{C}^*\big[L_{(m-k+1)}\big]\Big], \end{aligned}$$

where we used the property of the Bell polynomials, which can be seen on Eq. (A.2), that, for any constant α:

$$\mathcal{B}_{m,k}\big[\alpha x_1, \cdots, \alpha^{m-k+1} x_{m-k+1}\big] = \alpha^m\, \mathcal{B}_{m,k}\big[x_1, \cdots, x_{m-k+1}\big].$$

Finally, using the simplified notation introduce above, we obtain

$$\frac{\partial^m}{\partial s^m}\Big[G \circ \mathcal{C}^*[Q_t](s)\Big]_{s=0} = (-1)^m \sum_{k=1}^{m} \nu_k\, \mathcal{B}_{m,k}\Big[\mathcal{C}^*\big[L_i\big]\Big]. \tag{A.7}$$

The same way, we can show that

$$\frac{\partial^m}{\partial s^m}\Big[G \circ \mathcal{C}^*[W_t](s)\Big]_{s=0} = \sum_{k=1}^{m} \nu_k\, \mathcal{B}_{m,k}\Big[\mathcal{C}^*\big[\langle\, N_V^i \,\rangle\big]\Big], \tag{A.8}$$

where $\langle\, N_V^i \,\rangle$ is given by Eq. (II.68):

$$\langle\, N_V^i \,\rangle(\mathbf{r}_0, \mathbf{v}_0, t) = \frac{\partial^i W_t(\mathbf{r}_0, \mathbf{v}_0|s)}{\partial\, s^i}\Big|_{s=0}. \tag{A.9}$$

2 FLUCTUATIONS – ZERO DIMENSIONAL MODEL

c. without control

The calculations performed in this annex gives more details on the derivation of Sec. II.1.2. Consider a system of one single cell in which we initially deposit N_0 particles. At time $t = 0$ we let them start to randomly reproduce and die following the Galton-Watson process described in Sec. I.1.2. Note that in this problem, we are not interested in the diffusion process: either particles are not allowed to diffuse, either we consider the whole cell as a unique point. The number N of individuals in the cell is thus a random variable, and we denote by $P(N,t)$ the probability of observing exactly N individuals at time t in the cell. Following the lines of [Houchmandzadeh 2009], we can show that this probability, for this zero dimensional model, follows the master equation:

$$\frac{dP}{dt}(N,t) = \underbrace{-P(N,t)\left[W^-(N,t) + \sum_{k\geqslant 1} W_k^+(N,t)\right]}_{\text{Losses}} + \underbrace{P(N+1,t)\,W^-(N+1,t)}_{\text{gain by death}} + \underbrace{\sum_{k=1}^{N-1} P(N-k,t)\,W_k^+(N-k,t)}_{\text{gain by birth}}, \tag{A.10}$$

where, $W^-(N,t)dt$ is the probability that the population of N particles undergoes one death during dt:

$$\forall N \geqslant 1, \qquad W^-(N,t)dt = \lambda_0 N(t)dt\,, \tag{A.11}$$

and $W_k^+(N,t)dt$ is the probability that it earns k new particles during dt:

$$\forall N \geqslant 1, \qquad W_k^+(N,t)dt = \lambda_{k+1} N(t)dt\,. \tag{A.12}$$

Note that for this latter case, the population actually observes $k+1$ birth, but earns only k new particles, as the incident particles is absorbed. For instance, the probability that a population of size $N \geqslant 1$ earns one new particle during dt is $W_1^+(N,t)dt = \lambda_2 N(t)dt$. Replacing these expressions, the master equation (A.10) for $P(N,t)$ then becomes

$$\boxed{\frac{dP}{dt}(N,t) = -\lambda\, N\, P(N,t) + \sum_{i=0}^{N} \lambda_i\,(N+1-i)\,P(N+1-i,t)\,,} \tag{A.13}$$

where we have used that $\lambda_0 + \sum_{k\geqslant 1} \lambda_{k+1} = \lambda - \lambda_1$ and that

$$\begin{aligned} P(N+1,t)\, W^-(N+1,t) + \sum_{k=1}^{N-1} P(N-k,t)\, W_k^+(N-k,t) \\ = \lambda_0(N+1)\, P(N+1,t) + \sum_{k=1}^{N-1} \lambda_{k+1}(N-k) P(N-k,t) \\ = \sum_{i=0}^{N} \lambda_i (N+1-i)\, P(N+1-i,t) - \lambda_1 N\, P(N,t)\,, \end{aligned}$$

with the change of variable $i = k+1$ in the sum. Then, equations for the various moments of N, can be extracted directly from the master equation, using the definition $\langle N^k \rangle = \sum_{N\geqslant 0} N^k P(N,t)$:

$$\boxed{\frac{d\langle N^k\rangle}{dt} = -\lambda \langle N^{k+1}\rangle + \sum_{i\geqslant 0} \lambda_i \langle (N-1+i)^k N\rangle\,.} \tag{A.14}$$

Here as well we used a computational trick:

$$\begin{aligned} \sum_{N\geqslant 0} \sum_{i=0}^{N} \lambda_i N^k (N+1-i)\, P(N+1-i,t) &= \sum_{i\geqslant 0} \lambda_i \sum_{N\geqslant i} N^k (N+1-i)\, P(N+1-i,t) \\ &= \sum_{i\geqslant 0} \lambda_i \sum_{N'\geqslant 1} (N'-1+i)^k\, N'\, P(N',t)\,, \end{aligned}$$

with a change of variable $N' = N+1-i$ in the second sum.

In particular, for $k = 1$,

$$\frac{d\langle N\rangle}{dt} = \lambda(\nu_1 - 1)\langle N\rangle\,, \tag{A.15}$$

and for $k = 2$,

$$\frac{d\langle N^2\rangle}{dt} = \lambda\big[\nu_2 - (\nu_1 - 1)\big]\langle N\rangle + 2\lambda(\nu_1 - 1)\langle N^2\rangle\,. \tag{A.16}$$

The variance of N, $\sigma^2(t) = \langle N^2\rangle - \langle N\rangle^2$ then verifies/follows the same equation

$$\frac{d\sigma^2}{dt} = \lambda\big[\nu_2 - (\nu_1 - 1)\big]\langle N\rangle + 2\lambda(\nu_1 - 1)\sigma^2\,, \tag{A.17}$$

and with the initial conditions $\langle N \rangle(0) = N_0$ and $\sigma^2(0) = 0$ (initially particles are not correlated) we get

$$\boxed{\begin{cases} \langle N \rangle(t) = N_0 \, e^{\lambda(\nu_1 - 1)\, t} \\ \sigma^2(t) = \left[\dfrac{\lambda \nu_2}{\lambda(\nu_1 - 1)} - 1 \right] \left[\dfrac{\langle N \rangle^2}{N_0} - \langle N \rangle(t) \right] . \end{cases}} \tag{A.18}$$

3 APPENDIX FOR THE CAUCHY FORMULA

The numerator in Eq. (IV.96) can be rearrange as follows,

$$\begin{aligned}
A &= \int_0^\infty ds\, t(s)\, s \int_0^s dr\, w(r) \\
&= \int_0^\infty ds\, t(s) \int_0^s dx \int_0^s dr\, w(r) \\
&= \int_0^\infty dx \int_x^\infty ds\, t(s) \left[\int_0^\infty dr\, w(r) - \int_s^\infty dr\, w(r) \right] \\
A &= \lambda \int_0^\infty dx\, h(x) \int_0^\infty dr\, w(r) - \lambda \int_0^\infty dx \int_x^\infty dr\, w(r) \int_x^r ds\, t(s)\,, \qquad \text{(A.19)}
\end{aligned}$$

where we used the definition of $h(x)$ given in Eq. (IV.77). The same definition leads for the last integral $\int_x^r ds\, t(s) = \lambda\,[h(x) - h(r)]$, and for A:

$$\begin{aligned}
A &= \lambda \int_0^\infty dx\, h(x) \int_0^x dr\, w(r) + \lambda \int_0^\infty dx \int_x^\infty dr\, w(r)\, h(r)\,, \qquad \text{(A.20)} \\
&= \lambda \int_0^\infty dx\, h(x) \int_0^x dr\, w(r) + \lambda \int_0^\infty dr\, r\, w(r)\, h(r)\,. \qquad \text{(A.21)}
\end{aligned}$$

Then, from the definition of $w(r)$ in Eq. (IV.90), we get

$$\begin{aligned}
\int_0^x dr\, w(r) &= 1 - \int_x^{+\infty} dr\, \frac{1}{\langle c \rangle} \int_r^{+\infty} f(c)\, dc\,, \\
&= 1 - \frac{1}{\langle c \rangle} \int_x^{+\infty} dc\, f(c) \int_x^c dr\,, \\
&= 1 - \frac{1}{\langle c \rangle} \int_x^{+\infty} dc\, c\, f(c) + x\, w(x)\,, \\
\int_0^x dr\, w(r) &= \frac{1}{\langle c \rangle} \int_0^x dc\, c\, f(c) + x\, w(x)\,. \qquad \text{(A.22)}
\end{aligned}$$

Finally using this last identity in Eq. (A.21) yields for the constant A of Eq. (IV.96),

$$A = \lambda \left[\frac{1}{\langle c \rangle} \int_0^\infty dr\, h(r) \int_0^r dc\; c\, f(c) + 2 \int_0^\infty dr\, r\, w(r)\, h(r) \right]. \qquad \text{(A.23)}$$

4 COMPUTATIONAL SAMPLING METHODS FOR RANDOM VARIABLES

In this short document, we give an insight into how to sample certain types of random variables that can be useful from a computational point of view. This document was originally written to go along with a small C/C++ library, whose functions are now commented throughout this appendix. There are many ways of sampling random variables [Gobet 2013]; only direct sampling methods, using the cumulative distribution function or Box-Muller like methods, will be presented here.

A.4.1 Random number generator in C/C++

In C/C++, the simplest generators are

- `rand`, with a period of $2^{32} \sim$ 4.3e9:
  `rand()` return a random integer uniformly distributed between 0 and `RAND_MAX`

- `drand48`, with a period of $2^{48} \sim$ 2.8e14:
  `drand48()` return a random number, uniformly distributed over $[0, 1]$.

The Mersenne Twister pseudorandom number generator is one of the most widely used generator for Monte Carlo simulations in many fields. In C++, its most commonly-used version (`mt19937`, of period $(2^{19937} - 1) \sim$ 1e6000) is implemented in the library `random` since the C++11 standard.
These generators can be initialised using:

```
std::mt19937 gen;       //only for mt19937

void initialise_generator()
{
    int seed = (unsigned)time(NULL);
    srand(seed);        //for rand
    srand48(seed);      //for drand48
    gen.seed(seed_val); //for mt19937
}
```

A.4.2 Few well-known pdf

a. Uniform distribution

We can define the function `double rand_uni(double a=0, double b=1)` that return a random variable uniformly distributed over $[a, b]$, thanks to one of the generators above (for instance, with `drand48`):

```
double rand_uni(double a=0, double b=1)
{       return a + (b-a)*drand48();      }
```

```
//For mt19937:
std::uniform_real_distribution<double> uni(0.,1.);
double rand_uni(double a=0, double b=1)
{       return a + (b-a)*uni(gen);      }
```

b. Exponential distribution

Let x be an exponentially distributed random variable, its pdf is of the form:

$$p(x) = \begin{cases} \Sigma\, e^{-\Sigma x}, & x \geqslant 0 \\ 0, & x < 0 \end{cases} \tag{A.24}$$

where $\Sigma = \frac{1}{\mathbb{E}(x)}$ is the parameter of the distribution (*rate parameter*). The exponential distribution is supported on the interval $[0, +\infty)$, and its cumulative distribution function is

$$F(X) = \begin{cases} 1 - e^{-\Sigma X}, & X \geqslant 0 \\ 0, & X < 0 \end{cases} \tag{A.25}$$

This cumulative can be inverted easily, such that the sampling of an exponentially distributed random variable E_Σ, of parameter Σ, is given by

$$E_\Sigma = F^{-1}(U) = -\frac{1}{\Sigma} \ln[U]\,. \tag{A.26}$$

The following function `double rand_exp(double)` thus return an exponentially distributed variable, whose parameter Σ is passed as argument ($\Sigma = 1$ by default).

```
double rand_exp (double sigma = 1.)
{       return -log(rand_uni())/sigma;      }
```

c. Normal or Gaussian distribution

The normal distribution is a continuous probability distribution of two parameters: its mean (or expectation), denoted μ, and its variance, noted σ^2. The probability density of the normal distribution reads:

$$p(x) = \frac{1}{\sqrt{2\pi\sigma^2}}\, e^{-\dfrac{(x-\mu)^2}{2\,\sigma^2}}\,. \tag{A.27}$$

A random variable x with a normal distribution is said to be normally distributed, and is noted: $x \sim \mathcal{N}(\mu, \sigma^2)$. Let x be a normally distributed random variable, and let us set $z = (x - \mu)/\sigma$. The random variable z is distributed

with a *standard normal distribution* ($\mu = 0$ and $\sigma = 1$) (z is a standard normal deviate):

$$p(z) = \frac{1}{\sqrt{2\pi}} e^{-\frac{z^2}{2}}. \tag{A.28}$$

Thus, a random variable $X \sim \mathcal{N}(\mu, \sigma^2)$ can be given by $X = \mu + \sigma Z$ where $Z \sim \mathcal{N}(0, 1)$. To sample Z from a standard normal distribution, a first idea would be to use the cumulative distribution function (as for the exponential distribution):

$$F(Z) = \frac{1}{\sqrt{2\pi}} \int_{-\infty}^{y} e^{-\frac{y^2}{2}} dy = \frac{1}{\sqrt{\pi}} \int_{-\infty}^{y/\sqrt{2}} e^{-z^2} dz$$

$$F(Z) = \frac{1}{2}\left[1 - \text{erf}\left(\frac{Z}{2}\right)\right], \qquad \text{where } \text{erf}(x) = \frac{2}{\sqrt{\pi}} \int_0^x e^{-t^2} dt \tag{A.29}$$

is the error function. However, the inverse of this latter function is defined in terms of a series expansion (Maclaurin series), which is not convenient numerically. Several methods exist then to sample Z. A well-know one is the *Box-Muller method* - Let X and Y be two independent standard normal deviates. We have

$$p(X)\,dX\,p(Y)\,dY = \frac{1}{2\pi} e^{-\frac{X^2+Y^2}{2}} dX\,dY$$

With the changes of variable $X = r\cos(\theta)$ and $Y = r\sin(\theta)$, and then $s = \frac{r^2}{2}$,

$$\begin{aligned} p(X)\,dX\,p(Y)\,dY &= \left(\frac{1}{2\pi} d\theta\right)\left(r\, e^{-\frac{r^2}{2}} dr\right) \\ &= \left(\frac{1}{2\pi} d\theta\right)\left(e^{-s}\, ds\right), \end{aligned} \tag{A.30}$$

where s and θ are two independent random variables: θ is uniformly distributed over $[0, 2\pi]$ and s is exponentially distributed, with a rate parameter $\Sigma = 1$. Thus, X and Y can be obtained thanks to:

$$\begin{cases} X &= \sqrt{2\,E_1}\cos(2\pi U_1) = \sqrt{-2\ln(U_2)}\cos(2\pi U_1) \\ Y &= \sqrt{2\,E_1}\sin(2\pi U_1) = \sqrt{-2\ln(U_2)}\sin(2\pi U_1) \end{cases} \tag{A.31}$$

The sampling of a standard deviate can be thus given by the function

```
double rand_Gauss (double mu=0., double sigma=1.)
{
return mu + sigma * sqrt(2*rand_exp())*cos(rand_uni(0,2*M_PI));
}
```

that takes in argument the mean μ and the standard deviation σ. By default $\mu = 0$ and $\sigma = 1$.

A.4.3 Stable distributions

Stable distributions (or α-stable distributions) were first introduced by Lévy [1925]. They are fully described by four parameters: an index of stability $\alpha \in (0, 2]$, a skewness parameter $\beta \in [-1, 1]$, a scale parameter $c > 0$ and location parameter $\mu \in \mathbb{R}$ [Borak et al. 2005].

A symmetric distribution has a parameter $\beta = 0$; the asymmetry of a distribution increases with $|\beta|$. A stability index $\alpha = 2$, corresponds to the Gaussian distribution with a variance $\sigma^2 = 2\,c^2$. For $\alpha < 2$, the variance of the distribution is undefined. The tail exhibit a power-law behaviour, becoming asymptotically equivalent to a Pareto law (see Sec. A.4.4):

$$p(x) \sim \begin{cases} \dfrac{C\,(1+\beta)}{x^{\alpha+1}}, & \text{for } x \to +\infty \\ \dfrac{C\,(1-\beta)}{|x|^{\alpha+1}}, & \text{for } x \to -\infty \end{cases} \tag{A.32}$$

where C is an amplitude parameter that can be express in terms of α and c:

$$C = \frac{c^{\alpha}\,\sin(\alpha\pi/2)\,\Gamma(\alpha+1)}{\pi} \tag{A.33}$$

This can be shown from the generalised central limit theorem. For $\alpha \in (1, 2]$, the parameter μ corresponds to the mean of the distribution, whereas the mean is undefined for $\alpha \leqslant 1$.

Let X be a α-stable random variable of parameter α, c, β and μ, it is denoted $X \sim \mathcal{S}_\alpha(c, \beta, \mu)$. The most popular parameterisation of the characteristic function of X is given by [Samoradnitsky and Taqqu 1994; Weron 1996]:

$$\psi(t) = \exp\left[it\mu - |ct|^{\alpha}(1 - i\beta\,\mathrm{sgn}(t)\,\delta)\right] \tag{A.34}$$

$$\text{with} \qquad \delta = \begin{cases} \tan(\frac{\pi\alpha}{2}), & \text{if } \alpha \neq 1 \\ -\frac{2}{\pi}\ln|t|, & \text{if } \alpha = 1 \end{cases}$$

The complexity of the sampling of an α stable random variable is due to the absence of direct analytical expression for stable distributions. In most cases, there exist no analytical expression for F^{-1}. In some particular cases, however, it is possible to write the cumulative F and obtain a simple analytical expression for F^{-1}, such as for the Cauchy Law $\mathcal{S}_1(c, 0, \mu)$, or the Lévy law $\mathcal{S}_{1/2}(c, 1, \mu)$.

a. Cauchy distribution, $X \sim \mathcal{S}_1(c, \beta = 0, \mu)$

The Cauchy distribution, also known as Lorentz distribution in physics, is fully characterised by two parameters, a location parameter μ and a scale parameter $c > 0$, and is given by:

$$p(x; \mu, c) = \frac{1}{\pi c \left(1 + \frac{(x-\mu)^2}{c^2}\right)} \tag{A.35}$$

This distribution is symmetric ($\beta = 0$) centered around μ, and as $\alpha = 1$, it admits neither a variance nor a mean. Note that a random variable that is the ratio of two independent standard deviates follows a Cauchy distribution. The cumulative distribution function of the standard Cauchy distribution is:

$$F(X) = \frac{1}{\pi} \arctan(X) + \frac{1}{2}\,. \tag{A.36}$$

The sampling of $X \sim \mathcal{S}_{\alpha=1}(c, \beta = 0, \mu)$ can thus be obtained thanks to the inverse function F^{-1}:

$$X = \mu + c\, F^{-1}(U) = \mu + c\, \tan\left[\pi\left(U - \frac{1}{2}\right)\right]\,. \tag{A.37}$$

The sampling of a random variable distributed according to a Cauchy distribution is given by:

```
double rand_Cauchy(double mu=0., double c=1.)
{       return mu+c*tan(M_PI*(rand_uni()-0.5));       }
```

By default the function return a standard random variable ($\mu = 0, c = 1$).

b. The Lévy distribution $X \sim \mathcal{S}_{1/2}(c, \beta = 1, \mu)$ *(or Levy*(μ, c)*)*

The lévy distribution was named after the mathematicien Paul Lévy. It is an asymmetric stable distribution of parameters $\alpha = 1/2$ and $\beta = 1$. The distribution is thus fully described with 2 parameters: the location parameter $\mu \in \mathbb{R}$ and the scale parameter $c > 0$:

$$p(x; \mu, c) = \begin{cases} \sqrt{\frac{c}{2\pi}}\, \frac{1}{(x-\mu)^{3/2}}\, \exp\left(-\frac{c}{2(x-\mu)}\right) & \text{si } x > \mu \\ 0 & \text{else} \end{cases} \tag{A.38}$$

The cumulative distribution function of the standard Lévy distribution is

$$\begin{aligned} F(X) &= \int_0^X \frac{1}{\sqrt{2\pi}x^{3/2}} e^{-\frac{1}{2x}} dx \\ &= -2\int_{+\infty}^{Y} \frac{1}{\sqrt{2\pi}} e^{-y^2/2} dy \qquad \text{o } y = \frac{1}{\sqrt{x}} \\ &= \text{erfc}\left(\frac{1}{\sqrt{2X}}\right) \qquad \text{avec } \text{erfc}(X) = 1 - \text{erf}(X) \end{aligned} \tag{A.39}$$

As for the Gaussian distribution, we can not use the inverse function F^{-1} to sample X. However, comparing the two cumulative distribution in Eq. (A.39) and in Eq. (A.29) (Gaussian distribution), we can see that, if Y is a standard deviate $Y \sim \mathcal{N}(0,1)$, then the random variable Y^{-2} is distributed according to a standard Lévy distribution, $Y^{-2} \sim \text{Levy}(0,1)$. We thus finally obtain a simple method to sample $\text{Levy}(\mu, c)$:

```
Y=rand_Gauss(); return mu+c/(Y*Y);
```

which we will rather write

```
double rand_Levy(double mu=0., double c=1.)
{
      double co=1./cos(2*M_PI*rand_uni());
      return mu+0.5*c*co*co/rand_exp();
}
```

to not lose in efficiency by taking the square (`Y*Y`) of the square root that inside the `rand_Gauss` function.

c. *Lois stables,* $X \sim \mathcal{S}_\alpha(c, \beta, \mu)$

Note that any random variable distributed according to a stable distribution can be written in term of a random variable distributed according to a standard stable distribution, $\mathcal{S}_\alpha(1, \beta, 0)$, noted $\mathcal{S}_\alpha(\beta)$:

$$\mathcal{S}_\alpha(c, \beta, \mu) \sim \begin{cases} \mu + c\,\mathcal{S}_\alpha(\beta), & \text{if } \alpha \neq 1 \\ \mu + c\,\mathcal{S}_\alpha(\beta) + \dfrac{2}{\pi}\beta\, c \ln(c), & \text{if } \alpha = 1 \end{cases} \tag{A.40}$$

The algorithm to sample a standard random variable $X \sim \mathcal{S}_\alpha(\beta)$ is based on the method of Chambers, Mallows, and Stuck [Chambers et al. 1976] and is proposed in [Weron 1996]:

1. Generate two independent random variable: one V uniformly distributed on $\left[-\frac{\pi}{2}, \frac{\pi}{2}\right]$, and an exponential random random variable E with mean 1.

2. **For** $\alpha \neq 1$, compute

$$X = S\,\frac{\sin[\alpha(V+B)]}{\cos(V)^{1/\alpha}}\,\left[\frac{\cos[V-\alpha(V+B)]}{E}\right]^{(1-\alpha)/\alpha} \tag{A.41}$$

where

$$\begin{cases} B = \dfrac{\arctan(\beta\tan\frac{\pi\alpha}{2})}{\alpha} \\ S = \left[1+\beta^2\tan^2\left(\dfrac{\pi\alpha}{2}\right)\right]^{1/(2\alpha)} \end{cases} \tag{A.42}$$

For $\alpha = 1$, compute

$$X = \frac{2}{\pi}\left[\left(\frac{\pi}{2}+\beta V\right)\tan V - \beta\ln\left(\frac{\frac{\pi}{2}E\cos V}{\frac{\pi}{2}+\beta V}\right)\right] \tag{A.43}$$

This algorithm gives, on a C code, for $\alpha = 1$:

```
double rand_alpha1(double c=1, double beta=0, double mu=0)
//Cauchy law by default
{
      double V=M_PI*(rand_uni()-0.5);
      double E=rand_exp();

      const double Pi_2=M_PI/2.;
      double X = ((Pi_2+beta*V)*tan(V)
                - beta*log((Pi_2*E*cos(V))/(Pi_2+beta*V)) )/Pi_2;
      return mu + c*X + beta*c*log(c)/Pi_2;
}
```

and for the case $\alpha \neq 1$:

```
double rand_alpha(double alpha=0.5, double c=1., double beta=1.,
    double mu=0.)
//loi de Levy par defaut
{
    double V=M_PI*(rand_uni()-0.5);
    double E=rand_exp();
    double alpha_=1./alpha;

    double tana=tan(M_PI*alpha/2.);
    double B = alpha_*atan(beta*tana);
    double S = pow(1+beta*beta*tana*tana, alpha_/2.);

    double X = S * sin(alpha*(V+B))/pow(cos(V), alpha_)
```

```
                * pow(cos(V-alpha*(V+B))/E , alpha_ -1 );

    return mu + c*X;
}
```

In the cases ($\alpha = 1$, $\beta = 0$) and ($\alpha = 1/2$, $\beta = 1$), we recover respectively the algorithm for the Cauchy law and the Lévy law.

A.4.4 Other fat-tailed distributions, Pareto distribution

The Pareto distribution is an asymmetric distribution with a power-law tail: (for $\mu = 0$)

$$p(x) = \begin{cases} \dfrac{C}{x^{\alpha+1}}, & \text{if } x \geqslant b \\ 0, & \text{elsewhere .} \end{cases} \tag{A.44}$$

where the parameter b is given by normalisation of $p(x)$. As for α-stable laws, the Pareto law admits a mean value for $\alpha > 1$ and a variance for $\alpha \geqslant 2$. α is the stability index, and C an amplitude parameter.

```
double rand_Pareto_b1(double alpha = 1.5, double c = 1.)
{       return pow(c/(alpha*rand_uni()), 1./alpha);      }
```

This law can be generalised for different values of asymmetry:

$$p(x) = \begin{cases} \dfrac{C\,(1+\beta)}{x^{\alpha+1}}, & \text{if } x \geqslant b^{+} \\ \dfrac{C\,(1-\beta)}{x^{\alpha+1}}, & \text{if } x \leqslant b^{-} \\ 0, & \text{elsewhere ,} \end{cases} \tag{A.45}$$

where the parameter b^{+} and b^{-} are given by normalisation of $p(x)$, and by setting a location parameter μ. The parameter β is a skewness parameter and C is an amplitude parameter. The sampling of random variable distributed according to a Pareto law with parameters α, C, β, and μ can be computed with the function:

```
double rand_Pareto(double alpha=1.5, double c=1., double beta=0.,
        double mu=0.)
// valid only for alpha > 1
{
    double g = (1.+beta)/(1.-beta);     //skewness
    //double beta = (g-1.)/(1+g);
```

```
    double b_alpha = c1 * (1+pow(g, (1./(1.-alpha))) ) / alpha;
    double a_alpha = (b_alpha*g*c1) /(alpha*b_alpha - c1);

    double A = c / (alpha * a_alpha);
    double B = c1/g / (alpha * b_alpha);

    double U = rand_uniform(-B, A);

    if (U < 0){
        double xi_ = 1./rand_uniform(0.,1./b_alpha);
        return mu - pow(xi_, 1./alpha);
        }
    else {
        double xi_ = 1./rand_uniform(0.,1./a_alpha);
        return mu + pow(xi_, 1./alpha);
        }
}
```

A.4.5 Example and numerical simulations

Landau distribution, $\mathcal{S}_{\alpha=1}(c, \beta = 1, \mu)$ of characteristic function

$$\varphi(x; \mu, c) = \exp\Big[\, it\mu - |c\,t|(1 + \tfrac{2i}{\pi}\log(|t|)\Big] \tag{A.46}$$

is the stable law with parameters $\alpha = 1$ and $\beta = 1$.

```
double rand_Landau(double c=1, double mu=0)
{
    const double Pi_2=M_PI/2.;
    double V=rand_uni(-Pi_2,Pi_2);
    double E=rand_exp();

    double X = ((Pi_2+V)*tan(V) - log((Pi_2*E*cos(V))/(Pi_2+V)) )/Pi_2;
    return c*X+c*log(c)/Pi_2 + mu;
}
```

In Fig. A.1, we compare the right tail of a Landau distribution (in red) of parameters $c = 1$ and $\mu = 0$:

```
    rand_Landau();
```

to the tail of a Pareto distribution (in green) of parameters $\alpha = 1$, $C = 2 * c/\pi$, $\beta = 1$ and $\mu = 0$:

```
    double c=1.;
    rand_Pareto_b1(1., 2*c/pi);
```

The figure also exhibit the theoretical curve for the Pareto distribution (in blue):

$$p(x) = \begin{cases} \dfrac{2\,c/\pi}{x^2}\,, & \text{if } x \geqslant b = 2\,c \\ 0\,, & \text{otherwise}\,. \end{cases} \tag{A.47}$$

The log-log scale curves on the right panel show that the two distributions have the same asymptotic behaviour on $+\infty$.

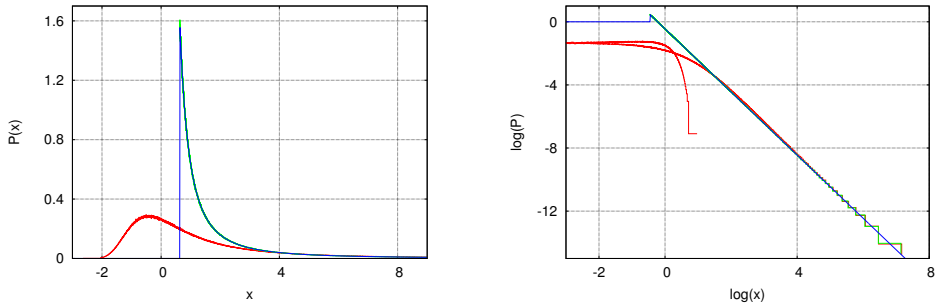

Figure A.1: Numerical simulation of a Landau distribution (blue) vs a Pareto distribution (green). The blue curve corresponds to the theoretical Pareto distribution Eq. (A.47). Log-log scale on the right panel.

5 COMPUTATIONAL METHOD FOR SIMULATING BRANCHING RANDOM WALKS

A.5.1 General algorithm

Branching random walks can be followed in generation n or in time t. Starting with one particle in the system, we still may have to follow more than one particle at a time. The main difficulty in simulating this type of walks is to find a way to deal with the fluctuating number of particles in the system. To tackle this problem with a simple program, the easiest way is to use a list containing the current particles and to follow particles in generation. For the sake of simplicity, I will discuss here an example in one dimension. The generalisation of the full code in higher dimension can be then obtained by generalising each jump in higher dimension.

Let us first define a structure for each particle,

```
struct particle_
{
    int n;     //generation n>=0
    double t;  //time of the last collision
    double x;  //coordinate x of the last collision in V
    int w;     //direction = +1 or -1
    double v;   //current speed (may change at each collision)
};
typedef struct particle_ particle;
```

and then a function that will transport a particle exiting a collision to its next collision point (taking as argument a pointer to particle):

```
void diffuse(particle *M)
{
    (*M).n ++;                      //generation +1
    (*M).w = direction1D((*M).w);   //change direction
    double l=jump();
    (*M).x += (*M).w*l; //position of the next collision
    (*M).t += l/(*M).v; //time at the next collision
    //change the speed if needed
}
```

where `doublejump()` is a function that gives the random length of a jump for the considered random walk (see Appendix 4 concerning the generation of random variables), and `int direction1D(int)` returns the new direction of the particle after the collision (isotropically distributed or not).

To take into account the fluctuations of the number of particles in the system and follow simultaneously several particles, the simplest way is to store every particles at each generation in a list, using for instance the `list` class provided by the C++ STL.

Let us write the main transport:
Initialisation – we start with one particle `M0` in the list

```
particle M0={0, 0, x0, w0, v0};  //1st particle at n=0
list<particle> li;   //contains particles of the current generation
```

For the need of the loop, we introduce a list buffer, where we store the particles that stay alive from one generation to the next:

```
list<particle> li_buffer;  //buffer
li_buffer.push_back(M0);   //starts with the initial particle
```

Loop – the loop is taken over the generations and runs while there are still particles in the buffer. To be sure that the loop will stop, we impose a maximum generation `nmax` (or a maximum time `tmax`). The algorithm for the loop is the following:

⟶ empty the buffer `li_buffer` in the list `li` of current particles;
⟶ for each particle of `li`:
- with probability p_1: `//transport`
  - transport the particle until the next collision
  - if the new position is still in V and the generation `n<nmax`, add the particle to the buffer
- with probability p_k: `//branching`
  - create k copies of the particle
  - for each copy:
    - transport the particle until the next collision
    - if the new position is still in V and the generation `n<nmax`, add the particle to the buffer
- with probability p_0, do nothing `//absorption`

For transport in a finite domain V, after transporting each particle, we check if the particle is still in the considered volume. To follow the particle in time, we keep particles in the loop as long as their current time $t < tmax$.

Example for a binary branching (p_0, p_1, p_2):

```
//variables
particle M;
bool V;
double dummy;
list<particle>::const_iterator l_head;
//loops
```

```
while (!li_buffer.empty()) {
    li_buffer.swap(li);//exchange li_buffer and li

    for(l_head=li.begin(); l_head!=li.end(); ++l_head)
    //for each element of li
    {
        M=*l_head;
        dummy=drand48();

        if (dummy < p_1) { //transport
            V=transport(&M);
            if (V && M_act.t < tmax )
                { li_buffer.push_back(M_act); }
        }
        else if (dummy < p_1+p_2){ //branching
            M2 = M;
            V=transport(&M);
            if (V && M_act.t < tmax )
                { li_buffer.push_back(M); }

            V=transport(&M2);
            if (V && M_act2.t < tmax )
                { li_buffer.push_back(M2); }
            }
        }
    li.clear();
}
```

where the functions `bool transport(particle* M)` transports the particle `M` to its next collision (calling the function `void diffuse(particle *M)`), records the interesting quantity (see the following section), and returns a Boolean variable, `true` if the particle is still within the finite domain V, `false` otherwise.

A.5.2 Details for each simulation

a. Travelled length and number of collisions

Any quantity of interest is then recorded during this loop. For instance, in Sec. II.3.1 and Chapter IV, we compute the total length travelled by `M0` and all its descendants until a certain time (or generation), or the total number of collisions encountered by these particles. For Sec. II.3.1, a first average of these quantities is obtained by averaging over the different realisations of the system (starting with the same initial particle `M0`). In Chapter IV, the average is also taken over the possible positions and directions taken by

the initial particles. Using this algorithm it is then possible to compute any moment of the total length travelled by particles, or the total number of collisions undergone in a finite domain V.

b. Clustering and pair correlation function

Free systems – Concerning the clustering of neutrons discussed in Chapter III, the pair correlation function corresponds exactly to the histogram of the distances between each pair of particles in the system at a given time t. Thus, to simulate numerically the pair correlation functions appearing in the different figures of Chapter III, we start with an initial number N_0 of particles in the list of particles `li_buffer`, and, using the previous algorithm, we let the system evolve up to a time t (loop); we finally compute the inter-particle distance histogram, which gives the pair correlation function $g(\mathbf{x}, \mathbf{y}, t)$ at time t.

Controlled systems – Adding the control, we further need to implement the control procedure described in Sec. III.3.1. In the previous algorithm, every time we copy one particle in the system we must now kill another particle of the system. As the number of particles in the system is now constant (always equal to N_0), an array will be now more convenient than a list to store the N_0 particles. Furthermore there is now a faster way to simulate this system up to a time t. Indeed, one particle gives rise to $k-1$ new particles (and $k-1$ other particles are killed) with a rate λ_k, so that we obtain the following algorithm: with a rate $N_0\lambda_k$ one of the N_0 particles is randomly chosen; $k-1$ other randomly chosen particles are then replaced by a copy of this particle. Between two events of this type, particles evolve as Brownian particles. We then let the system evolve up to a time t, and compute the pair correlation function (inter-particle distance histogram).

INDEX

BIBLIOGRAPHY

N. Agmon. The residence time equation. *Chemical Physics Letters*, 497(4): 184–186, 2010. *Cited at page 167*

N. Agmon. Single molecule diffusion and the solution of the spherically symmetric residence time equation. *The Journal of Physical Chemistry A*, 115(23):5838–5846, 2011. *Cited at page 63*

E. S. Andersen. On the fluctuations of sums of random variables ii. *Math. Scand*, 2(195-223):3, 1954. *Cited at pages 185 and 186*

E. S. Anderson. On the fluctuations of sums of random variables. *Math. Scand*, 1:263–285, 1953. *Cited at page 187*

R. Antoni and L. Bourgois. *Physique appliquée à l'exposition externe: Dosimétrie et radioprotection*. Springer Science & Business Media, 2013. *Cited at page 17*

W. Appel. *Probabilités pour les non-probabilistes*. H& K, 2013. *Cited at page 72*

L. F. A. Arbogast. *Du Calcul des derivations*. 1800. *Cited at pages 73, 221, 222, and 223*

K. B. Athreya and P. E. Ney. *Branching processes*, volume 196. Springer Science & Business Media, 2012a. *Cited at pages 55 and 89*

K. B. Athreya and P. E. Ney. *Branching processes*, volume 196. Springer Science & Business Media, 2012b. *Cited at page 45*

F. Aurzada and T. Simon. Persistence probabilities\ & exponents. *arXiv preprint arXiv:1203.6554*, 2012. *Cited at page 190*

N. T. J. Bailey. *The Mathematical Theory of Infectious Diseases and its Applications*. London: Griffin, 1968. *Cited at page 89*

A. Baldassarri, J. Bouchaud, I. Dornic, and C. Godreche. Statistics of persistent events: An exactly soluble model. *Physical Review E*, 59(1):R20, 1999. *Cited at page 186*

A. Barbarino, S. Dulla, and P. Ravetto. Integral neutron transport and new computational methods: A review. In *Integral Methods in Science and Engineering*, pages 41–56. Springer, 2013. *Cited at page 37*

J. Bardsley and A. Dubi. The average transport path length in scattering media. *SIAM Journal on Applied Mathematics*, 40(1):71–77, 1981. *Cited at pages 143 and 151*

P. Barthelemy, J. Bertolotti, and D. S. Wiersma. A lévy flight for light. *Nature*, 453(7194):495–498, 2008. *Cited at pages 46, 47, 48, and 211*

P. Barthelemy, J. Bertolotti, K. Vynck, S. Lepri, and D. S. Wiersma. Role of quenching on superdiffusive transport in two-dimensional random media. *Physical Review E*, 82(1):011101, 2010. *Cited at pages 47 and 211*

C. Beenakker, C. Groth, and A. Akhmerov. Nonalgebraic length dependence of transmission through a chain of barriers with a lévy spacing distribution. *Physical Review B*, 79(2):024204, 2009. *Cited at page 211*

D. Behrens. The effect of holes in a reacting material on the passage of neutrons. *Proceedings of the Physical Society. Section A*, 62(10):607, 1949. *Cited at page 47*

E. T. Bell. Partition polynomials. *Annals of Mathematics*, pages 38–46, 1927. *Cited at page 222*

G. I. Bell. On the stochastic theory of neutron transport. *Nuclear Science and Engineering*, 21(3):390–401, 1965. *Cited at pages 55, 82, 83, 100, and 103*

G. I. Bell and S. Glasstone. *Nuclear Reactor Theory*. Van Nostrand Reinhold Company, 1970. *Cited at pages 9, 10, 11, 13, 22, 23, 24, 28, 29, 30, 31, 33, 35, 37, 41, 63, 67, 75, 90, and 142*

O. Bénichou, M. Coppey, M. Moreau, P. Suet, and R. Voituriez. Averaged residence times of stochastic motions in bounded domains. *EPL (Europhysics Letters)*, 70(1):42, 2005. *Cited at pages 63, 143, 144, 146, 148, 149, 151, 167, 168, and 176*

O. Bénichou, C. Loverdo, M. Moreau, and R. Voituriez. Intermittent search strategies. *Reviews of Modern Physics*, 83(1):81, 2011. *Cited at page 176*

A. M. Berezhkovskii, V. Zaloj, and N. Agmon. Residence time distribution of a brownian particle. *Physical Review E*, 57(4):3937, 1998. *Cited at pages 63 and 167*

P. Bernabó, R. Burioni, S. Lepri, and A. Vezzani. Anomalous transmission and drifts in one-dimensional lévy structures. *Chaos, Solitons & Fractals*, 67:11–19, 2014. *Cited at pages 47, 48, and 211*

A. T. Bharucha-Reid. *Elements of the Theory of Markov Processes and Their Applications*. New York:Academic, 1968. *Cited at page 89*

G. Biroli, J.-P. Bouchaud, and M. Potters. On the top eigenvalue of heavy-tailed random matrices. *EPL (Europhysics Letters)*, 78(1):10001, 2007. *Cited at page 181*

S. Blanco and R. Fournier. An invariance property of diffusive random walks. *EPL (Europhysics Letters)*, 61(2):168, 2003. *Cited at pages 143, 144, 156, 159, and 176*

S. Blanco and R. Fournier. Short-path statistics and the diffusion approximation. *Physical review letters*, 97(23):230604, 2006. *Cited at pages 63 and 156*

S. Borak, W. Härdle, and R. Weron. Stable distributions. In *Statistical tools for finance and insurance*, pages 21–44. Springer, 2005. *Cited at page 231*

J.-P. Bouchaud and A. Georges. Anomalous diffusion in disordered media: statistical mechanisms, models and physical applications. *Physics reports*, 195(4):127–293, 1990. *Cited at page 181*

A. Brahme and J. Kempe. *Comprehensive Biomedical Physics, Vol 9: Radiation Therapy Physics and Treatment Optimization, Chap 2: Particle Transport Theory and Absorbed Dose*. Elsevier, 2014. *Cited at page 144*

A. J. Bray, S. N. Majumdar, and G. Schehr. Persistence and first-passage properties in nonequilibrium systems. *Advances in Physics*, 62(3):225–361, 2013. *Cited at page 184*

E. Brun, E. Dumonteil, F. Hugot, N. Huot, C. Jouanne, Y. Lee, F. Malvagi, A. Mazzolo, O. Petit, J. Trama, et al. Overview of tripoli-4 version 7, continuous-energy monte carlo transport code. 2011. *Cited at pages 44 and 65*

E. Brun, F. Damian, E. Dumonteil, F.-X. Hugot, Y.-K. Lee, F. Malvagi, A. Mazzolo, O. Petit, J.-C. Trama, T. Visonneau, et al. Tripoli-4 r version 8 user guide. Technical report, CEA Saclay, Direction de l'Energie Nucleaire, Departement de Modelisation des Systemes et Structures, Service d'etudes des Reacteurs et de Mathematiques Appliquees, DEN/-DANS/DM2S/SERMA/LTSD, CEA/Saclay, 91191 Gif-sur-Yvette Cedex (France), 2013. *Cited at pages 44, 65, and 90*

E. Brunet and B. Derrida. Statistics at the tip of a branching random walk and the delay of traveling waves. *EPL (Europhysics Letters)*, 87(6):60010, 2009. *Cited at pages 84 and 89*

P. Buonsante, R. Burioni, and A. Vezzani. Transport and scaling in quenched two-and three-dimensional lévy quasicrystals. *Physical Review E*, 84(2):021105, 2011. *Cited at pages 47 and 211*

R. Burioni, L. Caniparoli, S. Lepri, and A. Vezzani. Lévy-type diffusion on one-dimensional directed cantor graphs. *Physical Review E*, 81(1):011127, 2010. *Cited at page 211*

J. Bussac and P. Reuss. *Traité de neutronique: Physique et calcul des réacteurs nucléaires avec application aux réacteurs à eau pressurisée et aux réacteurs à neutrons rapides*. 1978. *Cited at pages 7 and 10*

K. M. Case and P. F. Zweifel. *Linear transport theory*. Addison-Wesley, 1967. *Cited at pages 36, 37, 46, 142, and 157*

CEA collectif, M. Coste-Delclaux, C. Diop, A. Nicolas, and B. Bonin. *Neutronique*. CEA Saclay; Groupe Moniteur, 2013. *Cited at pages 19, 28, 37, 66, 67, and 90*

C. Cercignani. *The Boltzmann equation and its applications*. Springer New York, 1988. *Cited at page 28*

J. Chadwick. Possible existence of a neutron. *Nature*, 129(3252):312, 1932. *Cited at page 28*

M. Challet, V. Fourcassie, S. Blanco, R. Fournier, G. Theraulaz, and C. Jost. A new test of random walks in heterogeneous environments. *Naturwissenschaften*, 92(8):367–370, 2005. *Cited at page 144*

J. M. Chambers, C. L. Mallows, and B. Stuck. A method for simulating stable random variables. *Journal of the American statistical association*, 71 (354):340–344, 1976. *Cited at page 233*

S. Chandrasekhar. Stochastic problems in physics and astronomy. *Reviews of modern physics*, 15(1):1, 1943. *Cited at page 142*

A. V. Chechkin, R. Metzler, V. Y. Gonchar, J. Klafter, and L. V. Tanatarov. First passage and arrival time densities for lévy flights and the failure of the method of images. *Journal of Physics A: Mathematical and General*, 36 (41):L537, 2003. *Cited at page 185*

K. L. Chung. *Lectures from Markov processes to Brownian motion*, volume 249. Springer Science & Business Media, 2013. *Cited at page 12*

L. Comtet. *Advanced Combinatorics: The art of finite and infinite expansions*. Springer Science & Business Media, 1974. *Cited at page 222*

S. Condamin, O. Bénichou, V. Tejedor, R. Voituriez, and J. Klafter. First-passage times in complex scale-invariant media. *Nature*, 450(7166):77–80, 2007. *Cited at page 63*

R. Courant and D. Hilbert. *Methods of Mathematical Physics Vol. 2 (Partial Differential Equations)*. *Cited at page 33*

D. Cox and P. Lewis. The statistical analysis of series of events. 1966. *Cited at page 56*

J. T. Cox and D. Griffeath. Occupation times for critical branching brownian motions. *The Annals of Probability*, pages 1108–1132, 1985. *Cited at pages 89, 135, and 167*

A. D. Craik. Prehistory of faà di bruno's formula. *American Mathematical Monthly*, pages 119–130, 2005. *Cited at pages 73, 83, and 222*

A. Davis and A. Marshak. Lévy kinetics in slab geometry: Scaling of transmission probability, 1997. *Cited at pages 48 and 211*

A. B. Davis. Effective propagation kernels in structured media with broad spatial correlations, illustration with large-scale transport of solar photons through cloudy atmospheres. In *Computational Methods in Transport*, pages 85–140. Springer, 2006. *Cited at page 46*

A. B. Davis and A. Marshak. Photon propagation in heterogeneous optical media with spatial correlations: enhanced mean-free-paths and wider-than-exponential free-path distributions. *Journal of Quantitative Spectroscopy and Radiative Transfer*, 84(1):3–34, 2004. *Cited at pages 46 and 47*

D. Dawson. The critical measure diffusion process. *Zeitschrift für Wahrscheinlichkeitstheorie und Verwandte Gebiete*, 40(2):125–145, 1977. *Cited at page 89*

L. De Broglie. *Recherches sur la théorie des quanta*. PhD thesis, 1924. *Cited at page 9*

C. De Mulatier, A. Rosso, and G. Schehr. Asymmetric lévy flights in the presence of absorbing boundaries. *Journal of Statistical Mechanics: Theory and Experiment*, 2013(10):P10006, 2013. *Cited at pages xiii, 3, 180, and 217*

C. De Mulatier, A. Mazzolo, and A. Zoia. Universal properties of branching random walks in confined geometries. *EPL (Europhysics Letters)*, 107(3): 30001, 2014. *Cited at pages xii, 2, 155, and 217*

C. de Mulatier, A. Zoia, A. Rosso, and C. M. Diop. Generalisation of opacity formulas for neutron transport. In *SNA+ MC 2013-Joint International Conference on Supercomputing in Nuclear Applications+ Monte Carlo*, page 05304. EDP Sciences, 2014. *Cited at pages x, 215, and 216*

C. de Mulatier, E. Dumonteil, A. Rosso, and A. Zoia. The critical catastrophe revisited. *Journal of Statistical Mechanics: Theory and Experiment*, 2015 (8):P08021, 2015. *Cited at pages xi, 2, 88, 135, and 216*

B. Derrida and D. Simon. The survival probability of a branching random walk in presence of an absorbing wall. *EPL (Europhysics Letters)*, 78(6): 60006, 2007. *Cited at page 84*

B. Diu, C. Guthmann, and D. Lederer. *Thermodynamique*. Hermann, 2007. *Cited at page 42*

M. Dixmier. Une nouvelle description des empilements aléatoires et des fluides denses. *Journal de Physique*, 39(8):873–895, 1978. *Cited at page 173*

J. J. Duderstadt and L. J. Hamilton. *Nuclear reactor analysis*. John Wiley and Sons, Inc., New York, 1976. *Cited at pages 21, 22, 62, and 84*

J. J. Duderstadt and W. R. Martin. Transport theory. *Transport theory., by Duderstadt, JJ; Martin, WR. Chichester (UK): John Wiley & Sons, 10+ 613 p.*, 1, 1979. *Cited at pages 28, 35, 36, 41, 42, 46, and 142*

S. Dulla, R. Sanchez, and P. Ravetto. Neutron transport and diffusion models for molten-salt reactor dynamics. Technical report, American Nuclear Society, 555 North Kensington Avenue, La Grange Park, IL 60526 (United States), 2006. *Cited at page 30*

S. Dulla, E. H. Mund, and P. Ravetto. The quasi-static method revisited. *Progress in Nuclear Energy*, 50(8):908–920, 2008. *Cited at page 28*

S. Dulla, E. Mund, and P. Ravetto. The quasi-static method for nuclear reactor kinetics: a review and a look ahead. *Transactions of the American Nuclear Society*, 104:872–874, 2011. *Cited at page 28*

E. Dumonteil, F. Malvagi, A. Zoia, A. Mazzolo, D. Artusio, C. Dieudonné, and C. De Mulatier. Particle clustering in monte carlo criticality simulations. *Annals of Nuclear Energy*, 63:612–618, 2014. *Cited at pages ix, 1, 43, 44, 45, 84, 88, 90, 135, and 215*

B. Dybiec, E. Gudowska-Nowak, and P. Hänggi. Lévy-brownian motion on finite intervals: Mean first passage time analysis. *Physical Review E*, 73(4): 046104, 2006. *Cited at page 190*

B. Dybiec, E. Gudowska-Nowak, and P. Hänggi. Escape driven by α-stable white noises. *Physical Review E*, 75(2):021109, 2007. *Cited at page 186*

E. B. Dynkin. *Markov processes*. Springer, 1965. *Cited at page 71*

B. S. Everitt and A. Skrondal. *The Cambridge dictionary of statistics*. Cambridge University Press, 2002. *Cited at page 57*

F. Faà di Bruno. *Sullo sviluppo delle funzioni*, volume 6. 1855. *Cited at pages 73, 83, 221, 222, and 223*

U. Fano. Ionization yield of radiations. ii. the fluctuations of the number of ions. *Physical Review*, 72(1):26, 1947. *Cited at page 56*

W. Feller. *An Introduction to Probability Theory, volume I*. 1968. *Cited at page 181*

W. Feller. *An introduction to probability theory and its applications*, volume 2. John Wiley & Sons, 2008. *Cited at page 163*

H. C. Fogedby. Lévy flights in random environments. *Physical review letters*, 73(19):2517, 1994. *Cited at page 47*

M. Frank and T. Goudon. On a generalized boltzmann equation for non-classical particle transport. *Kinetic and Related Models*, 3:395–407, 2010. *Cited at page 47*

R. García-García, A. Rosso, and G. Schehr. Lévy flights on the half line. *Physical Review E*, 86(1):011101, 2012. *Cited at page 193*

A. Gelimson and R. Golestanian. Collective dynamics of dividing chemotactic cells. *Phys. Rev. Lett.*, 114:028101, Jan 2015. *Cited at page 116*

E. Gobet. *Méthodes de Monte-Carlo et processus stochastiques: du linéaire au non-linéaire*. Editions de l'Ecole Polytechnique, 2013. *Cited at pages 19 and 228*

I. Golding, Y. Kozlovsky, I. Cohen, and E. Ben-Jacob. Studies of bacterial branching growth using reaction–diffusion models for colonial development. *Physica A: Statistical Mechanics and its Applications*, 260(3):510–554, 1998. *Cited at page 89*

G. Gradenigo, A. Sarracino, D. Villamaina, T. S. Grigera, and A. Puglisi. The ratchet effect in an ageing glass. *Journal of Statistical Mechanics: Theory and Experiment*, 2010(12):L12002, 2010. *Cited at page 181*

D. Grebenkov. Residence times and other functionals of reflected brownian motion. *Physical Review E*, 76(4):041139, 2007. *Cited at pages 63 and 167*

D. S. Grebenkov and B.-T. Nguyen. Geometrical structure of laplacian eigenfunctions. *SIAM Reviews*, 55:601–667, 2013. *Cited at pages 108 and 112*

G. Grimmett and D. Stirzaker. *Probability and random processes*. Oxford university press, 2001. *Cited at pages 67 and 80*

M. Grimod. *Neutronic modeling of pebble bed reactors in APOLLO2*. Theses, Université Paris Sud - Paris XI, Dec. 2010. *Cited at page 47*

C. Groth, A. Akhmerov, and C. Beenakker. Transmission probability through a lévy glass and comparison with a lévy walk. *Physical Review E*, 85(2):021138, 2012. *Cited at pages 47 and 211*

T. E. Harris. *The Theory of Branching Processes*. Springer-Verlag, Berlin, 1963. *Cited at pages 18, 55, 56, 58, 76, 84, and 89*

W. Heisenberg. *The physical principles of the quantum theory*. Dover Publ., first publication 1930, 2013. *Cited at page 9*

C. C. Heyde and E. Seneta. *IJ Bienaymé: statistical theory anticipated*, volume 3. Springer-Verlag, New York, 1977. *Cited at page 18*

B. Houchmandzadeh. Clustering of diffusing organisms. *Physical Review E*, 66(5):052902, 2002. *Cited at pages 45 and 94*

B. Houchmandzadeh. Neutral clustering in a simple experimental ecological community. *Physical review letters*, 101(7):078103, 2008. *Cited at pages 45, 89, 94, and 96*

B. Houchmandzadeh. Theory of neutral clustering for growing populations. *Physical Review E*, 80(5):051920, 2009. *Cited at pages 45, 56, 89, 94, 95, 96, 99, 105, 130, 135, and 224*

B. D. Hughes. Random walks and random environments. 1996. *Cited at pages 12, 19, 181, and 183*

P. Jagers et al. *Branching processes with biological applications*. London:Wiley, 1975. *Cited at page 89*

R. Jeanson, S. Blanco, R. Fournier, J.-L. Deneubourg, V. Fourcassié, and G. Theraulaz. A model of animal movements in a bounded space. *Journal of Theoretical Biology*, 225(4):443–451, 2003. *Cited at page 144*

R. Jeanson, C. Rivault, J.-L. Deneubourg, S. Blanco, R. Fournier, C. Jost, and G. Theraulaz. Self-organized aggregation in cockroaches. *Animal behaviour*, 69(1):169–180, 2005. *Cited at page 144*

M. Kac. On distributions of certain wiener functionals. *Transactions of the American Mathematical Society*, 65(1):1–13, 1949. *Cited at pages 63 and 67*

M. Kac. On some connections between probability theory and differential and integral equations. *Proc. 2nd Berkeley Symp. on Mathematical Statistics and Probability*, pages 189–215, 1951. *Cited at page 67*

L. P. Kadanoff. *Statics, Dynamics and Renormalization*. World Scientific, 2000. *Cited at page 60*

M. H. Kalos and P. A. Whitlock. *Monte carlo methods*. John Wiley & Sons, 2008. *Cited at pages 11, 12, and 13*

E. Kennard. Zur quantenmechanik einfacher bewegungstypen. *Zeitschrift für Physik*, 44(4-5):326–352, 1927. *Cited at page 9*

T. Koren, A. Chechkin, and J. Klafter. On the first passage time and leapover properties of lévy motions. *Physica A: Statistical Mechanics and its Applications*, 379(1):10–22, 2007a. *Cited at pages 181 and 186*

T. Koren, M. A. Lomholt, A. V. Chechkin, J. Klafter, and R. Metzler. Leapover lengths and first passage time statistics for lévy flights. *Physical review letters*, 99(16):160602, 2007b. *Cited at page 186*

A. Kostinski and R. Shaw. Scale-dependent droplet clustering in turbulent clouds. *Journal of fluid mechanics*, 434:389–398, 2001. *Cited at page 46*

W. Krauth. *Statistical mechanics: algorithms and computations*, volume 13. OUP Oxford, 2006. *Cited at pages 19, 67, and 195*

E. W. Larsen and R. Vasques. A generalized linear boltzmann equation for non-classical particle transport. *Journal of Quantitative Spectroscopy and Radiative Transfer*, 112(4):619–631, 2011. *Cited at pages 43, 46, 47, and 48*

D. J. Lawson and H. J. Jensen. Neutral evolution in a biological population as diffusion in phenotype space: reproduction with local mutation but without selection. *Physical review letters*, 98(9):098102, 2007. *Cited at page 89*

J. F. Le Gall. *Spatial Branching Processes, Random Snakes and Partial Differential Equations*. Zurich: Birkhäuser, 2012. *Cited at page 89*

P. Levitz. Random flights in confining interfacial systems. *Journal of Physics: Condensed Matter*, 17(49):S4059, 2005. *Cited at page 144*

P. Lévy. *Calcul des probabilités*, volume 9. Gauthier-Villars Paris, 1925. *Cited at page 231*

J. Lieberoth and A. Stojadinović. Neutron streaming in pebble beds. *Nuclear Science and Engineering*, 76(3):336–344, 1980. *Cited at page 47*

M. A. Lomholt, T. Ambjörnsson, and R. Metzler. Optimal target search on a fast-folding polymer chain with volume exchange. *Physical review letters*, 95(26):260603, 2005. *Cited at page 181*

I. Lux and L. Koblinger. *Monte Carlo particle transport methods: neutron and photon calculations*, volume 102. CRC press Boca Raton, 1991. *Cited at pages 14, 63, 64, and 80*

D. G. Madland and J. R. Nix. New Calculation of Prompt Fission Neutron Spectra and Average Prompt Neutron Multiplicities. *Nuclear Science and Engineering*, 81(2):213–271, June 1982. *Cited at page 17*

S. N. Majumdar. Persistence in nonequilibrium systems. *Current Science*, 77:370, 1999. *Cited at page 184*

S. N. Majumdar. Brownian functionals in physics and computer science. *CURRENT SCIENCE-BANGALORE-*, 89(12):2076, 2005. *Cited at page 67*

S. N. Majumdar, G. Schehr, and G. Wergen. Record statistics and persistence for a random walk with a drift. *Journal of Physics A: Mathematical and Theoretical*, 45(35):355002, 2012. *Cited at page 208*

S. N. Majumdar, G. Schehr, D. Villamaina, and P. Vivo. Large deviations of the top eigenvalue of large cauchy random matrices. *Journal of Physics A: Mathematical and Theoretical*, 46(2):022001, 2013. *Cited at page 181*

B. Mandelbrot. The variation of certain speculative prices. *The Journal of Business*, 36(4):pp. 394–419, 1963. *Cited at page 181*

A. Mazzolo. Properties of diffusive random walks in bounded domains. *EPL (Europhysics Letters)*, 68(3):350, 2004. *Cited at pages 63, 143, 148, 151, 160, and 173*

A. Mazzolo. An invariance property of generalized pearson random walks in bounded geometries. *Journal of Physics A: Mathematical and Theoretical*, 42(10):105002, 2009. *Cited at pages 148, 159, 160, and 169*

A. Mazzolo, B. Roesslinger, and W. Gille. Properties of chord length distributions of nonconvex bodies. *Journal of Mathematical Physics*, 44:6195–6208, 2003. *Cited at pages 143 and 168*

A. Mazzolo, C. De Mulatier, and A. Zoia. Cauchy's formulas for random walks in bounded domains. *Journal of Mathematical Physics*, 55(8):083308, 2014. *Cited at pages xii, 2, 168, 173, and 216*

N. Mercadier, W. Guerin, M. Chevrollier, and R. Kaiser. Lévy flights of photons in hot atomic vapours. *Nature physics*, 5(8):602–605, 2009. *Cited at pages 46 and 181*

R. Metzler and J. Klafter. The random walk's guide to anomalous diffusion: a fractional dynamics approach. *Physics reports*, 339(1):1–77, 2000. *Cited at pages 47 and 181*

M. Meyer, S. Havlin, and A. Bunde. Clustering of independently diffusing individuals by birth and death processes. *Physical Review E*, 54(5):5567, 1996. *Cited at pages 89, 96, 116, 117, 118, 119, 121, 124, 125, 127, 130, 134, and 135*

M. F. Modest. *Radiative heat transfer*. Academic press, 2013. *Cited at page 142*

J. D. Murray. *Mathematical Biology*. Berlin: Springer, 1989. *Cited at page 89*

J. P. Nolan. *Stable distributions*, volume 1177108605. ISBN, 2012. *Cited at page 155*

J. D. Northum and S. B. Guetersloh. The application of microdosimetric principles to radiation hardness testing. *Science and Technology of Nuclear Installations*, 2014. *Cited at page 144*

L. Pal. Nuovo cimento. *VII (Suppl.)*, page 25, 1958. *Cited at page 82*

V. Pareto. *Cours d'économie politique*. Librairie Droz, 1964. *Cited at page 181*

I. Pázsit and L. Pál. *Neutron fluctuations: a treatise on the physics of branching processes*. Elsevier, 2007. *Cited at pages 55, 63, 69, 74, 80, 81, 82, 83, 84, 89, 100, 103, and 147*

R. Pierrat, P. Ambichl, S. Gigan, A. Haber, R. Carminati, and S. Rotter. Invariance property of wave scattering through disordered media. *Proceedings of the National Academy of Sciences*, 111(50):17765–17770, 2014. *Cited at page 176*

J. Pitman. *Combinatorial Stochastic Processes: Ecole D'Eté de Probabilités de Saint-Flour XXXII-2002*. Springer, 2006. *Cited at pages 73 and 222*

B. Podobnik, A. Valentinčič, D. Horvatić, and H. E. Stanley. Asymmetric lévy flight in financial ratios. *Proceedings of the National Academy of Sciences*, 108(44):17883–17888, 2011. *Cited at page 181*

S. D. Poisson and C. H. Schnuse. *Recherches sur la probabilité des jugements en matière criminelle et en matière civile*. Meyer, 1841. *Cited at pages 13 and 56*

A. D. Polyanin. *Nonhomogeneous Heat Equation* at eqworld. http://eqworld.ipmnet.ru/en/solutions/lpde/lpde102.pdf. *Cited at pages 108 and 112*

A. D. Polyanin. *Handbook of linear partial differential equations for engineers and scientists*. CRC press, 2001. *Cited at pages 108 and 112*

G. C. Pomraning. *Linear kinetic theory and particle transport in stochastic mixtures*, volume 7. World Scientific, 1991. *Cited at pages 11, 12, 21, 31, 33, 35, 39, and 41*

A. K. Prinja. Notes on the lumped backward master equation for the neutron extinction/survival probability. Technical report, Los Alamos National Laboratory (United States). Funding organisation: DOE/LANL (United States), 2012. *Cited at pages 45, 62, and 84*

K. Ramola, S. N. Majumdar, and G. Schehr. Universal order and gap statistics of critical branching brownian motion. *Physical Review Letters*, 112 (21):210602, 2014. *Cited at page 89*

K. Ramola, S. N. Majumdar, and G. Schehr. Spatial extent of branching brownian motion. *Physical Review E*, 91(4):042131, 2015. *Cited at page 89*

J. Randon-Furling. A bijection between markovian and non-markovian persistence exponents. *arXiv preprint arXiv:1412.7393*, 2014. *Cited at page 208*

S. Redner. *A guide to first-passage processes*. Cambridge University Press, 2001. *Cited at pages 83, 108, and 146*

P. Reuss. *Précis de neutronique*. EDP Sciences, 2003. *Cited at page 29*

P. Reuss. *Neutron physics*. EDP sciences, 2012. *Cited at pages 6, 7, 9, 10, 12, 15, 17, 22, 24, 25, 26, 29, 36, 37, 142, and 149*

S. Ross. *Simulation*. Academic Press, 2013. ISBN 9780124158252. *Cited at page 13*

D. Rozon. *Introduction to nuclear reactor kinetics*. Polytechnic International, 1998. *Cited at page 10*

G. Samoradnitsky and M. S. Taqqu. *Stable non-Gaussian random processes: stochastic models with infinite variance*, volume 1. CRC Press, 1994. *Cited at pages 182 and 231*

L. A. Santaló. *Integral geometry and geometric probability*. Cambridge University Press, first publication 1976, 2004. *Cited at pages 142 and 148*

S. Sawyer and J. Fleischman. Maximum geographic range of a mutant allele considered as a subtype of a brownian branching random field. *Proceedings of the National Academy of Sciences*, 76(2):872–875, 1979. *Cited at pages 89 and 167*

T. Scholl, K. Pfeilsticker, A. Davis, H. Klein Baltink, S. Crewell, U. Löhnert, C. Simmer, J. Meywerk, and M. Quante. Path length distributions for solar photons under cloudy skies: Comparison of measured first and second moments with predictions from classical and anomalous diffusion theories. *Journal of Geophysical Research: Atmospheres (1984–2012)*, 111(D12), 2006. *Cited at page 47*

P. M. Schwarz and J. H. Schwarz. *Special relativity: from Einstein to strings*. Cambridge University Press, 2004. *Cited at page 7*

M. F. Shlesinger, G. M. Zaslavsky, and U. Frisch. Lévy flights and related topics in physics. In *Levy flights and related topics in Physics*, volume 450, 1995. *Cited at page 181*

J. Spanier and E. M. Gelbard. *Monte Carlo principles and neutron transport problems*. Addison-Wesley Publ., Reading, 1969. *Cited at pages 14, 19, 28, and 63*

T. Svensson, K. Vynck, M. Grisi, R. Savo, M. Burresi, and D. S. Wiersma. Holey random walks: Optics of heterogeneous turbid composites. *Physical Review E*, 87(2):022120, 2013. *Cited at pages 46 and 48*

T. Svensson, K. Vynck, E. Adolfsson, A. Farina, A. Pifferi, and D. S. Wiersma. Light diffusion in quenched disorder: Role of step correlations. *Physical Review E*, 89(2):022141, 2014. *Cited at pages 46, 47, 48, and 211*

J. Terrell. Distributions of Fission Neutron Numbers. *Physical Review*, 108 (3):783–789, Nov. 1957. *Cited at page 17*

D. Tilman and P. M. Kareiva. *Spatial ecology: the role of space in population dynamics and interspecific interactions*, volume 30. Princeton University Press, 1997. *Cited at page 89*

V. V. Tuchin. *Tissue optics: light scattering methods and instruments for medical diagnosis*. SPIE press Bellingham, 2007. *Cited at page 142*

L. Turgeman, S. Carmi, and E. Barkai. Fractional feynman-kac equation for non-brownian functionals. *Physical review letters*, 103(19):190201, 2009. *Cited at page 67*

R. Vasques and E. W. Larsen. Non-classical particle transport with angular-dependent path-length distributions. i: Theory. *Annals of Nuclear Energy*, 70:292–300, 2014a. *Cited at page 47*

R. Vasques and E. W. Larsen. Non-classical particle transport with angular-dependent path-length distributions. ii: Application to pebble bed reactor cores. *Annals of Nuclear Energy*, 70:301–311, 2014b. *Cited at page 47*

A. Vezzani, R. Burioni, L. Caniparoli, and S. Lepri. Local and average behaviour in inhomogeneous superdiffusive media. *Philosophical Magazine*, 91(13-15):1987–1997, 2011. *Cited at page 211*

G. Viswanathan, V. Afanasyev, S. Buldyrev, E. Murphy, P. Prince, and H. E. Stanley. Lévy flight search patterns of wandering albatrosses. *Nature*, 381 (6581):413–415, 1996. *Cited at page 176*

H. W. Watson and F. Galton. On the probability of the extinction of families. *The Journal of the Anthropological Institute of Great Britain and Ireland*, 4:138–144, 1875. *Cited at page 18*

G. Weiss. Aspects and applications of the random walk (random materials & processes s.). 2005. *Cited at pages 12, 19, and 146*

E. W. Weisstein. Delta function. From MathWorld–A Wolfram Web Resource, 2010. *Cited at page 32*

G. Wergen, S. N. Majumdar, and G. Schehr. Record statistics for multiple random walks. *Physical Review E*, 86(1):011119, 2012. *Cited at page 193*

R. Weron. On the chambers-mallows-stuck method for simulating skewed stable random variables. *Statistics & Probability Letters*, 28(2):165–171, 1996. *Cited at pages 182, 231, and 233*

M. M. R. Williams. *Random processes in nuclear reactors*. Oxford: Pergamon, 1974. *Cited at pages x, 55, 59, 84, and 89*

G. M. Wing. *An introduction to transport theory*. Wiley, 1962. *Cited at page 76*

W. Young, A. Roberts, and G. Stuhne. Reproductive pair correlations and the clustering of organisms. *Nature*, 412(6844):328–331, 2001. *Cited at pages 45, 59, 84, 89, 92, 96, and 134*

A. Yue, M. Dewey, D. Gilliam, G. Greene, A. Laptev, J. Nico, W. Snow, and F. Wietfeldt. Improved determination of the neutron lifetime. *Physical review letters*, 111(22):222501, 2013. *Cited at page 10*

V. Zaburdaev, S. Denisov, and J. Klafter. Lévy walks. *Reviews of Modern Physics*, 87(2):483, 2015. *Cited at pages 47 and 176*

M. Zaider and H. H. Rossi. *Microdosimetry and its Applications*. Springer, 1996. *Cited at page 144*

Y.-C. Zhang, M. Serva, and M. Polikarpov. Diffusion reproduction processes. *Journal of Statistical Physics*, 58(5-6):849–861, 1990. *Cited at pages 89, 96, 116, 134, and 135*

A. Zoia, A. Rosso, and M. Kardar. Fractional laplacian in bounded domains. *Physical Review E*, 76(2):021116, 2007. *Cited at page 193*

A. Zoia, E. Dumonteil, and A. Mazzolo. Collision densities and mean residence times for d-dimensional exponential flights. *Physical Review E*, 83 (4):041137, 2011. *Cited at page 63*

A. Zoia, E. Dumonteil, and A. Mazzolo. Properties of branching exponential flights in bounded domains. *EPL (Europhysics Letters)*, 100(4):40002, 2012a. *Cited at pages 58, 74, 143, 144, 146, 149, 151, 167, 168, and 169*

A. Zoia, E. Dumonteil, A. Mazzolo, and S. Mohamed. Branching exponential flights: travelled lengths and collision statistics. *Journal of Physics A: Mathematical and Theoretical*, 45(42):425002, 2012b. *Cited at pages 63, 64, 66, 67, 72, 73, 74, 80, 83, and 84*

A. Zoia, E. Dumonteil, A. Mazzolo, C. de Mulatier, and A. Rosso. Clustering of branching brownian motions in confined geometries. *Physical Review E*, 90(4):042118, 2014. *Cited at pages xi, 2, 88, 135, and 216*

V. M. Zolotarev. *One-dimensional stable distributions*, volume 65. American Mathematical Soc., 1986. *Cited at page 187*

G. Zumofen and J. Klafter. Absorbing boundary in one-dimensional anomalous transport. *Physical Review E*, 51(4):2805, 1995. *Cited at pages 185 and 197*

ÉCOLE DOCTORALE
Physique en île-de-France (EDPIF)

Titre : Contributions de la théorie des marches aléatoires au transport stochastique des neutrons

Mots clés : marches aléatoires branchantes, théorie du transport des neutrons, statistiques de fluctuations, diffusion anormale, géométries confinées, simulations Monte-Carlo

Résumé : L'un des principaux objectifs de la physique des réacteurs nucléaires est de caractériser la répartition aléatoire de la population de neutrons au sein d'un réacteur. Les fluctuations de cette population sont liées à la nature stochastique des intéractions des neutrons avec les noyaux fissiles du milieu : diffusion, capture stérile, ou encore émission de plusieurs neutrons lors de la fission d'un noyau. L'ensemble de ces mécanismes physiques confère une structure aléatoire branchante à la trajectoire des neutrons, alors modélisée par des marches aléatoires. Avec environs 10^8 neutrons par centimètre cube dans un réacteur de type REP à pleine puissance en conditions stationnaires, les grandeurs physiques du système (flux, taux de réaction, énergie déposée) sont, en première approximation, bien représentées par leurs valeurs moyennes respectives. Ces observables physiques moyennes obéissent alors à l'équation de transport linéaire de Boltzmann.

Au cours de ma thèse, je me suis penchée sur deux aspects du transport qui ne sont pas décrits par cette équation, et pour lesquels je me suis appuyée sur des outils issus de la théorie des marches aléatoires. Tout d'abord, grâce au formalisme de Feynman-Kac, j'ai étudié les fluctuations statistiques de la population de neutrons, et plus particulièrement le phénomène de « clustering neutronique », qui a été mis en évidence numériquement pour de faibles densités de neutrons (typiquement un réacteur au démarrage). Je me suis ensuite intéressée à différentes propriétés de la statistique d'occupation des neutrons effectuant un transport anormal (càd non-exponentiel). Ce type de transport permet de modéliser le transport dans des matériaux fortement hétérogènes et désordonnés, tel que les réacteurs à lit de boulets. L'un des aspects novateurs de ce travail est la prise en compte de la présence de bords. En effet, bien que les systèmes réels soient de taille finie, la plupart des résultats théoriques pré-existants sur ces thématiques ont été obtenus sur des systèmes de taille infinie.

Université Paris-Saclay
Espace Technologique / Immeuble Discovery
Route de l'Orme aux Merisiers RD 128 / 91190 Saint-Aubin, France

Title : A random walk approach to stochastic neutron transport

Keywords : branching random walks, neutron transport theory, fluctuation statistics, anomalous diffusion, confined geometries, Monte Carlo simulations

Abstract : One of the key goals of nuclear reactor physics is to determine the distribution of the neutron population within a reactor core. This population indeed fluctuates due to the stochastic nature of the interactions of the neutrons with the nuclei of the surrounding medium: scattering, emission of neutrons from fission events and capture by nuclear absorption. Due to these physical mechanisms, the stochastic process performed by neutrons is a branching random walk. For most applications, the neutron population considered
is very large, and all physical observables related to its behaviour, such as the heat production due to fissions, are well characterised by their average values. Generally, these mean quantities are governed by the classical neutron transport equation, called linear Boltzmann equation.

During my PhD, using tools from branching random walks and anomalous diffusion, I have tackled two aspects of neutron transport that cannot be approached by the linear Boltzmann equation. First, thanks to the Feynman-Kac backward formalism, I have characterised the phenomenon of "neutron clustering" that has been highlighted for low-density configuration of neutrons and results from strong fluctuations
in space and time of the neutron population. Then, I focused on several properties of anomalous (non-exponential) transport, that can model neutron transport in strongly heterogeneous and disordered media, such as pebble-bed reactors. One of the novel aspects of this work is that problems are treated in the presence of boundaries. Indeed, even though real systems are finite (confined geometries), most of previously existing results were obtained for infinite systems.